



السلوك الفيزيائي والكيميائي لخليط من خوافض التوتر السطحي اللاأيونيه

إعداد

وائل ضامن سيد صلاح الدين

بكالوريوس كيمياء/ جامعة بيت لحم/ فلسطين

إشراف

د. منذر فنون

قدمت هذه الرسالة استكمالاً لمتطلبات

درجة الماجستير

في الكيمياء الصناعية والتطبيقية

دائرة الكيمياء والكيمياء الصناعية

كلية العلوم والتكنولوجيا

جامعة القدس

أيار 2005

الإهداء

إلى اللّذين كانا لي مدرسةً في البذلِّ والجِدِّ والعطاءِ والصبرِ والمُصابرةِ.... إلى

اللّذين جعلوا لي من أيامهم أ وثيقةَ عزّةٍ لا يفنى سناؤها ورايةَ مجدٍ لا يبلى

بهاؤها.... إلى أبي وأمي

إلى اللّذين نشقتُ من أنفاسهم عبيرَ المؤازرةِ وأريجَ العونِ والتأييدِ.... إلى اللّذين لم

أجدُ في عيونهم غيرَ أنوارِ فرحةٍ متوهجةٍ بما أسعى لقطفِ ثماره من بستانِ

المستقبلِ الباسطِ جناحهُ ليطيّرَ بي إلى قمةِ المجدِ وذروةِ

العزّةِ.... إلى إخوتي وأخواتي

إلى قناديلِ العلمِ ومصابيحِ المعرفةِ والثّقافةِ.... إلى فرسانِ غارةِ العلمِ ورُماةِ الحدقِ

في سراياه.... إلى اللّذين يصفُلون للوطنِ بالعلمِ سُيوفًا لا تنبؤُ ويُسرِجونَ أحصنةً لا

تكبؤُ ويببئونَ عقولًا تهتّرُ عظمةً وتتألقُ معرفةً وعلماً.... إلى أسرةِ جامعةِ القدسِ



**Physicochemical Behavior
of Mixed Nonionic Surfactant Systems**

By

Wail Damin Al-Sayyd Salah Al-Diyn

B. Sc. Chemistry / Bethlehem University / Palestine

Supervised by:

Dr. Monzer Fanun

A THESIS

Submitted in Partial fulfillment of requirements for the degree of

Master of Applied & Industrial Technology

Department of Chemistry & Chemical Technology

Faculty of Science and Technology

Al-Quds University

May, 2005

**Deanship of Graduate Studies
Al-Quds University**

**Physicochemical Behavior
of Mixed Nonionic Surfactant Systems**

Wail Damin Al-Sayyd Salah Al-Diyn

M.Sc. Thesis

Jerusalem- Palestine

2005

Program for Postgraduate Studies in Applied and Industrial Technology
Faculty of Science and Technology
Department of Chemistry & Chemical Technology
Deanship of Graduate Studies

Physicochemical Behavior

of Mixed Nonionic Surfactant Systems

Student Name: Wail Damin Al-Sayyd Salah Al-Diyn

Registration No: 9810955

Supervisor: Dr. Monzer Fanun

Master thesis submitted and accepted, Date: 22/5/2005

The names and signatures of the examining committee members are as follows:

1. Dr. Monzer Fanun/ **Supervisor**

Signature.....

2. Dr. Alfred Aded Rabbo/ **External Examiner**

Signature.....

3. Dr. Mohammed Abul Haj/ **Internal Examiner**

Signature.....

AL-QUDS UNIVERSITY

(2005)

Declaration

I certify that this thesis submitted for the degree of Master is the results of my own research, except where otherwise acknowledged, and that this thesis has not been submitted for a higher degree to any other university or institution.

Signed:

Wail Damin Al-Sayyed Salah Al-Diyn

Date:

22/5 /2005

Acknowledgement

I would like first of all to express my deep gratitude to my supervisor Dr. Monzer Fanun for his special concern and tremendous efforts on my experiments and analysis that I respect and admire the most.

I would also like to thank the Department of Chemistry at Al-Quds University for their help and advice through this work,

I also like to thank Bierzeit Pharmaceutical Co. for its helping to supply me with the needed materials for this work. In addition to my great thanks and appreciation for the helping that I received from Hebrew University which enable me to get the best characterization and results analysis.

Finally, but by no means least, I wish to thank all of my friends and colleagues for the support and encouragement they generously provided through my study period.

Abstract

This study aims to examine the effect of temperature, co-surfactant content, mixed surfactant content and oil content on the phase behavior of mixed nonionic surfactant system with vegetable oils.

The systems studied are: Water/ Surfactants/ Co-surfactants/ Oil or Water/ mixed surfactants/ Oil. The surfactants used in this study are sucrose esters; sucrose monolaurate (L₁₆₉₅) and sucrose monostearate (S₁₅₇₀) beside ethoxylated mono diglycerides (EMDG) which are nonionic surfactants varying in their structure and hydrophilicity. The head group of the sucrose esters is sucrose, and the lipophilic tail is the ester of fatty acids. In the case of EMDG, the head group is the result of the ethoxylation of 20 moles of ethylene oxide per one mole of a mixture of stearate and palmitate esters of glycerin.

The co-surfactants used are food, cosmetic and pharmaceutical grade short chain alcohol (ethanol) and its substitute 1, 2-propandiol (propylene glycol, (PG)) which is one of the least hydrophilic simple polyols that are soluble in water but practically insoluble in the oil phase.

The oils used are: R (+)-limonene, Isopropylmyristate (IPM) and caprylic-capric triglyceride (MCT).

The mono terpene hydrocarbon (R (+)-limonene), the major constituent of citrus essential oils, is often used in food, cosmetic, and coating materials. R (+)-limonene is essentially insoluble in water, IPM is a straight chain oil used in many pharmaceutical formulations owing its compatibility with biological systems and is expected to be environment friendly.

Medium chain triglyceride (MCT) is fully saturated and stable to oxidation and used in many foods, cosmetic and pharmaceutical formulations.

In the system: Water/ L₁₆₉₅/ PG/ Oil, R (+)-limonene was not able to form three-phase region over all of the range of temperatures studied or mixed surfactant and co-surfactant contents when the $Oil/(Oil + water)$, weight ratio was constant (α) = 50 wt% only one or two-phase region were formed. For $PG/(PG + L_{1695})$, weight ratio (δ) = 25 wt% the minimum amount of surfactant and co-surfactant needed to form the one phase region is $\gamma_{\min} = 50$ wt% and the temperature at which this one phase region was formed is 55°C. This γ_{\min} increases as δ increases. IPM and MCT formed three-phase region, beside the one and two-phase regions formed. The efficiency ($\bar{\gamma}$) of the mixed surfactant and co-surfactant increases from 50 to 65 wt%, as δ increases in the case of IPM and decreases from 60 to 45 wt% as δ increases in the case of MCT. The phase inversion temperature $\bar{T}_{(PIT)}$ increases from 82 to 92°C as δ increases in the case of IPM and decreases from 91 to 87.5 °C as δ increases in the case of MCT.

In the system: Water/ S₁₅₇₀/ PG/ Oil, no three-phase formation with R(+)-limonene and IPM only one or two-phase region were formed, while in the case of MCT the three-phase was formed over all of the range of δ studied.

Using the system: Water/ EMDG/ PG/ Oil, no three-phase formation for δ values ≥ 25 wt% with IPM and MCT. In the case of R (+)-limonene, the three-phase is formed for δ values ≥ 75 wt%.

While in the case of the system: Water/ L₁₆₉₅/ EMDG/ Oil , three-phase is formed for the three oils when δ values ≥ 25 wt%, $\bar{\gamma}$ increases as δ increases in the presence of R (+)-limonene and decreases in the case of IPM or MCT. The \bar{T} increases as δ increases in the case of R (+)-limonene and decreases in the case of IPM and MCT.

In the system: Water/ S₁₅₇₀/ EMDG/ Oil, no three-phase formation in the case of R(+)-limonene, only one-phase region beside the two-phase region. In

the case of IPM, the three-phase region is formed when δ values ≥ 75 wt% and in MCT, the three-phase is formed in the whole range of δ studied.

In the pseudo-ternary phase behavior at constant T, the systems: Water/ L_{1695} / EMDG/ Oil + EtOH, were studied. The oils were R (+)-limonene and IPM, and the weight ratio of L_{1695} /EMDG was varied from 1 to 1/3, and the weight ratio of *Oil/EtOH* was 1 in the case where EtOH was present in the system.

The solubilization parameters calculated were the maximum amount of solubilized water (W_m) and total area of the one-phase region (A_T). The system: Water/ L_{1695} + EMDG (1/1)/ EtOH + R (+)-limonene (1/1), gave the maximum amount of $W_m = 100$ wt% in the presence and absence of EtOH, the A_T in the presence of EtOH was 74.2 % and in its absence was 61.6%.

Another objective of this study is to elucidate the microstructure of the one-phase region which was formed. This was done by using electrical conductivity and self-diffusion NMR techniques. The systems studied by electrical conductivity were: Water/ L_{1695} / EMDG/ Oil where δ and γ (wt %), were constant equal 50 and 31 wt%, respectively. α (wt %) and T were varied.

The oils were R (+)-limonene and IPM. The electrical conductivity (κ) of the system containing R (+)-limonene varies from 1.8×10^{-3} S/cm at $\alpha = 10$ wt% to 4.7×10^{-6} S/cm at $\alpha = 90$ wt%, While in the case of IPM κ varies from 4.26×10^{-3} S/cm at $\alpha = 10$ wt% to 1.26×10^{-4} S/cm at $\alpha = 90$ wt% and varies linearly with temperature.

The system containing IPM was investigated using self-diffusion NMR, and was found that the relative self-diffusion coefficient of water and oil varies as α varies. It decreases from 0.83 to 0.1 in the case of water, and from 0.001 to 0.36 in the case of oil when α values 10 and 85 wt%.

The hydrodynamic radius (R_H) was calculated at 90 wt% water and was equal to 7.3 nm and the area (a) per polar head group was estimated at 75 \AA^2 .

A third objective explored in this study was the solubilization of pharmaceutical active ingredients, sodium diclofenac in model microemulsion systems studied in this work which were: Water/ L₁₆₉₅/ EMDG/ EtOH + Oil.

The solubilization capacity in the microemulsion systems passes, through a maximum at $\alpha = 61.5 \text{ wt\%}$ in the systems: water/ L₁₆₉₅/ EMDG/ Oil for the two oils studied (R (+)-limonene, and IPM).

In the case where ethanol is present in the system: Water/ L₁₆₉₅/ EMDG/ Oil+ EtOH (1/1), the maximum solubilization capacity passes through a maximum at $\alpha = 23 \text{ wt\%}$. If we suppose that ethanol is present only in the oil phase, then the α where is the maximum solubilization occurs, equals 37.5 wt\% .

ملخص البحث:

تهدف هذه الدراسة الى اختبار وقياس بتأثير درجة الحرارة، ومساعدات خوافض التوتر السطحي، وخليط عدد من خوافض التوتر السطحي، وكذلك بتأثير الزيت على مظهر وسلوك أنظمة مكونة من زيوت نباتية وخوافض توتر سطحي لأيونية.

الأنظمة التي تناولتها هذه الدراسة هي اما: ماء / خوافض توتر سطحي/ مساعدات خوافض التوتر السطحي/ زيت، أو: ماء / خليط من خوافض التوتر السطحي / زيت. خوافض التوتر السطحي المستخدم في هذه الدراسة هي: سكروز استر (سكروز أحادي اللوريت (L1695)، سكروز أحادي الستيريت (S1570)، و اثوكسيلاند احادي وثنائي الجليسيريد (EMDG)، وتعتبر هذه المواد خوافض توتر سطحي لأيونية تختلف فيما بينها بتركيبها البنائي ومدى قابليتها للذوبان في الماء. رأس المجموعة في السكروز استر هو السكروز، والذنب الدهني هو استر الاحماض الدهنية. رأس المجموعة في EMDG نتاج الاثوكسيلاشن (Ethoxylation) لعشرين مول من اكسيد الاثيلين لكل مول من خليط الاستيريت والبالميتيت استر للجليسيرين.

مساعدات خوافض التوتر السطحي المستخدمة في هذه الدراسة تدخل في مجالات الغذاء ومواد التجميل والصناعات الدوائية، وهي حلقة صغيرة من الكحول (الايثانول) أو بديل عنها مثل بروبيلين جلايكول (PG) الذي يتميز بسهولة ذوبانه في الماء، لكنه عمليا غير قابل للذوبان في الزيت.

الزيوت المستخدمة و التي تناولتها هذه الدراسة هي: الليمونين (R(+)-limonene)، الأيزوبروبيل مريستيت (IPM)، والكابريك-كابريك ثلاثي الجليسيريد (MCT). تعتبر الزيوت العطرية أحادية الهيدروكربون ومنها (R(+)-limonene) من المكونات الرئيسية للزيوت الاساسية في الليمون (Citrus)، والتي تستخدم احيانا في الطعام ومواد التجميل ومواد التغليف، وال (R(+)-limonene) غير قابل للذوبان في الماء. ال (IPM) هو زيت خطي البناء ويستخدم في كثير من الصناعات الدوائية بسبب كونه يمتلك خاصية التوافق مع النظام البيولوجي، ويعتبر أيضاً من المواد غير الضارة بالبيئة. ثلاثي الجليسيريد (MCT) هو زيت متوسط البناء الجزيئي (ومتشعب)، مشعب و عملية الاكسدة بالنسبة اليه مستقرة أو ثابتة، ويستخدم في كثير من مجالات الطعام ومواد التجميل وصناعة الادوية.

عند اختبار نظام مكون من: ماء / L1695 / بروبيلين جلايكول / زيت، وجد أن R(+)-limonene لم يكن قادراً على تكوين منطقة تحتوي على ثلاث طبقات (طبقة ماء وجزء من خافض التوتر السطحي مذاب فيه وطبقة زيت وجزء من خافض التوتر السطحي مذاب فيه والطبقة الثالثة مكونه من خوافض التوتر التي لم تذوب في الزيت ولا في الماء) حتى بوجود خليط من خوافض التوتر السطحي ومساعداته في أي من درجات الحرارة

المدروسة، عندما كانت نسبة الزيت إلى الزيت والماء ثابتة وتساوي 50% من نسبة الوزن الكلي، فقط استطاع الليمونين تشكيل منطقة مكونة من طبقة واحدة (منطقة المستحلبات الجزيئية الدقيقة (Microemulsion)) ومنطقة مكونة من طبقتان (مكونة من خواص التوتر السطحي المذابة في الماء وطبقة مكونة من الزيت لوحده أو خواص توتر سطحي مذابة في الزيت وطبقة أخرى مكونة من الماء لوحده). عندما كانت نسبة وزن البروبيلين جلايكول الى خليط من البروبيلين جلايكول مع L₁₆₉₅ تساوي 25% من نسبة وزنها، استطاعت أقل كمية منها وهي 50% من نسبة الوزن من تكوين منطقة تشتمل على طبقة واحدة وكانت درجة الحرارة عندها تساوي 55 درجة مئوية في حين أن هذه النسبة تزداد بازدياد نسبة البروبيلين جلايكول.

أما بالنسبة ل IPM وال MCT فانه تشكلت منطقة تحتوي على ثلاث طبقات الى جانب تشكل مناطق مكونة من طبقة وطبقتين. فاعلية خليط خواص التوتر السطحي ومساعداتها ازدادت من 50 الى 65% من نسبة الوزن ومع ازدياد نسبة البروبيلين جلايكول عند استخدام زيت IPM , وتنخفض من 60 الى 45% من نسبه الوزن بازدياد نسبة البروبيلين جلايكول عند استخدام زيت MCT . عند استخدام زيت ال IPM نلاحظ أنه مع زيادة نسبة وزن البروبيلين جلايكول فان درجة الحرارة التي تحدث عندها عملية الانتقال والانقلاب (من مرحلة ذوبان خافض التوتر السطحي ومساعداته في الماء الى ذوبانها في الزيت (phase inversion temperature(T_{PI})) تزداد من 82 الى 92 درجة مئوية وهذه القيمة تنخفض من 91 الى 87.5 درجة مئوية اذا كان الزيت المستخدم MCT.

عند اختبار نظام مكون من: ماء / S₁₅₇₀ / بروبلين جلايكول / زيت، وجد انه لم يكن بإمكان أي من الزيوت (R(+)-limonene, IPM) من تكوين منطقة تحتوي على ثلاث طبقات، بينما استطاعت هذه الزيوت تكوين مناطق تحتوي على طبقة وطبقتين، في حين استطاع زيت MCT تكوين منطقة تحتوي على ثلاث طبقات عند جميع نسب البروبيلين جلايكول المدروسة.

باستخدام نظام مكون من: ماء/ EMDG / بروبلين جلايكول / زيت، عندما كانت الزيوت المستخدمة MCT و IPM لم تتكون منطقة تحتوي على ثلاث طبقات عندما كانت نسبة البروبيلين جلايكول أكبر أو تساوي 25% من نسبة الوزن , لكن عند استخدام زيت R(+)-limonene تكونت منطقة تحتوي على ثلاث طبقات عندما كانت نسبة البروبيلين جلايكول اكبر او تساوي 75% من نسبة الوزن.

باستخدام نظام مكون من: ماء/ EMDG/L₁₆₉₅ / زيت، تكونت منطقة من ثلاث طبقات عندما كانت نسبة وزن EMDG أكبر أو تساوي 25% من نسبة الوزن. فاعلية خافض التوتر السطحي (L₁₆₉₅) ازدادت مع زيادة نسبة EMDG ، بوجود زيت R(+)-limonene ، وانخفضت هذه القيمة عند استخدام زيوت MCT أو

IPM . درجة الحرارة الرئيسية \bar{T} (Mean temperature,) ازدادت مع ازدياد نسبة EMDG باستخدام زيت - R(+)-limonene وانخفضت باستخدام زيت MCT و IPM.

باستخدام نظام مكون من: ماء / EMDG / S₁₅₇₀ / زيت، لم تتكون منطقة تحتوي على ثلاث طبقات في حالة استخدام زيت R(+)-limonene، وتكونت منطقة تحتوي على طبقة واحدة فقط الى جانب منطقة تحتوي على طبقتين، وعند استخدام زيت IPM تكونت منطقة تحتوي على ثلاث طبقات عندما كانت نسبة وزن EMDG اكبر او تساوي 75% من نسبة الوزن الكلي، و عند استخدام زيت MCT تكونت منطقة من ثلاث طبقات في جميع تراكيز EMDG المدروسة.

لدراسة مظهر السلوك للنظام الرباعي (Quaternary or Pseudo-ternary) على درجة حرارة ثابتة لنظام مكون من: ماء / EMDG / L₁₆₉₅ / زيت+ ايثانول، حيث أن الزيوت المستخدمة في هذه الدراسة هي: IPM و R(+)-limonene، وكانت نسبة وزن L₁₆₉₅ الى EMDG متغيرة (1 و 1/3) وكانت نسبة وزن الزيت الى الايثانول واحد في حال وجود الايثانول في هذا النظام.

معاملات الذائبية التي تم حسابها في هذه الدراسة هي اكبر نسبة ماء مذابة (W_m) والمساحة الكلية للمنطقة المكونة من طبقة واحدة (A_T). كانت اكبر نسبة للماء التي تم تذويبها هي 100% سواءً بوجود الايثانول او عدم وجوده في النظام المذكور أعلاه، في حين ان المساحة الكلية (A_T) للمنطقة المكونة من طبقة واحدة كانت 74.2% في حال وجود الايثانول في هذا النظام، و 61.6% في حال عدم وجود الايثانول.

ومن الأهداف الأخرى لهذه الدراسة هو تبيان و توضيح البناء الجزيئي الدقيق للمنطقة المكونة من طبقة واحدة، وقد تمت هذه الدراسة باستخدام جهاز التوصيل الكهربائي (Electric Conductivity) وجهاز الانتشار الذاتي (Self-Diffusion NMR) وقد استخدم جهاز التوصيل الكهربائي (Electric Conductivity) في مكون من: ماء / EMDG / L₁₆₉₅ / زيت، حيث كانت نسبة وزن EMDG تساوي 50% من نسبة الوزن لخليط خوافض التوتر السطحي، ونسبة وزن خوافض التوتر السطحي ومساعداتها ثابتة وتساوي 31% من نسبة الوزن الكلي، بينما تم تغيير نسبة الزيت الى الزيت والماء، وكذلك تغيير درجة الحرارة.

تغيرت قيمة التوصيل الكهربائي من $1.8 \times 10^{-3} \text{ s/cm}$ عندما كانت نسبة وزن الزيت إلى الزيت والماء (α) = 10% من نسبة الوزن الى $4.7 \times 10^{-6} \text{ s/cm}$ عندما كانت $\alpha = 90\%$ من نسبة الوزن، في حال استخدام زيت R(+)-limonene. بينما اختلفت هذه القيمة من $4.26 \times 10^{-3} \text{ s/cm}$ عندما كانت α

= 10% إلى 1.26×10^{-4} s/cm عندما كانت $\alpha = 90\%$ من نسبة الوزن في حال استخدام زيت IPM ، وكان هذا التغيير خطياً مع درجة الحرارة.

تم دراسة نظام يحتوي على زيت IPM باستخدام جهاز (Self-diffusion NMR) ووجد ان معامل الانتشار الذاتي النسبي (Relative self diffusion coefficient) بالنسبة للماء والزيت يتغير مع تغير نسبة وجودهما، تقل من 0.83 الى 0.1 في حالة الماء ومن 0.001 الى 0.36 في حالة الزيت عندما كانت نسبة الزيت الى الزيت والماء 10 و 85% من نسبة الوزن الكلي.

لقد تم حساب نصف القطر الهيدروديناميكي (Hydrodynamic Radius R_H) عندما كانت نسبة الماء تساوي 90% من نسبة الوزن، ووجد انه يساوي 7.3 نانوميتر (7.3 nm) وقد قدرت مساحة رأس المجموعة ب 75 أنجستروم تربيع (75 \AA^2).

أما الهدف الثالث لهذه الدراسة هو استكشاف مدى قدرة نظام مكون من: ماء / EMDG / L₁₆₉₅ / ايثانول / زيت، على تذويب مواد رئيسية تستخدم في الصناعات الدوائية مثل ديكلوفيناك الصوديوم (Sodium Diclofenac). لقد تبين ان نظام مكون من: ماء / EMDG / L₁₆₉₅ / زيت، حيث ان الزيت المستخدم هنا هو R(+)-limonene وIPM، تكون فيه أكبر نسبة تذويب عندما تكون نسبة الزيت الى الزيت والماء تساوي 61.5% من نسبة الوزن. وفي حال وجود الايثانول في هذا النظام بنسبة واحد الى واحد مع الزيت كانت اكبر نسبة للذائبية عندما كانت نسبة الزيت الى الزيت والماء تساوي 23% من نسبة الوزن. اذا فرضنا ان الايثانول موجود مع الزيت فقط في هذه الحالة، فان أكبر نسبة للذائبية تتحقق عندما تكون نسبة الزيت الى الزيت والماء تساوي 37.5% من نسبة الوزن.

To my dear Parents

TABLE OF CONTENTS

	Page
Declaration	i
Acknowledgement	ii
Abstract	iii
Arabic Abstract	vii
Dedication	xi
Table of Contents	xii
List of Abbreviations	xiv
List of Tables	xvi
List of Figures	xx
Chapter one: Introduction	1
Chapter two: Objectives	19
Chapter three: Materials and Methods	22
III.1 Materials	23
III.1.1 Surfactant (surface active agent)	23
III.1.2 Oils	24
III.1.3 Co-surfactant and Co-solvents	25
III.1.4 Water	26
III.1.5 Solubilization Materials	26
III.1.6 Others	26
III.2 Methods	27
III.2.1 Phase behavior determination	27
III.2.1.1 Samples preparation for temperature dependent phase behavior	27
III.2.1.2 Temperature dependent phase behavior determination	27
III.2.1.3 Sample preparation for pseudo-ternary phase diagram at constant temperature	30

III.2.1.4 Solubilization parameters	31
III.2.2 Active ingredients solubilization evaluation	32
III.2.3 Electrical conductivity	33
III.2.4 Pulsed gradient echo (PGSE) nuclear magnetic resonance (NMR)	34
Chapter four: Results and Discussion	35
IV.1 Phase Behavior Results	36
IV.1.1 Binary Phase Behavior	36
IV.1.2 Ternary Phase Behavior	43
IV.1.3 Quaternary Phase Behavior	51
IV.1.4 Discussion of the Phase Behavior	117
IV.1.5 Pseudo-ternary Phase Diagram	144
IV.2 Microemulsion Structure	154
IV.2.1 Electrical Conductivity	154
IV.2.2 Pulsed Gradient Spin-Echo (PGSE)-NMR	162
IV.3 Solubilization in Microemulsion	176
IV.3.1 Introduction	176
IV.3.2 Results and Discussion	178
Chapter five: General Conclusions	185
Chapter six: References	192

List of Abbreviations

1ϕ (Winsor IV), L_2	One-phase region
$M\phi$, 2ϕ (Winsor I, and Winsor II)	Two-phase or multi-phase region
3ϕ (Winsor III), (W+D+O)	Three-phase region (Water + Surfactant + Oil)
L_{1695}	Sucrose monolourate
S_{1570}	Sucrose monostearat
PG	Propylene glycol
EMDG	Ethoxylated mono-diglycerides
MCT	Caprylic/ capric triglyceride
IPM	Isopropyl myristatate
W/ O	Water in oil
O/ W	Oil in water
PIT	Phase inversion temperature
CMC	Critical micelle concentration
HLB	Hydrophilic lipophilic balance
T_1	The temperature where the three-phase body appears
$L\alpha$, LC	The lamellar phase (liquid crystal region)
T_u	The temperature where the three-phase body disappears
T_α	Temperature at the upper critical end point
T_β	Temperature at the lower critical end point
cp_α (cep_α)	Upper critical end point
cp_β (cep_β)	Lower critical end point
T_{cp}	Tricritical point
ΔT	The three-phase temperature interval
α or Φ	The mass fraction of oil in the mixture of water and oil

δ	The mass ratio of surfactants in the mixture
γ	Mass fraction of surfactant in the whole mixture
W_m	Surfactant in water
O_m	Surfactant in oil
\bar{T}	Mean temperature
$\bar{\gamma}$	Mean concentration
γ_{\min}	Minimum concentration
W_m	Maximum solubilization of water
S_m	Amount of surfactant needed to obtain maximum solubilization
A_T	Total mono phasic area
R_H	Hydrodynamic radius
a	The area per polar head group
D_{obs}	Observed diffusion coefficients
κ	Electrical conductivity
D_0	Diffusion coefficient of the neat component
D/D_0	Relative diffusion coefficient
SC	Solubilization capacity

List of Tables

Table	Description	Page
Table 3.1:	Type and composition of sucrose esters used in this research project.	23
Table 4.1:	Summary of the results of the system: Water/ L ₁₆₉₅ / PG/ Oil at constant $Oil/(Oil + Water)$ weight ratio, $\alpha = 50$ wt%, and variable δ (wt %), γ (wt %) and T (°C).	119
Table 4.2:	Summary of the analysis of the system: Water/ L ₁₆₉₅ / PG/ Oil at constant $Oil/(Oil + Water)$ weight ratio, $\alpha = 50$ wt%, and variable δ (wt %), γ (wt %) and T (°C).	121
Table 4.3:	Summary of the results of the system: Water/ S ₁₅₇₀ / PG/ Oil at constant $Oil/(Oil + Water)$ weight ratio, $\alpha = 50$ wt%, and variable δ (wt %), γ (wt %) and T (°C).	122
Table 4.4:	Summary of the analysis of the system: Water/ S ₁₅₇₀ / PG/ Oil at constant $Oil/(Oil + Water)$ weight ratio, $\alpha = 50$ wt%, and variable δ (wt %), γ (wt %) and T (°C).	124
Table 4.5:	Summary of the results of the system: Water/ EMDG/ PG/ Oil at constant $Oil/(Oil + Water)$ weight ratio, $\alpha = 50$ wt%, and variable δ (wt %), γ (wt %) and T (°C).	125
Table 4.6:	Summary of the analysis of the system: Water/ EMDG/ PG/ Oil at constant $Oil/(Oil + Water)$ weight ratio, $\alpha = 50$ wt%, and variable δ (wt %), γ (wt %) and T (°C).	127
Table 4.7:	Summary of the results of the system: Water/ L ₁₆₉₅ / EMDG/ Oil at constant $Oil/(Oil + Water)$ weight ratio, $\alpha = 50$ wt%, and variable δ (wt %), γ (wt %) and T (°C).	129
Table 4.8:	Summary of the analysis of the system: Water/ L ₁₆₉₅ / EMDG/ Oil at constant $Oil/(Oil + Water)$ weight ratio, $\alpha = 50$ wt%, and variable δ (wt %), γ (wt %) and T (°C).	130
Table 4.9:	Summary of the results of the system: Water/ S ₁₅₇₀ / EMDG/ Oil at constant $Oil/(Oil + Water)$ weight ratio, $\alpha = 50$ wt%, and variable δ (wt %), γ (wt %) and T (°C).	133

Table 4.10: Summary of the analysis of the system: Water/ S ₁₅₇₀ / EMDG/ Oil at constant $Oil/(Oil + Water)$ weight ratio, $\alpha = 50$ wt%, and variable δ (wt %), γ (wt %) and T (°C).	135
Table 4.11: Summary of the analysis of the results of the System: Water/ Surfactant/ PG/ Oil at constant $Oil/(Oil + Water)$ weight ratio, $\alpha = 50$ wt%, and variable δ (wt %), γ (wt %) and T (°C).	137
Table 4.12: Summary of the analysis of the results of the System: Water/ Surfactant/ EMDG/ Oil at constant $Oil/(Oil + Water)$ weight ratio, $\alpha = 50$ wt%, and variable δ (wt %), γ (wt %) and T (°C).	137
Table 4.13: System used in the study of variation of $Oil/(Oil + Water)$, α (wt %) as function of (T (°C)) for constant γ (wt %) and δ (wt %).	138
Table 4.14: Summary of the results of the system: water/ S ₁₅₇₀ / PG/ Oil, for variable $Oil/(Oil + Water)$ weight ratio, α (wt %) and temperature (°C).	141
Table 4.15: Summary of the results of the system: Water/ L ₁₆₉₅ / EMDG/ Oil, for variable $Oil/(Oil + Water)$ weight ratio, α (wt %) and temperature (°C).	142
Table 4.16: Summary of the results of the system: water/ S ₁₅₇₀ / EMDG/ Oil, for variable $Oil/(Oil + Water)$ weight ratio, α (wt %) and temperature (°C).	142
Table 4.17: Summary of the results of the pseudo-ternary phase behavior of the system: Water/ L ₁₆₉₅ / EMDG/ EtOH/ R (+)-Limonene at 25°C.	146
Table 4.18: Summary of the results of the pseudo-ternary phase behavior of the system: Water/ L ₁₆₉₅ / EMDG/ EtOH/ R (+)-Limonene at 25°C.	148
Table 4.19: Summary of the results of the pseudo-ternary phase behavior of the system: Water/ L ₁₆₉₅ / EMDG/ EtOH/ IPM at 25°C.	150

Table 4.20: summary of the results of the pseudo-ternary phase behavior of the system: Water/ L ₁₆₉₅ / EMDG/ EtOH/ IPM at 25°C.	152
Table 4.21: Electrical conductivity of the system: Water/ L ₁₆₉₅ / EMDG/ IPM ($\gamma = 31$ wt%, $\delta = 50$ (wt %)) as a function of α (wt %) and temperature (°C).	156
Table 4.22: Electrical conductivity of the system: Water / L ₁₆₉₅ / EMDG / R (+)-limonene ($\gamma = 31$ wt%, $\delta = 50$ wt%) as a function of α (wt%) and temperature (°C).	160
Table 4.23: Self-diffusion coefficients in the system Water/ L ₁₆₉₅ / EMDG/ IPM as function of α (wt %) and T (°C) for constant $\gamma = 31$ wt% and $\delta = 50$ wt%.	166
Table 4.24: Self-diffusion coefficients in the system Water/ L ₁₆₉₅ / EMDG/ IPM as function of α (wt %) and T (°C) for constant $\gamma = 26$ wt% and $\delta = 25$ wt%.	170
Table 4.25: Hydrodynamic radius of the System: Water/ L ₁₆₉₅ / EMDG/ IPM as function of α (wt %) for ($\gamma = 31$ wt%, $\delta = 50$ wt%).	172
Table 4.26: Hydrodynamic radius of the System: Water/ L ₁₆₉₅ / EMDG/ IPM as function of α (wt%) for ($\gamma = 26$ wt%, $\delta = 25$ wt%).	173
Table 4.27: Diclofenac sodium solubility at 25°C in the different microemulsion components.	178
Table 4.28: Solubilization capacity (SC) of diclofenac sodium in the system: Water/ L ₁₆₉₅ + EMDG(1/1)/ R(+)-limonene, along the dilution line D 60:40, at constant temperature (T = 25°C).	179
Table 4.29: Solubilization capacity (SC) of diclofenac sodium in the system: Water/ L ₁₆₉₅ + EMDG(1/1)/ R(+)-limonene + EtOH(1/1), along the dilution line D 60:40, at constant temperature (T = 25°C).	180
Table 4.30: Solubilization capacity (SC) of diclofenac sodium in the system: Water/ L ₁₆₉₅ + EMDG (1/1)/ IPM, along the dilution line D 60:40, at constant temperature (T = 25°C).	181

Table 4.31: Solubilization capacity (SC) of diclofenac sodium in the system: Water/ L₁₆₉₅ + EMDG (1/1)/ IPM + EtOH (1/1), along the dilution line D 60:40, at constant temperature (T= 25°C). 182

List of Figures

Figure	Description	page
Fig. 1.1:	A droplet microemulsion phase (A) can be of the O/ W (B) or the W/ O type (C). Typically, but not exclusively, the drops are nearly spherical and have a small size polydispersity.	3
Fig.1.2:	A bicontinuous structure.	3
Fig.1.3:	(A) A series of phase diagrams of a ternary system transformed from Winsor I {(a) and (b)} via Winsor II {(c), (d) and (e)} to Winsor II {(f) and (g)}. The dark triangles are three-phase regions. Tie lines indicate the composition of the two-phase regions. S, W and O stand for surfactant, water, and oil, respectively. (B) Phase changes of a system containing equal amounts of oil and water and a given (low) amount of surfactant.	6
Fig. 1.4:	The schematic change in phase behavior in a mixed-surfactant system. W _m and O _m are aqueous micellar and reverse micellar solution phases. W and O are excess water and oil phases. D indicates a microemulsion (surfactant) phase. W ₁ is the weight fraction of lipophilic surfactant in the mixed surfactant.	7
Fig.1.5:	A schematic view of the "unfolded" phase prism highlighting the three relevant binary phase diagrams. The most important features are the upper critical point on the oil-surfactant binary diagram, cp _α (which occurs at the temperature T _α), and the lower critical point on the water-surfactant binary diagram, cp _β (which occurs at the temperature T _β).	8
Fig. 1.6:	Formation of a three-phase body with nonionic amphiphiles by breaking the connected critical line at a tricritical point (tcp) by increasing the carbon number of the oil.	10
Fig.3.1:	Schematic phase prism in temperature-composition space. Showing the two vertical sections at either constant value of the oil fraction α , or at constant surfactant concentration γ . The lamellar phase L _α also is shown at high surfactant	28

concentrations.

- Fig.3.2:** The pseudo-binary phase diagram at $\alpha = 50$ wt% as a function of temperature and surfactant concentration, γ is the minimum surfactant concentration needed to make a single phase containing equal amounts of oil and water, and is a measure of the efficiency of the surfactant. γ_0 marks the lowest possible surfactant concentration where three liquid phases form. The temperatures T_1 and T_u are the temperature boundaries of the three-phase region. The phase boundaries trace the shape of a "fish". 30
- Fig.3.3:** Solubilization parameters for a schematic phase diagram. The weight ratio alcohol/ oil is varied from 1/ 2 in some cases to 1/ 1 or 3/ 1 in others, 1ϕ (L_2) is the area the W/ O microemulsion (one phase region), 2ϕ is the area two phase region. W_m is the maximum amount of solubilized water, S_m is the amount of surfactant needed to obtain maximum solubilization, and P is a point on the boundary of the monophasic area at which the water content reaches maximum. 33
- Fig.4.1:** Binary phase behavior of the System: L_{1695} / Oil as a function of surfactant concentration (γ (wt%)) and Temperature (T ($^{\circ}C$)). 37
- Fig.4.2:** Binary phase behavior of the System: S_{1570} / Oil as a function of surfactant concentration (γ (wt%)) and Temperature (T ($^{\circ}C$)). 38
- Fig.4.3:** Binary phase behavior of the System: EMDG/ Oil as a function of surfactant concentration (γ (wt%)) and Temperature (T ($^{\circ}C$)). 39
- Fig.4.4:** Binary phase behavior of the System: Water/ Surfactant as a function of surfactant concentration (γ (wt%)) and Temperature (T ($^{\circ}C$)) 40
- .
- Fig.4.5:** Binary phase behavior of the Systems: Surfactant/ PG as a function of surfactant concentration (γ (wt%)) and Temperature (T ($^{\circ}C$)). 42

- Fig.4.6:** Phase behavior of the System: Water/ L_{1695} / Oil as a function of γ (wt%) and temperature at constant $Oil/(Oil + Water)$ weight ratio $\alpha = 50$ (wt%). 45
- Fig.4.7:** Phase behavior of the System: Water/ S_{1570} / Oil as a function of γ (wt %) and temperature at constant $Oil/(Oil + Water)$ weight ratio, $\alpha = 50$ (wt %). 47
- Fig.4.8:** Phase behavior of the System: Water/ EMDG/ Oil as a function of γ (wt %) and temperature at constant $Oil/(Oil + Water)$ weight ratio, $\alpha = 50$ (wt %) 49
- .
- Fig.4.9:** Phase behavior of the System: Water/ PG/ Oil as a function of γ (wt %) and temperature at constant $Oil/(Oil + Water)$ weight ratio, $\alpha = 50$ (wt %). 50
- Fig.4.10:** Phase behavior of the System: Water/ L_{1695} / PG/ R(+)-Limonene as a function of δ , γ (wt%) and temperature at constant $Oil/(Oil + Water)$ weight ratio, $\alpha = 50$ (wt%). 52
- Fig.4.11:** Phase diagram for the system: Water/ L_{1695} / PG/ R (+)-Limonene at constant temperature ($T = 50^{\circ}\text{C}$ (A) and 80°C (B)) as a function of δ and γ (wt%). The $Oil/(Oil + Water)$ weight ratio, $\alpha = 50$ (wt %). 54
- Fig.4.12:** Phase behavior of the System: Water/ S_{1570} / PG/ R (+)-Limonene as a function of δ (wt%), γ (wt%) and temperature at constant $Oil/(Oil + Water)$ weight ratio, $\alpha = 50$ (wt%). 56
- Fig.4.13:** Vertical section through the phase prism for the system: Water/ S_{1570} / PG/ R (+)-Limonene at constant surfactant concentration (γ) equals 20 wt% and constant PG weight content in the mixture of surfactant (δ) and equals 0 wt% and 25 wt% as a function of temperature and $Oil/(Oil + Water)$ weight ratio, α (wt %). 58
- Fig.4.14:** Phase diagram for the system: Water/ S_{1570} / PG/ R (+)-Limonene at constant temperature ($T = 60^{\circ}\text{C}$) as a function of δ and γ (wt %). The $Oil/(Oil + Water)$ weight ratio, $\alpha = 50$ (wt%). 59

- Fig.4.15:** Phase behavior of the System: Water/ EMDG/ PG/ R (+)- Limonene as a function of δ , γ (wt %) and temperature at constant $Oil/(Oil + Water)$ weight ratio, $\alpha = 50$ (wt%). 61
- Fig.4.16:** Phase diagram for the system: Water/ L₁₆₉₅/ EMDG/ IPM at constant temperature (T = 72.5°C) as a function of δ and γ (wt %). The $Oil/(Oil + Water)$ weight ratio, $\alpha = 50$ (wt %). 62
- Fig.4.17:** Phase behavior of the System: Water/ L₁₆₉₅/ PG/ IPM as a function of δ , γ (wt%) and temperature at constant $Oil/(Oil + Water)$ weight ratio, $\alpha = 50$ (wt%). 64
- Fig.4.18:** Vertical section through the phase prism for the system: Water/ L₁₆₉₅/ PG/ IPM at constant surfactant concentration (γ) equals 26 wt% and 35.5 wt% and constant PG weight content in the mixture of surfactant (δ) and equals 0 wt% and 25 wt% as a function of temperature and $Oil/(Oil + Water)$ weight ratio, α (wt %). 66
- Fig.4.19:** Phase diagram for the system: Water/ L₁₆₉₅/ PG/ IPM at constant temperature (T = 80°C (A) and 85°C (B)) as a function of δ and γ (wt %). The $Oil/(Oil + Water)$ weight ratio, $\alpha = 50$ (wt %). 68
- Fig.4.20:** Phase behavior of the System: Water/ S₁₅₇₀/ PG/ IPM as a function of δ , γ (wt%) and temperature at constant $Oil/(Oil + Water)$ weight ratio, $\alpha = 50$ (wt%). 70
- Fig.4.21:** Vertical section through the phase prism for the system: Water/ S₁₅₇₀/ PG/ IPM at constant surfactant concentration (γ) equals 31 wt% and 26 wt% and constant PG weight content in the mixture of surfactant (δ) and equals 0 wt% and 25 wt% as a function of temperature and $Oil/(Oil + Water)$ weight ratio, α (wt%). 72
- Fig.4.22:** Phase diagram for the system: Water/ S₁₅₇₀/ PG/ IPM at constant temperature (T = 70°C) as a function of, δ and γ (wt%). The $Oil/(Oil + Water)$ weight ratio, $\alpha = 50$ (wt %). 73
- Fig.4.23:** Phase behavior of the System: Water/ EMDG/ PG/ IPM as a function of δ , γ (wt%) and temperature at constant 75

Oil/(Oil + Water) weight ratio, $\alpha = 50$ (wt%).

- Fig.4.24:** Phase diagram for the system: Water/ EMDG/ PG/ IPM at constant temperature ($T = 87^{\circ}\text{C}$) as a function of δ and γ (wt%). The *Oil/(Oil + Water)* weight ratio, $\alpha = 50$ (wt %). 76
- Fig.4.25:** Phase behavior of the System: Water/ L₁₆₉₅/ PG/ MCT as a function of δ , γ (wt%) and temperature at constant *Oil/(Oil + Water)* weight ratio, $\alpha = 50$ (wt%). 77
- Fig.4.26:** Phase diagram for the system: Water/ L₁₆₉₅/ PG/ MCT at constant temperature ($T = 90^{\circ}\text{C}$) as a function of δ and γ (wt%). The *Oil/(Oil + Water)* weight ratio, $\alpha = 50$ (wt %). 79
- Fig.4.27:** Phase behavior of the System: Water/ S₁₅₇₀/ PG/ MCT as a function of δ , γ (wt%) and temperature at constant *Oil/(Oil + Water)* weight ratio, $\alpha = 50$ (wt%). 81
- Fig. 4.28:** Vertical section through the phase prism for the system: Water/ S₁₅₇₀/ PG/ MCT at constant surfactant concentration (γ) equals 35.5 wt% and constant PG weight content in the mixture of surfactant (δ) and equals 25 wt% as a function of temperature and *Oil/(Oil + Water)* weight ratio, α (wt %). 83
- Fig.4.29:** Phase diagram for the system: Water/ S₁₅₇₀/ PG/ MCT at constant temperature ($T = 85^{\circ}\text{C}$) as a function of δ and γ (wt%). The *Oil/(Oil + Water)* weight ratio, $\alpha = 50$ (wt %). 83
- Fig.4.30:** Phase behavior of the System: Water/ EMDG/ PG/ MCT as a function of δ , γ (wt%) and temperature at constant *Oil/(Oil + Water)* weight ratio, $\alpha = 50$ (wt%). 85
- Fig.4.31:** Phase diagram for the system: Water/ EMDG/ PG/ MCT at constant temperature ($T = 60^{\circ}\text{C}$) as a function of δ and γ (wt%). The *Oil/(Oil + Water)* weight ratio, $\alpha = 50$ (wt %). 86
- Fig.4.32:** Phase behavior of the System: Water/ L₁₆₉₅/ EMDG/ R (+)-Limonene as a function of δ , γ (wt%) and temperature at constant *Oil/(Oil + Water)* weight ratio, $\alpha = 50$ (wt%). 88

- Fig.4.33:** Vertical section through the phase prism for the system: Water/ L₁₆₉₅/ EMDG/ R (+)-Limonene at constant surfactant concentration (γ) equals 26 wt% and 31 wt% and constant EMDG weight content in the mixture of surfactant (δ) and equals 25 wt% and 50 wt% as a function of temperature and $Oil/(Oil + Water)$ weight ratio, α (wt %). 90
- Fig. 4.34:** Phase diagram for the system: Water/ L₁₆₉₅/ EMDG/ R (+)-Limonene at constant temperature ($T = 85^\circ\text{C}$) as a function of δ and γ (wt %). The $Oil/(Oil + Water)$ weight ratio, $\alpha = 50$ (wt%). 91
- Fig. 4.35:** Phase behavior of the System: Water/ S₁₅₇₀/ EMDG/ R (+)-Limonene as a function of δ , γ (wt %) and temperature at constant $Oil/(Oil + Water)$ weight ratio, $\alpha = 50$ (wt %). 93
- Fig. 4.36:** Phase diagram for the system: Water/ S₁₅₇₀/ EMDG/ R (+)-Limonene at constant temperature ($T = 65^\circ\text{C}$) as a function of δ and γ (wt %). The $Oil/(Oil + Water)$ weight ratio, $\alpha = 50$ (wt%). 94
- Fig. 4.37:** Phase behavior of the System: Water/ L₁₆₉₅/ EMDG/ IPM as a function of δ , γ (wt %) and temperature at constant $Oil/(Oil + Water)$ weight ratio, $\alpha = 50$ (wt %). 96
- Fig. 4.38:** Vertical section through the phase prism for the system: Water/ L₁₆₉₅/ EMDG/ IPM at constant surfactant concentration (γ) equals 26 wt% and 31 wt% and constant EMDG weight content in the mixture of surfactant (δ) and equals 25 wt% and 50 wt% as a function of temperature and $Oil/(Oil + Water)$ weight ratio, α (wt %). 98
- Fig. 4.39:** Phase diagram for the system: Water/ L₁₆₉₅/ EMDG/ IPM at constant temperature ($T = 72.5^\circ\text{C}$) as a function of δ and γ (wt %). The $Oil/(Oil + Water)$ weight ratio, $\alpha = 50$ (wt %). 100
- Fig. 4.40:** Phase behavior of the System: Water/ S₁₅₇₀/ EMDG/ IPM as a function of δ , γ (wt %) and temperature at constant $Oil/(Oil + Water)$ weight ratio, $\alpha = 50$ (wt %). 102

- Fig. 4.41:** Vertical section through the phase prism for the system: Water/ S₁₅₇₀/ EMDG/ IPM at constant surfactant concentration (γ) equals 16.6 wt% and constant EMDG weight content in the mixture of surfactant (δ) and equals 25 wt% as a function of temperature and $Oil/(Oil + Water)$ weight ratio, α (wt %). 104
- Fig. 4.42:** Phase diagram for the system: Water/ S₁₅₇₀/ EMDG/ IPM at constant temperature (T = 65°C (A) and 70°C (B)) as a function of δ and γ (wt %). The $Oil/(Oil + Water)$ weight ratio, $\alpha = 50$ (wt %). 105
- Fig. 4.43:** Phase behavior of the System: Water/ L₁₆₉₅/ EMDG/ MCT as a function of δ , γ (wt %) and temperature at constant $Oil/(Oil + Water)$ weight ratio, $\alpha = 50$ (wt %). 108
- Fig. 4.44:** Vertical section through the phase prism for the system: Water/ L₁₆₉₅/ EMDG/ MCT at constant surfactant concentration (γ) equals 31 wt% and constant EMDG weight content in the mixture of surfactant (δ) and equals 25 wt% as a function of temperature and $Oil/(Oil + Water)$ weight ratio, α (wt%). 110
- Fig. 4.45:** Phase diagram for the system: Water/ L₁₆₉₅/ EMDG/ MCT at constant temperature (T = 80°C (A) and 85°C (B)) as a function of δ and γ (wt %). The $Oil/(Oil + Water)$ weight ratio, $\alpha = 50$ (wt %). 111
- Fig. 4.46:** Phase behavior of the System: Water/ S₁₅₇₀/ EMDG/ MCT as a function of δ , γ (wt%) and temperature at constant $Oil/(Oil + Water)$ weight ratio, $\alpha = 50$ (wt%). 113
- Fig. 4.47:** Vertical section through the phase prism for the system: Water/ S₁₅₇₀/ EMDG/ MCT at constant surfactant concentration (γ) equals 23.1 wt% and constant EMDG weight content in the mixture of surfactant (δ) and equals 25 wt% as a function of temperature and $Oil/(Oil + Water)$ weight ratio, α (wt %). 115
- Fig. 4.48:** Phase diagram for the system: Water/ S₁₅₇₀/ EMDG/ MCT at constant temperature (T = 80°C) as a function of δ and γ (wt%). The $Oil/(Oil + Water)$ weight ratio, $\alpha = 50$ (wt %). 116

- Fig. 4.49:** Phase inversion temperature $\bar{T}_{(PIT)}$ ($^{\circ}\text{C}$) [A] and the mean concentration ($\bar{\gamma}$) in wt% [B], for the system: Water/ L₁₆₉₅/ PG/ Oil at constant $Oil/(Oil + Water)$ weight ratio, $\alpha = 50$ wt%, and variable δ (wt %). 120
- Fig. 4.50:** Phase inversion temperature $\bar{T}_{(PIT)}$ ($^{\circ}\text{C}$) [A] and the mean concentration ($\bar{\gamma}$) in wt% [B], for the system: Water/ S₁₅₇₀/ PG/ Oil at constant $Oil/(Oil + Water)$ weight ratio, $\alpha = 50$ wt%, and variable δ (wt %). 123
- Fig. 4.51:** Phase inversion temperature $\bar{T}_{(PIT)}$ ($^{\circ}\text{C}$) [A] and the mean concentration ($\bar{\gamma}$) in wt% [B], for the system: Water/ EMDG/ PG/ Oil at constant $Oil/(Oil + Water)$ weight ratio, $\alpha = 50$ wt%, and variable δ (wt %). 126
- Fig. 4.52:** Phase inversion temperature $\bar{T}_{(PIT)}$ ($^{\circ}\text{C}$) [A] and the mean concentration ($\bar{\gamma}$) in wt% [B], for the system: Water/ L₁₆₉₅/ EMDG/ Oil at constant $Oil/(Oil + Water)$ weight ratio, $\alpha = 50$ wt%, and variable δ (wt %). 131
- Fig. 4.53:** Phase inversion temperature $\bar{T}_{(PIT)}$ ($^{\circ}\text{C}$) [A] and the mean concentration ($\bar{\gamma}$) in wt% [B], for the system: Water/ S₁₅₇₀/ EMDG/ Oil at constant $Oil/(Oil + Water)$ weight ratio, $\alpha = 50$ wt%, and variable δ (wt %). 134
- Fig. 4.54:** Phase diagrams of the systems: Water/ L₁₆₉₅/ EMDG/ R (+)-Limonene (A) and Water / L₁₆₉₅ / EMDG / EtOH / R (+)-Limonene (B) at 25 $^{\circ}\text{C}$. The weight ratio of L₁₆₉₅/ EMDG = 1/1 in the two systems (A), (B) and that of R (+)-Limonene/ Ethanol = 1 in the system (B). The one phase region is designated by 1ϕ , and the multiple-phase region is designated by $M\phi$. 145
- Fig. 4.55:** Phase diagrams of the systems: Water/ L₁₆₉₅/ EMDG/ R (+)-Limonene (A) and Water/ L₁₆₉₅/ EMDG/ EtOH/ R (+)-Limonene (B) at 25 $^{\circ}\text{C}$. The weight ratio of L₁₆₉₅/ EMDG = 1/3 in the two systems (A), (B) and that of R (+)-Limonene/ Ethanol = 1 in the system B. The one phase region is designated by 1ϕ , and the multiple-phase region is designated by $M\phi$. 147

- Fig. 4.56:** Phase diagrams of the systems: Water/ L₁₆₉₅/ EMDG/ IPM (A) and Water / L₁₆₉₅ / EMDG / EtOH / IPM (B) at 25°C. The weight ratio of L₁₆₉₅/ EMDG = 1/1 in the two systems (A), (B) and that of IPM/ Ethanol = 1 in the system (B). The one phase region is designated by 1 ϕ , and the multiple-phase region is designated by M ϕ 149
- Fig. 4.57:** Phase diagrams of the systems: Water/ L₁₆₉₅/ EMDG/ IPM (A) and Water/ L₁₆₉₅/ EMDG/ EtOH/ IPM (B) at 25°C. The weight ratio of L₁₆₉₅/ EMDG = 1/3 in the two systems (A), (B) and IPM/ Ethanol = 1 in the system (B). The one phase region is designated by 1 ϕ , and the multiple-phase region is designated by M ϕ . 151
- Fig. 4.58:** Phase diagram shown in Fig. 4.38.A. The \otimes are the points where we measured the electrical conductivity in the system: Water/ L₁₆₉₅/ EMDG/ IPM. At $\gamma = 31$ wt% and $\delta = 50$ wt% for variable α (wt%) and T (°C). 156
- Fig. 4.59:** Plot of κ as a function of T (°C) (A) and as a function of $Oil/(Oil + Water)$ weight ratio, α (wt %) (B) For the system: Water/ L₁₆₉₅/ EMDG/ IPM ($\gamma = 31$ wt%, $\delta = 50$ wt %) at points presented in Fig. 4.58. 157
- Fig. 4.60:** Phase diagram shown in Fig. 4.33.B. The \otimes are the points where we measured the Electrical conductivity in the system: Water/ L₁₆₉₅/ EMDG/ R (+)-limonene. At $\gamma = 31$ wt% and $\delta = 50$ wt% for variable α (wt %) and T (°C). 159
- Fig. 4.61:** Plot of κ as a function of T (°C) (A) and as a function of $Oil/(Oil + Water)$ weight ratio, α (wt %) (B) For the system: Water/ L₁₆₉₅/ EMDG/ R (+)-limonene ($\gamma = 31$ wt% and $\delta = 50$ wt%) at the points indicated in (Fig. 4.60). 161
- Fig. 4.62:** Effects of temperature and oil volume fraction (Φ or α) on the surfactant monolayer spontaneous curvature and on the surfactant oil water phase behavior for a system containing a fixed surfactant concentration. At low or zero content of oil (a) at low water content (b). At similar water and oil contents, a bicontinuous structure with a surfactant monolayer separating the water and oil domains can be stable. 163

- Fig. 4.63:** Schematic phase diagram of the system: Water/ L₁₆₉₅/ EMDG/ IPM, where the mixed surfactants content (i.e. γ) are 26 wt% in (A) and 31 wt% in (B). The EMDG ratio (i.e. δ) is 25 wt% in (A) and 50 wt% in (B). The cross filled circles \otimes are experimental points investigated by self diffusion measurements. 165
- Fig. 4.64:** Relative diffusion coefficients, D/D_0 , for the system: Water/ L₁₆₉₅/ EMDG/ IPM as a function of the weight fraction of $Oil/(Oil + Water)$, (α) for $\gamma = 31$ wt% and $\delta = 50$ wt%, where (\circ)-are the relative diffusion coefficient of the water and (Δ)-is for the oil. 168
- Fig. 4.65:** Relative diffusion coefficients, D^W/D^{W_0} , for the system: Water/ L₁₆₉₅/ EMDG/ IPM as a function of the weight fraction of $Oil/(Oil + Water)$ (α) for different surfactant and co-surfactant concentrations, (\circ) $\gamma = 31$ wt% , $\delta = 50$ wt%, and (\bullet) $\gamma = 26$ wt% , $\delta = 25$ wt%. 169
- Fig. 4.66:** Relative diffusion coefficients, D^O/D^{O_0} , for the system: Water/ L₁₆₉₅/ EMDG/ IPM as a function of the weight fraction of $Oil/(Oil + Water)$ (α) for different surfactant and co-surfactant concentrations, (\circ) $\gamma = 31$ wt% , $\delta = 50$ wt%, and (\bullet) $\gamma = 26$ wt% , $\delta = 25$ wt%. 171
- Fig. 4.67:** Hydrodynamic radius for the system: Water/ L₁₆₉₅/ EMDG/ IPM as function of $Oil/(Oil + Water)$ weight ratio, α (wt %) for ($\gamma = 31$ wt%, $\delta = 50$ wt %). 173
- Fig. 4.68:** Hydrodynamic radius for the system: Water/ L₁₆₉₅ / EMDG/ IPM as function of $Oil/(Oil + Water)$ weight ratio α (wt %) for ($\gamma = 26$ wt%, $\delta = 25$ wt %). 174
- Fig. 4.69:** Solubilization capacity (SC) curve of Diclofenac sodium along the dilution line D 60:40 at 25°C, in the system: Water/ L₁₆₉₅ + EMDG (1/1)/ R (+)-limonene. 179
- Fig. 4.70:** Solubilization capacity (SC) curve of Diclofenac sodium along the dilution line D 60:40 at 25°C, in the system: Water/ L₁₆₉₅ + EMDG (1/1)/ R (+)-limonene + EtOH (1/1). 180

Fig. 4.71: Solubilization capacity (SC) curve of Diclofenac sodium 181
along the dilution line D 60:40 at 25°C, in the system:
Water/ L₁₆₉₅ + EMDG (1/1)/ IPM.

Fig. 4.72: Solubilization capacity (SC) curve of Diclofenac sodium 182
along the dilution line D 60:40 at 25°C, in the system:
Water/ L₁₆₉₅ + EMDG (1/1)/ IPM + EtOH (1/1).

Physicochemical Behavior of Mixed Nonionic Surfactant Systems

By

Wail Damin Al-Sayyd Salah Al-Diyn

B. Sc. Chemistry / Bethlehem University / Palestine

Supervised by:

Dr. Monzer Fanun

A THESIS

**Submitted in Partial fulfillment of requirements for the degree of
Master of Applied & Industrial Technology
Department of Chemistry & Chemical Technology
Faculty of Science and Technology
Al-Quds University**

I. May, 2005

II. Introduction

Microemulsions are macroscopically homogeneous thermodynamically stable mixture of water, oil and surfactant, which on the microscopic level consist of individual domains of oil and water separated by monolayer of amphiphile (see Fig. 1.1 and 1.2). Schulman scientifically described them in 1943⁽¹⁾. The concept had appeared in the parent literature before that^(2,3).

Understanding microstructure of the microemulsion is needed for any scientific or industrial application of microemulsion, thus we find much work over the last three decades in this particular area⁽⁴⁻⁶⁾. A microemulsion has a microstructure (droplets) with small oil and water domains (approximately 100 \AA) separated by a monolayer of surfactant, also microemulsions exhibit ultra low interfacial tensions ($< 0.01 \text{ dyn cm}^{-1}$)⁽⁷⁾. The variables which affect the phase behavior and microstructure of microemulsions are the surfactant type and concentration, co-solvent type and concentration, electrolyte type and concentration, temperature and pH⁽⁸⁻¹¹⁾.

Microemulsions are of growing importance in many industries such as cosmetics, foods, pharmaceuticals, pesticides and coating materials^(12,13). Over the last 20 years the results of researches have greatly increased our knowledge of the nature of microemulsion. It gives us powerful new tools for the design of microemulsions and relation of surfactant structure to the formation of microemulsions⁽¹⁴⁾. There are many researches who relate the conditions for microemulsion formation to the formulation of stable emulsions and dispersions, and to the selection of surfactant for maximum

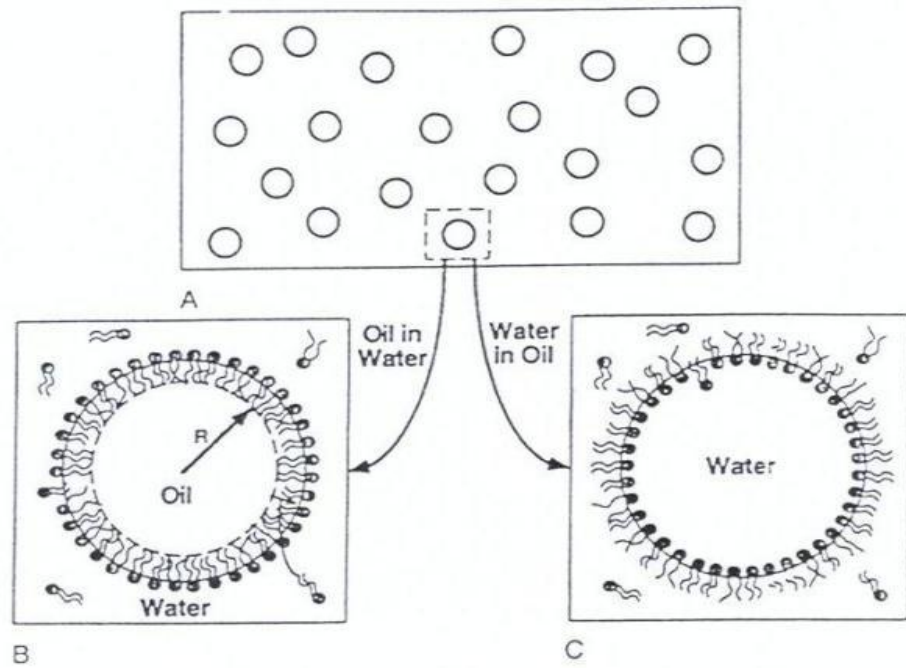


Fig. 1.1: A droplet microemulsion phase (A) can be of the O/ W (B) or the W/ O type (C). Typically, but not exclusively, the drops are nearly spherical and have a small size polydispersity ⁽¹⁵⁾.

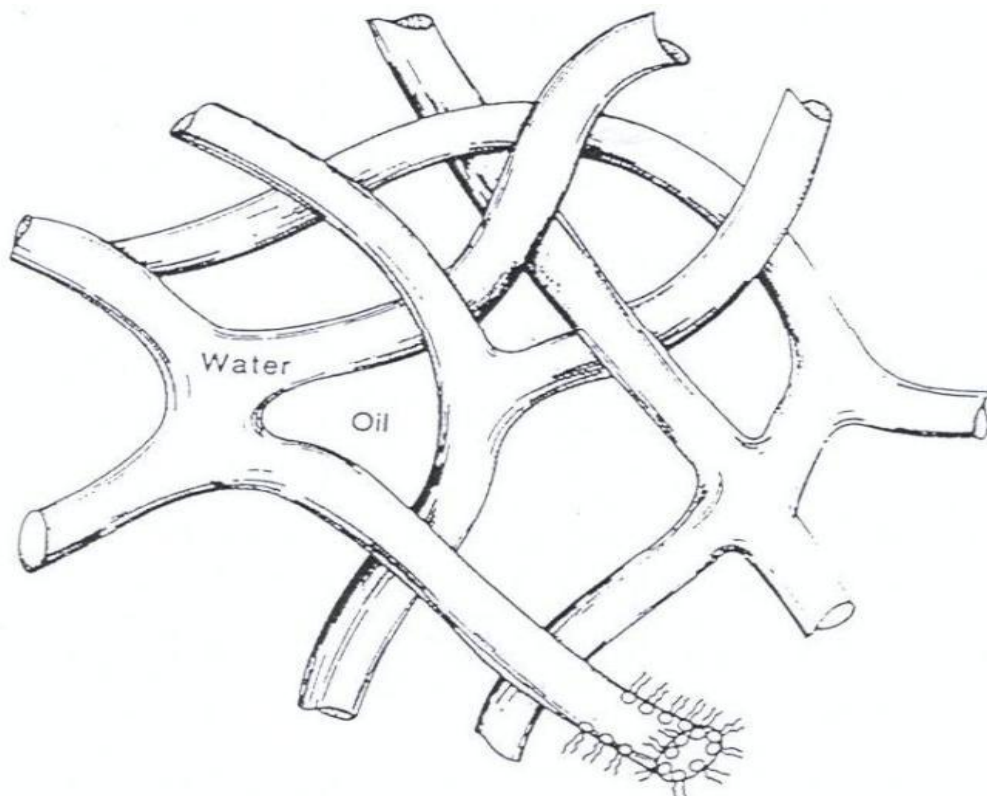


Fig. 1.2: A bicontinuous structure ⁽¹⁵⁾.

efficiency in the use of surfactants in environmental remediation and cleaning applications and to adopt tools developed for microemulsion formulation to the design of emulsions, dispersions, and cleaning systems⁽¹⁴⁾.

In his study, Per Ekwall investigated the phase equilibria in systems of water, surfactants and third components, he covered a large number of three component systems. In this study he has a solid foundation⁽¹⁶⁻¹⁸⁾. In such systems it is important to point out that there will occur a variety of structures like micelles, liquid crystals with different geometries, and reversed micelles. To understand the nature of a microemulsion it is important to understand all interrelated association structures occurring in the systems and not just to analyze the microemulsion as an isolated association phenomenon. Gunilla Gillberg ⁽¹⁹⁾ is the first one who extended these three-component systems to include a fourth component and demonstrated the identity of the W/O microemulsions according to Schulman and the inverse micellar solutions investigated by Ekwall ⁽²⁰⁾. A fifth component also can be added to the system (i.e. Salt, additive, etc).

The pioneer investigations of the phase equilibria of water, nonionic surfactant and oil is the Japanese professor Shinoda who emphasized the connection between nonionic surfactant properties and temperature ⁽²¹⁻²³⁾. For aqueous systems, Shinoda clarified the clouding, and in ternary systems he introduced the concepts of the phase inversion temperature (PIT). For a descriptive understanding of microemulsions, it is of central importance to correlate molecular properties of the surfactants, maximal solubilization and temperature (hydrophilic/lipophilic balance HLB, temperature).

Extensive theoretical and experimental work has been devoted to different kind of microemulsion systems in order to build up an

unambiguous picture of these systems with regard to structure and molecular processes. On the other hand, there has been a development of a large variety of technical application of these systems ⁽²⁴⁾.

Generally, surfactants are classified according to their structure. We can classify surfactants into ionic, zwitterionic and nonionic according to their charges or to the lack those charges. Also surfactant can be classified according to their micelle formation properties or to their swelling capacity and the concomitant mesophase formation in aqueous solutions. The balance between electrostatic or polar interactions, and geometry packing factor, topology will, at the end, by far determine the geometry of the colloidal structure formed. The monomer activity with regard to aggregation, and formation of micelles are defined by the micelle forming surfactants, the critical micelle concentration (CMC) and the Kraft point (KP) ⁽²⁵⁻²⁸⁾.

Phase behavior of nonionic amphiphiles is characterized by the change in the distribution of the amphiphile over the water-rich and oil -rich phase with the change in temperature. Upon increasing temperature the phase behavior sequence will depend on the total amphiphile concentration. At low amphiphile concentration the sequence will be: Winsor I (2) (W_m+O) → Winsor III (3) (W+D+O) → Winsor II (2) (W+O_m) (**see Fig. 1.3 and 1.4**), while at high amphiphile concentration the sequence will be: Winsor I (W_m+O) → Winsor IV (microemulsion) (1φ) → Winsor II (W+O_m). Winsor I indicates that at ambient temperature, nonionic amphiphiles are more soluble in the aqueous phase, while at high temperatures they are more soluble in the oleic phase (Winsor II).

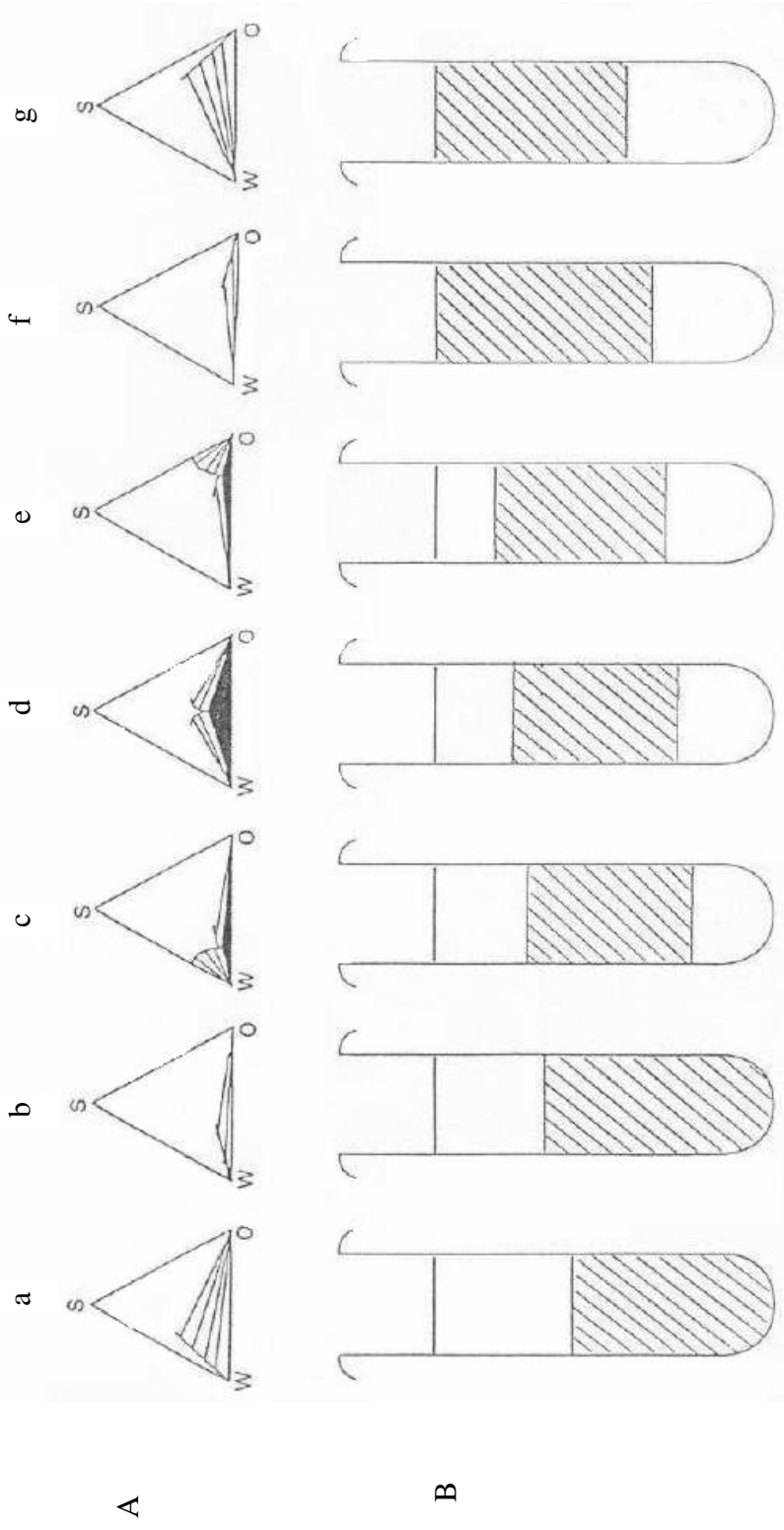


Fig. 1.3: (A) A series of phase diagrams of a ternary system transformed from Winsor I {(a) and (b)} via Winsor III {(c), (d) and (e)} to Winsor II {(f) and (g)}. The dark triangles are three-phase regions. The lines indicate the composition of the two-phase regions. S, W and O stand for surfactant, water, and oil, respectively. (B) Phase changes of a system containing equal amounts of oil and water and a given (low) amount of surfactant⁽⁶⁾.

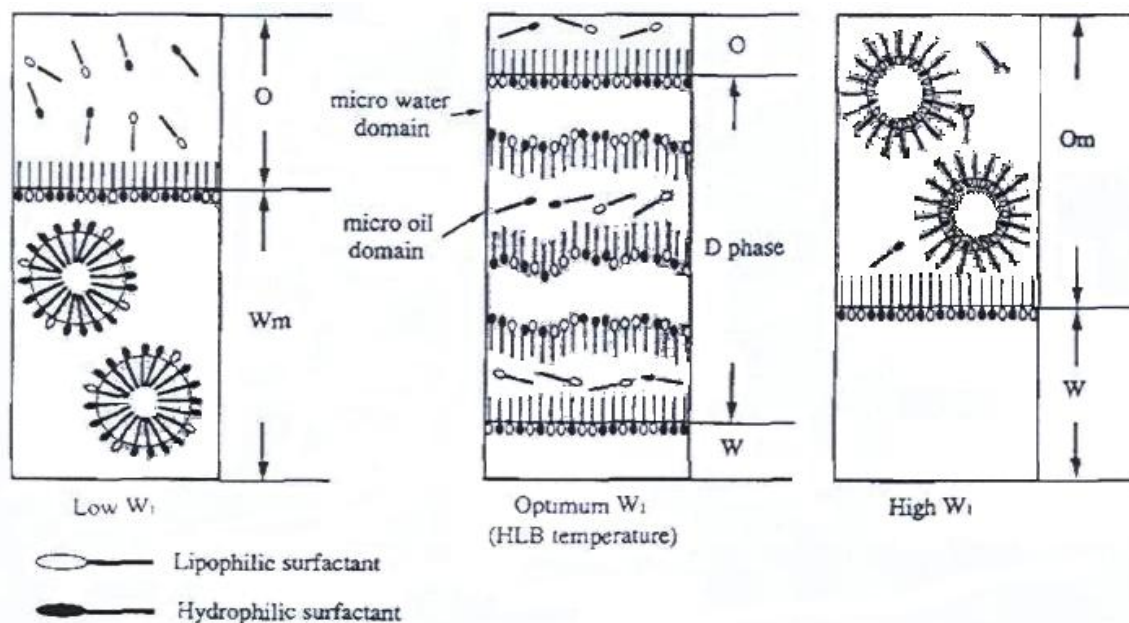


Fig. 1.4: The schematic change in phase behavior in a mixed-surfactant system. W_m and O_m are aqueous micellar and reverse micellar solution phases. W and O are excess water and oil phases. D indicates a microemulsion (surfactant) phase. W_1 is the weight fraction of lipophilic surfactant in the mixed surfactant ⁽²⁹⁾.

Within a definite temperature interval ΔT in between, the mixture may break up into three coexisting liquid phases, Winsor III, a water-rich (W , lower), amphiphile-rich (D , middle), and an oil-rich (O , upper), at sufficiently elevated amphiphile concentration, the mixture of water-oil-amphiphile becomes homogeneous (Winsor IV or microemulsion). This leads to the formation of "fish" diagrams.

The temperature related to the critical endpoint (cep_β) of the critical line extending from the critical point (cep_β at T_β) in the water-nonionic amphiphile mixture and the temperature related to the critical endpoint (cep_α) of the critical line extending from the critical point (cep_α at T_α) in the oil-nonionic amphiphile binary mixture; are the most significant properties concerned in determining the temperature range of the three-phase body, and hence the Winsor I \rightarrow Winsor III \rightarrow Winsor II phase progression is

developed see (Fig. 1.5). It is impossible at specific conditions for extreme values of T_α or T_β (or both) to produce a homogeneous mixture of water-oil-amphiphile. Therefore, knowledge of T_α and T_β is decisive for choosing amphiphiles and forming microemulsions within a particular temperature range.

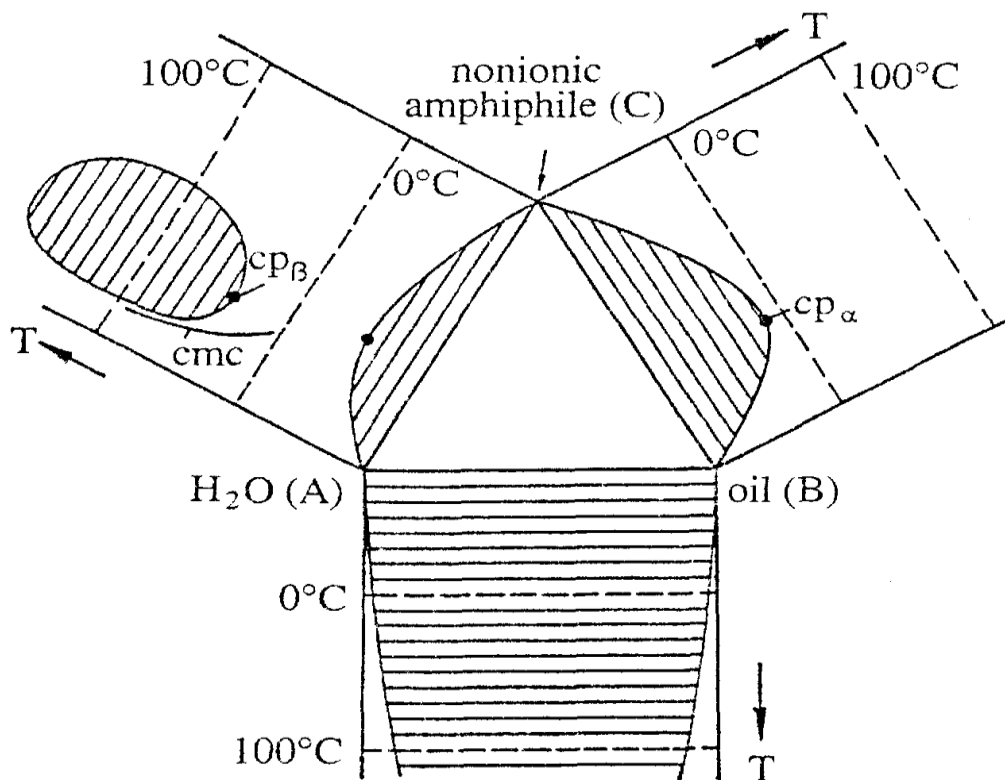


Fig. 1.5: A schematic view of the "unfolded" phase prism highlighting the three relevant binary phase diagrams (redrawn from Kahlweit et al. ⁽³⁰⁾). The most important features are the upper critical point on the oil-surfactant binary diagram, cp_α (which occurs at the temperature T_α), and the lower critical point on the water-surfactant binary diagram, cp_β (which occurs at the temperature T_β)

The formation of three liquid equilibrium phase is the consequence of the inversion of the distribution of the amphiphile over two solvents. For A-

B-C (Water/ Oil/ Surfactant) mixtures raising temperatures eventually enforces a separation of the lower aqueous phase at the critical end point , cep_{β} , into a water-rich phase and an amphiphile-rich phase, which leads to the formation of isothermal three-phase triangle within the central miscibility gap.

With a further increase of temperature, the amphiphile-rich phase moves on an ascending trajectory around the surface of the body of heterogeneous phases to the oil-rich phase.

The three-phase body thus appears at T_1 at the lower cep_{β} on the water rich side and disappears at T_u at the upper cep_{α} on the oil rich side. In the three-phase temperature interval

$$\Delta T = T_u - T_1 \quad (1)$$

and $\bar{T}_{(PIT)} = (T_1 + T_u) / 2 \quad (2)$

the isothermal three-phase triangle changes its shape, and so the amphiphile rich phase moves clock wise from cep_{β} to cep_{α} ⁽³¹⁾ (see Fig. 1.6).

Conceptually, the critical line around the central gap can be looked at as an elastic spring, ⁽³²⁾ the upper part of which, on the water-rich side, is fixed by the (lurking) nose of the H₂O-surfactant system, whereas its lower end, on the oil-rich side, is fixed by the upper critical point of the oil-surfactant gap. Consequently, if for a given surfactant one increases the hydrophobicity of the oil; one expects the inflection point to rise temperature wise. Simultaneously, the tangent to the inflection point will become increasingly more horizontal, indicating the increasing "bending tension" of the critical line. If one increases the hydrophobicity of the oil further, the critical line will eventually break at a tricritical point, which then gives rise to a three-phase body within the prism.

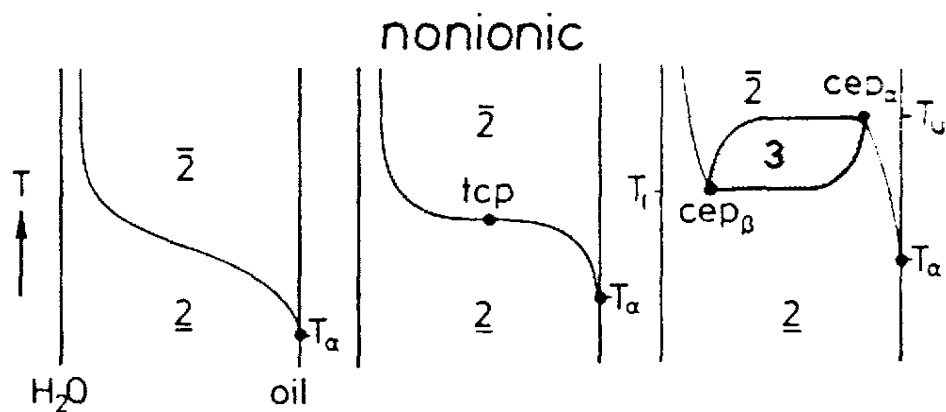


Fig. 1.6: Formation of a three-phase body with nonionic amphiphiles by breaking the connected critical line at a tricritical point (tcp) by increasing the carbon number of the oil ⁽³³⁾.

Close to the tricritical point, the end points of the two critical lines, cep_α and cep_β , are still close to each other. Accordingly, the three-phase triangle is small, being located close to the boundary of the central gap. The more hydrophobic the oil, the further the two end points move apart, cep_α moving toward the oil corner, cep_β toward the H₂O corner. Accordingly, the three-phase body becomes increasingly large, and the three-phase temperature interval increasingly wide.

Considering first single-tailed nonionic amphiphiles, the hydrophobic interaction between their head groups and water makes their lower miscibility gap lie, in general, below the melting point. At ambient temperatures, water and nonionic amphiphiles are thus completely miscible. With rising temperature, however, water becomes an increasingly poorer solvent for nonionic amphiphiles, which makes the miscibility gap reappear at elevated temperatures at a lower critical point (cep_β) that plays an important role in the phase behavior of ternary A-B-C mixtures. This upper

gap is, again for thermodynamic reasons, a "closed loop". For a given head group, the composition of cep_{β} moves toward the water-rich side with increasing carbon number of the tail. The critical temperature T_{β} rises with increasing hydrophilicity of the head (for a given tail), but drops, with increasing carbon number of the tail (for a given head).

In the same sequence, the" extension of the central gap as well as the (relative) area covered by the three-phase triangle within that gap shrinks as, with given surfactant, one proceeds from one oil to the next less hydrophobic homologue, the area covered by the three-phase triangle shrinks and moves close to the boundary of the central gap, as a consequence of the fact that the end points of cep_{α} and cep_{β} increasingly approach each other. If one could change the properties of the oils continuously, one could, accordingly, imagine a system in which the three-phase triangle reduces to a point on the boundary of the central gap, i.e., in which the two critical lines cep_{α} and cep_{β} merge. Such a point is called the "tricritical point", because" three coexisting fluid phases simultaneously become identical as some appropriate thermodynamic variable is altered"⁽³⁴⁾. In this case the chemical potential of the oil. Accordingly, the interfacial tensions between the three phases, including between the aqueous and the oil phase, decrease as one approaches the tricritical point to, finally, vanish simultaneously.

Factors determining the phase behavior of the ternary mixture Water/ Amphiphile/ Oil be changed by the effective carbon number of the oil, the hydrophilicity of head group, or the lipophilic tail of the amphiphile .

Considering first changing the effective carbon number of the oil for a given surfactant, increase the chain length of the oil or its nature will rise T_{α} , this decreases the tendency of nonionic amphiphile to leave the water-

rich phase for the oil-rich phase as T raises, accordingly, \bar{T} rises with nonionic amphiphiles with rising the effective chain length of oils.

The width on the temperature scale of the three-phase region narrows as one proceeds from an oil to the next less hydrophobic homologue until it disappears for the lower hydrophobic one.

If we now consider the effect of varying the hydrophobicity of the amphiphile which can be made by changing the effective carbon number of its tail for a given head group or by changing the nature of the head group and the nature of the hydrophobic part. This affects both T_α and T_β . With nonionic amphiphiles both T_α and T_β drop with increasing the hydrophobicity of the amphiphile which makes $\bar{T}_{(PII)}$ drops.

Considering now the effect of adding a fourth component to the Water/ Amphiphile/ Oil mixture. In our case the fourth component can be alcohols or alcohol substitutes or another amphiphile.

Alcohols is distributed over the water-rich and the oil-rich phase. Adding an alcohol affects both the water-amphiphile and oil-amphiphile diagram. Their distribution coefficient depends weakly on temperature, but sensitively on their carbon number and on the chain length of the oils.

Adding short chain alcohols that is completely miscible in water increases the mutual solubility between water and amphiphile, this is equivalent to decreasing the hydrophobicity of the amphiphile. Increasing the concentration of a short chain alcohol, thus, makes \bar{T} rises with nonionic amphiphiles. Adding medium and long chain alcohols makes \bar{T} drops with nonionic amphiphiles.

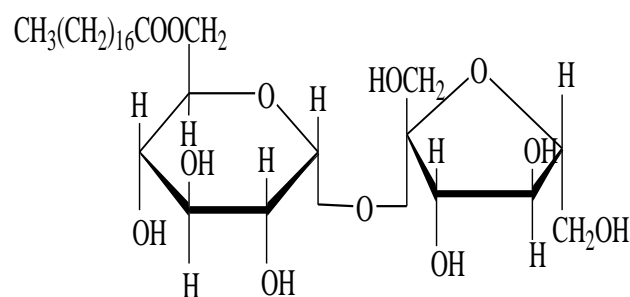
Considering finally the effect of adding a second amphiphile to the mixture of Water/ Amphiphile/ Oil. If the added amphiphile is more

hydrophilic amphiphile than the first one originally presented in the mixture this will increase the hydrophilicity of the amphiphile mixture and thus \bar{T} rises. If it is less hydrophilic, \bar{T} drops.

The efficiency of surfactant which is the minimum amount of surfactant needed to solubilize equal weights of oil and water, is defined as, $(\bar{\gamma})$ ⁽³⁵⁾. The efficiency depends on the nature of the amphiphile, and on that of the oil and, in particular, on temperature, reaching its maximum in the three-phase temperature interval. Close to the mean temperature \bar{T} one finds the highest efficiency of the amphiphile with respect to homogenizing equal masses of water and oil, and a minimum of interfacial tension between the water and the oil.

Phase transitions will also occur without any addition of a solubilizate (i.e. Salt), mainly due to the packing of and the interaction between the aggregates when the concentration of the surfactant monomer is gradually increased. The structure change in this last phase transition is not a consequence of the packing ratio from the molecular surfactant structure, but a result of structure changes due to intermicellar interaction⁽²⁴⁾.

The possibilities of using sucrose as a raw material in the chemical industry have excited interest because sucrose is an inexpensive raw material, and fatty acids or fats, also inexpensive raw materials to form sucrose fatty acid esters^(36,37). Sucrose has 8 free hydroxyl groups that can be esterified (**Scheme 1**). If most of them are esterified, the products will be very hydrophobic, with good solubility in oil, but partial esterification will yield sucrose esters with amphiphilic properties. Sucrose fatty acid esters (mono-di-and triesters of sucrose) may be used as emulsifiers in foods and in other applications (cosmetics, detergents, etc).



Scheme 1: Chemical structure of Sucrose monostearate.

Numerous attempts have been made in the last 50 years to manufacture these esters in a simple and inexpensive way. However, the heat sensitivity of sucrose, high activation energy of the esterification process and the difference in hydrophilicity/ hydrophobicity of the two components, make this process difficult to achieve⁽³⁸⁾.

Sugar esters in general and sucrose esters in particular, are available in a wide range of different hydrophile/ lipophile balances⁽³⁹⁾.

Several papers have been written over the years on topics such as manufacture, structure, hydrophile/ lipophile balance, emulsifying properties, solubility stability, interaction with starch and interaction with proteins, crystallization retardation on sucrose and detergency. Many possible food applications have been considered including ice cream, coffee whiteners, mousse products imitation whipped cream, bread, bakery products, fondants and margarines. In addition, many cosmetic, detergency, cleaning and pharmaceutical applications have been studied. Because of high prices and Legislation restrictions, sucrose-ester products have limited application⁽³⁹⁾.

Lately, studies on sucrose-esters derived from other mono-di-or oligomeric sucrose, and used as emulsifiers, have been made⁽⁴⁰⁾.

Hundreds of applications in which sucrose esters are used in combination with other emulsifiers, organic acids, proteins, carbohydrates, etc. have been described in patents ⁽⁴¹⁻⁴³⁾ and literature ⁽⁴⁴⁻⁴⁹⁾. Hundreds of papers have been written on polyesters of sucrose and sweeteners, sucrose less fat and fatless sucrose for nutritional, health diet, nutraceutical and other related applications ⁽⁵⁰⁻⁶⁵⁾.

The emulsification properties of sucrose-esters are somewhat unique, since almost any hydrophilic-lipophilic balance can be obtained, and since the sucrose esters don't change their HLB balance with temperature (unlike the ethoxylated derivatives). Commercial sucrose ester, which is a complex mixture of various internal compositions of different chain-lengths of fatty acids, mono-, di-, tri-, or polysubstitutions on the hydroxyl groups, free fats or fatty acids, etc ⁽³⁹⁾.

The complex structure might influence the emulsification properties, and might have some effect on the reproducibility of the results in many of the applications, and will have very pronounced effects on the self-aggregation of these esters in water or in oil ⁽³⁹⁾.

The solubility of sucrose esters in many classes of oils is very low and consequently, T_{α} is exceptionally high, requiring the use of a co-surfactant to augment sucrose esters oil solubility, and create microemulsions in water-oil-sucrose ester mixtures. Numerous groups ⁽⁶⁶⁻⁷¹⁾ have explored this approach and studied the phase behavior and properties of water-oil - Sucrose esters-co-surfactant microemulsions. It was found that sucrose esters in the presence of $C_2 - C_8$ alcohols as co-surfactants can form microemulsions used for pharmaceutical and food applications. Non-toxic co-surfactants for pharmaceutical purposes also have been used to make sucrose ester microemulsions. In this research, we substituted alcohol by

1,2-propanediol (propylene glycol, (PG)) which shows to be efficient substitute .

In this study we evaluate the effect of adding propylene glycol (1,2-propane diol) (PG) to the mixture water/ Sucrose Esters/ Oil on the phase behavior of the system. Some surfactant molecules are known to self-assemble in polar organic solvents like propylene glycol (1,2-propanediol) glycerol, and formamide ^(72,73) . PG is one of the least hydrophilic simple polyols. These solvents like water, form hydrogen bonds, have relatively high dielectric constants and are immiscible with hydrocarbon solvents, ⁽⁷⁴⁾ and sometimes they are used as water substitutes. Critical micelle concentrations are higher in polar nonaqueous solvents than in water ^(75,76). Adding polyols to the surfactant mixture will decrease the polarity and the freezing point of water. For these reasons, some water-soluble polyols such as propylene glycol (1,2-propanediol) and glycerol protect biological systems from massive ice crystallization ⁽⁷⁷⁻⁷⁹⁾.

Also we investigated the addition of ethoxylated type nonionic surfactant which is ethoxylated mono diglyceride. Ethoxylated Mono\Diglyceride, The (EMDG) (MAZOL 80 MG KOSHER) is a mixture of stearate and palmitate partial esters of glycerin ethoxylated with approximately 20 moles of ethylene oxide per mole of alpha-monoglyceride reaction mixture.

The oils used were caprylic/capric triglyceride (MCT), isopropylmyristate (IPM) and (R (+)-limonene). MCT are used mainly because they are fully saturated and "oxidation-free" oil and, therefore, it is considered to be "safe oil" and is widely used in food formulations. IPM is used in many pharmaceutical formulations owing its compatibility with biological systems and is expected to be environment friendly ⁽⁸⁰⁾. The

monoterpene hydrocarbon R (+)-limonene is a unique and interesting solvent (the major constituent of citrus essential oils, lipophilic perfume constituent) that is present in several natural products. R (+)-limonene is often used in foods, cosmetics, and coating materials. R (+)-Limonene is essentially insoluble in water and requires addition of a surfactant to be solubilized or emulsified in water ⁽⁸¹⁾. R (+)-Limonene is used in the preparation of cloudy macroemulsions for beverages. Citrus essential oils are also used in some “green” cleaning formulations and known to have powerful detergency abilities (solubilization) ^(81,82).

The development of microemulsion with specific properties like high solubilization power and temperature insensitivity was focused in many researches in the past. But the most basic studies on microemulsions have been conducted with standard surfactants, such as polyoxyethylene- type nonionic surfactants, alkyl sulfates, quaternary ammonium salts and dialkyl sulfosuccinate that are not permitted in food systems (health restrictions), so it is important to search for new surfactants for the preparation of microemulsions. On the other hand the food-grade surfactants are limited in their number and structure. The mono and diglycerides of fatty acids, sorbitan esters, polyglycerol esters, such as polyglycerol polyricinoleate (PGPR), and sucrose ester (sucrose polystearate) are hydrophobic surfactants, where's the ethoxylated sorbitan esters, polyglycerol esters, sodium stearyl lactylate and sucrose esters are hydrophilic surfactants. And all of these are food grade compounds ⁽³⁹⁾.

The nonionic microemulsions have higher potential for many applications, so we concentrated our efforts on studying and developing new microemulsion based on water-nonionic surfactant-oil, and co-

emulsifier (short chain of alcohol; i.e. ethanol and PG), where all components of our microemulsion are safe for general use ^(83,84).

CHAPTER TWO

OBJECTIVES

II.1 Objectives

Food, cosmetics, and pharmaceutical formulations are very complicated multi-component dispersed systems; where proteins, polysaccharides and fats are dispersed in an aqueous phase in a very complex way. This complexity, precisely, stands in the way of innovation. The trend in systems, today, is to bring new ideas into the area of functional food (introducing functional, health and nutrition additives to existing products) and to obtain functional food with additional health or nutritional values.

In our laboratory at Al-Quds University, we are working on subjects related to the introduction of functional additives to food systems, using microemulsions as carriers for the entrapment and controlled minerals, mostly for the consumption of babies and elderly people.

The unique properties of food grade microemulsions based on surfactants including sucrose ester, ethoxylated mono diglyceride, etc, might find application in systems requiring solubilization of food ingredients and monitoring of chemical reactions carried out in microemulsions serving as microreactors. To the best of our knowledge, this work is supposed to be the first work that will try to increase our understanding of the structure and stability of these systems. In order to accomplish this objective, we fixed the aims of this research project in the following points:

- Study of the phase behavior of mixed nonionic food and pharmaceutical grade surfactants, co-surfactant, co-solvents and vegetable oils as the oil phase in order to determine the regions of microemulsion phase. This is accomplished by the investigation of

ternary and quaternary phase diagrams, "fish" and χ cuts.

- Evaluation of the water solubilization capacity of the prepared microemulsion systems.
- Exploring the microstructures of the formed microemulsions, Pulsed gradient spin echo (PGSE) nuclear magnetic resonance (NMR), and electrical conductivity. These techniques will be used to study how changes in the relative amounts of the surfactant and in the chain length of the surfactant or oil, the presence of co-surfactant and the addition of water that influence the microemulsions micro-structure within the one-phase region.
- Solubilization of food or pharmaceutical active ingredients in the dispersed phase of the microemulsions, introducing the solubilize containing microemulsions in new pharmaceutical formulations and find a correlation between the microstructure of microemulsions and the quantity of solubilized materials.
- Developing new food or pharmaceutical products containing the formulated microemulsions.

This work will open new avenues in the field of food, cosmetic and pharmaceutical dispersions. The new inventions will definitely contribute to future development of new, functional products that will be healthier.

CHAPTER THREE

MATERIALS and METHODS

III.1 Materials

III.1.1 Surfactant (surface active agent)

The sucrose esters (sucrose alkanoates) where it is produced by a reaction between sucrose and fatty acids. There is a mono-, di- or poly substitution on the sucrose (**Scheme 1**). These surfactants are food grade and were obtained from Mitsubishi Kasei food Corp, (Mie, Japan).

Table 3.1: Type and composition of sucrose esters used in this research project ⁽⁸⁵⁾.

Type	HLB	Purity of combined fatty acids %	Ester composition %			Melting Point(°C)	
			Monoester	Di, tri and polyester	start point	Peak point	
S ₁₅₇₀	15	Stearic 70	70	30	49	56	
L ₁₆₉₅	16	Lauric 95	80	20	35	47	

Ethoxylated Mono\Diglyceride, The (EMDG) (MAZOL 80 MG KOSHER) is a mixture of stearate and palmitate partial esters of glycerin ethoxylated with approximately 20 moles of ethylene oxide per mole of alpha-monoglyceride reaction mixture. It is a pale yellow oily liquid or semi gel that has a faint characteristic odor and mild taste.

Approved for many direct foods additive applications. The principal uses-Emulsifier in pan release aids, cake and cake mixes icing and icing mixes, frozen conditioner in yeast leavened backing products.

Specifications of EMDG:

Acid Value, mg KOH/g.....	2.0 Max.
Saponification Value, mg KOH/g.....	65.0 – 75.0
Hydroxyl Value, mg KOH/g.....	65.0 – 80.0
Form 25°C.....	amber liquid
POE, % Anhydrous Basis.....	60.5 – 65.0
1, 4 Dioxane, ppm.....	1.0 Max.
Color, Gardner.....	2.0 Max.
Water, %.....	1.0 Max.
Iodine Value, %.....	2.0 Max.
In water	soluble

This surfactant is food grade and was obtained from BASF Corporation, (Gurnee, Illinois, USA).

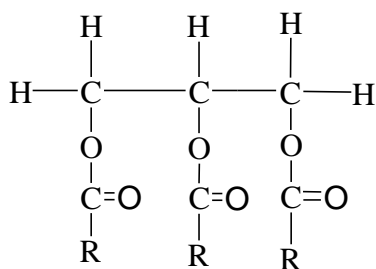
III.1.2 Oils

- Caprylic/capric triglyceride (MCT) "Neobee M5" a food grade triglyceride containing 60 wt% C_7 and 40 wt% C_9 , was obtained from Stepan Europe (Vorepe, France) (**Scheme 2-a**).

- Isopropyl myristate (98%) (IPM) was purchased from Sigma-Aldrich Chemie GmbH, Riedel Germany (**Scheme 2-b**).

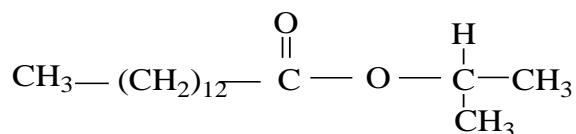
- R (+)-limonene (98%) was purchased from Fluka Chemie GmbH (**Scheme 2-c**).

a-

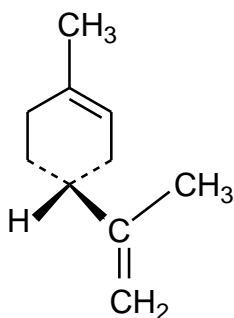


$R = 66\% C_7H_{15}$ and $34\% C_9H_{19}$

b-



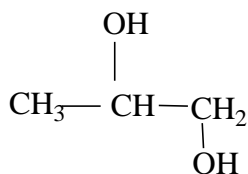
c-



Scheme 2: Chemical structure of MCT (a) ⁽⁸⁶⁾, IPM(b) and R(+)-limonene(c).

III.1.3 Co-surfactant and Co-solvents

The co-surfactant used is 1,2-Propanediol (Propylene glycol, PG) ($\geq 99.5\%$) was purchased from BDH (poole, UK) (see **Scheme 3 for chemical structure**). The co-solvent is absolute ethanol (minimum 99.8%) was obtained from Frutarom (Haifa, Israel).



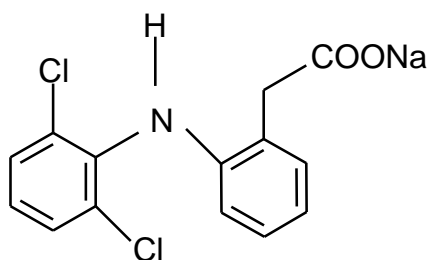
Scheme 3: Chemical structure of 1,2-Propanediol (propylene glycol, PG)

III.1.4 Water

Water was double distilled.

III.1.5 Solubilization materials

Sodium diclofenac contains not less than 99.0% and not more than equivalent of 101.0% of sodium [2-[(2,6-dichlorophenyl) amino] phenyl] acetate, calculated with reference to the dried substance (**scheme 4**)⁽⁸⁷⁾. Was obtained from Marsing and Co. Ltd. Denmark.



Scheme 4: Chemical structure of Diclofenac sodium ($C_{14}H_{10}Cl_2NNaO_2$).

III.1.6 Others

Sodium chloride of analytical grade was purchased from J.T. Baker Inc. (Phillipsburg, USA).

III.2 Methods

III.2.1 Phase Behavior Determination

III.2.1.1 Samples preparation for temperature dependant phase behavior.

Various amounts of water, oil, surfactant, and co-surfactant were sealed in ampoules. A series of ampoules sealed by Benson burner and kept in a thermostat were well shaken and left at constant temperature ($\pm 0.05\text{ C}^\circ$) for one to two days depending on the stability of emulsions. Phase equilibrium was determined by visual observation.

III.2.1.2 Temperature dependent phase behavior determination

The method introduced by Kahlweit and co-worker^(30,31,35,88), Fanun et al.⁽⁸⁹⁻⁹⁶⁾, Rayan et al.^(97,98) for ternary, pseudoternary and quaternary phase diagram for the mixtures of (A) water, (B) oil, (C) surfactant, and (D)co-surfactant⁽⁹⁷⁾. The phase behavior of these mixtures depends on five independent variables, pressure (P), temperature (T), and three mass fractions⁽⁹⁸⁾.

The pressure effect is weak so it's turned out while the effect of temperature is strong and it's important experimental parameter⁽³⁰⁾.

The ternary system at constant pressure has three independent variable⁽³⁰⁾, the temperature (T), the mass fraction of oil in the mixture of water and oil, α , defined as:

$$\alpha = \frac{B \times 100}{A + B} \quad \text{In wt \%} \quad (3)$$

And the mass fraction of surfactant in the whole mixture, γ , defined as:

$$\gamma = \frac{C \times 100}{A + B + C} \quad \text{In wt \%} \quad (4)^{(30,97,99)}$$

And in quaternary mixture which mean that two surfactants are used, the mass ratio of surfactants in the mixture, δ , defined as

$$\delta = \frac{D \times 100}{C + D} \quad \text{In wt \%} \quad (5)$$

For a ternary mixture, $\delta = 0$. At constant pressure two-dimensional phase space representation can be made by varying two of the defining variables, the phase behavior can be read as a function of temperature against one composition variable, with all others being held constant(see Fig. 3.1).

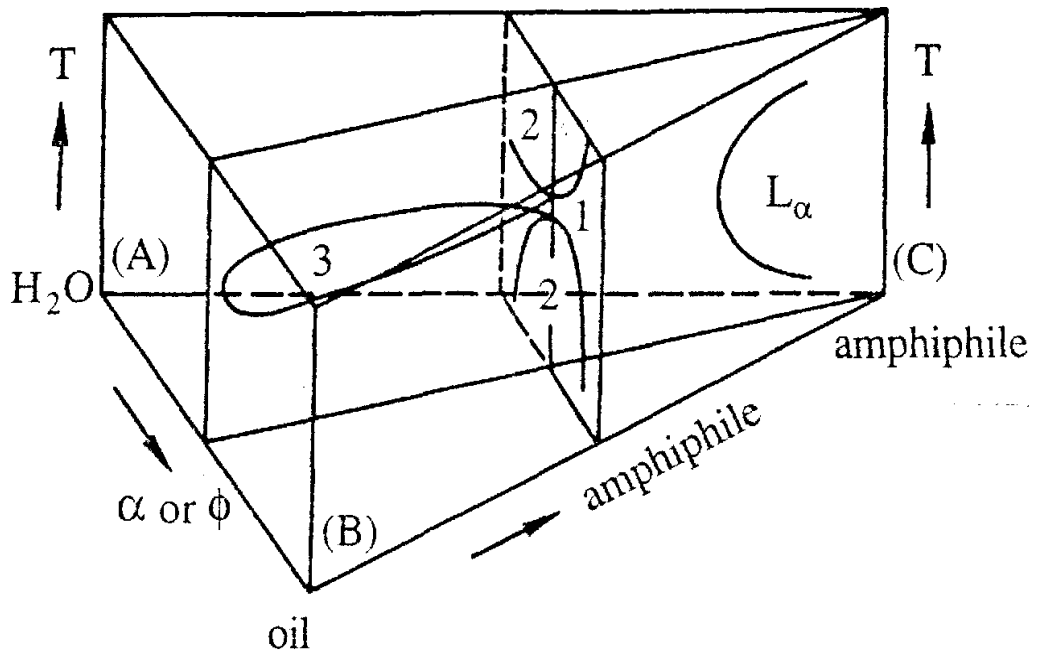


Fig. 3.1: Schematic phase prism in temperature-composition space (redrawn from Kahlweit et al. ⁽¹⁰⁰⁾) showing the two vertical sections at either constant values of the oil fraction α , or at constant surfactant concentration γ . The lamellar phase L_α also is shown at high surfactant concentrations.

When studying microemulsion phase behavior there are several sections through the phase prism have been shown ⁽⁹⁸⁾. One section is a section containing equal masses of oil and water ($\alpha = 50\%$) as a function of temperature and surfactant concentration, which allows to determine the efficiency of surfactant which is the minimum amount of surfactant necessary to completely solubilized equal weights of oil and water, denoted by, $(\bar{\gamma})$ and the phase inversion temperature (PIT) of the three phase body for a given oil (**see Fig. 3.2**) ^(35,97). There is another section where the surfactant concentration is constant as a function of temperature and oil shows the ability of the surfactant to solubilize oil in water (low α) and water in oil (high α), the phase prism were determined within $0.05 \pm C$. There is also another section where the ($\alpha = 50\%$) and temperature is constant as a function of the surfactant ratio (δ), which shows the evaluation of the one-phase microemulsion region and the phase body as the surfactant ratio are changed, the phase boundaries were determined within 1 wt%. These sections are used to describe the phase behavior of the quaternary mixture⁽⁹⁸⁾.

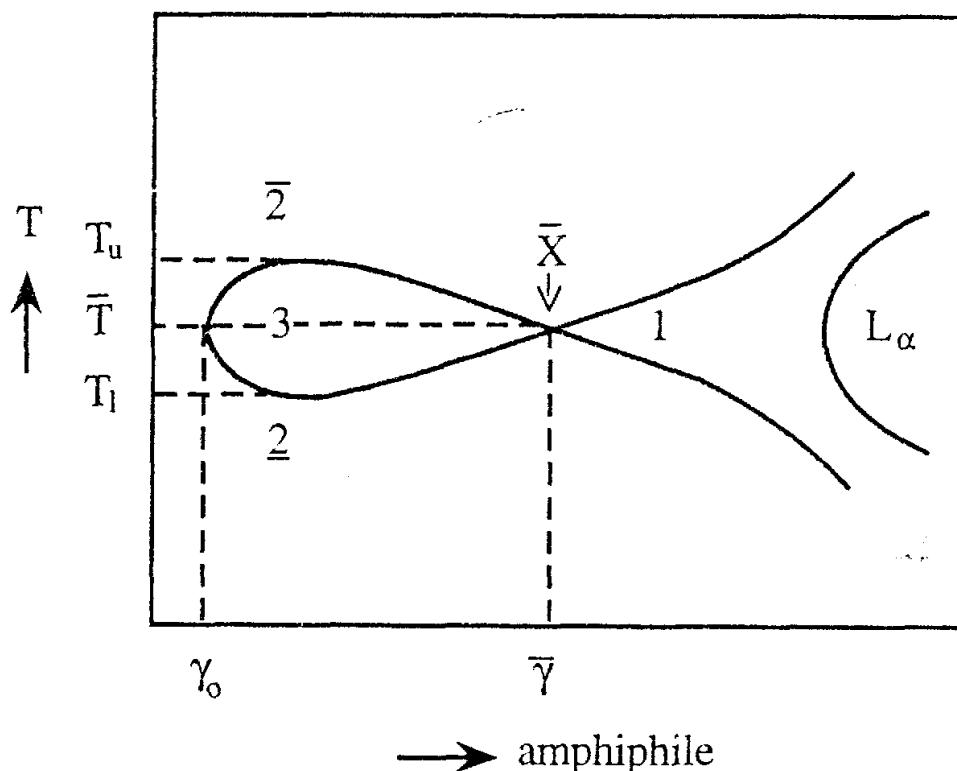


Fig. 3.2: The pseudobinary phase diagram at $\alpha = 50$ wt% as a function of temperature and surfactant concentration, γ is the minimum surfactant concentration needed to make a single phase containing equal amounts of oil and water, and is a measure of the efficiency of the surfactant. γ_0 marks the lowest possible surfactant concentration where three liquid phases form. The temperatures T_l and T_u are the temperature boundaries of the three-phase region. The phase boundaries trace the shape of a "fish". Redrawn from Kahlweit et al. ⁽¹⁰⁰⁾.

III.2.1.3 Sample preparation for pseudoternary phase diagram at constant temperature

The behavior of a four-component system is described on pseudoternary phase diagrams in which the weight ratio of two components was fixed. Usually, the oil/ alcohol weight ratio was held constant at 1:1 when alcohol is present in the system. The construction

of the phase diagram was conducted in a thermostatic bath ($25 \pm 0.2^\circ\text{C}$). Ten weighted samples composed of mixtures of surfactant, alcohol (cosurfactant), and oil were prepared in culture tubes sealed with viton-lined screw caps at predetermined weight ratios of (alcohol + oil) to surfactant. These mixtures were titrated with water. These aqueous mixtures are samples along water dilution lines drawn to the water apex from the opposite side of the triangle. In all of the samples tested, evaporative loss was negligible. Nearly all samples were equilibrated during a time interval of up to 24 h. The tubes were then inspected visually. Appearance of turbidity was considered as an indication for phase separation. The phase behavior of such samples was determined only after sharp interfaces had become visible. The completion of this process was hastened by centrifuging the samples. Every sample that remained transparent and homogeneous after vigorous vortexing was considered as belonging to a monophasic area in the phase diagram⁽¹⁰¹⁻¹⁰⁴⁾.

III.2.1.4 Solubilization Parameters.

The goal of our work was to incorporate a large amount of water into the microemulsion. Thus, the water solubilization was estimated as the monophasic area of the relevant phase diagrams. It is well documented that the water solubilization capacity of different amphiphilic systems should be strictly compared at optimal solubilization capacity⁽¹⁰⁵⁾. Because the maximum solubilization of water appears some on different water dilution lines (a line in the phase diagram beginning with a mixture of alcohol, oil, and surfactant at a fixed ratio, which is diluted with water), it is common to

list the maximum solubilization of water (W_m) on the dilution line in which maximum solubilization was obtained. The problem of comparing W_m values that lie on different dilution lines was discussed in previous papers⁽¹⁰¹⁻¹⁰³⁾. In our systems W_m values lie, within experimental error, on virtually the same specific dilution line^(103,106), and therefore we feel that the comparison between the W_m values is a proper way of estimating the maximum solubilization (see Fig. 3.3).

Li et al.⁽¹⁰⁷⁾ have employed as a solubilization parameter, the total monophasic area. It is the sum of the five cross-sectional area in the tetrahedral phase diagram, each with a different oil/ surfactant ratio. We will call this area A_T . The relative error in determining the A_T and W_m (wt%) was estimated to be $\pm 0.5\%$ for all systems studied. In our comparative studies we used both the A_T and W_m (wt%) values.

III.2.2 Active Ingredients Solubilization Evaluation

Free food or pharmaceutical active ingredient can be added to a ready-made microemulsion composed of oil, surfactant, co-surfactant or co-solvent and water. The mixture, which includes the food or pharmaceutical active ingredients, is heated to 80°C for 30 min. the samples once transparent, are cooled and stored at 25°C. Samples that remained transparent for at least 5 days will be considered to be microemulsions.

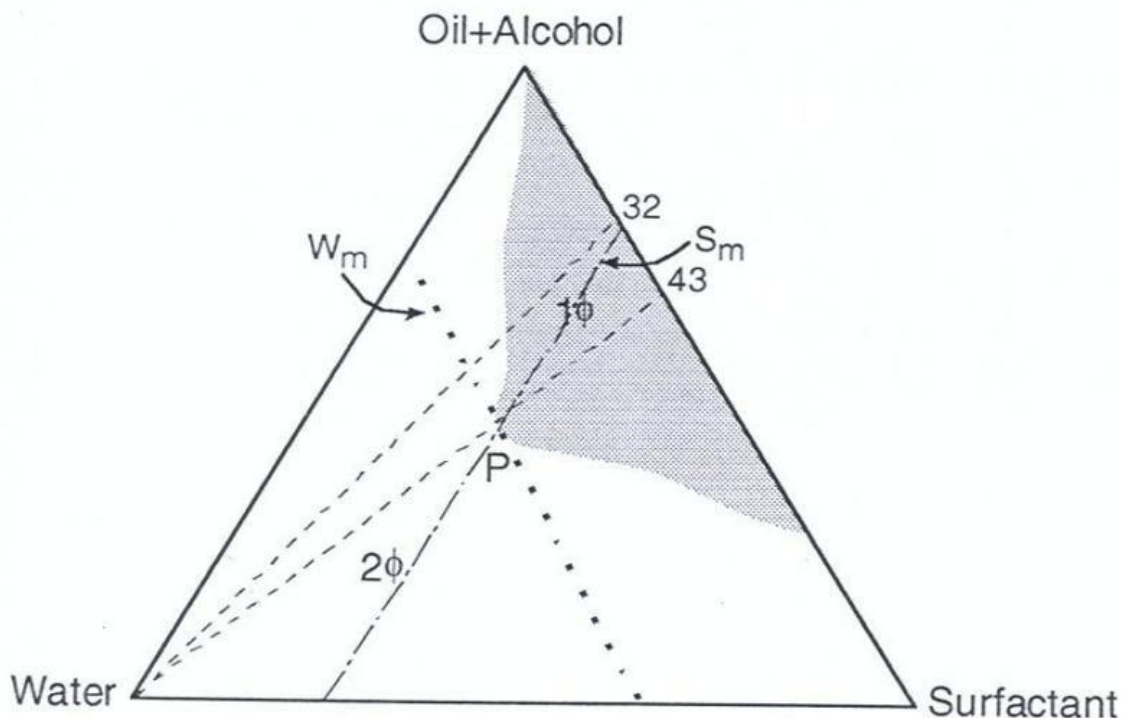


Fig. 3.3: Solubilization parameters for a schematic phase diagram. The weight ratio alcohol/ oil is 1/ 1, 1ϕ (L_2) is the area the W/ O microemulsion (one phase region), 2ϕ is the area two phase region. W_m is the maximum amount of solubilized water, S_m is the amount of surfactant needed to obtain maximum solubilization, and P is a point on the boundary of the monophasic area at which the water content reaches maximum ⁽⁹⁵⁾. 32 and 43 are dilution lines where the initial surfactant concentrations are 32 and 43 wt%, respectively.

III.2.3 Electrical Conductivity Measurements

Electrical conductivity of isotropic phases was measured with a conductivity meter, a model TetraCon® 325. For electrical conductivity measurements all microemulsions were made using a 0.05 M aqueous solution of NaCl. The electrode was dipped in the microemulsion sample until an equilibrium was reached and reading become stable.

III.2.4 Pulsed Gradient Spin Echo (PGSE) Nuclear Magnetic Resonance (NMR)

NMR measurements can be performed on Bruker DRX-400 spectrometer with a BGU II ⁽¹⁰⁸⁾ gradient amplifier unit and a 5-mm BBI probe equipped with a z-gradient coil, providing a z-gradient strength (g) of up to 55 G cm⁻¹. The self-diffusion coefficients were determined using bipolar-pulsed field gradient stimulated spin-echo (BPFG-SSE). In this work we used bipolar gradient pulses as described by Wu et al. ⁽¹⁰⁸⁾ to reduce the eddy-current effects.

Experiments were carried out by varying the gradient strength and keeping all other timing parameters constant. The self-diffusion coefficient (D) is given by

$$I = \frac{I_0}{2} e^{-R(t) - (\gamma G \delta)^2 D (\Delta - (\delta/3))} \quad (6)$$

where I is the measured signal intensity, I_0 is the signal intensity for $g = 0$, γ is the gyromagnetic ratio for the ¹H nucleus, δ is the gradient pulse length, Δ is the time between the two gradients in the pulse sequence (and hence defines the diffusion time), and $R(t)$ is a constant that takes into account nuclear relaxation. Since in our experiments $R(t)$ is constant, we do not consider it further. Typically, we use $\Delta = 100$ ms, $\delta = 8$ ms, and vary g from 1.7 to 32.3 G cm⁻¹ in 32 steps.

CHAPTER FOUR

RESULTS and DISCUSSION

IV.1 Phase Behavior Results

IV.1.1 Binary Phase Behavior

System A: Sucrose Laurate (L_{1695})/ Oils

Fig. 4.1 shows the temperature-composition phase diagrams of binary mixture of sucrose laurate (L_{1695}) and the oils, R(+)-Limonene (**A**), IPM (**B**), MCT (**C**). Sucrose laurate (L_{1695}) is completely miscible in R(+)-Limonene at low concentration $\gamma \leq 10$ wt% surfactant and high temperature $T \geq 57.5^\circ\text{C}$. At surfactant concentrations more than $\gamma > 10$ wt% there is no solubilization of surfactant in R(+)-Limonene .

Binary mixtures of sucrose laurate (L_{1695}) and IPM, MCT **Fig. 4.1 (B, C)** shows that the oil is a poor solvent for this amphiphilic compound and that there is practically no miscibility between the two compounds.

System B: Sucrose Stearate (S_{1570})/ Oils

Fig. 4.2 shows the temperature-composition phase diagrams of the binary mixtures of sucrose stearate (S_{1570}) and oils. Binary mixtures of sucrose stearate (S_{1570}) and R(+)-Limonene, **Fig. 4.2 (A)** shows that at low temperature the surfactant and oil are miscible with each other and they form a liquid crystal which is viscous and not fluid. Increasing the concentration of the surfactant (S_{1570}) (i.e. $\gamma > 50$ wt%) this miscible region is formed over all of the range of temperatures studied (i.e. $5^\circ\text{C} - 80^\circ\text{C}$).

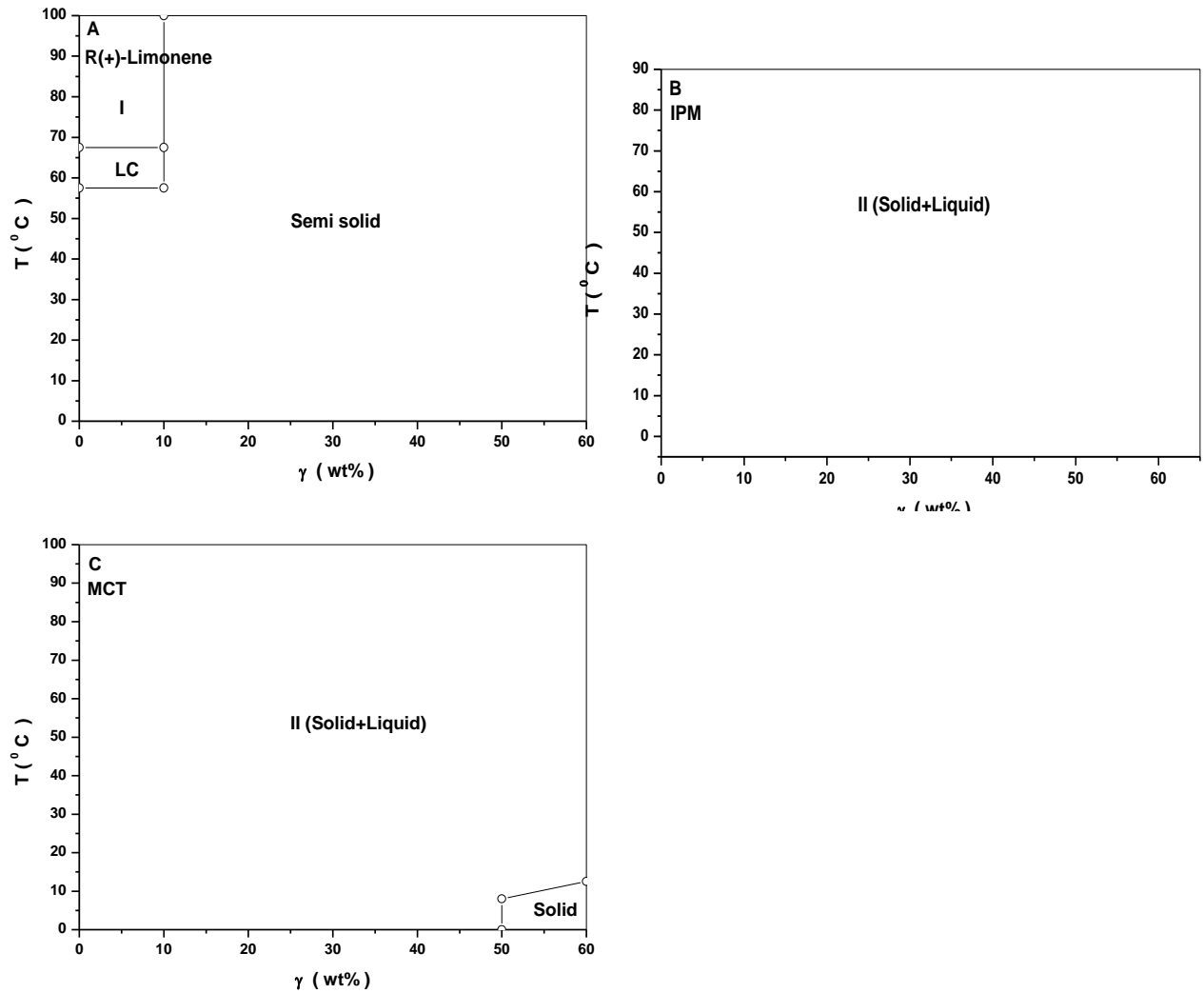


Fig. 4.1: Binary phase behavior of the System: L₁₆₉₅/ Oil as a function of surfactant concentration (γ (wt%)) and Temperature (T (°C)).

On the other hand at high temperatures and low concentration of surfactant this phase (liquid crystal) disappears and the surfactant and oil are separated into two phases solid and liquid at temperatures below the fusion point of the surfactant and two liquid phases at temperatures above the fusion point of the surfactant.

Binary mixtures of sucrose stearate (S_{1570}) and the oils IPM (B) and MCT (C) revealed that the oils is a poor solvent for these amphiphilic compounds and that there is a practically no miscibility between the two compounds. Sucrose stearate (S_{1570}) appears to be too hydrophilic for the dissolution into IPM and MCT.

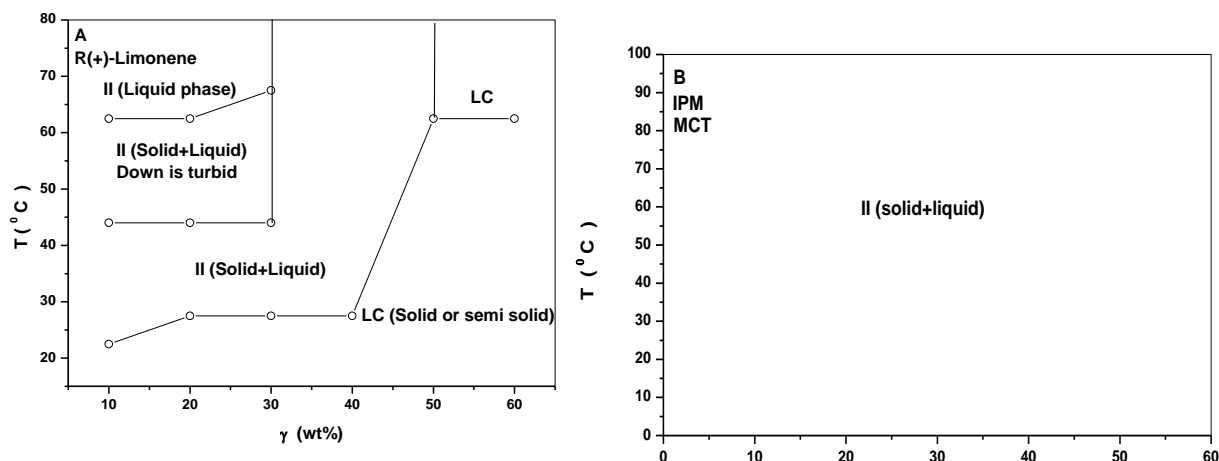


Fig. 4.2: Binary phase behavior of the System: S_{1570} / Oil (wt%) as a function of surfactant concentration (γ (wt%)) and Temperature (T ($^{\circ}C$)).

System C: Ethoxylated Mono-Diglyceride (EMDG)/ Oils

Fig. 4.3 shows the temperature-composition phase diagrams of binary mixture of ethoxylated mono-diglyceride (EMDG) and oils, R(+)-Limonene (A), IPM (B), MCT (C). Binary mixtures of ethoxylated mono-diglyceride (EMDG) and oils revealed that these oils are good solvents of this amphiphilic compound.

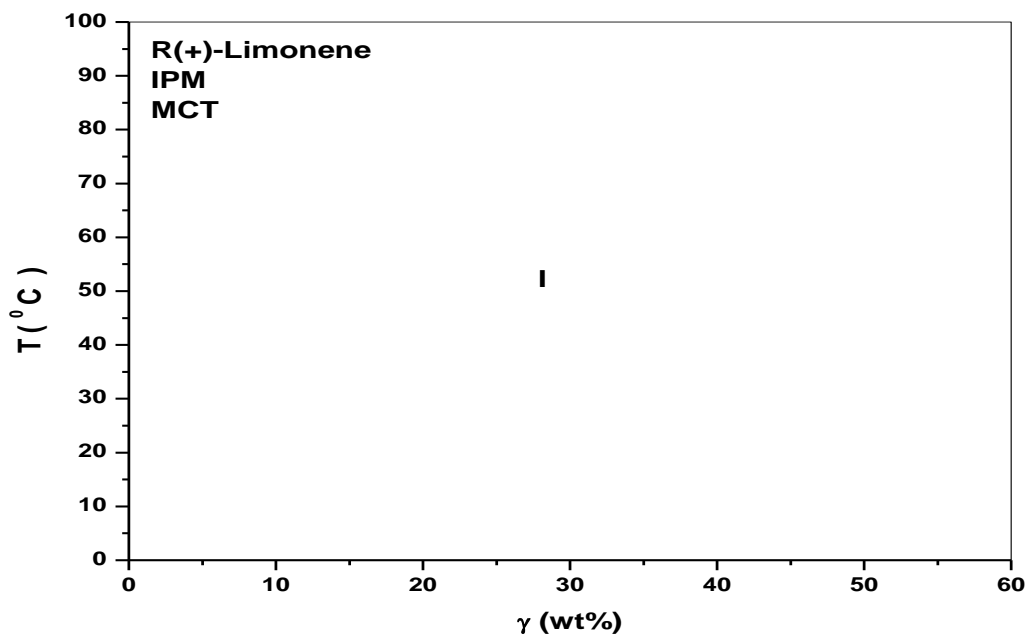


Fig. 4.3: Binary phase behavior of the System: EMDG/ Oil as a function of surfactant concentration (γ (wt%)) and Temperature (T ($^{\circ}\text{C}$)).

System D: Surfactants/ Water

Fig. 4.4 shows the temperature-composition phase diagrams of binary systems water-surfactant mixtures for L_{1695} (A), S_{1570} (B), EMDG(C). **Fig. 4.4 (A)** shows the binary mixture of sucrose laurate (L_{1695}) and water. As we can see in the Figure the surfactant is completely miscible in water at high concentration of surfactant (i.e. $\gamma > 40$ wt%) and forms liquid crystals. On the other hand, sucrose stearate (**Fig. 4.4 B**) is not miscible in water at any concentration of surfactant at low temperatures, it becomes miscible at $T_{\beta} = 49^{\circ}\text{C}$ for surfactant concentration from $\gamma = 15$ wt% to $\gamma = 70$ wt% and $T_{\beta} = 44^{\circ}\text{C}$ for surfactant concentration more than $\gamma = 70$ wt%, and forms a small region highly viscous gel. When we raise the temperature this region

disappears and the surfactant become not miscible with water as we can see in the Fig. 4.4 (B).

Fig. 4.4 (C), shows the binary mixtures of ethoxylated mono-diglyceride (EMDG) and water. The surfactant is completely miscible in water at $T_{\beta} \leq 35^{\circ}\text{C}$ for all concentrations of surfactant (EMDG). When we raise the temperature to $T > 60^{\circ}\text{C}$ the two phase region appears at low concentration of surfactant $\gamma \leq 40 \text{ wt\%}$, but at concentration above this concentration (i.e. $\gamma > 40 \text{ wt\%}$) the surfactant is still miscible in water.

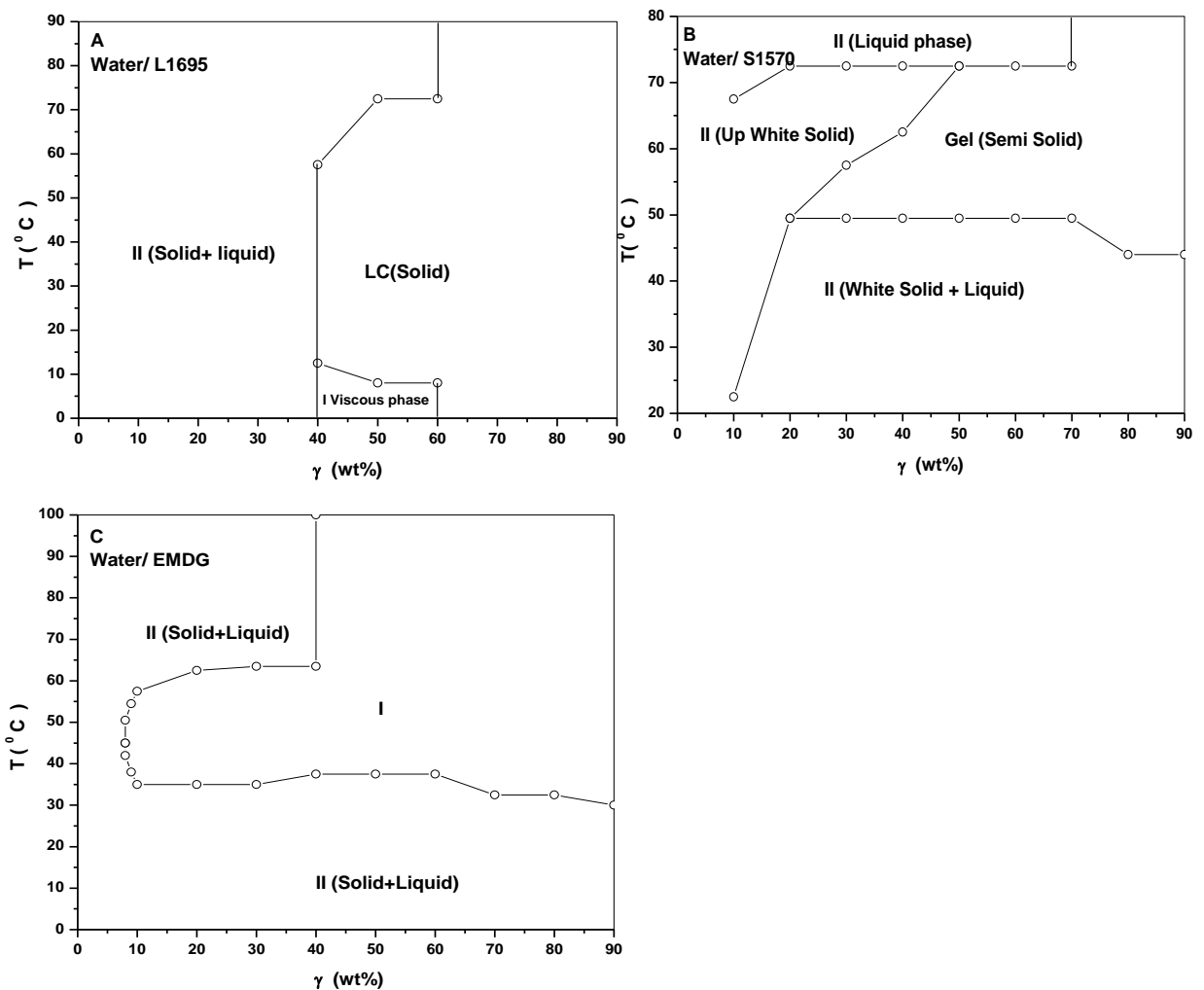


Fig. 4.4: Binary phase behavior of the System: Water/ Surfactant as a function of surfactant concentration ($\gamma \text{ (wt\%)}$) and Temperature ($T \text{ (}^{\circ}\text{C)}$).

System E: Surfactants/ PG.

Fig. 4.5 shows the temperature-composition phase diagrams of binary Surfactant/PG mixture for sucrose laurate (L_{1695})(A), sucrose stearate (S_{1570})(B), ethoxylated mono-diglyceride (EMDG)(C). Binary mixture of sucrose laurate (L_{1695}) and PG **Fig. 4.5 (A)** shows that at low concentration of surfactant less than $\gamma = 20$ wt%, and low temperature $T \leq 27.5^\circ\text{C}$ and $\gamma = 30$ wt%, and at $T = 22.5^\circ\text{C}$ the surfactant L_{1695} and cosurfactant (PG) are not miscible in each other. When we raise the temperature (i.e. $T > 27.5^\circ\text{C}$) at these concentration or increase the surfactant concentration, the surfactant and cosurfactant becomes miscible in each other .

Fig. 4.5 (B), shows that at low temperature (i.e. $T = 47.5^\circ\text{C}$ for $\gamma \leq 30$ wt% and $T = 42.5^\circ\text{C}$ for $\gamma > 30$ wt%) the surfactant sucrose stearate (S_{1570}) and cosurfactant (PG) are not miscible in each other. Raising the temperature (i.e. $T \geq 47.5^\circ\text{C}$ for $\gamma \leq 30$ wt% and $T \geq 42.5^\circ\text{C}$ for $\gamma > 30$ wt%), the S_{1570} and PG becomes miscible.

Fig. 4.5 (C), shows that when we increase the concentration of surfactant T_β decreases sharply and the surfactant ethoxylated mono-diglycerid (EMDG) and cosurfactant (PG) are miscible in each other.

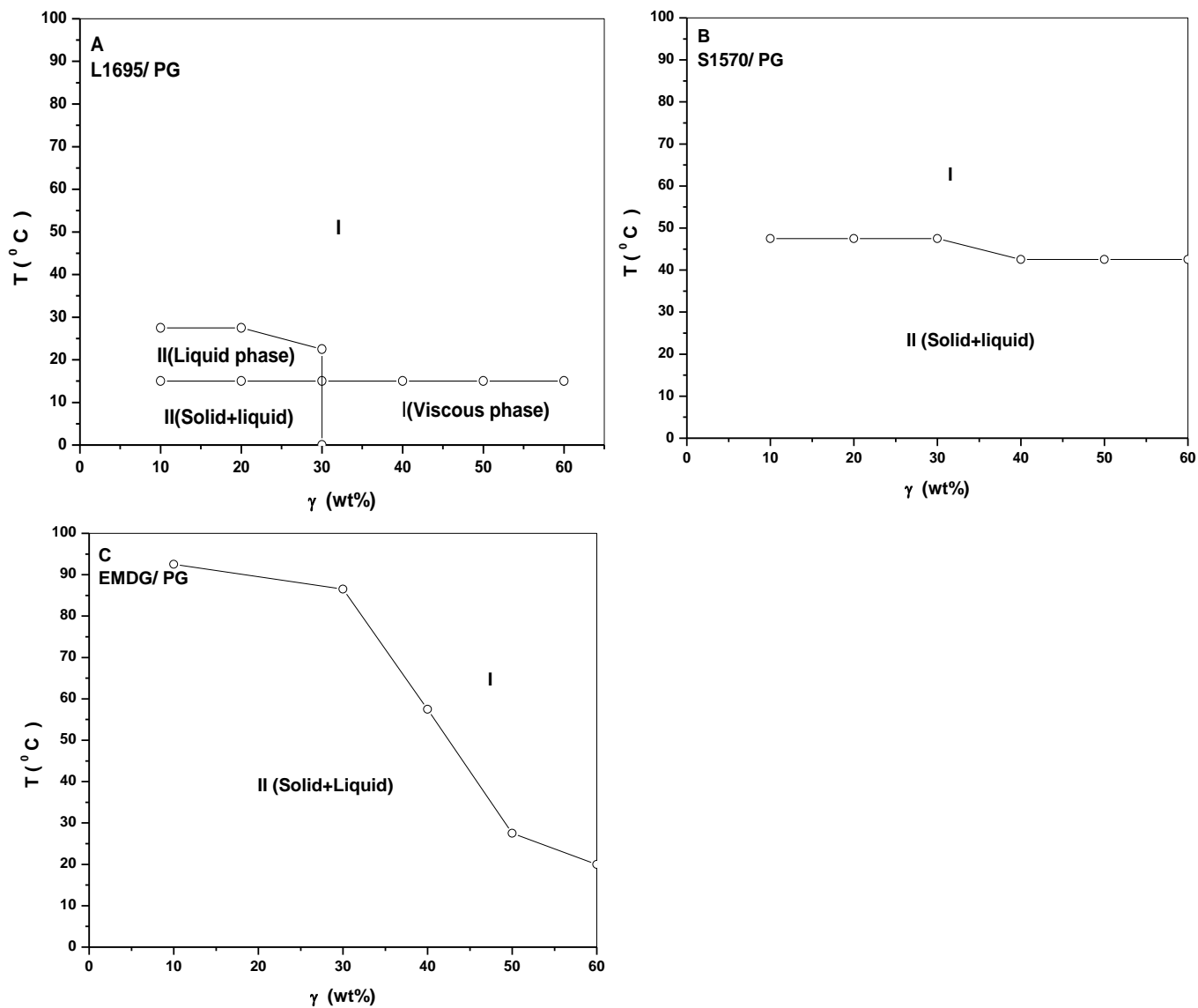


Fig. 4.5: Binary phase behavior of the Systems: Surfactant/ PG as a function of surfactant concentration (γ (wt%)) and Temperature (T ($^{\circ}\text{C}$)).

IV.2 Ternary Phase Behavior

Phase Behavior of the System A: Water/ L₁₆₉₅ / Oil

Fig. 4.6 shows the temperature composition phase diagram of the system: Water / L₁₆₉₅ / Oil mixture for R(+)-Limonene (A), IPM (B), MCT (C). This system was studied to determine the effect of oil chain length and type of oil on the maximum amount of solubilized water as a function of γ (wt%), and temperature at $\alpha = 50$ wt%.

As we can see in the Figures, at low temperatures, two separate phases are observed designated by II (Wm+O) which signifies water continuous micellar system with excess oil. At high temperature another two separate phases are observed and designated by II (W+Om), which means excess water with oil continuous micellar system. One phase region (microemulsion region) designated by I is also observed.

Using cyclic oils like R(+)-Limonene the three phase body does not appear and one phase region is formed at $\gamma = 32.5$ wt% of surfactant and temperature $T = 80^\circ\text{C}$. Using straight and long chain oil as in the case of IPM this will improve the solubilization and increase the one phase region, this region also moves downward in the temperature scale, as we can see this region is start to form at $\gamma = 25$ wt% of surfactant and $T = 72.5^\circ\text{C}$.

Using branched oils such as a triglycerides in the case of MCT, the three phase body designated by III (W+D+O) start to form at low concentration of surfactant but the one phase region is shifted up in the temperature scale, the mean temperature $\bar{T} = 87.5^\circ\text{C}$, $\bar{\gamma} = 37.5$ wt%, which means the existence of bicontinuous micellar system with excess water and

oil (see Fig. 1.4 page 7) presents these cases, but the one phase region becomes wider more than the use of cyclic chain oils.

It is important to note that for high content of surfactant (i.e. 70 wt%) the one phase region appears at lower temperatures (i.e. 20°C). Increasing the surfactant content decreases the temperature at which the one phase appears. For high temperatures (i.e. $T > 75^{\circ}\text{C}$), the transition temperature from one phase to two phase is dependent on the surfactant content. It increases when γ increases.

Increasing the surfactant content (i.e. 55 wt%) decreases the temperature at which the one phase is formed (i.e. 20°C). The same behavior as in the case of R (+)-limonene is observed with MCT for high temperatures.

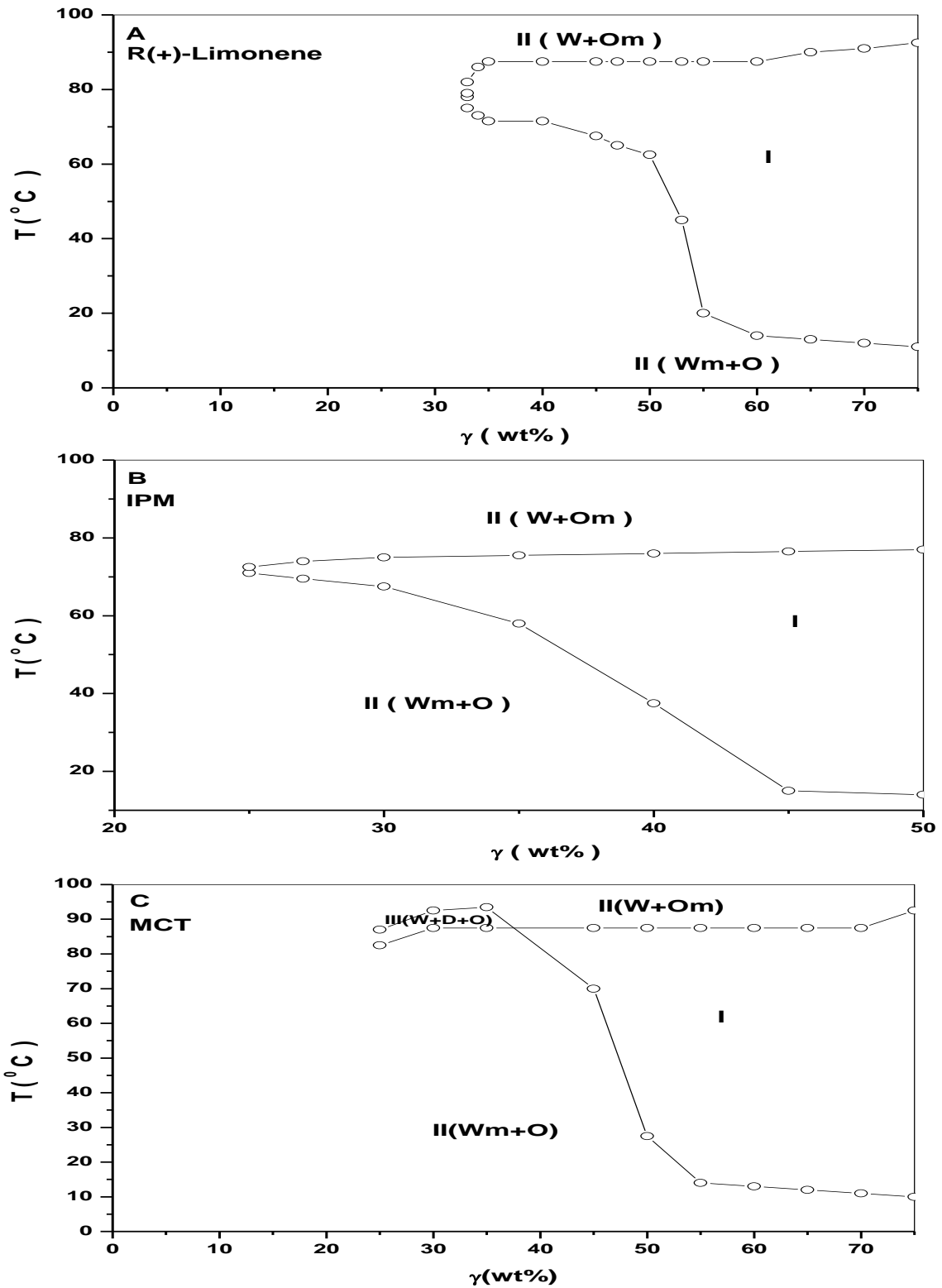


Fig. 4.6: Phase behavior of the System: Water/ L₁₆₉₅/ Oil as a function of γ (wt%) and temperature at constant $Oil/(Oil + Water)$ weight ratio, $\alpha = 50$ (wt%).

Phase Behavior of the System B: Water/ S₁₅₇₀/ Oil

Fig. 4.7 shows the phase behavior of the system: Water/ S₁₅₇₀/ Oil as a function of γ (wt%), and temperature at $\alpha = 50$ wt%, the oils were R (+)-limonene (A), IPM (B), MCT (C).

When we use a cyclic oils such as R (+)-limonene, as the oleic phase the three phase body does not appear and the one phase region appears at $T = 65.5^\circ\text{C}$ and $\gamma_{\min} = 25$ wt%, which mean that S₁₅₇₀ as a surfactant improves the solubilization of oil in water in comparasion with L₁₆₉₅. It is important to not that for high content of surfactant (i.e. 70 wt%) the one phase region appears at lower temperatures (i.e. 25°C). Increasing the surfactant content decreases the temperature at which the one phase appears. For high temperatures (i.e. $T > 75^\circ\text{C}$), the transion temperature from one phase to two phase is dependent on the surfactant content. It increases when γ increases. In the presence of branched oils such as triglycerides in case of MCT, we observe that the three phase region is formed, the mean temperature $\bar{T} = 77^\circ\text{C}$ and $\bar{\gamma} = 51$ wt%.

In the case of the long chain oil (IPM) as the oleic phase the one phase region appears at $T = 75^\circ\text{C}$ and $\gamma_{\min} = 42.5$ wt%, but the one phase is moved downward in the temperature scale. Increasing the surfactant content (i.e. 55 wt%) decreases the temperature at which the one phase is formed (i.e. 35°C). The same behavior as in the case of R (+)-limonene is observed with MCT for high temperatures. From these **Fig. 4.7 (A, B, C)** we can see that using cyclic oils as oil phase will give a wider one phase region better than the use of branched (MCT) or long chain oil (IPM) and this phase appears at low temperature at high concentration of surfactant (S₁₅₇₀).

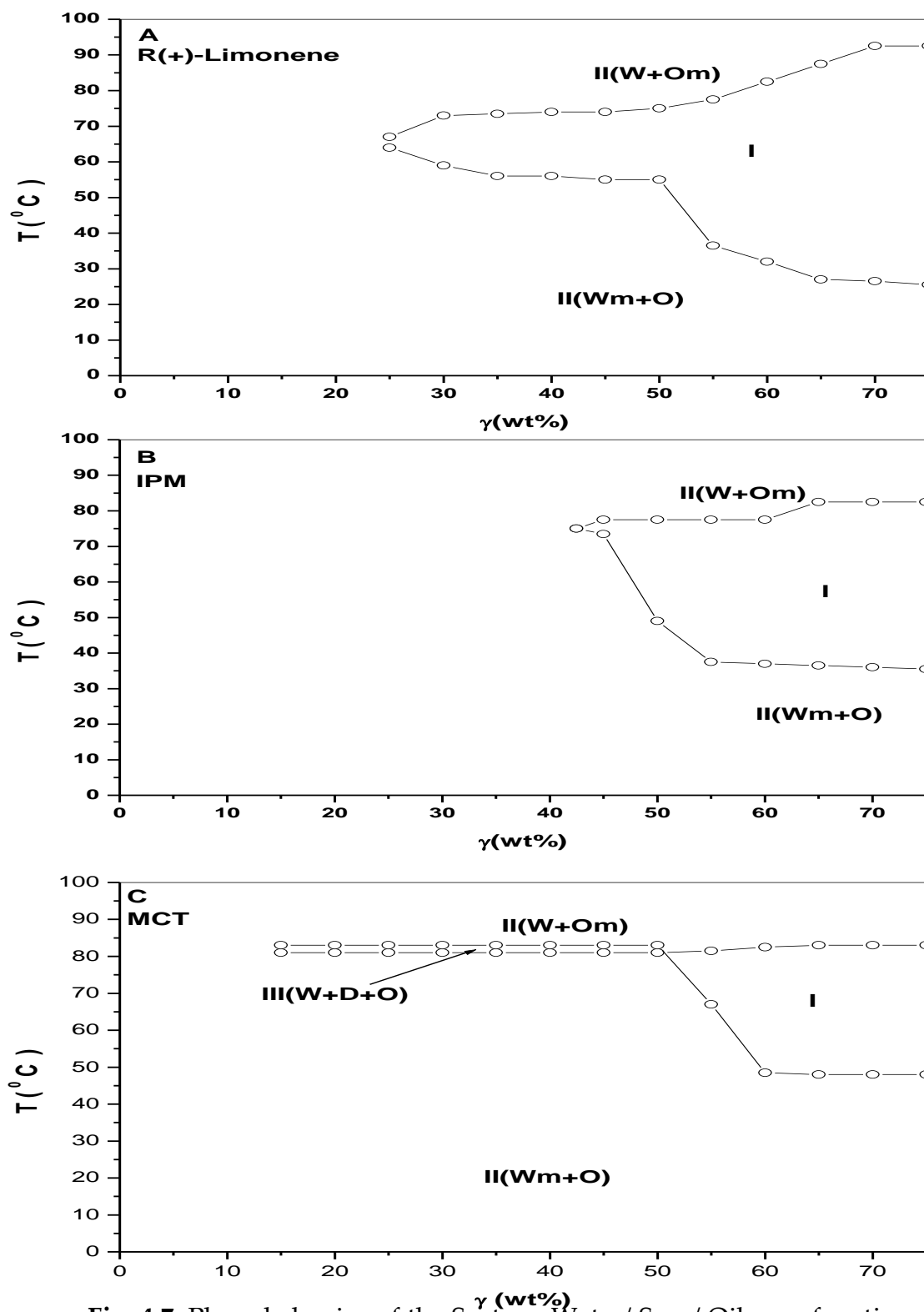


Fig. 4.7: Phase behavior of the System: Water/ S₁₅₇₀ / Oil as a function of γ (wt%) and temperature at constant $Oil/(Oil + Water)$ weight ratio, $\alpha = 50$ (wt%).

Phase Behavior of the System C: Water/ EMDG/ Oil

Fig. 4.8 shows the temperature-composition phase diagram of the system: Water/ EMDG/ Oil mixture for R (+)-limonene (A), IPM (B), MCT (C) at $\alpha = 50$ wt%. The following systems were studied to elucidate the effect of oil chain length and type of oil on the maximum amount of solubilized water in the system as a function of γ (wt%), and temperature at $\alpha = 50$ wt%.

In the presence of cyclic oils such as R (+)-limonene there is no formation of three phase region and the homogeneous microemulsion region (one phase region) shifted to high concentration of surfactant, while the presence of branched oils such as triglycerides in the case of MCT we can see that the mean temperature $\bar{T} = 85^\circ\text{C}$ and $\bar{\gamma} = 42$ wt%, the three phase body appears, this type of oil improve the solubilization of water because the one phase region becomes wider as we can see in the **Fig. 4.8(C)**, and this type of oil will increase the efficiency of the surfactant more than the use of cyclic oils (R(+)-limonene). Using IPM which have a long and linear structure, the mean temperature $\bar{T} = 105^\circ\text{C}$ and $\bar{\gamma} = 26.5$ wt% so as we can see that the $\bar{\gamma}$ moves down to low concentration of surfactant, the three phase body appears in this type of oils. It is important to not that for high content of surfactant (i.e. 70 wt%) the one phase region appears at lower temperatures (i.e. 25°C). Increasing the surfactant content decreases the temperature at which the one phase appears. For high temperatures (i.e. $T > 75^\circ\text{C}$), the transion temperature from one phase to two phase is dependent on the surfactant content. It increases when γ increases.

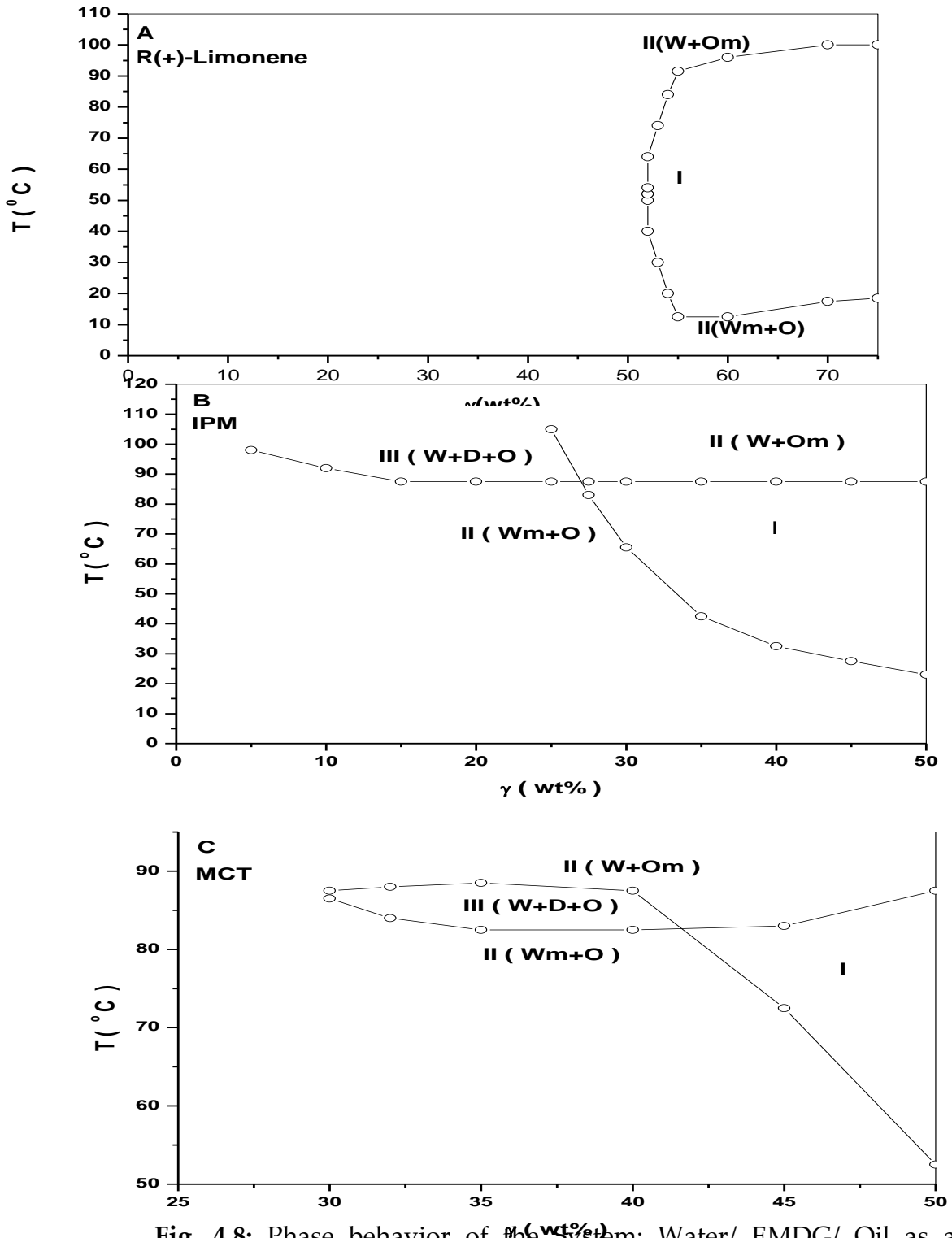


Fig. 4.8: Phase behavior of the System: Water/ EMDG/ Oil as a function of γ (wt%) and temperature at constant $Oil/(Oil + Water)$ weight ratio, $\alpha = 50$ (wt%).

Increasing the surfactant content (i.e. 55 wt%) decreases the temperature at which the one phase is formed (i.e. 25°C). The same behavior as in the case of R (+)-limonene is observed with MCT for high temperatures. One conclusion that the using of long chain oil will improve the solubilization of the surfactant (EMDG).

Phase Behavior of the System D: Water / PG / Oil

This system Fig. 4.9 shows that there is no solubilization of oil in water when using PG as a co-surfactant with different types of oils.

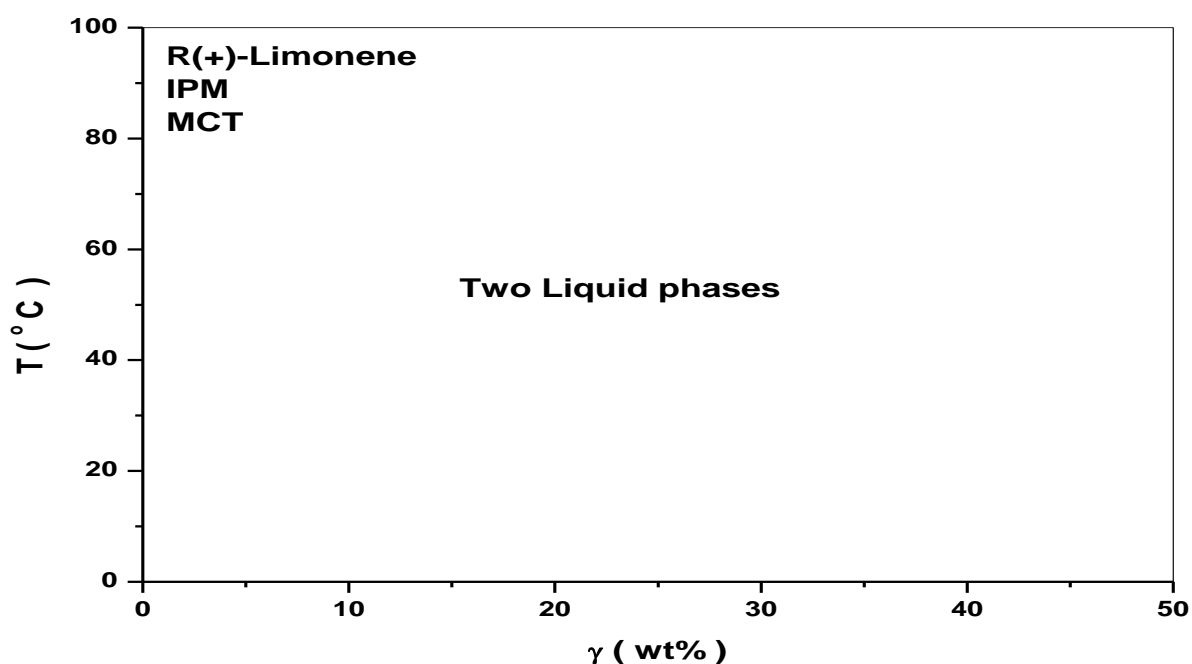


Fig. 4.9: Phase behavior of the System: Water/ PG/ Oil as a function of γ (wt%) and temperature at constant $Oil/(Oil + Water)$ weight ratio, $\alpha = 50$ (wt%).

IV.1.3 Quaternary phase behavior

Phase Behavior of the System A: Water/ L₁₆₉₅/ PG/ R (+)-limonene.

1-As a Function of δ, γ and Temperature at $\alpha = 50$ wt%.

Fig. 4.10 shows the temperature-composition phase diagrams of the system: Water/ L₁₆₉₅/ PG/ R (+)-limonene mixture for δ (wt%) = 25%(B), 40%(C), 50%(D), 75%(E), 90%(F) and 100%(G) at $\alpha = 50$ wt%. The system: water / L₁₆₉₅ / R (+)-limonene "fish" ($\delta = 0\%$ (A)) is shown in the first as reference. As we can see in the Figures, at low temperatures two separate phases are observed designated by II (Wm+O) which signifies water continuous micellar system with excess oil. At high temperature another two separate phases are observed and designated by II (W+Om), which means excess water with oil continuous micellar system. One phase region (microemulsion region) designated by I is also observed. At high concentrations of PG two phases are also observed liquid and white solid precipitate. With the addition of PG the homogeneous microemulsion region (fish tail) becomes smaller and the minimum amount of mixed L₁₆₉₅ + PG needed for the formation of one phase region (γ_{\min}) of the surfactant mixture decreases slightly (i.e $\gamma_{\min} = 32.5$ wt% and T = 80°C for $\delta = 0$ wt% to $\gamma_{\min} = 60$ wt% and T = 55°C for $\delta = 25$ wt% to $\gamma_{\min} = 75$ wt% and T = 55°C for $\delta = 40$ wt%) while there is no formation for the three-phase body (fish body).

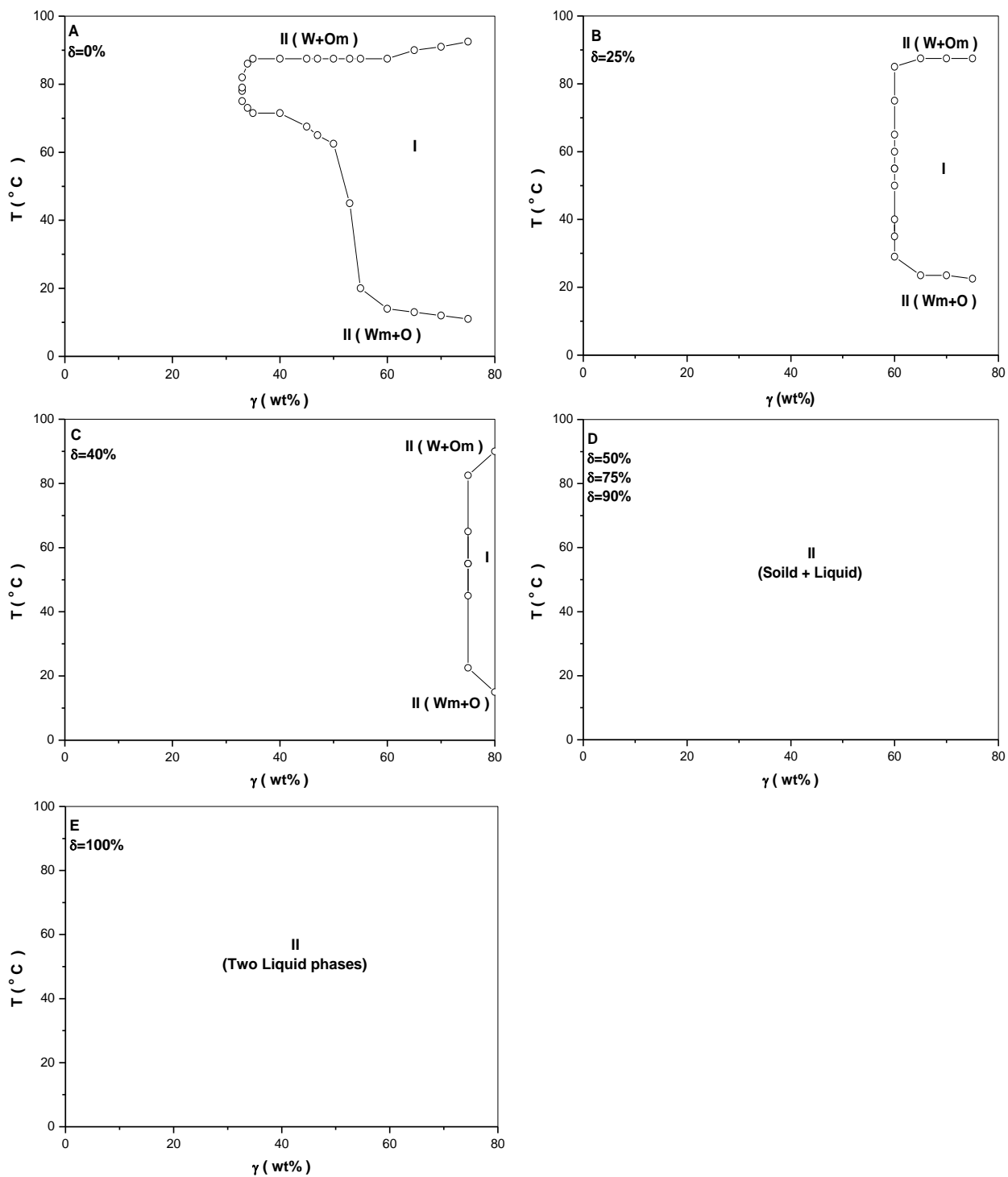


Fig. 4.10: Phase behavior of the System: Water/ L₁₆₉₅/ PG/ R (+)-limonene as a function of δ , γ (wt%) and temperature at constant $Oil/(Oil + Water)$ weight ratio, $\alpha = 50$ (wt%).

From this Figure we can say that increasing the ratio of PG/ L₁₆₉₅ (i.e. $\delta = 50$ wt% to $\delta = 100$ wt%), will shift the system to the solid and liquid two separated phases. No three phase region was observed in these systemes.

It is important to note that for high content of surfactant (i.e. 65 wt%) the one phase region appears at lower temperatures (i.e. 20°C) at low cosurfactant concentrations δ (i.e. < 25 wt%). Increasing the surfactant content decreases the temperature at which the one phase appears. For high temperatures (i.e. $T > 75^\circ\text{C}$), the transion temperature from one phase to two phase is dependent on the surfactant content. It increases when γ increases.

2-As a Function of δ, γ and Constant Temperature at $\alpha = 50$ wt%.

Fig. 4.11(A and B), shows the phase behavior of the system: Water/ L₁₆₉₅/ PG/ R (+)-limonene at $\alpha = 50$ wt% as a function of δ (wt%) and γ (wt%) at constant temperature ($T = 50$ and 80°C). At 50°C , L₁₆₉₅ is mainly dissolved in water to form II (W_m+O) at low values of surfactant and form one-phase microemulsion at high concentration of surfactant γ (i.e. $\gamma > 52$ wt%), by increasing δ concentration of co-surfactant the amount of surfactant needed to form one phase region is increased. At high concentration of co-surfactant ($\delta > 45$ wt%) the one phase region disappeared and the two phase region, is appeared which mean that the surfactant is dissolved in oil to form II (W+O_m). The three phase region does not form at any values of δ and γ . At 80°C , L₁₆₉₅ remains dissolved in the water at low concentration of surfactant but the one-phase

microemulsion appears by using surfactant concentration $\gamma \geq 32.5$ wt% at $\delta = 0$ wt%.

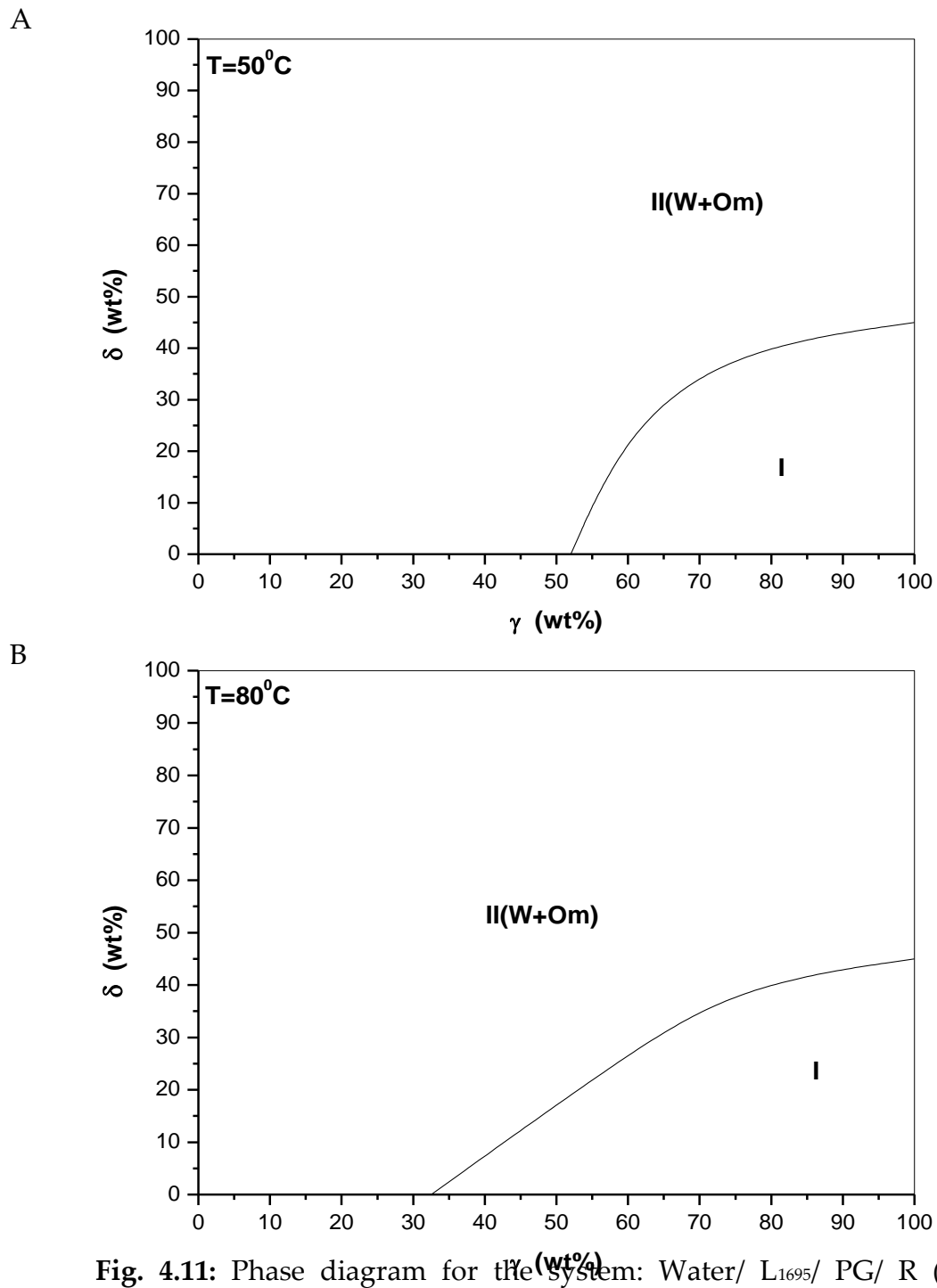


Fig. 4.11: Phase diagram for the system: Water/ L₁₆₉₅/ PG/ R (+)-limonene at constant temperature ($T = 50^{\circ}\text{C}$ (A) and 80°C (B)) as a function of δ and γ (wt%). The $\text{Oil}/(\text{Oil} + \text{Water})$ weight ratio, $\alpha = 50$ (wt%).

By raising the concentration of co-surfactant (δ) the one-phase microemulsion is shifted to high concentration of surfactant (γ) and it remain shifted toward high concentrations, so the one-phase region disappears and the two-phase region appears so the mixture of L₁₆₉₅ + PG is dissolved in oil at high concentration of δ . The three phase region does not appear at any concentration of surfactant (γ) and co-surfactant (δ).

Phase Behavior of the System B: Water/ S₁₅₇₀/ PG/ R(+)-limonene

1-As a Function of δ, γ and Temperature at $\alpha = 50$ wt%.

Fig. 4.12 shows the temperature-composition phase diagram of the system: Water/ S₁₅₇₀/ PG/ R (+)-limonene mixture for δ (wt%) = 25%(B), 40%(C), 50%(D), 75%(E), and 100%(F) at $\alpha = 50$ wt% and $\delta = 0$ %(A) as reference. As in the previous system we want to study the effect of increasing the ratio of PG/ S₁₅₇₀ on the solubilization of oil in water. The phase sequence II (W_m+O) → I → II (W+O_m) is also observed in this system. As we can see by the addition of PG, the homogeneous microemulsion region (fish tail) becomes wider and the minimum amount of mixed surfactant and co-surfactant needed to form the one phase region γ_{\min} of the surfactant mixture increases slightly (i.e $\gamma_{\min} = 25$ wt% and T = 65.5°C for $\delta = 0$ wt% and drops to $\gamma_{\min} = 24$ wt% and T = 61°C for $\delta = 25$ wt% and $\delta = 40$ wt% and T = 56.5°C and drops at $\gamma_{\min} = 20$ wt% and T = 56°C for $\delta = 50$ wt% and the same for $\delta = 75$ wt% but T = 58°C) compared to the pure S₁₅₇₀ case.

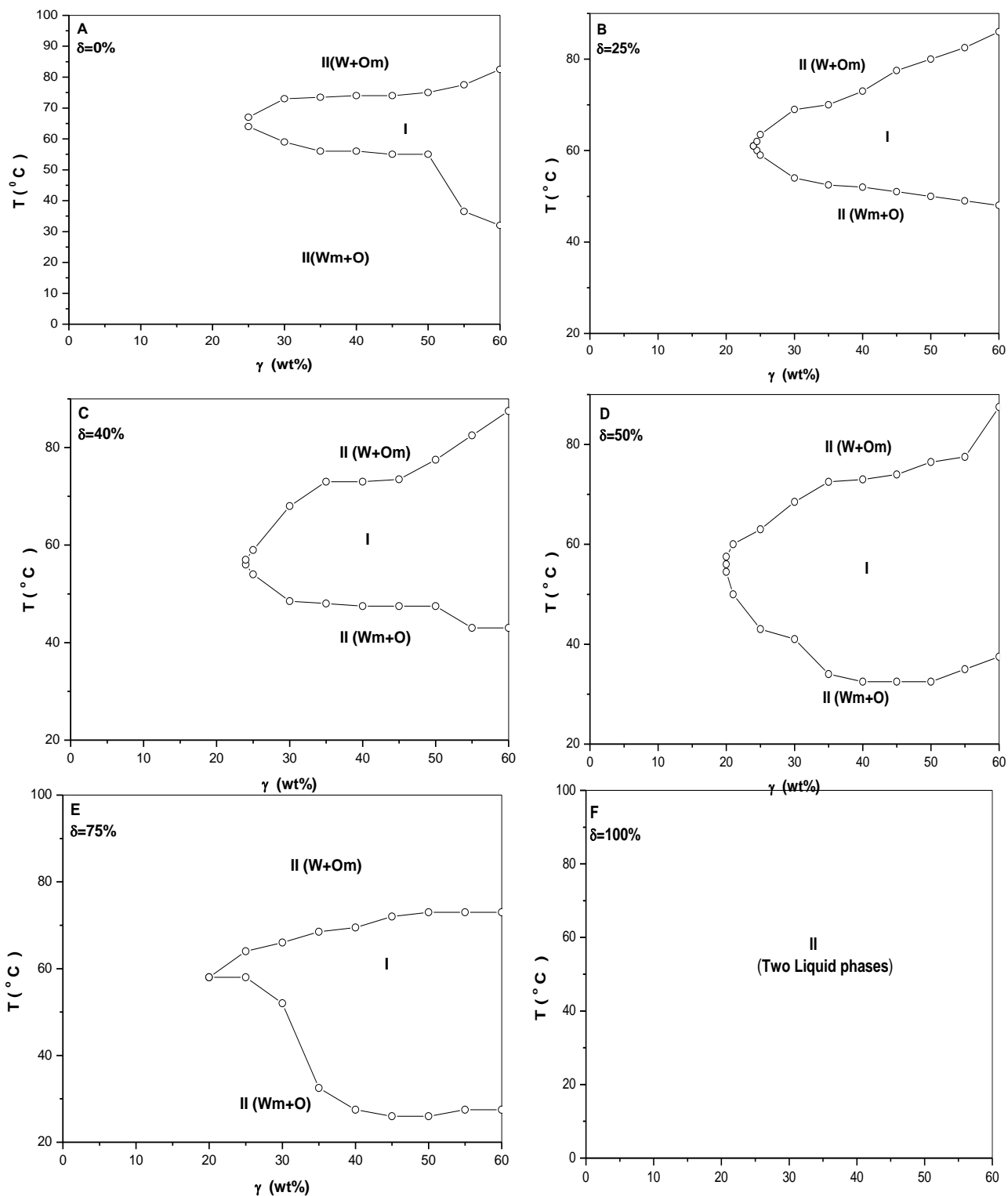


Fig. 4.12: Phase behavior of the System: Water/ S_{1570} / γ PG/ R (+)-limonene as a function of δ (wt%), γ (wt%) and temperature at constant $Oil/(Oil + Water)$ weight ratio, $\alpha = 50$ (wt%).

Also the formation of homogeneous microemulsion will occur at low temperature (i.e. at $\gamma = 45$ wt%, temperature at $\delta = 0$ wt % , $T_1 = 55^\circ\text{C}$ while at $\delta = 25$ wt% , $T_1 = 51^\circ\text{C}$ and drops to $\delta = 40$ wt%, $T_1 = 47^\circ\text{C}$ and at $\delta = 50$ wt% the $T_1 = 32^\circ\text{C}$ and at $\delta = 75$ wt% the $T_1 = 26^\circ\text{C}$).

On the other hand, high ratios of PG in the mixture $S_{1570} + \text{PG}$ more than $\delta = 75$ wt% will result in the shrinkage and disappearance at $\delta = 100$ wt% the homogenous microemulsion region. One important observation is that S_{1570} improve the Water/ Oil solubilization. Compered to L_{1695} in the previous system, the high content of surfactant (i.e. 55 wt%) the one phase region appears at lower temperatures (i.e. 30°C) when increasing the PG content δ (i.e. from 25 wt% to 75 wt%) in the mixed surfactnt system.

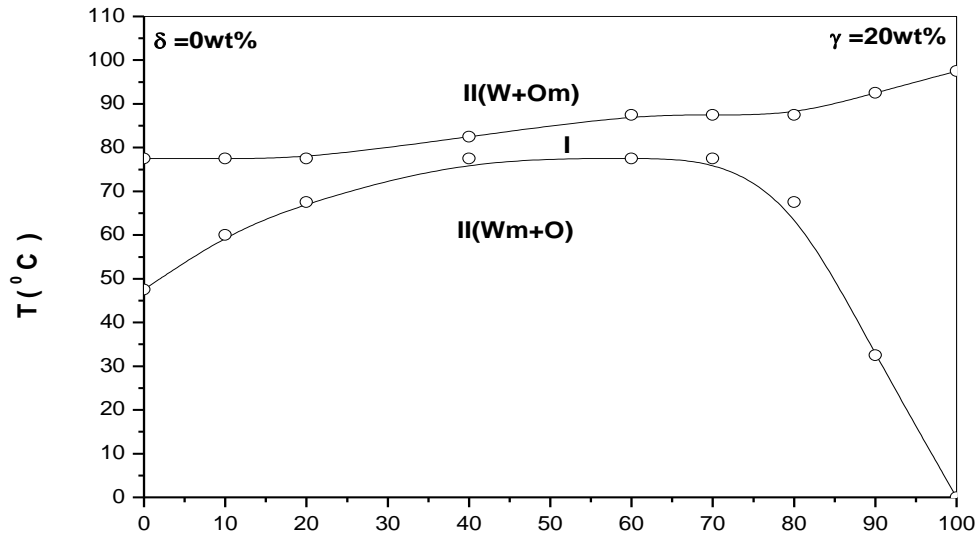
Increasing the surfactant content decreases the temperature at which the one phase appears. For high temperatures (i.e. $T > 75^\circ\text{C}$), the transion temperature from one phase to two phase is dependent on the surfactant content, it increases when γ increases.

2-As a Function of δ, α and Temperature at Constant γ .

Fig. 4.13 shows the phase behavior of the system: Water/ S_{1570} / PG/ R (+)-limonene at fixed surfactant concentration (i.e. $\delta = 0$ wt% for $\gamma = 20$ wt% (A) and $\delta = 25$ wt% for $\gamma = 20$ wt% (B)), while varying the temperature and weight ratios of oil and water. We confirmed that the one phase microemulsion regions are bounded at high temperatures by oil-continuous microemulsions with excess water (W+Om), and at low temperatures by water continuous microemulsion with excess oil (Wm+O).

The mono- and multiphase lamellar region appear at high oil concentrations and low temperatures. The one phase region is a water continuous at low α values and oil continuous one at high α values this one phase microemulsion becomes large when we increase the oil-water ratio.

A



B

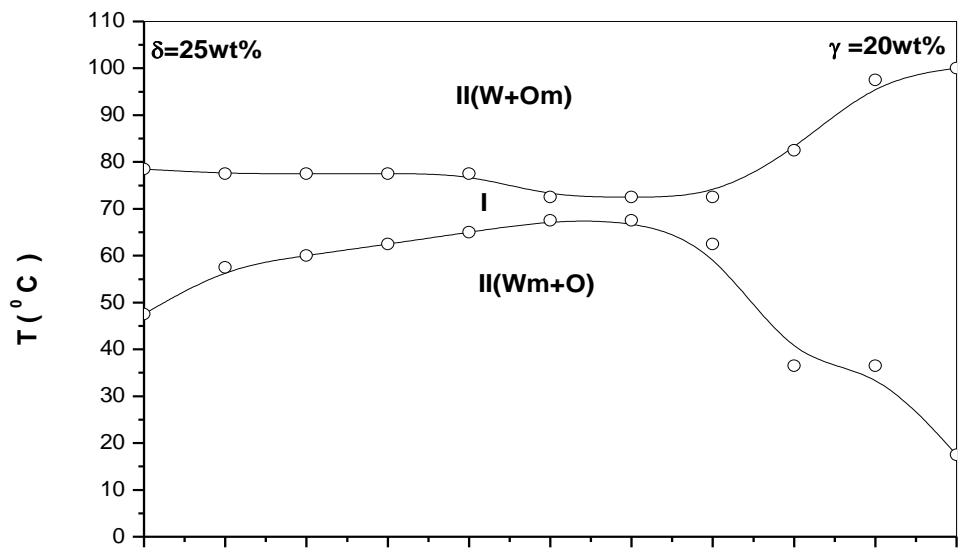


Fig. 4.13: Vertical section through the phase prism for the system: Water/ S_{1570} / PG/ R(+)-limonene at constant surfactant concentration (γ) equals 20 wt% and constant PG weight content in the mixture of surfactant (δ) and equals 0 wt% and 25 wt% as a function of temperature and $Oil/(Oil + Water)$ weight ratio, α (wt%).

3-As a Function of δ, γ and Constant Temperature at $\alpha = 50$ wt%.

Fig. 4.14 shows the phase behavior of the system: Water/ S_{1570} / PG/ R (+)-Limonene at $\alpha = 50$ wt% as a function of δ and γ (wt%) at constant temperature $T = 60^\circ\text{C}$. By increasing δ (wt%) the one phase microemulsion appears at low concentration of (S_{1570}) to reach its minimum amount of the surfactant S_{1570} ($\gamma = 20$ wt%) at $\delta = 40$ wt%. When we increase δ more than 40 wt% the presence of one phase microemulsion is shifted toward high concentrations of surfactant. With high values of δ , the one phase region disappears and the II (W+Om) is appeared which mean that the surfactant is mainly dissolved in oil. For this system there is no formation of the three phase body at any δ and γ concentrations.

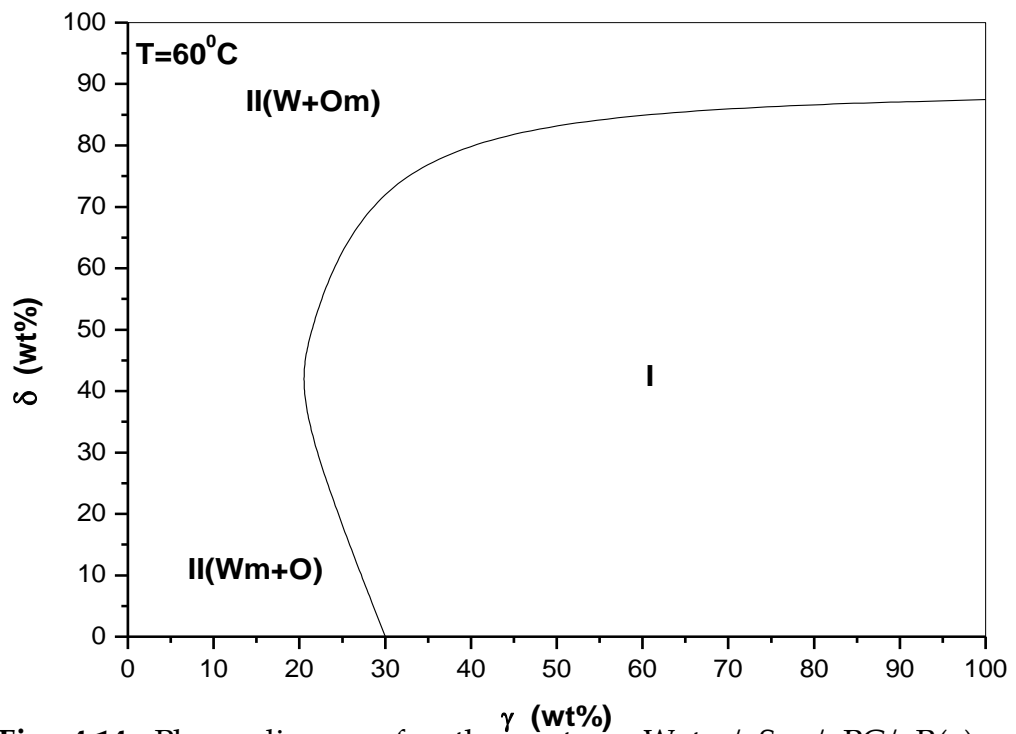


Fig. 4.14: Phase diagram for the system: Water/ S_{1570} / PG/ R(+)-Limonene at constant temperature ($T = 60^\circ\text{C}$) as a function of δ and γ (wt%). The $\text{Oil}/(\text{Oil} + \text{Water})$ weight ratio, $\alpha = 50$ (wt%).

Phase Behavior of the System C: Water/ EMDG/ PG/ R (+)-Limonene

1-As a Function of δ, γ and Temperature at $\alpha = 50$ wt%.

Fig. 4.15 shows the temperature-composition phase diagram of the system: Water/ EMDG/ PG/ R(+)-Limonene mixture for δ (wt%) = 25%(B), 50%(C), 75%(D) and 100%(E) at $\alpha = 50$ wt% and $\delta = 0$ wt% (A) as a reference. These figures show the effect of increasing the ratio of PG/ EMDG on the solubilization of R(+)-Limonene in water. Adding PG as cosurfactant to a mixture of EMDG will increase the homogeneous microemulsion region and increases the γ_{\min} of the surfactant, but PG weight ratio (i.e. $\delta = 25$ wt%) in the mixture of EMDG + PG gives a negative results on the homogeneous microemulsion region. This also was observed with high ratio of PG/ EMDG, the homogeneous one phase appears at $\gamma_{\min} = 68$ wt% and the $T = 47.5^{\circ}\text{C}$ at $\delta = 25$ wt% while at $\delta = 50$ wt% , $\gamma_{\min} = 35$ wt% and the $T = 87.5^{\circ}\text{C}$. Increasing PG/ EMDG ratio to $\delta = 75$ wt% the three-phase body (fish body) is formed at low concentrations of surfactant, less than $\gamma = 45$ wt%, the one phase region is formed at $\bar{\gamma} = 45$ wt% and the $\bar{T} = 92.5^{\circ}\text{C}$.

It is important to note that for high content of surfactant (i.e. 70 wt%) the one phase region appears at lower temperatures (i.e. 15°C). Increasing the surfactant content decreases the temperature at which the one phase appears. For high temperatures (i.e. $T > 80^{\circ}\text{C}$), the transition temperature from one phase to two phase is dependent on the surfactant content.

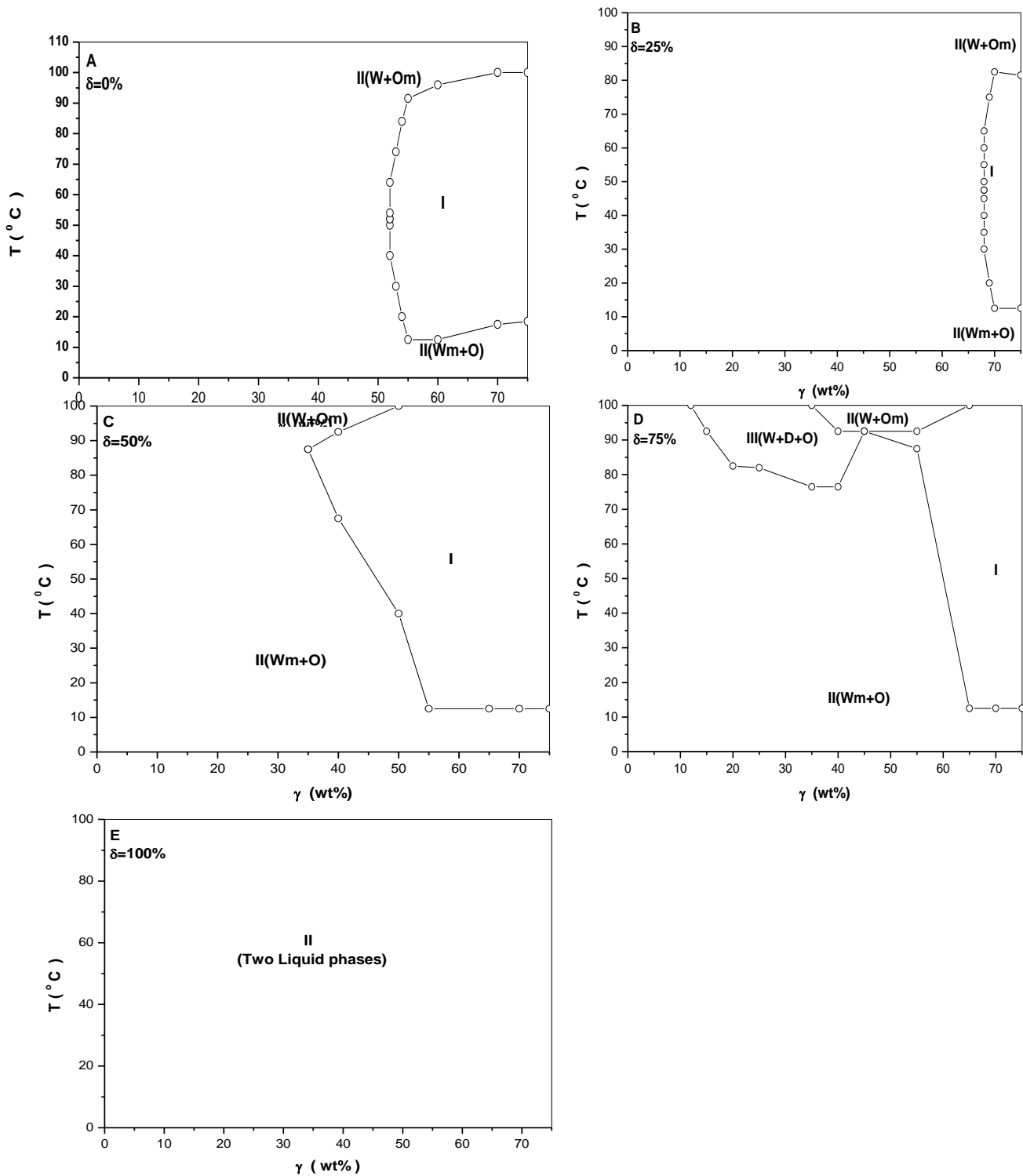


Fig. 4.15: Phase behavior of the System: Water/ EMDG/ PG/ R(+)-Limonene as a function of δ , γ (wt%) and temperature at constant $Oil/(Oil + Water)$ weight ratio, $\alpha = 50$ (wt%).

It increases when γ increases, when also increasing PG weight ratio in mixture of EMDG + PG.

2-As a Function of δ, γ and Constant Temperature at $\alpha = 50$ wt%.

Fig. 4.16 shows the phase behavior of the system: Water/ EMDG/ PG/ R (+)-limonene at $\alpha = 50$ wt% as a function of δ and γ (wt%) at constant temperature $T = 52^\circ\text{C}$. The one-phase microemulsion region for the ternary system appears at high mixed surfactant and cosurfactant concentration (i.e. $\gamma = 52$ wt%). By increasing δ (i.e. PG concentration) in the system more than 25 wt%, the one phase microemulsion region is shifted to the direction of low mixed surfactant and cosurfactant concentration to reach its minimum at $\delta = 50$ wt%.

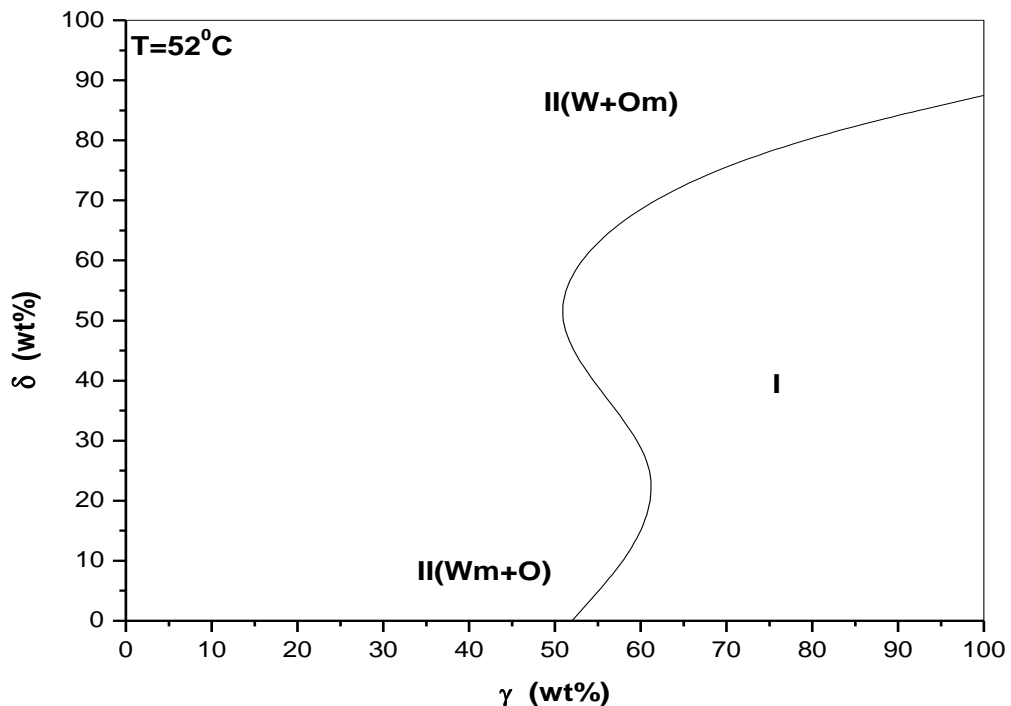


Fig. 4.16: Phase diagram for the system: Water/ L₁₆₉₅/ EMDG/ IPM at constant temperature ($T = 72.5^\circ\text{C}$) as a function of δ and γ (wt%). The *Oil/(Oil + Water)* weight ratio, $\alpha = 50$ (wt%).

Increasing PG content (i.e. more than 50 wt %) in the system, the one phase microemulsion region is shifted slightly toward high mixed surfactant and cosurfactant concentration. At very high PG concentration more than $\delta = 87.5$ wt% the surfactant becomes too oil soluble and an aqueous phase separates out and the II (W+Om) is present.

Phase Behavior of the System D: Water/ L₁₆₉₅/ PG/ IPM

1-As a Function of δ , γ and Temperature at $\alpha = 50$ wt%.

Fig. 4.17 shows the temperature-composition phase diagram of the system: Water/ L₁₆₉₅/ PG/ IPM mixture for δ (wt%) = 25%(B), 40%(C), 50%(D), 75%(E), and 100%(F). The system: Water/ L₁₆₉₅/ IPM “fish” ($\delta = 0$ wt% (A)) is shown as a reference. With the addition of PG, the homogeneous microemulsion region (fish tail) becomes smaller and the efficiency of the surfactant mixture is decreased (i.e. $\bar{\gamma} = 50$ wt% and $\bar{T} = 82^\circ\text{C}$ for $\delta = 25$ wt%, but at $\delta = 40$ wt%, $\bar{\gamma} = 62$ wt% and $\bar{T} = 85^\circ\text{C}$ and at $\delta = 50$ wt%, $\bar{\gamma} = 65$ wt% and $\bar{T} = 92.5^\circ\text{C}$) and as we can see the mean temperature moves upward on the temperature scale. On the other hand the area of the three-phase body increases with increasing δ . With highly addition of PG (i.e. for δ values bigger than 50 wt%), the homogeneous microemulsion region disappears and the two and three phase bodies are the only regions which are formed. At $\delta = 100$ wt% two liquid separate phases are the only formed for all the range of concentrations and temperatures.

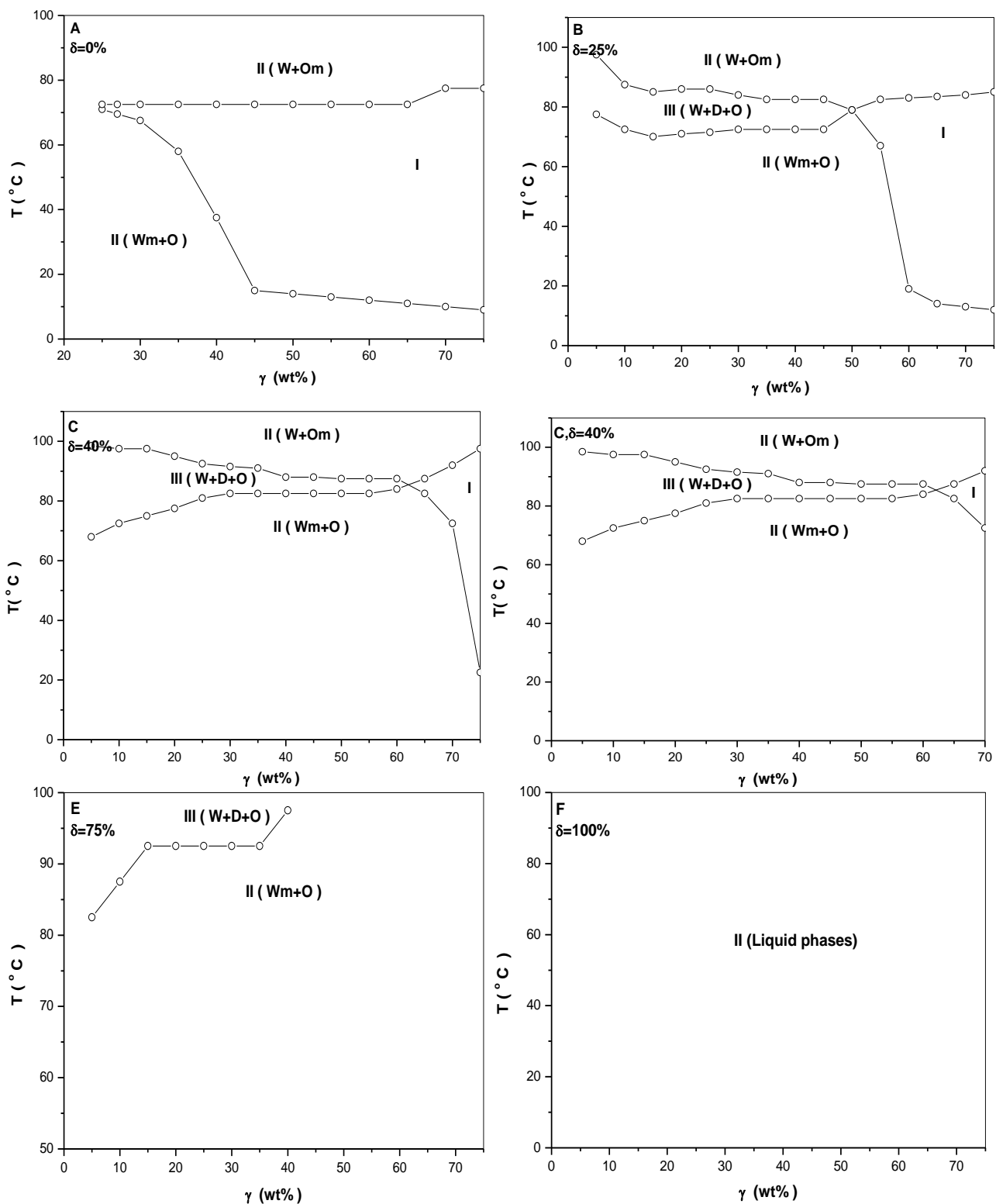


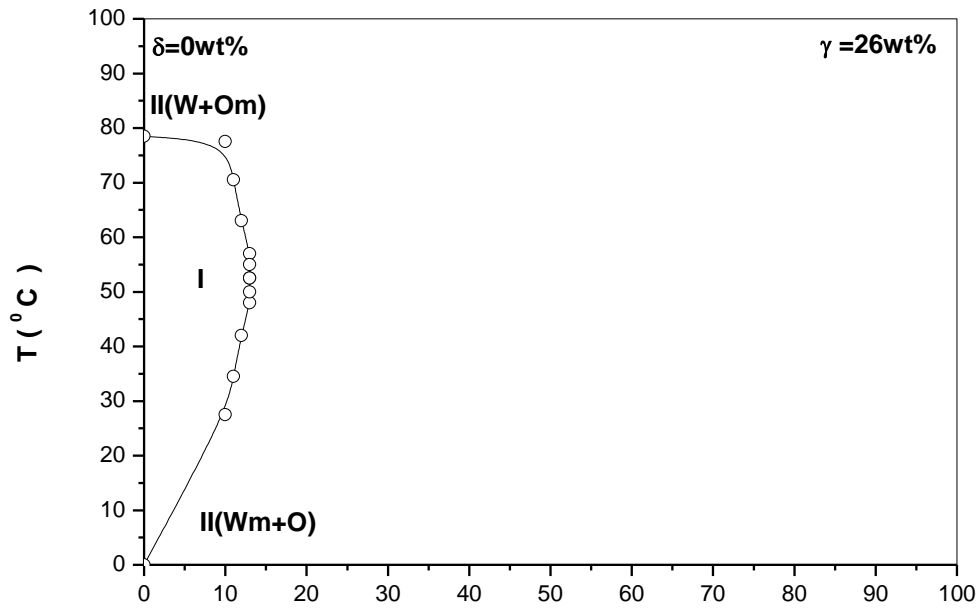
Fig. 4.17: Phase behavior of the System: Water/ L₁₆₉₅/ PG/ IPM as a function of δ , γ (wt%) and temperature at constant Oil/(Oil + Water) weight ratio, $\alpha = 50$ (wt%).

By comparing these results to results in the system: Water/ L₁₆₉₅/ IPM at $\delta = 0$ wt%, we can see that the minimum amount of L₁₆₉₅ needed to solubilize IPM in water is $\gamma_{\min} = 25$ wt% and $T = 72.5^{\circ}\text{C}$ which is bigger than those observed with the addition of PG and homogeneous microemulsion is the wider for all, and this happen at low temperature.

2-As a Function of δ, α and Temperature at Constant γ .

Fig. 4.18 shows the phase behavior of the system: Water/ L₁₆₉₅/ PG/ IPM for constant surfactant concentrations (i.e. $\delta = 0$ wt% for $\gamma = 26$ wt% (A) and $\delta = 25$ wt% for $\gamma = 31$ wt% (B)), while varying the temperature and weight ratio of oil and water. **Fig. 4.18 (A)** (i.e. $\delta = 0$ wt% for $\gamma = 26$ wt%) shows that the one phase region is shifted to the very high concentration of water (i.e. $\alpha \leq 13$ wt%) and this region becomes smaller than the region which is formed in **Fig. 4.18 (B)**. We observed that the one phase microemulsion regions appears at high water content (i.e. $\alpha \leq 21$ wt%) and this phase is bounded at high temperature by oil continuous microemulsion with excess water (W+Om) and low temperature by water continuous microemulsion with excess oil (Wm+O). Increasing α (i.e. $\alpha > 21$ wt%) the one phase microemulsion disappears and the two phase are dominant as we can see in the **Fig. 4.18 (B)**.

A



B

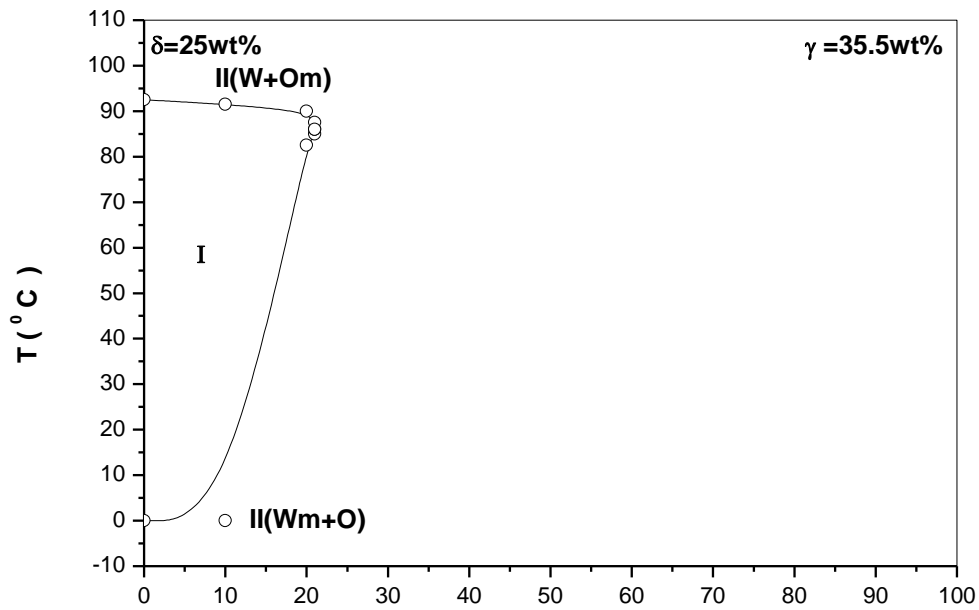


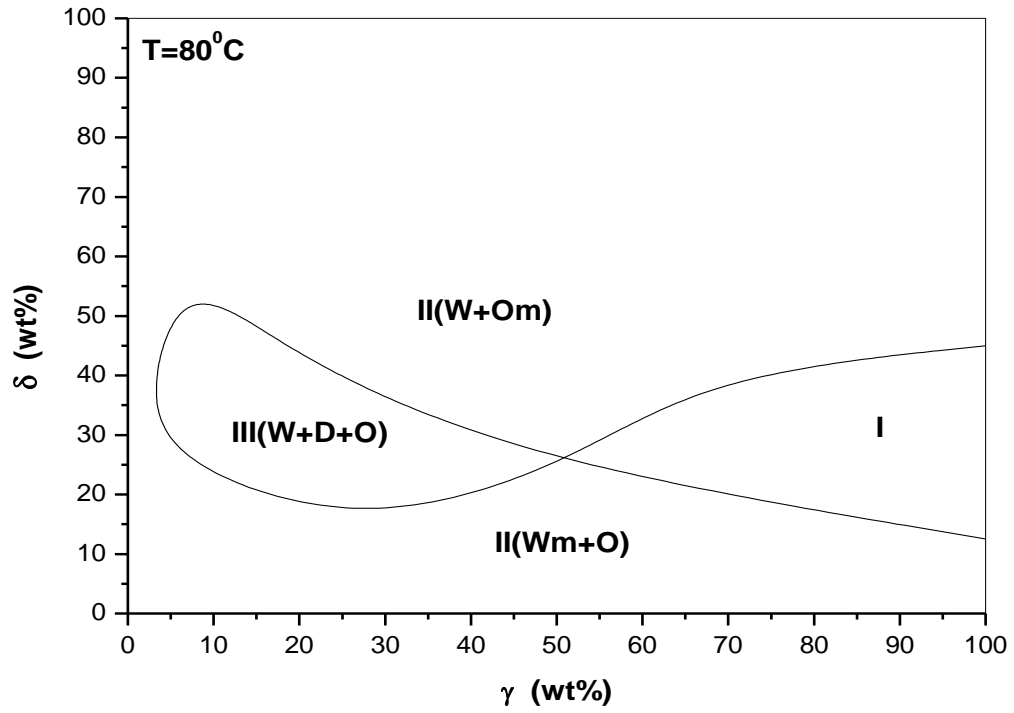
Fig. 4.18: Vertical section through the phase prism for the system: Water/ L₁₆₉₅/ PG/ IPM at constant surfactant concentration (γ) equals 26 wt% and 35.5 wt% and constant PG weight content in the mixture of surfactant (δ) and equals 0 wt% and 25 wt% as a function of temperature and $\text{Oil}/(\text{Oil} + \text{Water})$ weight ratio, α (wt%).

3-As a Function of δ, γ and Constant Temperature at $\alpha = 50$ wt%.

Fig. 4.19 (A and B), shows the phase behavior of the system: Water/ L_{1695} / PG/ IPM at $\alpha = 50$ wt% as a function of δ and γ (wt%) at constant temperature ($T = 80$ and 85°C). At 80°C , a fish phase diagram is observed; L_{1695} is mainly dissolved in water, so the two-phase region at low δ appears as II (Wm+O). As δ is increased, the three-phase body is traversed. At higher values of co-surfactant (δ) there is another two-phase region, since the mixture $L_{1695} + \text{PG}$ is mainly dissolved in oil (II (W+Om)) at 80°C . The three-phase body III (W+D+O) starts at low values of δ (i.e. $\delta = 17.5$ wt%) and at $\gamma = 27.5$ wt%, as γ increases, the amount of PG needed to promote the three-phase region also increases. When $\gamma = 51$ wt% and $\delta = 26.5$ wt% the minimum amount of total surfactant + co-surfactant necessary to form a one-phase microemulsion is present in the mixture.

At 85°C a fish phase diagram is also observed, L_{1695} remains dissolved in the water and the same II (Wm+O) \rightarrow III (W+D+O) \rightarrow II (Wm+O) phase sequence is seen as PG content increases. However, the three-phase body becomes very large and shifted toward higher δ (i.e. $\delta = 20$ wt%), indicating that more PG is present in the microemulsion. The minimum amount of total surfactant + co-surfactant necessary to form a one-phase microemulsion, is 60 wt% (i.e. $\bar{\gamma} = 60$ wt%).

A



B

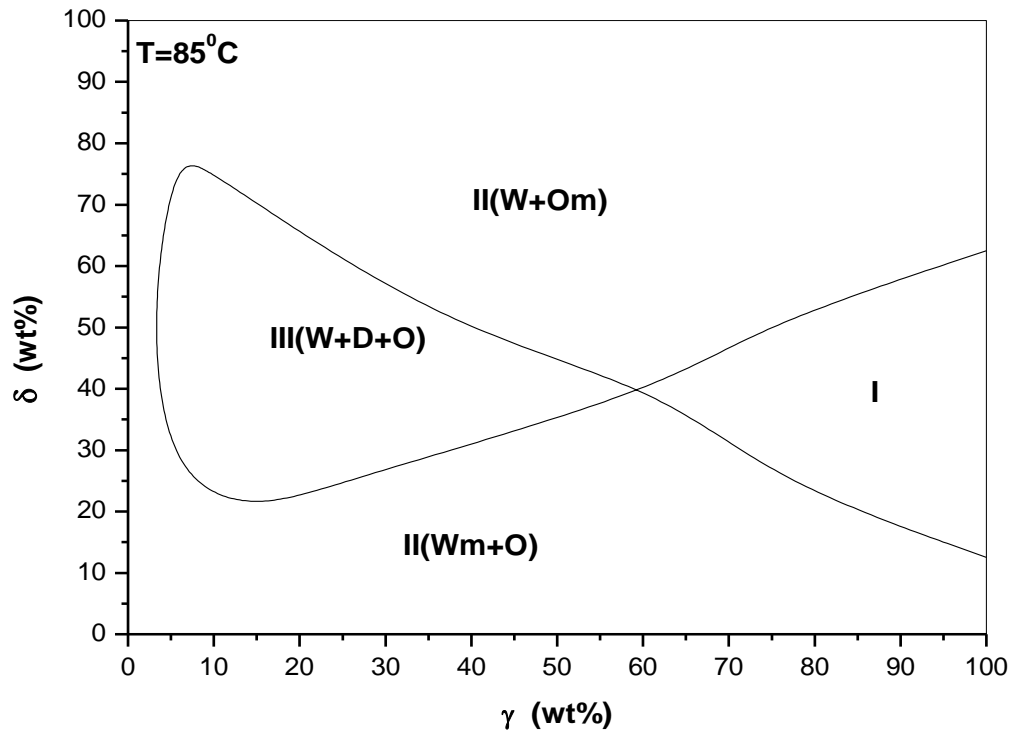


Fig. 4.19: Phase diagram for the system: Water/ L₁₆₉₅/ PG/ IPM at constant temperature ($T = 80^\circ\text{C}$ (A) and 85°C (B)) as a function of δ and γ (wt%). The *Oil/(Oil + Water)* weight ratio, $\alpha = 50$ (wt%).

Phase Behavior of the System E: Water/ S₁₅₇₀/ PG/ IPM.

1-As a Function of δ, γ and Temperature at $\alpha = 50$ wt%.

Fig. 4.20 shows the temperature-composition phase diagram of the system: Water/ S₁₅₇₀/ PG/ IPM mixture for δ (wt%) = 25%(B), 40%(C), 50%(D), 75%(E) and 100%(F) and $\delta = 0$ %(A) as reference. With the addition of PG the one phase region becomes wider and the minimum amount of mixed surfactant needed to form the one phase region increases slightly (i.e. $\gamma_{\min} = 42.5$ wt% and $T = 75^\circ\text{C}$ for $\delta = 0$ wt% to $\gamma_{\min} = 32.5$ wt% and $T = 71^\circ\text{C}$ for $\delta = 25$ wt% and $\gamma_{\min} = 25$ wt% and $T = 68^\circ\text{C}$ for $\delta = 40$ wt% while at $\delta = 50$ wt%, $\gamma_{\min} = 17.5$ wt% and $T = 67.5^\circ\text{C}$).

It is important to note that for high content of surfactant (i.e. 55 wt%) the one phase region appears at lower temperatures (i.e. 40°C) at low cosurfactant concentrations δ (i.e. < 50 wt%). And surfactant content (i.e. 65 wt%) the one phase region appears at the temperature lower temperature (i.e. 40°C) at δ (i.e. 75 wt%).

Increasing the surfactant content decreases the temperature at which the one phase appears. For high temperatures (i.e. $T > 75^\circ\text{C}$), the transition temperature from one phase to two phase is dependent on the surfactant content. It increases when γ increases.

From these results we can note that addition of PG less than $\delta = 50$ wt% will give a large one phase region, and increases the probability of the formation of homogeneous microemulsion at low concentration of surfactant. The one phase at these concentrations (low concentration of S₁₅₇₀) moves downward along the temperature scale. On the other hand the

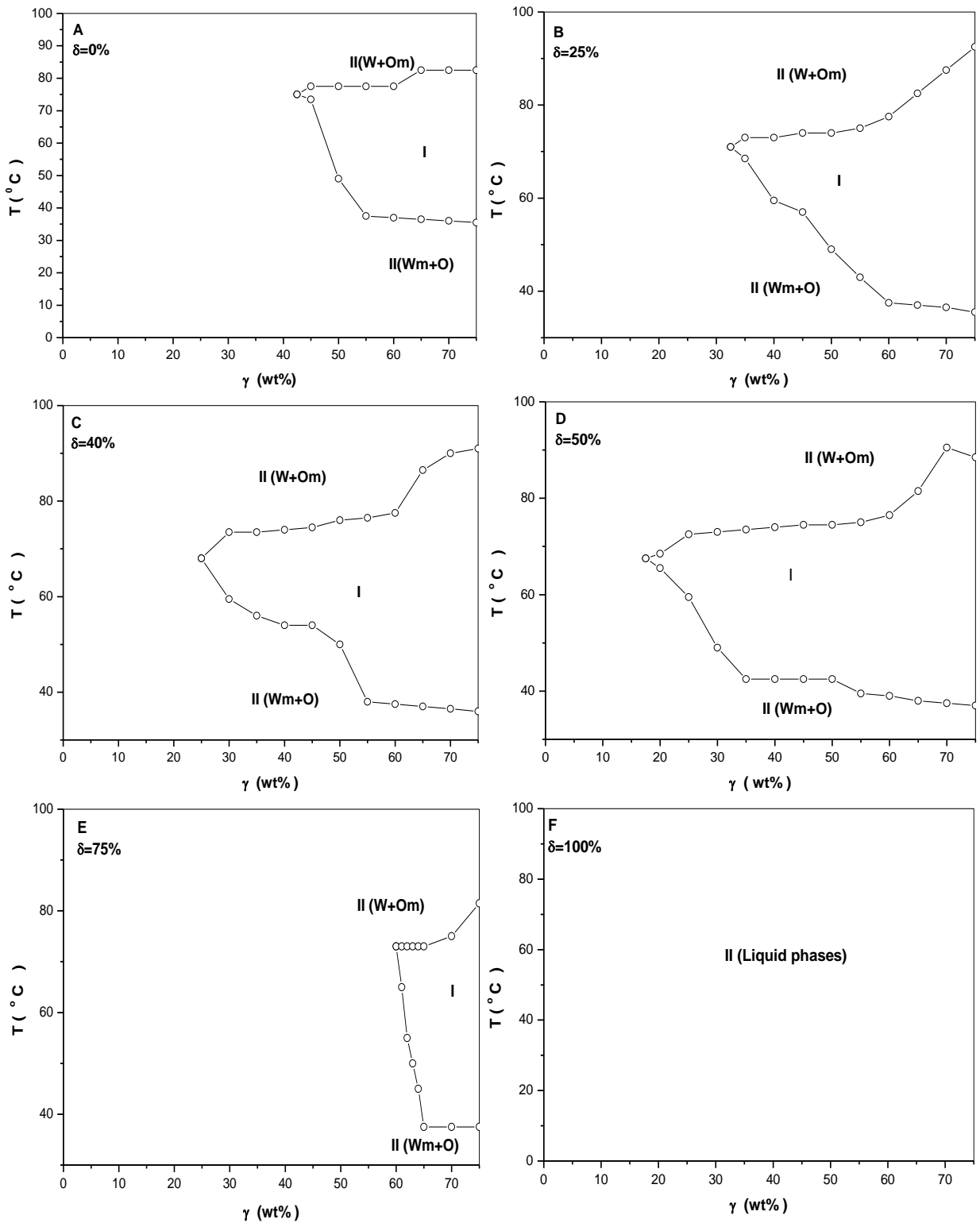


Fig. 4.20: Phase behavior of the System: Water/ S_{1570} / PG/ IPM as a function of δ , γ (wt%) and temperature at constant $Oil/(Oil + Water)$ weight ratio, $\alpha = 50$ (wt%).

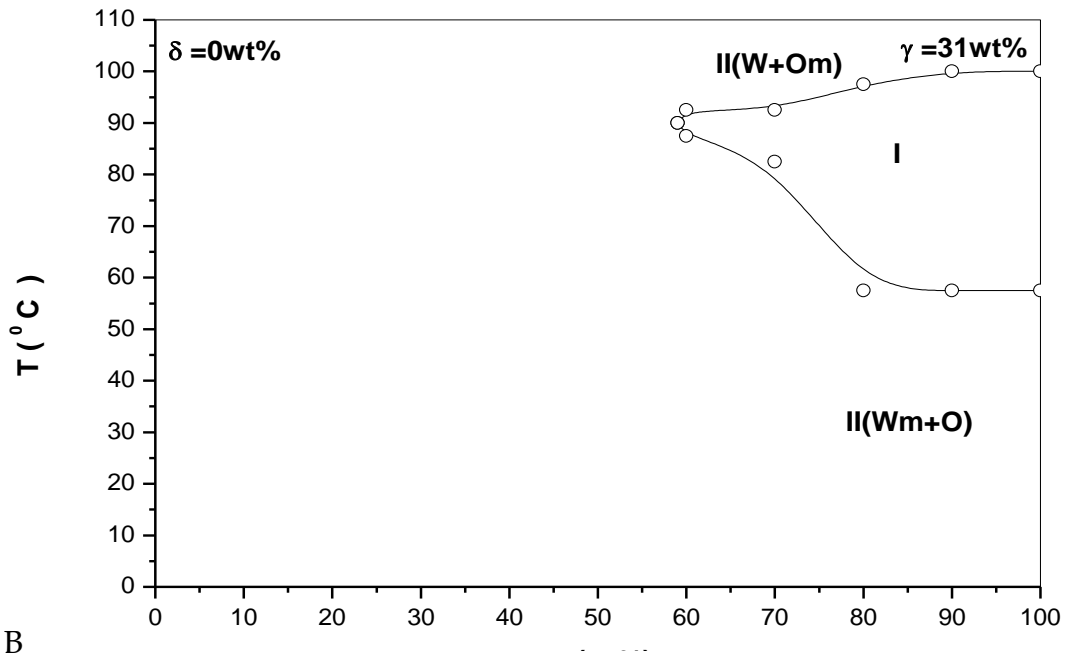
highly addition of PG more than $\delta = 50$ wt% will increase the propability of disappearance of the one phase body and the appearance of three phase body instead at $\delta = 90$ wt% (not shown), where the three phase region is formed with no formation of one phase region. At $\delta = 100$ wt% the system is separated into two liquid phases. We can say that the slightly addition of PG have a large effect on the formation of one phase region compared with no addition of PG (at $\delta = 0$ wt%).

2-As a Function of δ , α and Temperature at Constant γ .

Fig. 4.21 shows the phase behavior of the system: Water/ S₁₅₇₀/ PG/ IPM for fixed surfactant concentrations (i.e. $\delta = 0$ wt% for $\gamma = 31$ wt% (A) and $\delta = 25$ wt% for $\gamma = 26$ wt% (B)), while varying the temperature and weight ratios of oil and water. We can see that the one phase microemulsion regions are bounded at high temperatures by oil continuous microemulsions with excess water (W+Om) and at low temperatures by water continuous microemulsion with excess oil (Wm+O). With equal amounts of solubilized oil and water a bicontinuous microemulsion region appears. **Fig. 4.21 (A)** (i.e. $\delta = 0$ wt% for $\gamma = 31$ wt%) shows that at higher oil contents (i.e. $\alpha \geq 59$ wt%), the one phase microemulsion appears at high temperature (i.e. 65°C - 105°C). On the other hand there is no formation of one phase microemulsion at α values below (i.e. $\alpha < 60$ wt%) which means that the co-surfactant can not solubilize the oil in water at any temperature studied.

The presence of mono-and multiphasic lamellar regions appears at high α values, as we can see in **Fig. 4.21 (B)**. The one phase region extends over all of the range of α values and over a range of temperatures between

A



B

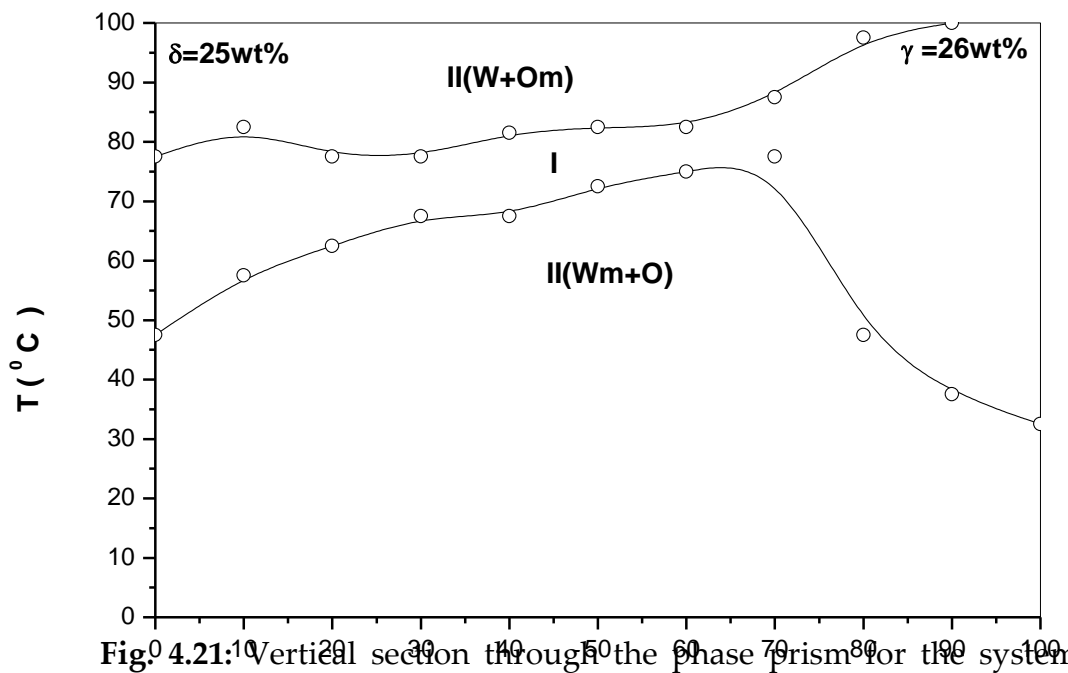


Fig. 4.21: Vertical section through the phase prism for the system: Water/ S_{1570} / PG/ IPM at constant surfactant concentration (γ) equals 31 wt% and 26 wt% and constant PG weight content in the mixture of surfactant (δ) and equals 0 wt% and 25 wt% as a function of temperature and $\text{Oil}/(\text{Oil} + \text{Water})$ weight ratio, α (wt%).

50°C - 80°C for low α values (water continuous microemulsion) and over the temperature range of 40-100°C for high α values (oil continuous microemulsion).

3-As a Function of δ, γ and Constant Temperature at $\alpha = 50$ wt%.

Fig. 4.22 shows the phase behavior of the system: Water/ S_{1570} / PG/ IPM at $\alpha = 50$ wt% as a function of δ and γ (wt%) at constant temperature $T = 70^\circ\text{C}$. At low concentrations of δ and γ the surfactant S_{1570} is mainly dissolved in water to form II (Wm+O) but with increasing the concentration γ the one phase microemulsion appears at $\gamma = 47.5$ wt%. With increasing the concentration of δ the amount of surfactant needed to form one phase region decreased (i.e. at $\delta = 46$ wt%, $\gamma = 29$ wt %).

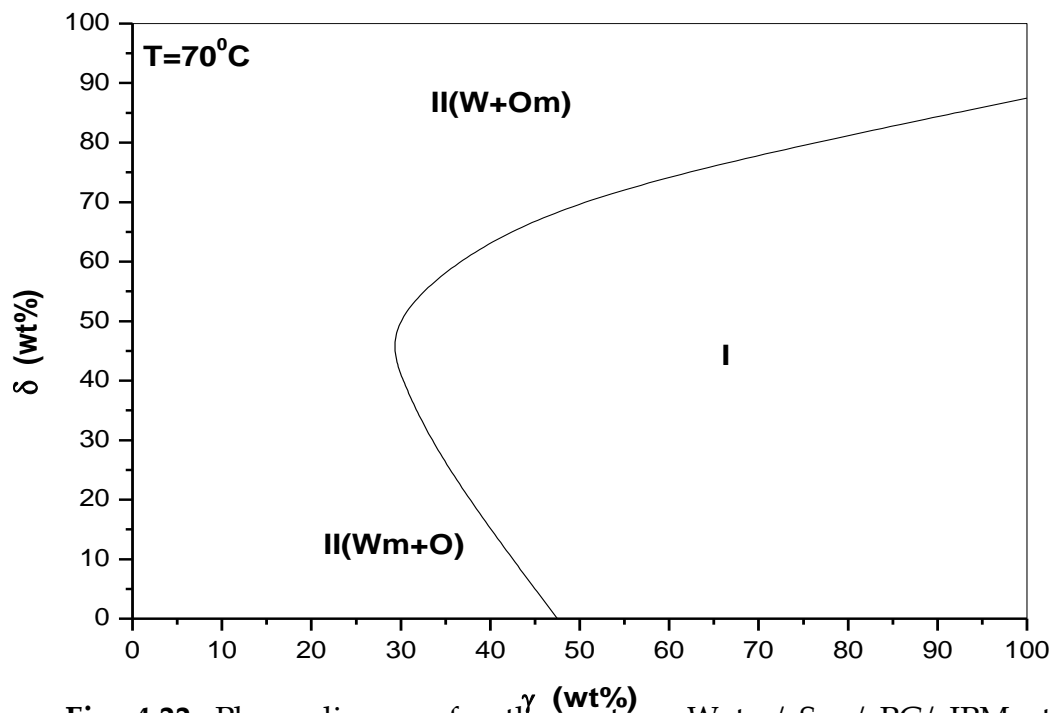


Fig. 4.22: Phase diagram for the system: Water/ S_{1570} / PG/ IPM at constant temperature ($T = 70^\circ\text{C}$) as a function of, δ and γ (wt%). The $Oil/(Oil + Water)$ weight ratio, $\alpha = 50$ (wt%).

At high concentration of δ the two phase region II (W+Om) is appeared at all γ concentrations. The three-phase body does not form at any concentrations of δ and γ .

Phase Behavior of the System F: Water/ EMDG/ PG/ IPM.

1-As a Function of δ, γ and Temperature at $\alpha = 50$ wt%.

Fig. 4.23 shows the temperature-composition phase diagram of the system: Water/ EMDG/ PG/ IPM for δ (wt%) = 50%(B), 75%(C) and 100%(D) and $\delta = 0$ %(A) as reference. Adding PG to the mixture of: Water/ EMDG/ IPM, the amount of mixed EMDG + PG needed for the formation of one phase region decreases as we can see in figures at $\delta = 50$ wt% and 75 wt%, but this is still bigger than the efficiency without PG added as we see in (A). The homogeneous microemulsion starts to form at $\delta = 50$ wt% at $\gamma_{\min} = 55$ wt% and $T = 55^\circ\text{C}$, and at low concentration of surfactant the one phase (fish tail) or the three phase (fish body) didn't form. While at $\delta = 75$ wt% the one phase region starts to form at $\gamma_{\min} = 35$ wt% and $T = 55^\circ\text{C}$ and at $\gamma = 55$ wt% the one phase region is formed at $T = 21.5^\circ\text{C}$. In comparison with $\delta = 0$ wt% (A) the homogeneous microemulsion region (fish tail) is formed at $\bar{\gamma} = 26.5$ wt% and $\bar{T} = 105^\circ\text{C}$. Increasing the ratio of PG/ EMDG will shift the system toward the formation of one phase region at higher concentrations of surfactant compared to ternary system when PG is absent, no three phase region is observed with high ratios of PG/ EMDG, in opposite to the L₁₆₉₅ containing system.

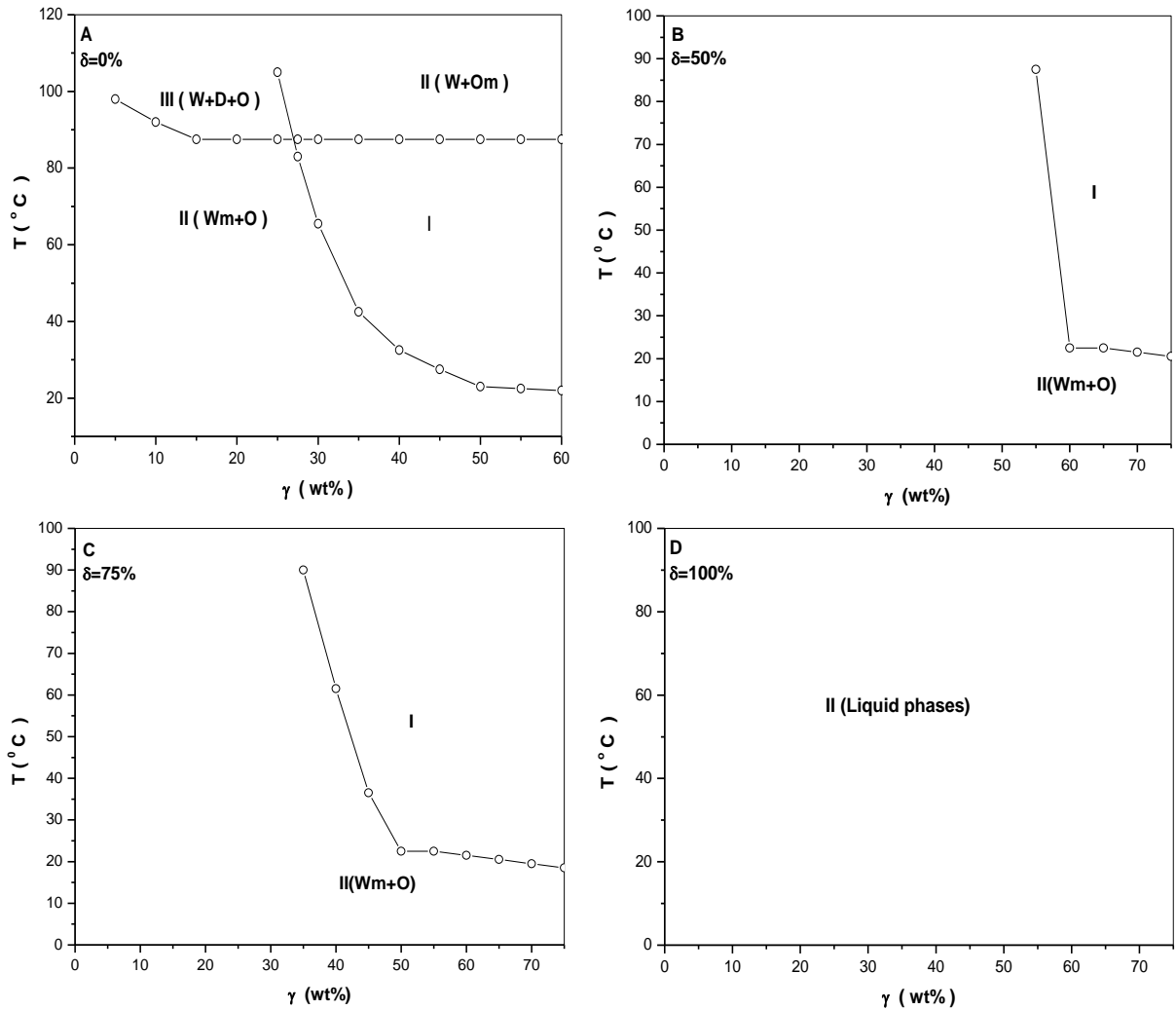


Fig. 4.23: Phase behavior of the System: Water/ EMDG/ PG/ IPM as a function of δ , γ (wt%) and temperature at constant $Oil/(Oil + Water)$ weight ratio, $\alpha = 50$ (wt%).

2-As a Function of δ , γ and Constant Temperature at $\alpha = 50$ wt%.

Fig. 4.24 shows the phase behavior of the system: Water/ EMDG/ PG/ IPM at $\alpha = 50$ wt% as a function of δ and γ (wt%) at constant temperature $T = 87^\circ\text{C}$. At 87°C , EMDG is mainly dissolved in water to form II(Wm+O) at very low values of surfactant content and the one phase microemulsion formed at mixed surfactant concentration $\gamma = 27.5$ wt%. By

increasing δ (i.e. co-surfactant concentration (PG)) the one phase microemulsion region is formed at mixed surfactant and cosurfactant concentration more than 27.5 wt%. Increasing co-surfactant concentration (i.e. δ (more than 75 wt%)) the mixed surfactant becomes too oil soluble and the aqueous phase separates out into II(W+Om).

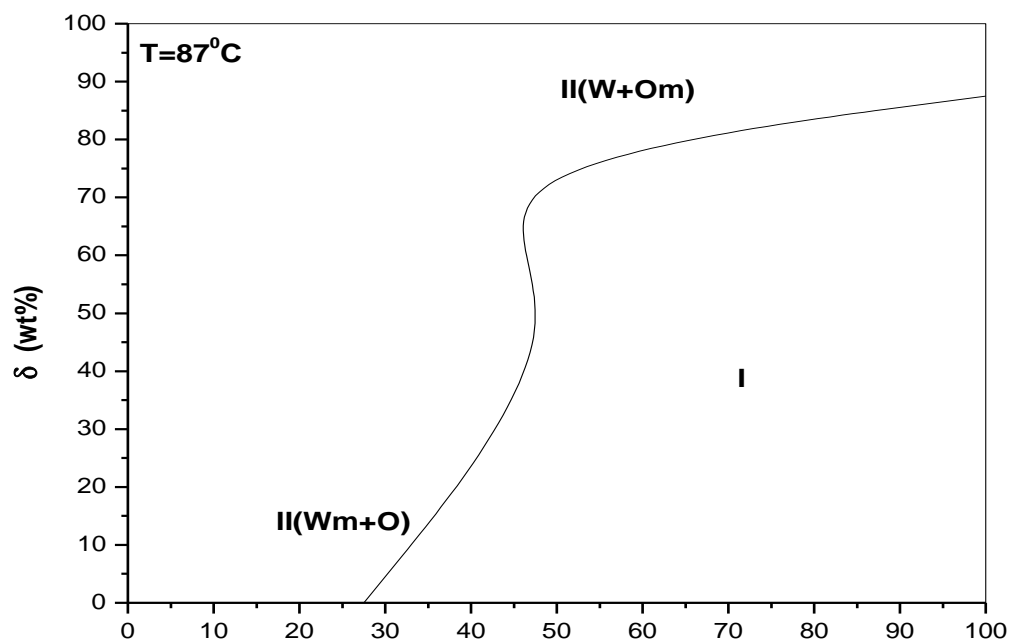


Fig. 4.24: Phase diagram for the system Water/ EMDG/ PG/ IPM at constant temperature ($T = 87^{\circ}\text{C}$) as a function of δ and γ (wt%). The Oil/(Oil + Water) weight ratio, $\alpha = 50$ (wt%).

Phase Behavior of the System G: Water/ L₁₆₉₅/ PG/ MCT.

1-As a Function of δ, γ and Temperature at $\alpha = 50$ wt%.

Fig. 4.25 shows the temperature-composition phase diagram of the system: Water/ L₁₆₉₅/ PG/ MCT for δ (wt%) = 25%(B), 40%(C), 50%(D), 90%(E) and 100%(F). The system: Water/ L₁₆₉₅/ MCT (fish) ($\delta = 0$ wt% (A)) is shown as a reference.

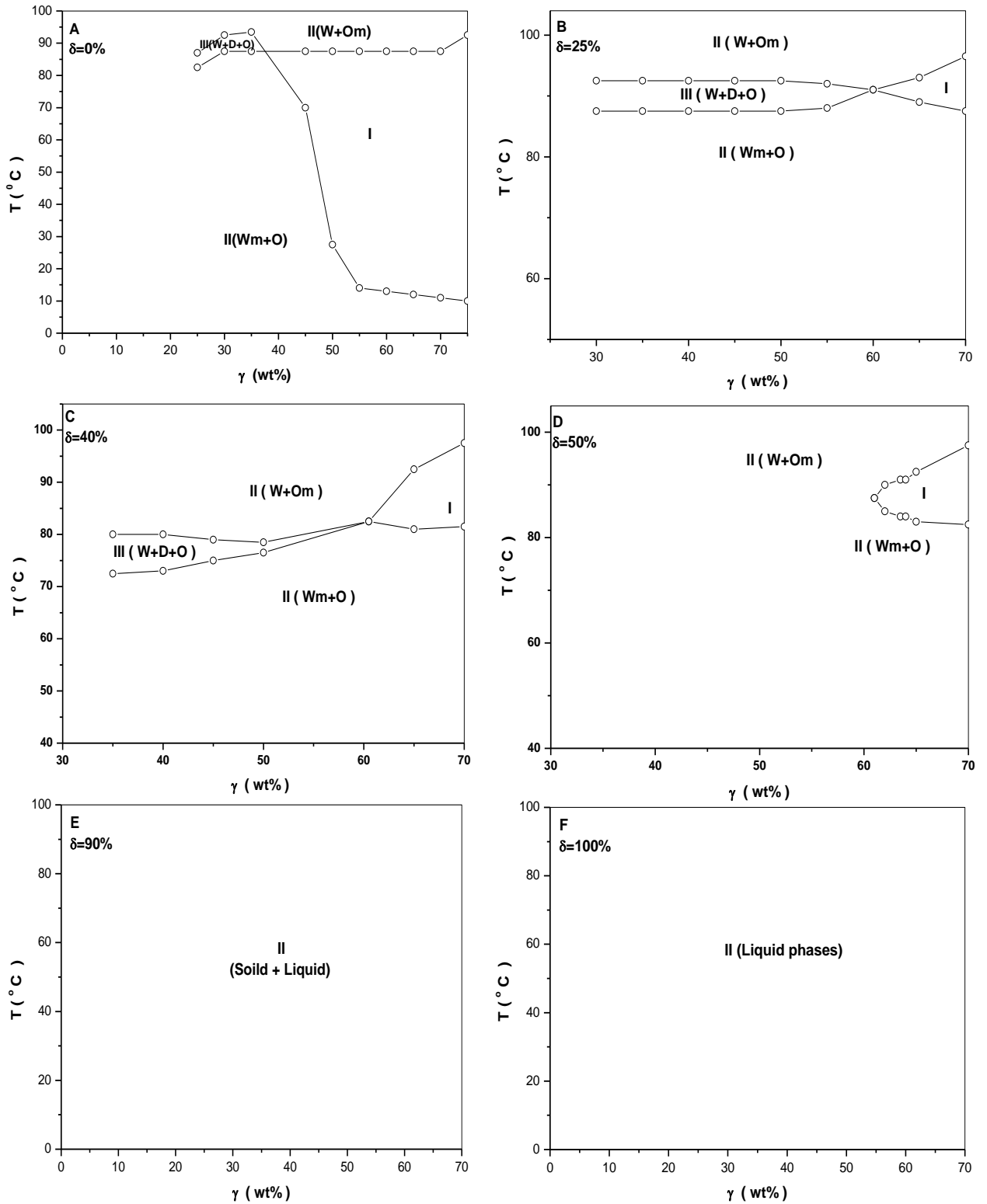


Fig. 4.25: Phase behavior of the System: Water/ L₁₆₉₅/ PG/ MCT as a function of δ , γ (wt%) and temperature at constant $Oil/(Oil + Water)$ weight ratio, $\alpha = 50$ (wt%).

The homogeneous microemulsion region (fish tail) becomes wide and the efficiency of the surfactant mixture increases (i.e. $\bar{\gamma} = 60$ wt% and $\bar{T} = 91^\circ\text{C}$ for $\delta = 25$ wt% and $\bar{\gamma} = 50$ wt% and the $\bar{T} = 82.5^\circ\text{C}$ for $\delta = 40$ wt% and $\gamma_{\min} = 45$ wt% and the $T = 87.5^\circ\text{C}$ for $\delta = 50$ wt%). While high addition of PG (i.e. $\delta = 75$ wt%) no homogeneous microemulsion one phase region is formed.

The three-phase body disappears with increasing the concentration of PG from $\delta = 40$ wt% to $\delta = 50$ wt%, and its appearance moves downward on the temperature scale. At high concentration of cosurfactant (PG) the three phase body appears another time without formation of homogenous microemulsion region.

It is important to note that for high content of surfactant (i.e. 55 wt%) the one phase region appears at lower temperatures (i.e. 20°C). Increasing the surfactant content decreases the temperature at which the one phase appears. For high temperatures (i.e. $T > 75^\circ\text{C}$), the transition temperature from one phase to two phase is dependent on the surfactant content. It increases when γ increases.

2-As a Function of δ, γ and Constant Temperature at $\alpha = 50$ wt%.

Fig. 4.26 shows the phase behavior of the system: Water/ L₁₆₉₅/ PG/ MCT at $\alpha = 50$ wt% as a function of δ and γ (wt%) at constant temperature ($T = 90^\circ\text{C}$). At low values of ($\delta =$ ratio of concentrations \Rightarrow number) the surfactant L₁₆₉₅ dissolved in the water II (Wm+O) and the sequence II (Wm+O) \rightarrow III (W+D+O) \rightarrow II (W+Om) is seen as δ increases. At higher values of δ there are another two-phase region II (W+Om) since L₁₆₉₅ + PG is

mainly dissolved in the oil. As the concentration of the surfactant increased (i.e. γ) the amount of the co-surfactant (i.e. δ) necessary to form the three phase is increased. The minimum amount of surfactant γ needed to form one phase microemulsion is $\gamma = 57.5$ wt% at $\delta = 27$ wt%.

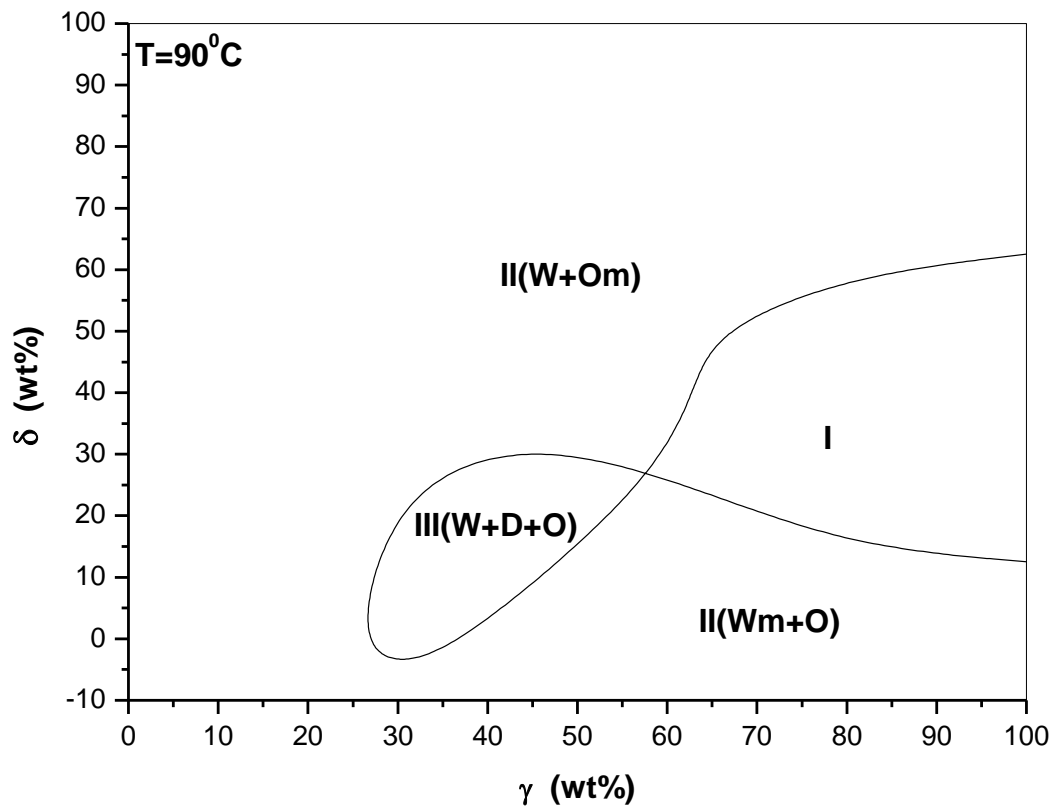


Fig. 4.26: Phase diagram for the system: Water/ L₁₆₉₅/ PG/ MCT at constant temperature ($T = 90^\circ\text{C}$) as a function of δ and γ (wt%). The $\text{Oil}/(\text{Oil} + \text{Water})$ weight ratio, $\alpha = 50$ (wt%).

Phase Behavior of the System H: Water/ S₁₅₇₀/ PG/ MCT.

1-As a Function of δ, γ and Temperature at $\alpha = 50$ wt%.

Fig. 4.27 shows the temperature-composition phase diagram of the system: water/ S₁₅₇₀/ PG/ MCT, for δ (wt%) = 25%(B), 40%(C), 50%(D) and 100%(E) and Water/ S₁₅₇₀/ MCT for $\delta = 0%$ (A) as a reference at $\alpha = 50$ wt%. With the addition of PG the homogeneous microemulsion region (one phase region) becomes larger and at high concentration of surfactant (S₁₅₇₀) we got this region at low temperature which means that the one phase moves downward on the temperature scale as we can see at $\delta = 25$ wt%.

The one phase region is formed at $T = 57^\circ\text{C}$ for $\gamma = 65$ wt% at $\delta = 25$ wt%, with increasing PG concentration (i.e. $\delta = 40$ wt%) this phase is formed at $T = 42.5^\circ\text{C}$ and $\gamma = 70$ wt% and at $\delta = 50$ wt% this phase formed at $T = 42.5^\circ\text{C}$ and $\gamma = 75$ wt%.

At low concentration of surfactant less than $\gamma = 51$ wt% the three phase region is formed. At high ratios of PG/ S₁₅₇₀ more than $\delta = 50$ wt% the homogeneous microemulsion (one phase region) will not form over all of the range of concentrations of surfactant but the three phase region is still present and disappears at $\delta = 100$ wt%.

As we can see in the **Fig. 4.27 (A)** at $\delta = 0$ wt%, the mean temperature $\bar{T} = 83^\circ\text{C}$ while with adding PG the mean temperature also the same (i.e. $\bar{T} = 83^\circ\text{C}$), and the addition of PG will not affect the homogeneous microemulsion region (fish tail) because it still formed at $\bar{\gamma} = 52$ wt% at all concentration of PG from $\delta = 0$ wt% to $\delta = 50$ wt%.

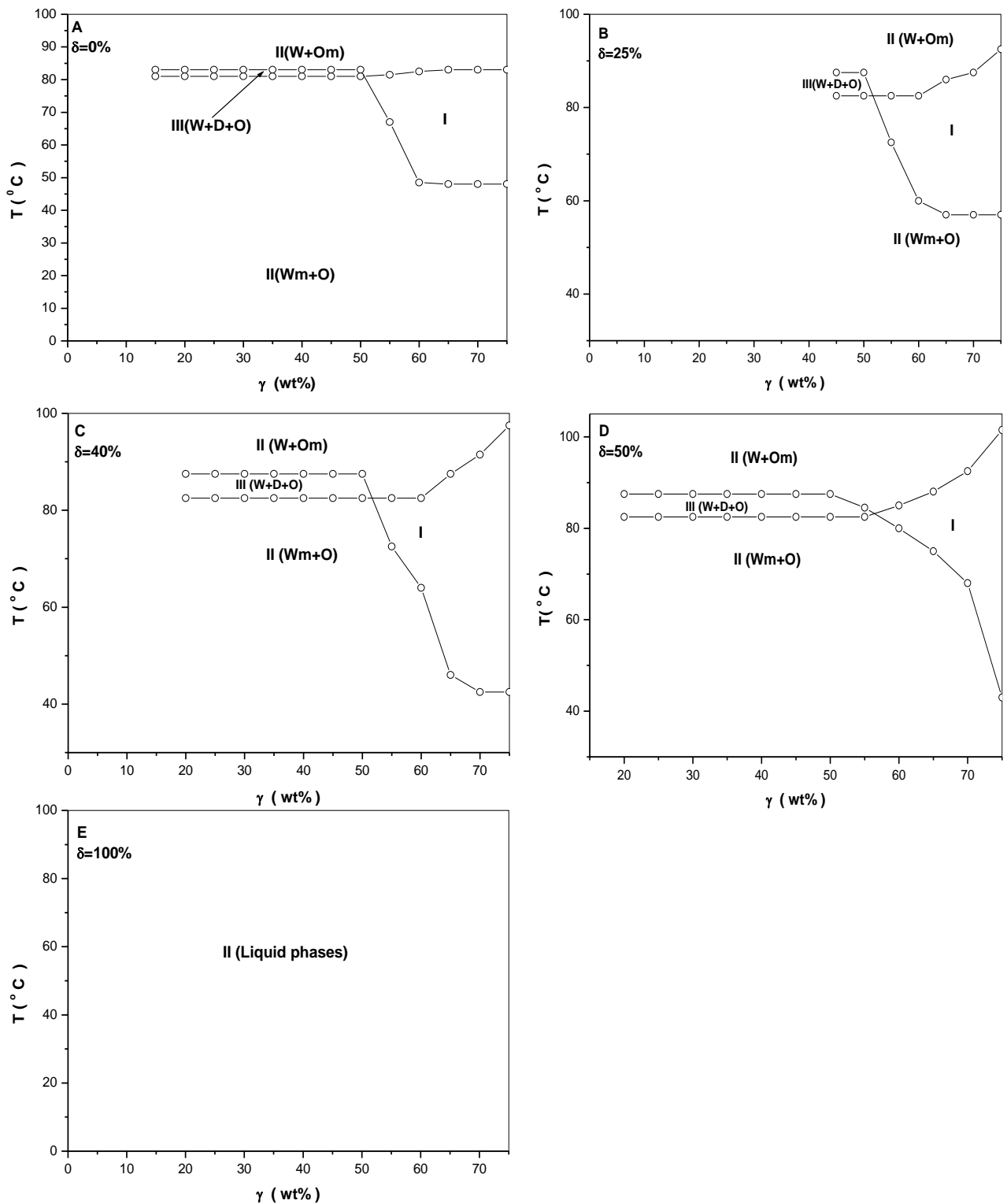


Fig. 4.27: Phase behavior of the System: Water/ S₁₅₇₀/ PG/ MCT as a function of δ , γ (wt%) and temperature at constant $Oil/(Oil + Water)$ weight ratio, $\alpha = 50$ (wt%).

2-As a Function of δ, α and Temperature at Constant γ .

Fig. 4.28 shows the phase behavior of the system: Water/ S₁₅₇₀/ PG/ MCT for constant surfactant concentration (i.e. $\delta = 25$ wt% for $\gamma = 35.5$ wt%) with varying temperature and weight ratios of oil and water. The one phase microemulsion regions are bounded at higher temperature by oil continuous microemulsions with excess water (W+Om) and at low temperature by water continuous microemulsion with excess oil (Wm+O). On the other hand the one phase microemulsion at high water concentrations (i.e. $\alpha < 60$ wt%) is not present at any temperature studied and the two phase region are formed.

3-As a Function of δ, γ and Constant Temperature at $\alpha = 50$ wt%.

Fig. 4.29 shows the phase behavior of the system: Water/ S₁₅₇₀/ PG/ MCT at $\alpha = 50$ wt% as a function of δ and γ (wt%) at constant temperature $T = 85^\circ\text{C}$. At low values of δ the S₁₅₇₀ is mainly dissolved in the water to form II (Wm+O). At higher values of δ there is another two phase region II (W+Om) since the mixture S₁₅₇₀ + PG is mainly dissolved in the oil. The three-phase III(W+D+O) body starts at low values of δ (i.e. $\delta > 20$ wt%) and extends to high values of δ (i.e. $\delta = 85$ wt%). As γ increases the amount of S₁₅₇₀ needed to promote the three-phase body also increases, with the three phase body extending to a minimum δ (i.e. $\delta = 25$ wt%) at $\gamma = 59$ wt%. When $\gamma = 60$ wt% the minimum amount of the total surfactant necessary to form a one phase microemulsion is present in the mixture, while the concentration of the co-surfactant is $\delta = 28$ wt%.

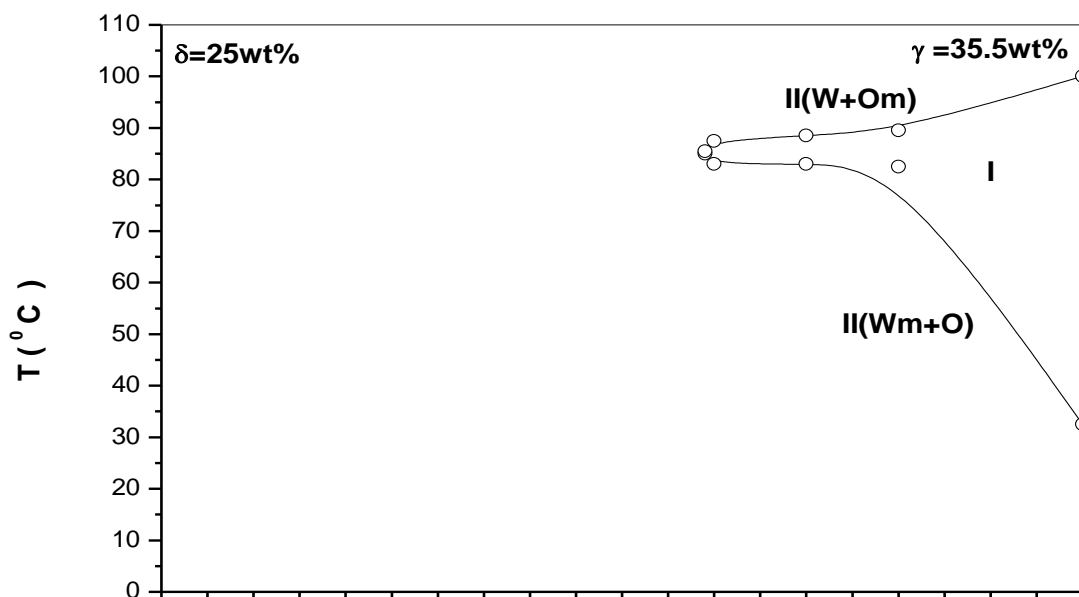


Fig. 4.28: Vertical section through the phase prism for the system: Water/ S₁₅₇₀/ PG/ MCT at constant surfactant concentration (γ) equals 35.5 wt% and constant PG weight content in the mixture of surfactant (δ) and equals 25 wt% as a function of temperature and *Oil/(Oil + Water)* weight ratio, α (wt%).

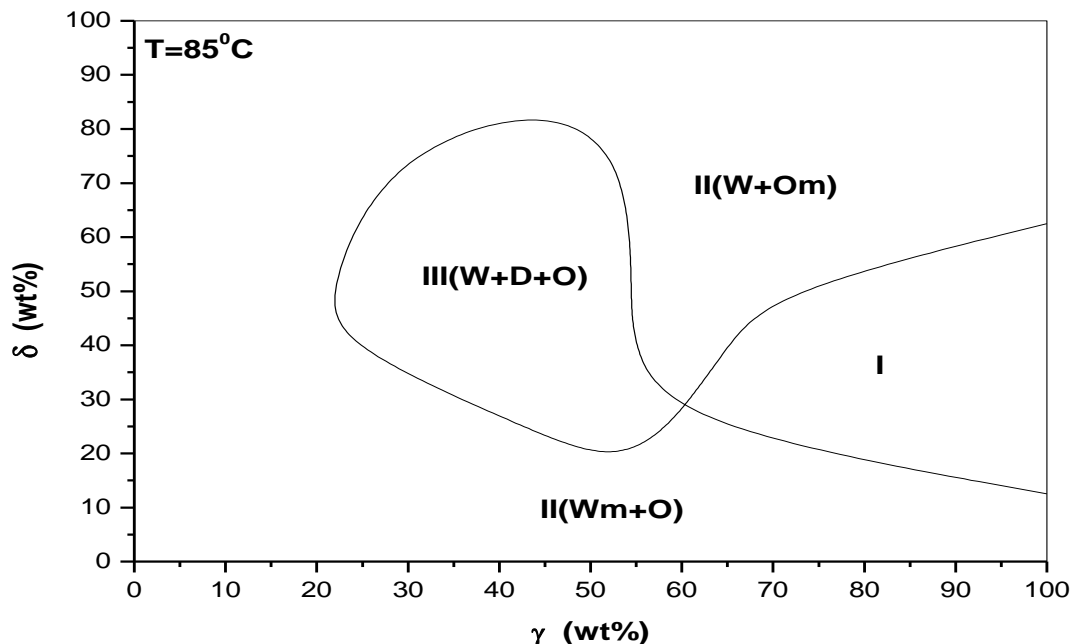


Fig. 4.29: Phase diagram for the system: Water/ S₁₅₇₀/ PG/ MCT at constant temperature ($T = 85^\circ\text{C}$) as a function of δ and γ (wt%). The *Oil/(Oil + Water)* weight ratio, $\alpha = 50$ (wt%).

Phase Behavior of the System I: Water/ EMDG/ PG/ MCT.

1- As a Function of δ, γ and Temperature at $\alpha = 50$ wt%.

Fig. 4.30 show the temperature-composition phase diagram of the system: Water/ EMDG/ PG/ MCT mixture for δ (wt%) = 0%(A), 50%(B), 75%(C), and (D)100%. With little addition of PG to the system there is no solubilization of oil in the water. The same behavior is observed with high ratios of PG/ EMDG (i.e. $\delta = 100$ wt%) as we can see in the **Fig. 4.30 (D)**. With medium addition of PG the one phase appears and increases slightly at high concentrations of surfactant more than $\gamma = 55$ wt% of EMDG (i.e. $T_1 = 50^\circ\text{C}$ at $\gamma = 75$ wt%, $\delta = 50$ wt%, $T_1 = 30^\circ\text{C}$ at $\gamma = 65$ wt%, $\delta = 75$ wt%). Adding PG to the systems will shift it toward the formation of the one phase region. At $\delta = 100$ wt% (**Fig. 4.30 D**) there is no solubilization of oil in water in the presence of PG.

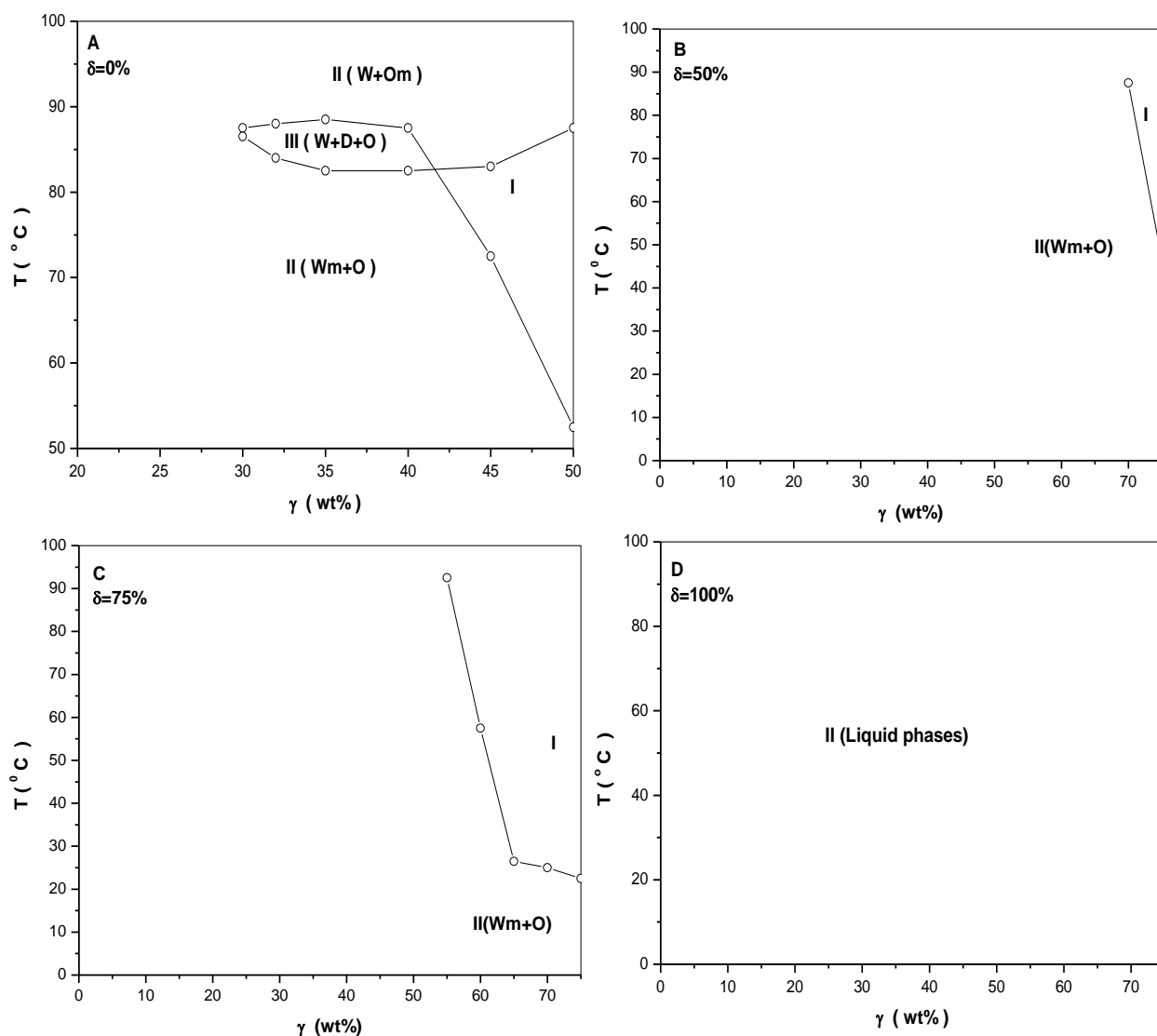


Fig. 4.30: Phase behavior of the System: Water/ EMDG/ PG/ MCT as a function of δ , γ (wt%) and temperature at constant $\text{Oil}/(\text{Oil} + \text{Water})$ weight ratio, $\alpha = 50$ (wt%).

2-As a Function of δ , γ and Constant Temperature at $\alpha = 50$ wt%.

Fig. 4.31 shows the phase behavior of the system: Water/ EMDG/ PG/ MCT at $\alpha = 50$ wt% as a function of δ and γ (wt%) at constant temperature $T = 60^{\circ}\text{C}$. At 60°C , EMDG is mainly dissolved in water to form II(Wm+O) at

low values of surfactant content, and form one phase microemulsion at surfactant concentration γ (i.e. $\gamma = 47.5$ wt%). By increasing the co-surfactant concentration (i.e. δ) the amount of the mixed surfactant and cosurfactant needed to form one phase microemulsion region is increased. At very high concentration of co-surfactant (i.e. PG) the mixed surfactant becomes too oil soluble and an aqueous phase separates out so the II (W+Om) is present.

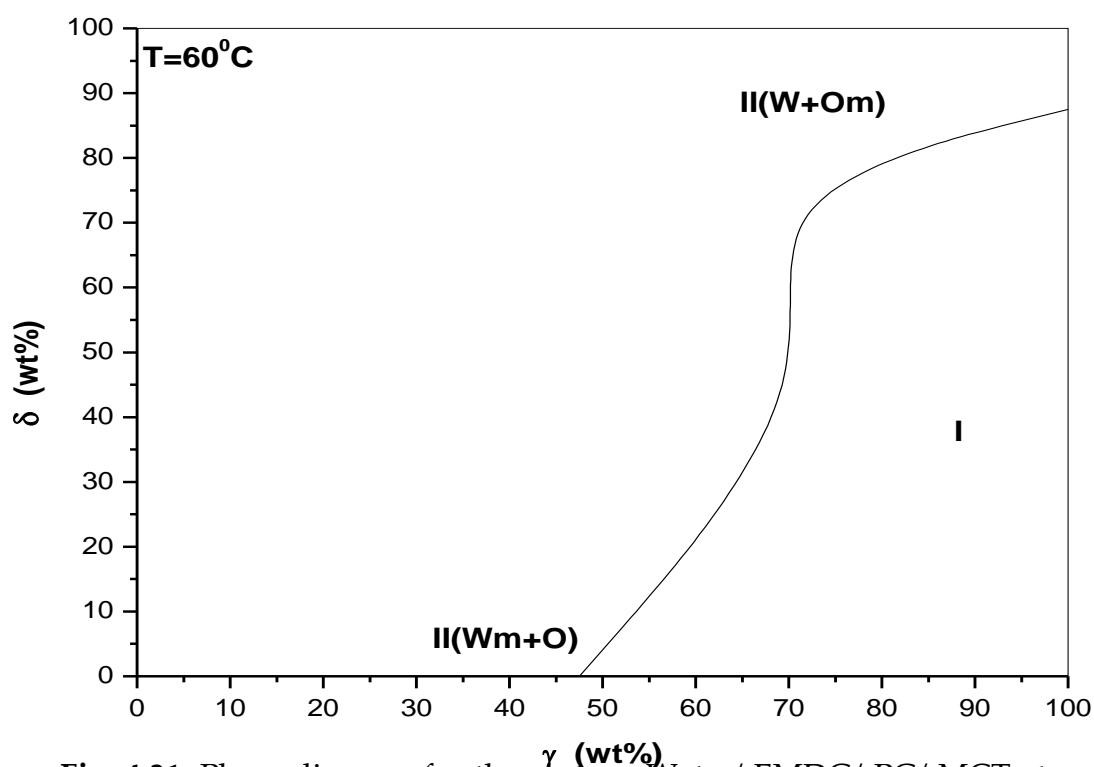


Fig. 4.31: Phase diagram for the system: Water/ EMDG/ PG/ MCT at constant temperature ($T = 60^\circ\text{C}$) as a function of δ and γ (wt%). The $Oil/(Oil + Water)$ weight ratio, $\alpha = 50$ (wt%).

Phase Behavior of the System J: Water/ L₁₆₉₅/ EMDG/ R(+)-Limonene.

1- As a Function of δ , γ and Temperature at $\alpha = 50$ wt%.

Fig. 4.32 shows the temperature-composition phase diagram of the system: Water/ L₁₆₉₅/ EMDG/ R(+)-Limonene for δ (wt%) = 0%(A), 25%(B), 50%(C), 75%(D), and 100%(E). Adding EMDG cause the homogeneous microemulsion region (fish tail) and the efficiency of the surfactant mixture to increase (i.e. $\bar{\gamma} = 21$ wt% for $\delta = 25$ wt% , $\bar{\gamma} = 16.5$ wt% for $\delta = 50$ wt%), when increasing the EMDG/ L₁₆₉₅ ratio, a three phase body appears at low concentration of surfactant (L₁₆₉₅) the one phase region becomes wider with increasing the ratio of EMDG/ L₁₆₉₅ as we can see in the Fig. 4.32 (B and D) and this region moves downward in the temperature scale, but the mean temperature move up ward in the temperature scale (i.e. $\bar{T} = 85^\circ\text{C}$ for $\delta = 25$ wt%, $\bar{T} = 90^\circ\text{C}$ for $\delta = 50$ wt%). When increasing the ratio of EMDG/ L₁₆₉₅ more than $\delta = 50$ wt% the three phase region disappears and, the one phase region is the dominant at high concentrations of surfactant. The minimum amount of mixed L₁₆₉₅ + EMDG needed for the formation of one phase region increases as EMDG content increases.

It is important to note that for high content of surfactant (i.e. 55 wt%) the one phase region appears at lower temperatures (i.e. 20°C). Increasing the surfactant content decreases the temperature at which the one phase appears. For high temperatures (i.e. $T > 75^\circ\text{C}$), the transition temperature from one phase to two phase is dependent on the surfactant content. It increases when γ increases.

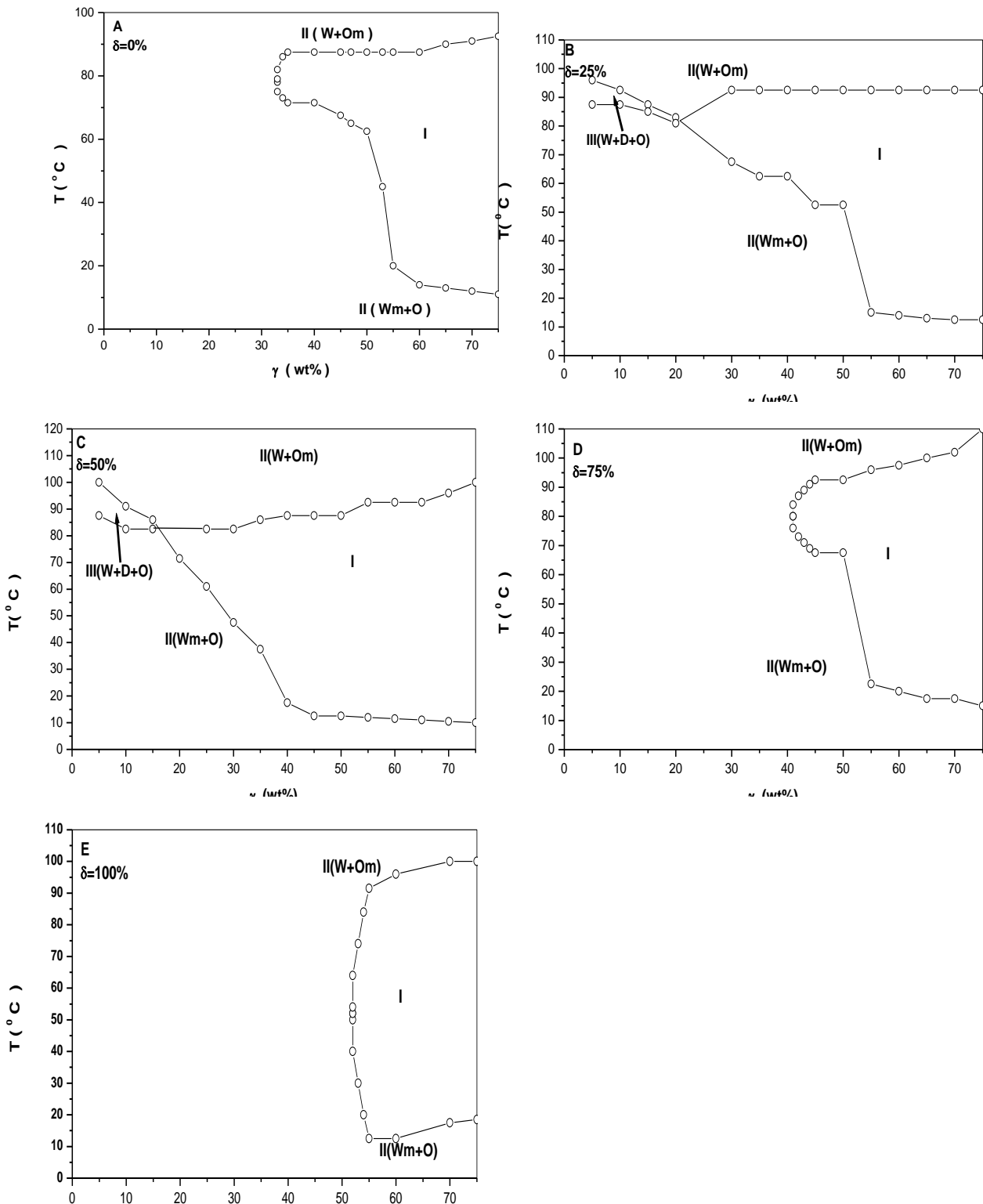


Fig. 4.32: Phase behavior of the System: Water/ L_{1695} / EMDG/ $R(+)$ -Limonene as a function of δ , γ (wt%) and temperature at constant $Oil/(Oil + Water)$ weight ratio, $\alpha = 50$ (wt%).

2-As a Function of δ , α and Temperature at Constant γ .

Fig. 4.33 shows the phase behavior of the system: Water/ L₁₆₉₅/ EMDG/ R (+)-Limonene for fixed surfactant concentration (i.e. $\delta = 25$ wt% for $\gamma = 26$ wt% (A), and $\delta = 50$ wt%, for $\gamma = 31$ wt% (B)), with varying the temperature and weight ratios of oil and water (i.e. α) the one phase microemulsion appears over all of the range of α values. When $\delta = 25$ wt% (**Fig. 4.33(A)**), the one phase channel becomes less wide on the temperature range, and shifts upward in the temperature scale (i.e. $80^\circ\text{C} < T < 90^\circ\text{C}$). When the α values are between 30 wt% and 70 wt%, it appears at $T = 83.5^\circ\text{C}$.

At low α value (i.e. $\alpha < 30$ wt%) the one phase region is a water continuous one and at high α value (i.e. $\alpha > 70$ wt%) the one phase region is converted to oil continuous one. For medium α values between (i.e. 30 wt% and 70 wt%) the one phase region can be a bicontinuous one. This type of behavior is also observed in all later systems studied that have a one phase region extended over all the range of α values. In the one-phase regions a lamellar liquid crystal phase can exist at low temperatures. The range of temperatures over which this one phase channel is wide extends from 15°C to 95°C for all of the range of α values, as shown in **Fig. 4.33(B)**.

A

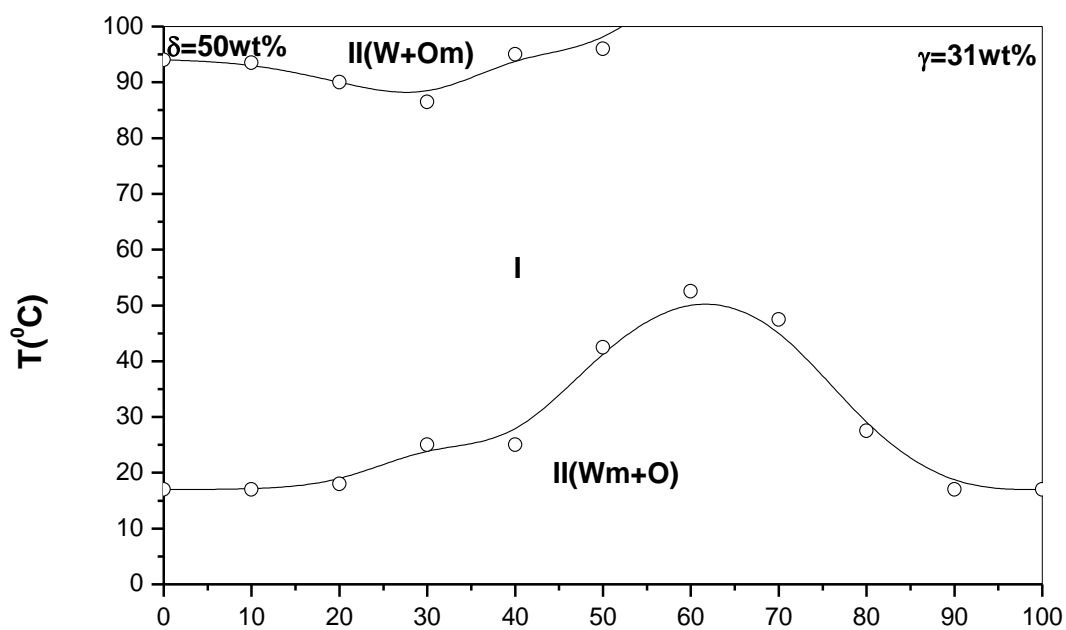
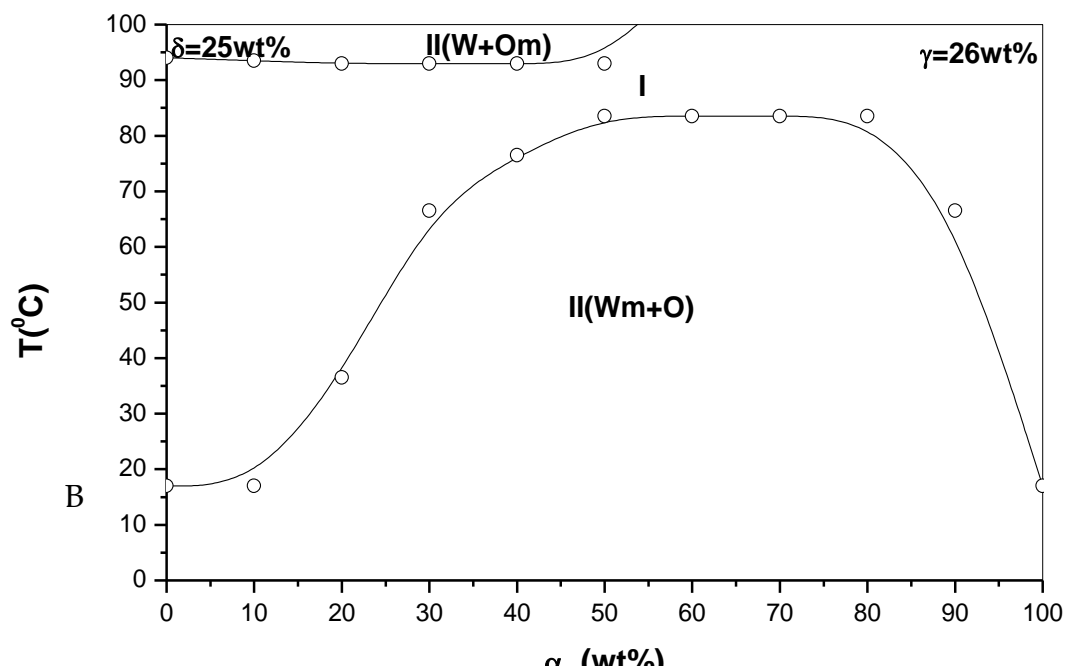


Fig. 4.33: Vertical section through the phase prism for the system: Water/ L_{1695} / EMDG/ R (+)-Limonene at constant surfactant concentration (γ) equals 26 wt% and 31 wt% and constant EMDG weight content in the mixture of surfactant (δ) and equals 25 wt% and 50 wt% as a function of temperature and *Oil/(Oil + Water)* weight ratio, α (wt%).

3-As a Function of δ, γ and Constant Temperature at $\alpha = 50$ wt%.

Fig. 4.34 shows the phase behavior of the system: Water/ L₁₆₉₅/ EMDG/ R (+)-Limonene at $\alpha = 50$ wt% as a function of δ and γ (wt%) at constant temperature $T = 85^\circ\text{C}$. At 85°C , a fish phase diagram is observed and low concentration of co-surfactant (δ) the two-phase region appeared at $\gamma \leq 28$ wt% but at $\gamma > 28$ wt% the one-phase microemulsion region appeared. By increasing the concentration of co-surfactant (δ) the three-phase body appears at very low concentration of surfactant (i.e. $\gamma = 6$ wt% at $\delta = 50$ wt%). Increasing δ promotes the sequence II (Wm+O) \rightarrow III (W+D+O) \rightarrow II (W+Om). The (W+Om) region is formed at low δ with increasing the concentration of surfactant + co-surfactant γ . On the other hand, the one-phase microemulsion is shifted slightly to high concentration of γ by increasing the concentration of δ .

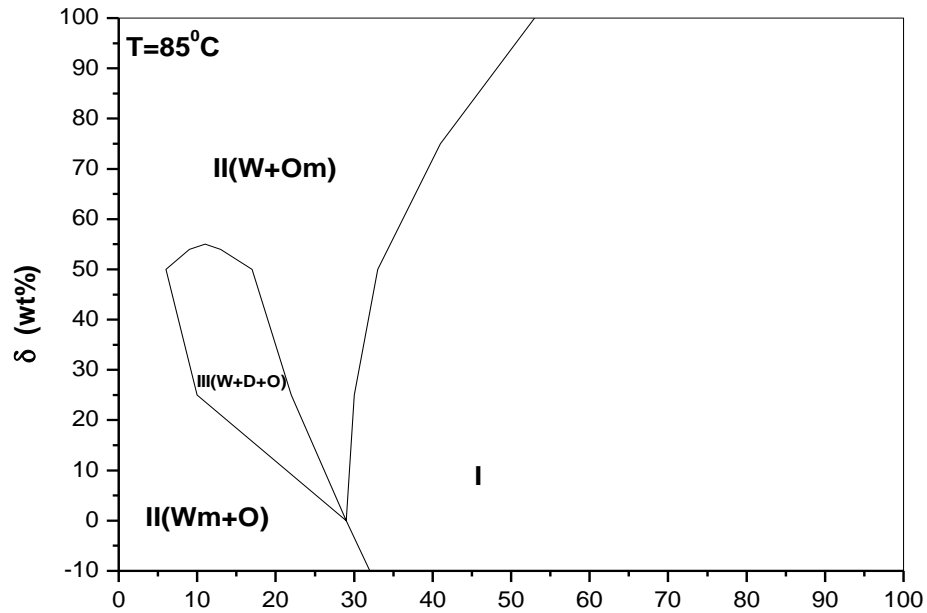


Fig. 4.34: Phase diagram for the γ system: Water/ L₁₆₉₅/ EMDG/ R(+)-Limonene at constant temperature ($T = 85^\circ\text{C}$) as a function of δ and γ (wt%). The $\text{Oil}/(\text{Oil} + \text{Water})$ weight ratio, $\alpha = 50$ (wt%).

Phase Behavior of the System K: Water/ S₁₅₇₀/ EMDG/ R(+)-limonene

1-As a Function of δ , γ and Temperature at $\alpha = 50$ wt%.

Fig. 4.35 shows the temperature-composition phase diagram of the system: Water/ S₁₅₇₀/ EMDG/ R(+)-Limonene mixture for δ (wt%) = 25%(B), 50%(C), 75%(D) and 100%(E) at $\alpha = 50$ wt%. The system: Water/ S₁₅₇₀/ R(+)-Limonene "fish" ($\delta = 0$ wt%(A)) is shown as reference. With the addition of EMDG the homogeneous micromulsion becomes smaller and the mean concentration goes to the direction of the high concentration of surfactant (i.e. at $\delta = 25$ wt%, the $\gamma_{\min} = 19$ wt% and $T = 65^{\circ}\text{C}$ and at $\delta = 50$ wt% the $\gamma_{\min} = 30$ wt% and $T = 70^{\circ}\text{C}$, while at $\delta = 75$ wt%, $\gamma_{\min} = 34$ wt% and $T = 70^{\circ}\text{C}$) the mean temperature moves up and downward on the temperature scale, with increasing the quantity of EMDG on the mixture as we can see in the figure the one phase region at high concentration of surfactant moves downward on the temperature scale. We can say that the addition of little quantity of EMDG will give a large one phase region, as we can see on the Figure at $\delta = 25$ wt% and this results is the best for all comparing with $\delta = 0$ wt% and with $\delta = 100$ wt%. At $\delta = 0$ wt% the $\gamma_{\min} = 25$ wt% and $T = 65^{\circ}\text{C}$, and at $\delta = 100$ wt% $\gamma_{\min} = 52$ wt% and $T = 60^{\circ}\text{C}$.

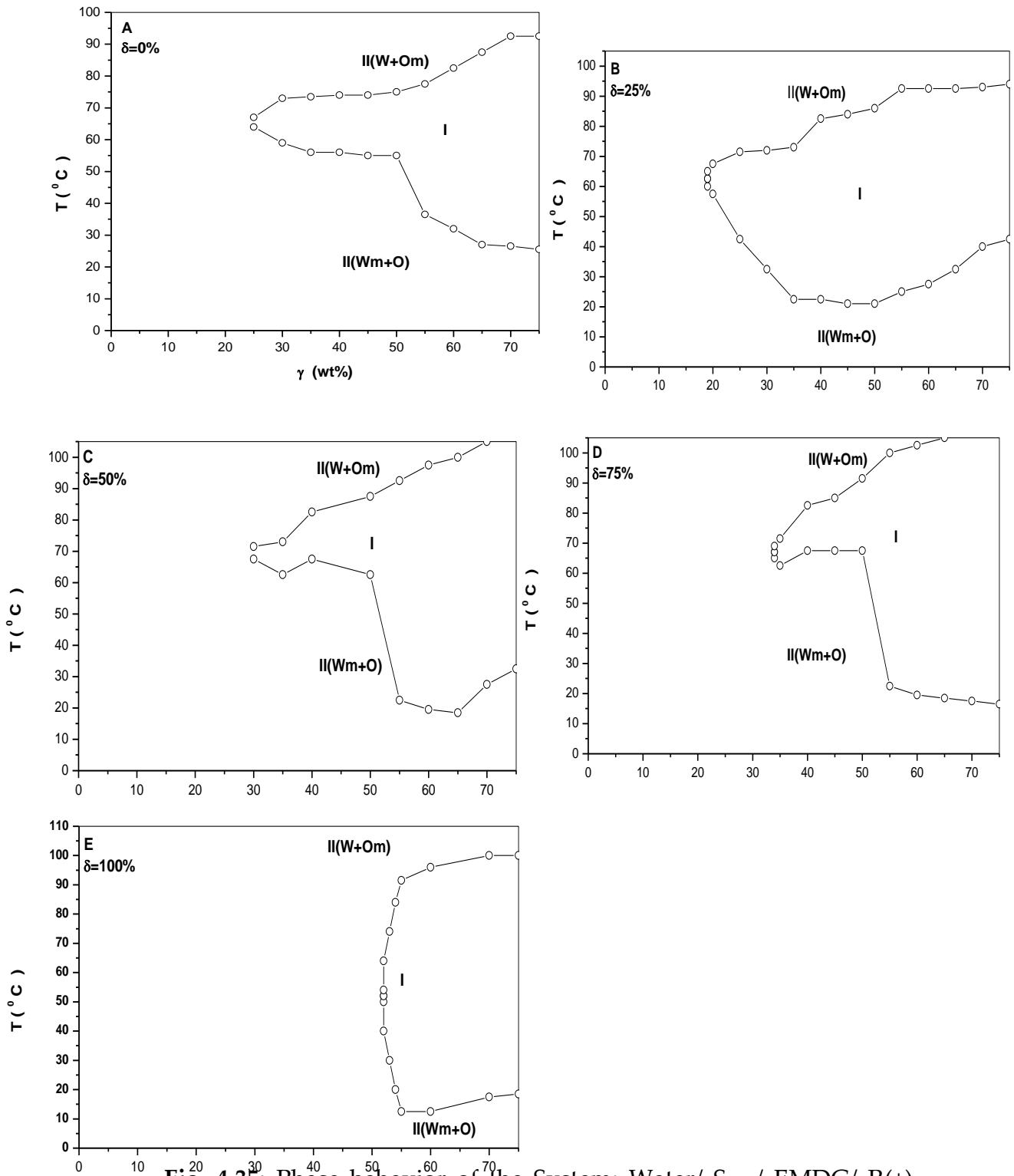


Fig. 4.35: Phase behavior of the System: Water/ S₁₅₇₀/ EMDG/ R(+)-Limonene as a function of δ , γ (wt%) and temperature at constant Oil/(Oil + Water) weight ratio, $\alpha = 50$ (wt%).

2-As a Function of δ, γ and Constant Temperature at $\alpha = 50$ wt%.

Fig. 4.36 shows the phase behavior of the system: Water/ S_{1570} / EMDG/ R (+)-Limonene at $\alpha = 50$ wt% as a function of δ and γ (wt%) at constant temperature $T = 65^\circ\text{C}$. At values of γ and δ below 25 wt% a two phase body is observed. Increasing the values of δ will shift the two phase body to higher values of γ . For $\delta = 80$ wt%, $\gamma = 35$ wt%. A one phase region is observed beside the two phase region. No three phase body III (W+D+O) is observed all over the range of δ and γ studied.

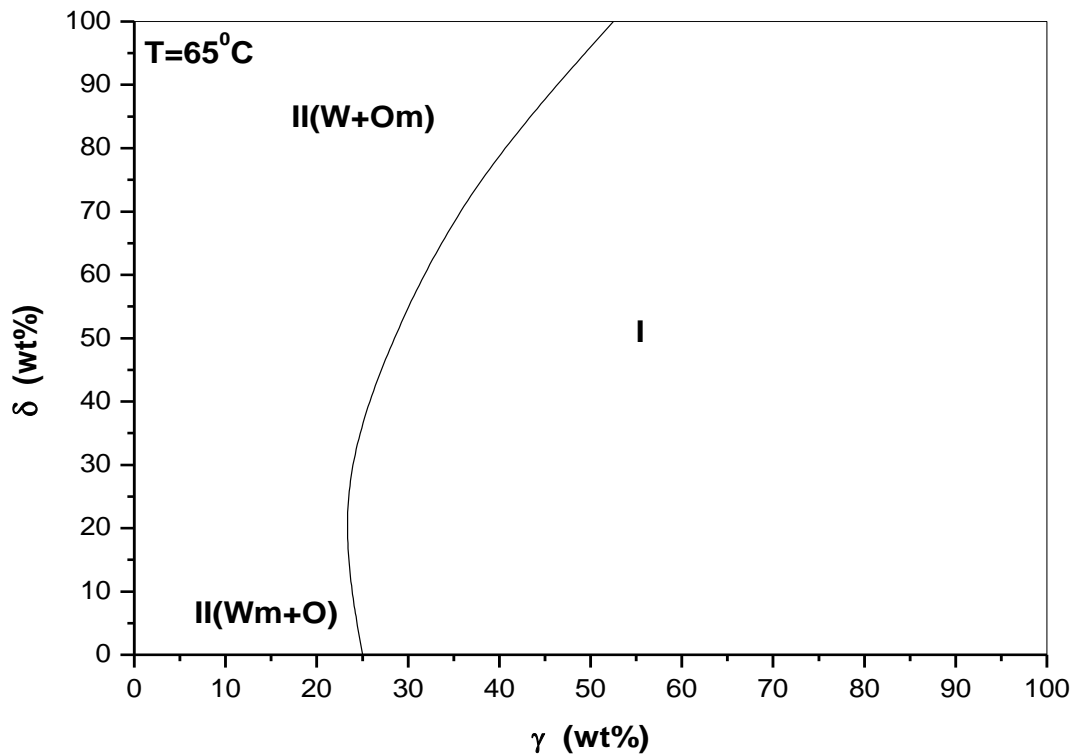


Fig. 4.36: Phase diagram for the system: Water/ S_{1570} / EMDG/ R(+)-Limonene at constant temperature ($T = 65^\circ\text{C}$) as a function of δ and γ (wt%). The $\text{Oil}/(\text{Oil} + \text{Water})$ weight ratio, $\alpha = 50$ (wt%).

Phase Behavior of the System L: Water/ L₁₆₉₅/ EMDG/ IPM.

1-As a Function of δ, γ and Temperature at $\alpha = 50$ wt%.

Fig. 4.37 shows the temperature-composition phase diagram of the system: Water/ L₁₆₉₅/ EMDG/ IPM, mixture for δ (wt%) = 25%(B), 50%(C), 75%(D) and 100%(E). The system: Water/ L₁₆₉₅/ IPM at $\delta = 0$ %(A) is shown as reference. With the addition of EMDG the homogeneous microemulsion region (fish tail) becomes larger, and moves downward in the temperature scale at medium concentration of surfactant (i.e from $\gamma = 30$ wt% to $\gamma = 50$ wt%) as we can see in the figure at ($\delta = 25, 50, 75$ and 100 wt%) that the mean concentration ($\bar{\gamma}$) move downward at the temperature scale (i.e at $\delta = 25$ wt%, $\bar{\gamma} = 28$ wt% and $\bar{T} = 87.5^\circ\text{C}$, $\delta = 50$ wt%, $\bar{\gamma} = 28$ wt% and $\bar{T} = 72.5^\circ\text{C}$ while at $\delta = 75$ wt%, $\bar{\gamma} = 23.5$ wt% and $\bar{T} = 72^\circ\text{C}$).

It is important to note that for high content of surfactant (i.e. 50 wt%) the one phase region appears at lower temperatures (i.e. 20°C) for co-surfactant concentrations δ (i.e. > 50 wt%) and for $\delta = 0$ wt%. Increasing the surfactant content decreases the temperature at which the one phase appears. For high temperatures (i.e. $T > 75^\circ\text{C}$), the transition temperature from one phase to two phase is dependent on the surfactant content. It increases when γ increases.

When adding EMDG the three phase body appears. At low concentration of surfactant the three phase is formed and this region is shrunk and moves upward in the temperature scale.

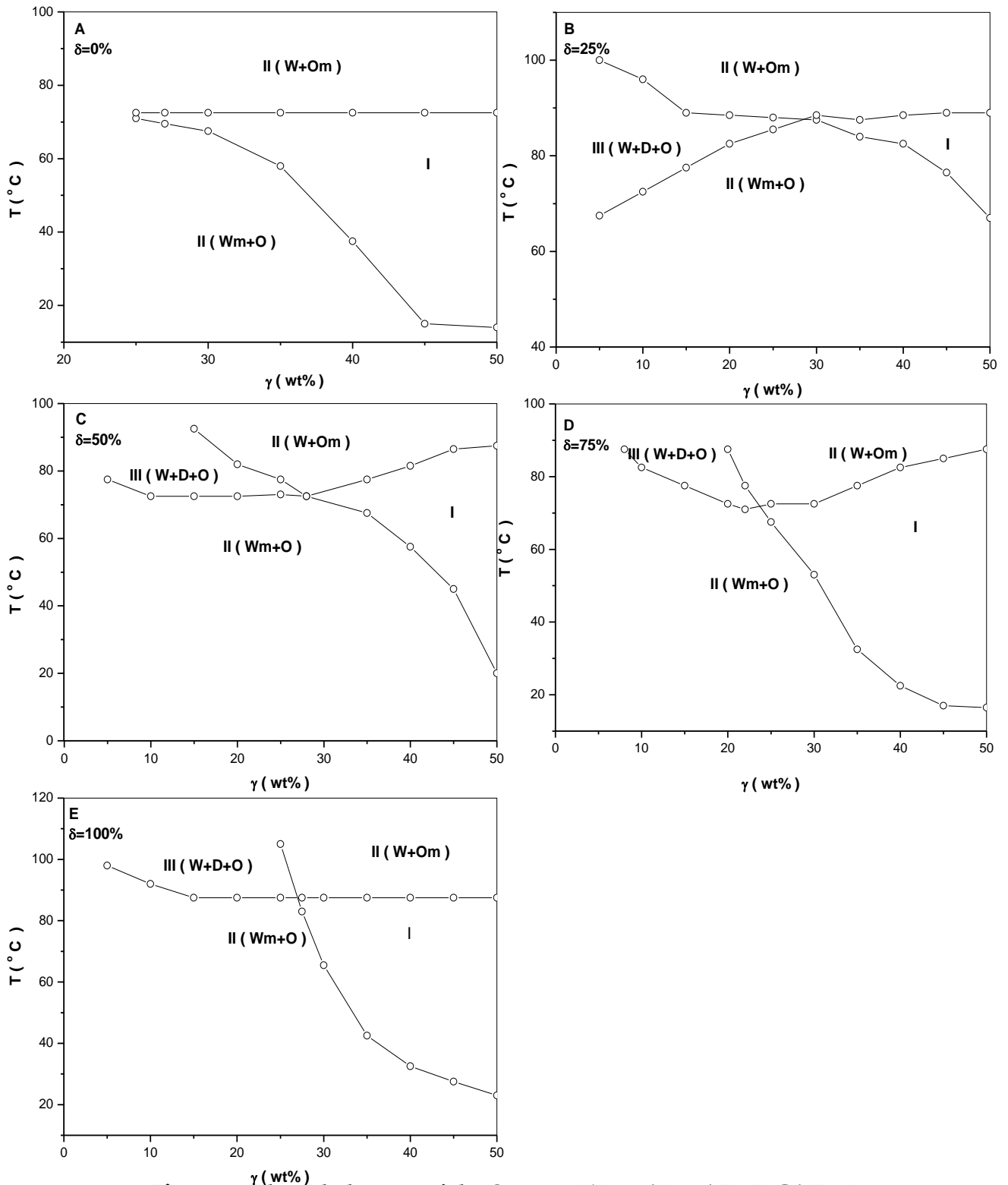


Fig. 4.37: Phase behavior of the System: Water/ L₁₆₉₅/ EMDG/ IPM as a function of δ , γ (wt%) and temperature at constant Oil/(Oil + Water) weight ratio, $\alpha = 50$ (wt%).

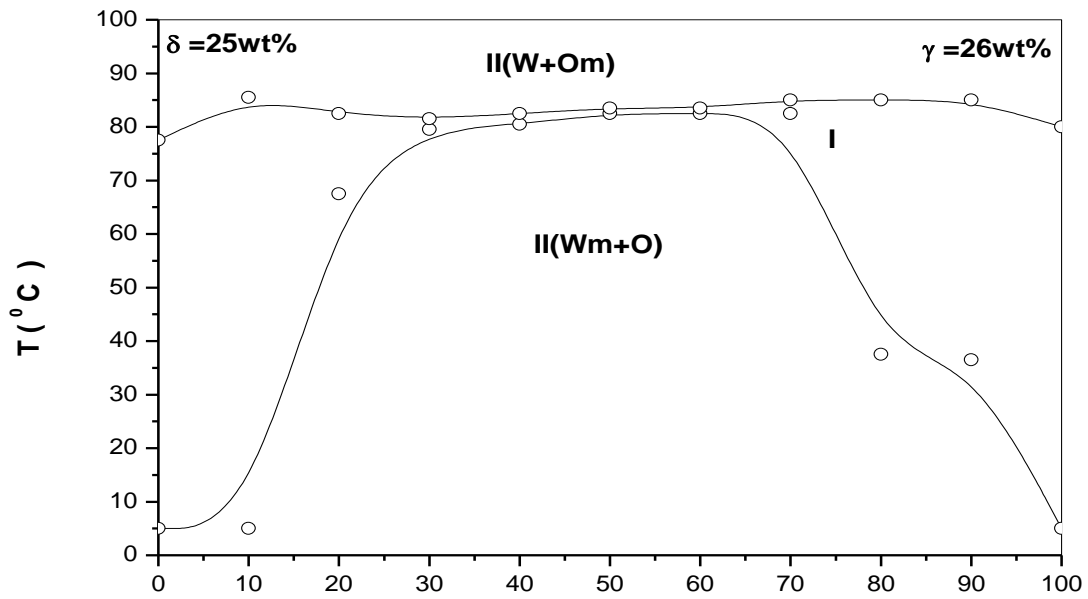
Increasing the EMDG concentration gives a larger one phase region but when comparing these results with the Water/ L₁₆₉₅/ IPM system at $\delta = 0$ wt%, we will see that the one phase body is the greater and formed at very low temperatures at $\delta = 0$ wt% as we can see at $\gamma = 45$ wt% the temperature is $T = 15^{\circ}\text{C}$, and at $\gamma = 50$ wt% the temperature is $T = 14^{\circ}\text{C}$, while the addition of the EMDG can't form one phase region at such low temperatures at these surfactant concentrations .

2-As a Function of δ, α and Temperature at Constant γ .

Fig. 4.38 shows the phase boundaries of the system: Water/ L₁₆₉₅/ EMDG/ IPM at fixed surfactant concentrations (i.e. $\delta = 25$ wt% for $\gamma = 26$ wt%(A), and $\delta = 50$ wt% for $\gamma = 31$ wt%(B)), while varying the temperature and weight ratios of oil and water. In **Fig. 4.38 (A)** we can see that the one-phase microemulsion region are bounded at temperatures below 70°C by an water continuous microemulsion with excess oil (W_m+O) and at high temperatures (over 85°C) by an oil continuous microemulsion with excess water (W+O_m). The one phase region extends for all the range of α values.

At low α values (i.e. $0 \text{ wt}\% \leq \alpha \leq 20 \text{ wt}\%$), this region is wide and extends over the temperature range of 5 to 85°C , the same behavior is observed at high α values (i.e. $70 \text{ wt}\% < \alpha < 100 \text{ wt}\%$). These one phase regions contain lamellar phase regions beside the fluid microemulsions. For α values between $20 \text{ wt}\%$ and $70 \text{ wt}\%$ the one phase region occurs at a narrow range of temperatures between $78^{\circ}\text{C} < T < 83^{\circ}\text{C}$. The mono-and multiphasic lamellar regions appears at high temperature and medium concentration of oil-to water ratio.

A



B

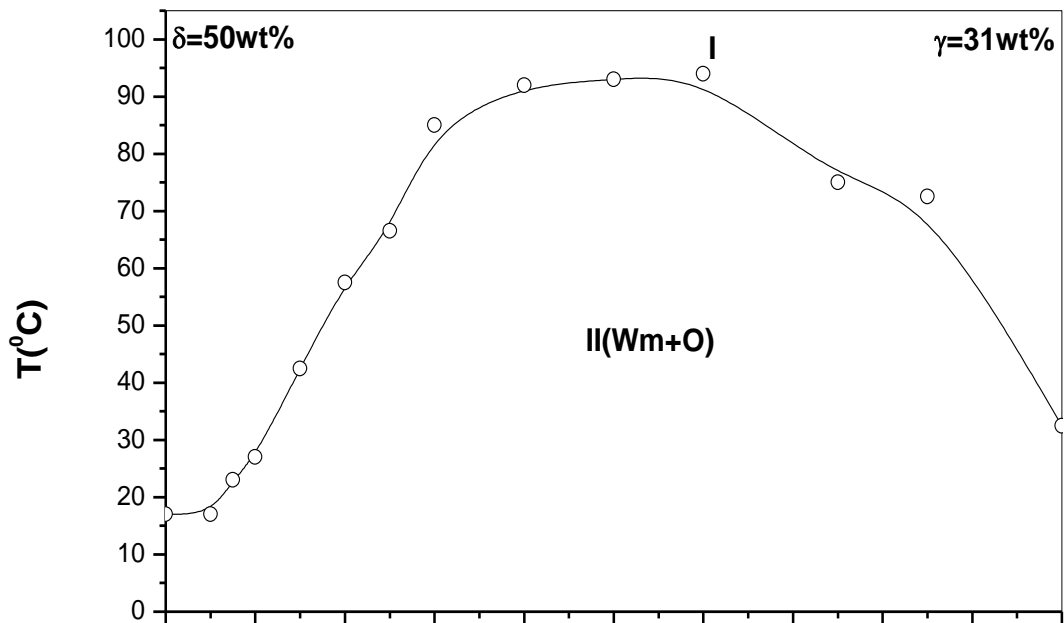


Fig. 4.389 Vertical section through the phase prism for the system: Water/ L₁₆₉₅/ EMDG/ IPM at constant surfactant concentration (γ) equals 26 wt% and 31 wt% and constant EMDG weight content in the mixture of surfactant (δ) and equals 25 wt% and 50 wt% as a function of temperature and $\text{Oil}/(\text{Oil} + \text{Water})$ weight ratio, α (wt%).

Fig. 4.38 B (i.e. $\delta = 50$ wt% for $\gamma = 31$ wt%) shows that at low temperature the one-phase microemulsion region are bounded by water continuous microemulsion with excess oil (W_m+O) and at medium temperature by oil continuous microemulsion with excess water. While at equal amounts of solubilized oil and water the one-phase region are shifted upward in the temperature scale. The one-phase microemulsion at low and high weight ratios of oil and water extends over the range of temperatures varying from 20°C to $T > 100^\circ\text{C}$. These one phase regions contain also lamellar liquid crystal phases.

3-As a Function of δ, γ and Constant Temperature at $\alpha = 50$ wt%.

Fig. 4.39 shows the phase behavior of the system: Water/ L_{1695} / EMDG/ IPM at $\alpha = 50$ wt% as a function of δ and γ (wt%) at constant temperature ($T = 72.5^\circ\text{C}$). A fish phase diagram is observed, L_{1695} is dissolved in water to form II (W_m+O) at low concentration of δ and γ (i.e. $\delta = 0$ wt%, $\gamma \leq 70$ wt %) but at high concentration $\gamma > 70$ wt% at $\delta = 0$ wt% the one-phase microemulsion appears. By increasing the concentration of co-surfactant (i.e. δ) the one-phase microemulsion is shifted to low concentration γ , while the three phase is appearing at low concentration of surfactant (i.e. $\gamma = 7.5$ wt% at $\delta = 22$ wt%) the sequence II (W_m+O) \rightarrow III ($W+D+O$) \rightarrow II ($W+O_m$) is observed at low concentration of surfactant by increasing δ .

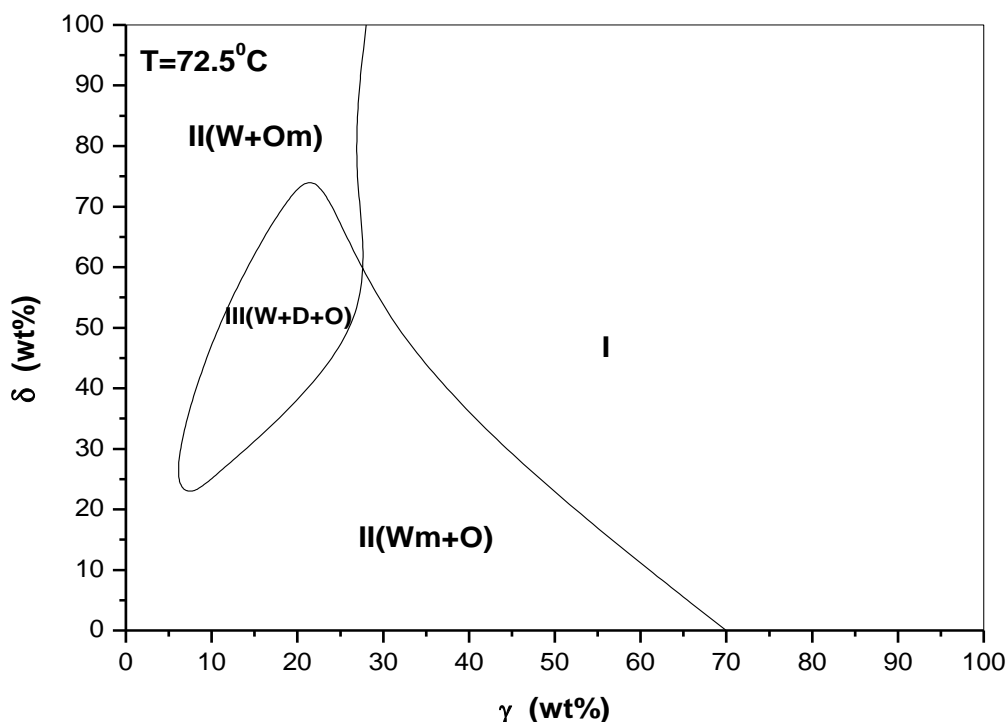


Fig. 4.39: Phase diagram for the system: Water/ L₁₆₉₅/ EMDG/ IPM at constant temperature (T = 72.5°C) as a function of δ and γ (wt%). The Oil/(Oil + Water) weight ratio, $\alpha = 50$ (wt%).

Phase Behavior of the System M: Water/ S₁₅₇₀/ EMDG/ IPM.

1-As a Function of δ, γ and Temperature at $\alpha = 50$ wt%.

Fig. 4.40 shows the temperature-composition phase diagram of the system: Water/ S₁₅₇₀/ EMDG/ IPM mixture for δ (wt%) = 0%(A), 25%(B), 50%(C), 75%(D) and 100%(E). The system: Water/ S₁₅₇₀/ IPM ($\delta = 0$ wt%) is shown as reference .

As we can see, when EMDG is added the homogeneous microemulsion region (fish tail) becomes wider and the minimum amount of S₁₅₇₀ + EMDG needed for formation of the one phase region of the

surfactant mixture increases slightly (i.e. $\gamma_{\min} = 42$ wt% and $T = 75^{\circ}\text{C}$ at $\delta = 0$ wt%, and at $\delta = 25$ wt% the $\gamma_{\min} = 15$ wt% and $T = 67.5^{\circ}\text{C}$, while at $\delta = 50$ wt% the $\gamma_{\min} = 5$ wt% and $T = 62.5^{\circ}\text{C}$) so the one phase becomes larger and the mean temperature moves downward in the temperature scale at these concentrations of EMDG with no formation of the three-phase body (fish body). It is important to note that for high content of surfactant (i.e. 40 wt%) the one phase region appears at lower temperatures (i.e. 30°C) at cosurfactant concentrations δ (i.e. > 25 wt%).

Increasing the surfactant content decreases the temperature at which the one phase appears. For high temperatures (i.e. $T > 75^{\circ}\text{C}$), the transition temperature from one phase to two phase is dependent on the surfactant content. It increases when γ increases.

Increasing the ratio of EMDG/ S_{1570} (i.e. $\delta \geq 75$ wt%) the three-phase region (fish body) start to form at low concentration of surfactant less than $\gamma = 15$ wt% and this region becomes large and moves upward on the temperature scale and surfactant concentration which is moved upward on the temperature scale so at $\delta = 75$ wt%, $\bar{\gamma} = 13$ wt%, and $\bar{T} = 80^{\circ}\text{C}$ while at $\delta = 100$ wt%, $\bar{\gamma} = 27$ wt% and $\bar{T} = 92^{\circ}\text{C}$.

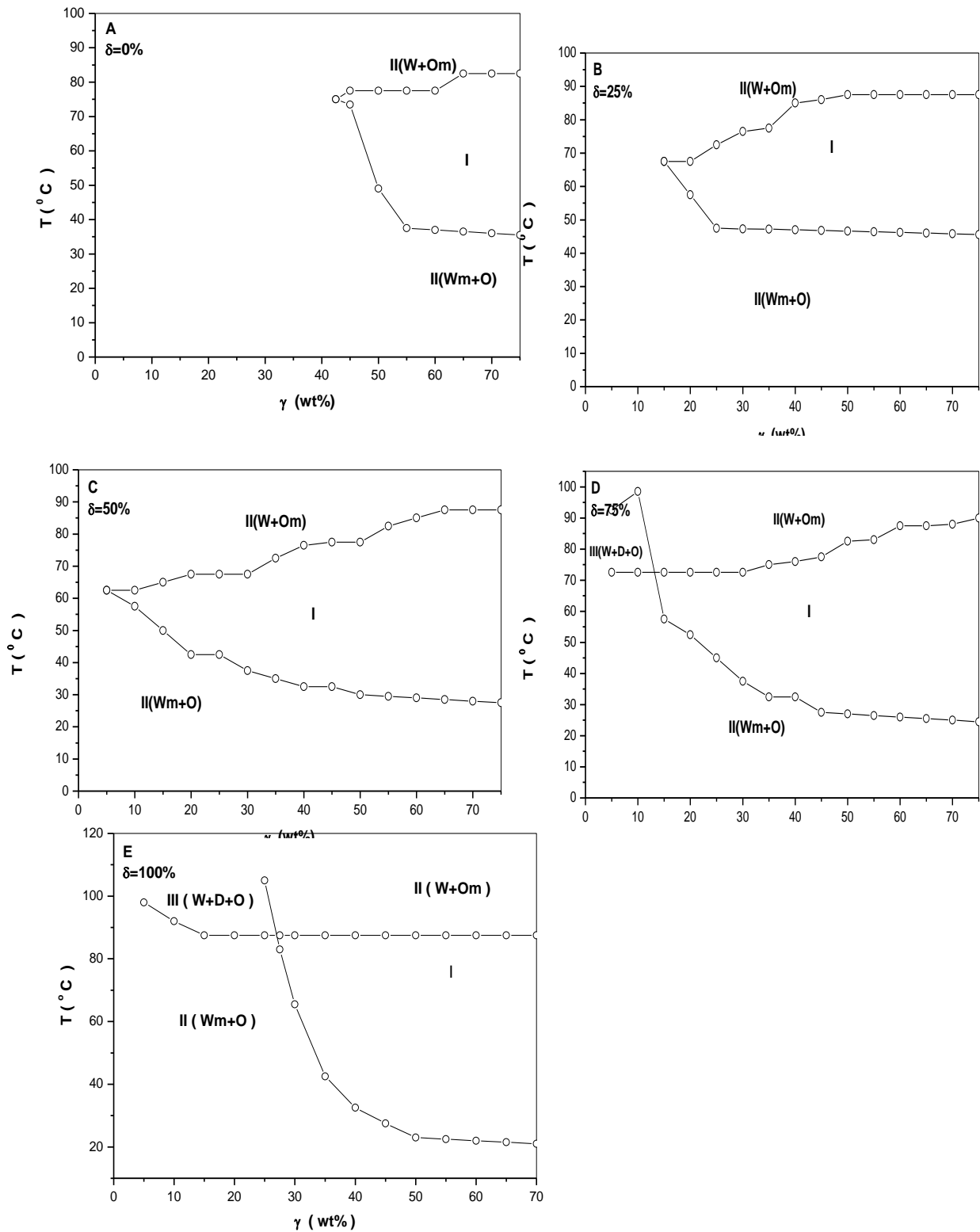


Fig. 4.40: Phase behavior of the System: Water/ S₁₅₇₀/ EMDG/ IPM as a function of δ , γ (wt%) and temperature at constant Oil/(Oil + Water) weight ratio, $\alpha = 50$ (wt%).

2-As a Function of δ, α and Temperature at Constant γ .

Fig. 4.41 shows the phase behavior of the system: Water/ S_{1570} / EMDG/ IPM at constant surfactant concentration (i.e. $\delta = 25$ wt% for $\gamma = 16.6$ wt%), as function of temperature and weight ratios of oil and water (i.e. α). At low oil contents one phase microemulsion appears at temperatures between ($T = 47.5^\circ\text{C}$ and $T = 67.5^\circ\text{C}$) while at high oil contents (i.e. oil continuous phase) the one phase microemulsion regions are bounded at high ($T > 70^\circ\text{C}$) temperatures by oil continuous microemulsion with excess water ($W+O_m$) and at low temperature ($T < 40^\circ\text{C}$) by water continuous microemulsion with excess oil. At equal amounts of solubilized oil and water, a bicontinuous mono-phase region can be present. The one phase region extends for all the range of α values. At α values below 60 wt%, the range of temperatures for which the phase region present is $45^\circ\text{C} \leq T \leq 68^\circ\text{C}$, while for high α values (i.e. $\alpha > 60$ wt%) the one phase region extends over the temperatures range 35°C to 90°C .

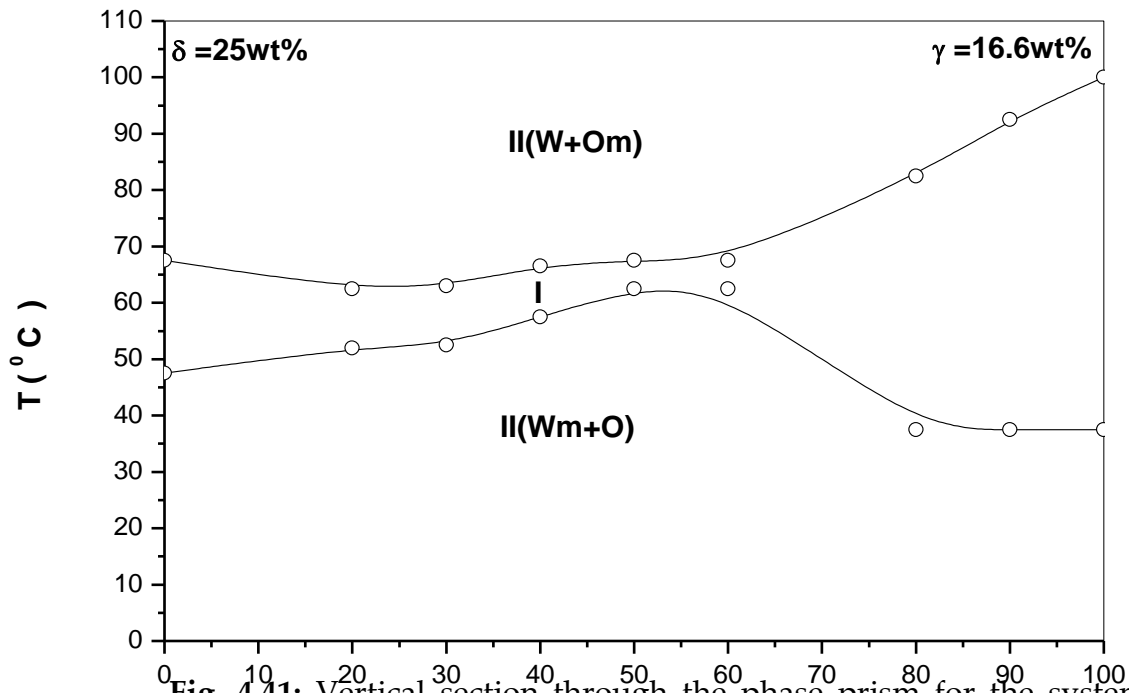


Fig. 4.41: Vertical section through the phase prism for the system: Water/ S_{1570} / EMDG/ IPM at constant surfactant concentration (γ) equals 16.6 wt% and constant EMDG weight content in the mixture of surfactant (δ) and equals 25 wt% as a function of temperature and $Oil/(Oil + Water)$ weight ratio, α (wt%).

3-As a Function of δ, γ and Constant Temperature at $\alpha = 50$ wt%.

Fig. 4.42 (A and B) shows the phase behavior of the system: Water/ S_{1570} / EMDG/ IPM at $\alpha = 50$ wt% as a function δ and γ (wt%) at constant temperature ($T = 65$ and 70°C). At 65°C (**Fig. 4.42 A**), S_{1570} is mainly dissolved in water to form two phase region II (Wm+O) at low δ and low concentration of, γ (i.e. $\gamma < 30$ wt %). For values more than $\gamma = 30$ wt% the one phase microemulsion region appears. With increasing δ the amount of the mixed surfactants needed to form one phase microemulsion is decreased to reach it is minimum amount at $\delta = 50$ wt% (i.e. $\gamma = 11$ wt %).

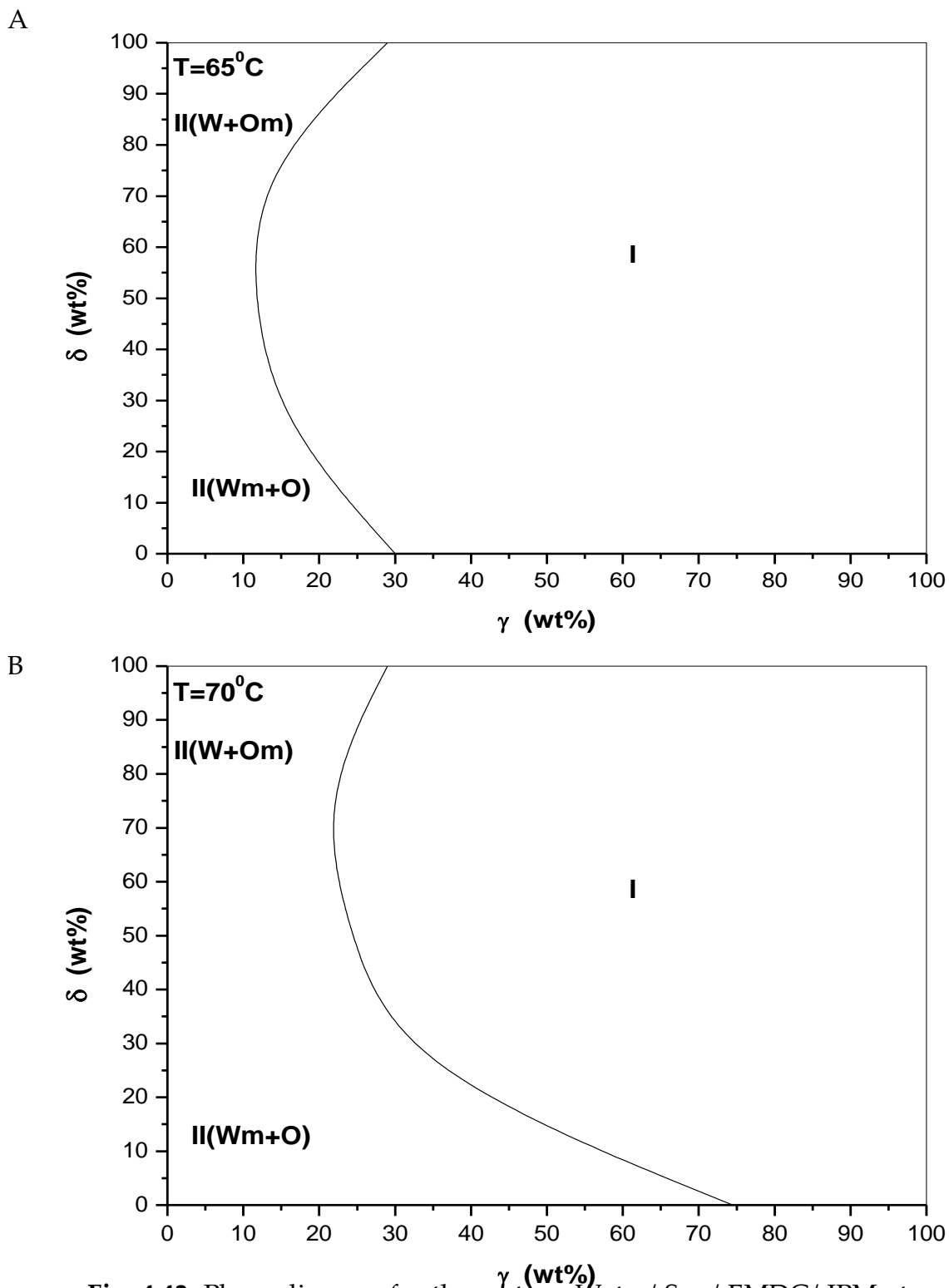


Fig. 4.42: Phase diagram for the system: Water/ S_{1570} / EMDG/ IPM at constant temperature ($T = 65^\circ\text{C}$ (A) and 70°C (B)) as a function of δ and γ (wt%). The *Oil/(Oil + Water)* weight ratio, $\alpha = 50$ (wt%).

At higher δ values the stable microemulsion formed at higher concentration (i.e. $\gamma > 11$ wt%). The three phase microemulsion is not formed. At 70°C S₁₅₇₀ remains dissolved in the water at low concentration of δ to form II (Wm+O). At these concentrations the one phase microemulsion formed at high concentration of surfactant γ (i.e. $\gamma = 75$ wt% at $\delta = 0$ wt%). With increasing δ the amount of surfactant needed to form one phase microemulsion is decreased (i.e. $\delta = 70$ wt%, $\gamma = 20$ wt%). At higher increase of δ the amount of the surfactant needed to form one phase microemulsion is increased. The three phase body is not formed at any concentrations of δ and γ .

Phase Behavior of the System N: Water/ L₁₆₉₅/ EMDG/ MCT.

1-As a Function of δ, γ and Temperature at $\alpha = 50$ wt%.

Fig. 4.43 shows the temperature-composition phase diagram of the system: Water/ L₁₆₉₅/ EMDG/ MCT mixture for δ (wt%) = 25%(B), 50%(C), 75%(D) and 100%(E). The system: water / L₁₆₉₅ / MCT "fish" ($\delta = 0$ wt% (A)) is shown as reference. With the addition of EMDG the homogeneous micromulsion region (fish tail) becomes wider and the efficiency of the surfactant mixture increases slightly (i.e. $\bar{\gamma} = 41$ wt% for $\delta = 25$ wt% and drops to $\bar{\gamma} = 36$ wt% for $\delta = 50$ wt%). The temperature interval for the three-phase body increases slightly with increasing δ , and the mean temperature moves downward on the temperature scale (i.e. the mean temperature for $\delta = 25$ wt% is $\bar{T} = 85^\circ\text{C}$ and for $\delta = 50$ wt% is $\bar{T} = 82.5^\circ\text{C}$ while at $\delta = 75$ wt% the mean temperature is $\bar{T} = 78^\circ\text{C}$).

The one phase region increases with increasing the EMDG / L₁₆₉₅ in system and this region moves downward in the temperature scale as shown in the figures. It is important to note that for high content of surfactant (i.e. 55 wt%) the one phase region appears at lower temperatures (i.e. 25°C).

Increasing the surfactant content decreases the temperature at which the one phase appears. For high temperatures (i.e. $T > 75^{\circ}\text{C}$), the transition temperature from one phase to two phase is dependent on the surfactant content. It increases when γ increases.

By doing a little comparison to the system: Water/ L₁₆₉₅/ MCT mixture at $\delta = 0$ wt% we can see that this system have a large one phase region and the mean concentration is $\bar{\gamma} = 37.5$ wt% but it's mean temperature $\bar{T} = 87.5^{\circ}\text{C}$ which is different from the other system and this system solubilizes more MCT in water than the highly addition of EMDG $\delta = 100$ wt% as we can see the mean concentration is $\bar{\gamma} = 42$ wt% and the mean temperature is $\bar{T} = 83^{\circ}\text{C}$ but the one phase region is smaller than the system $\delta = 0$ wt%.

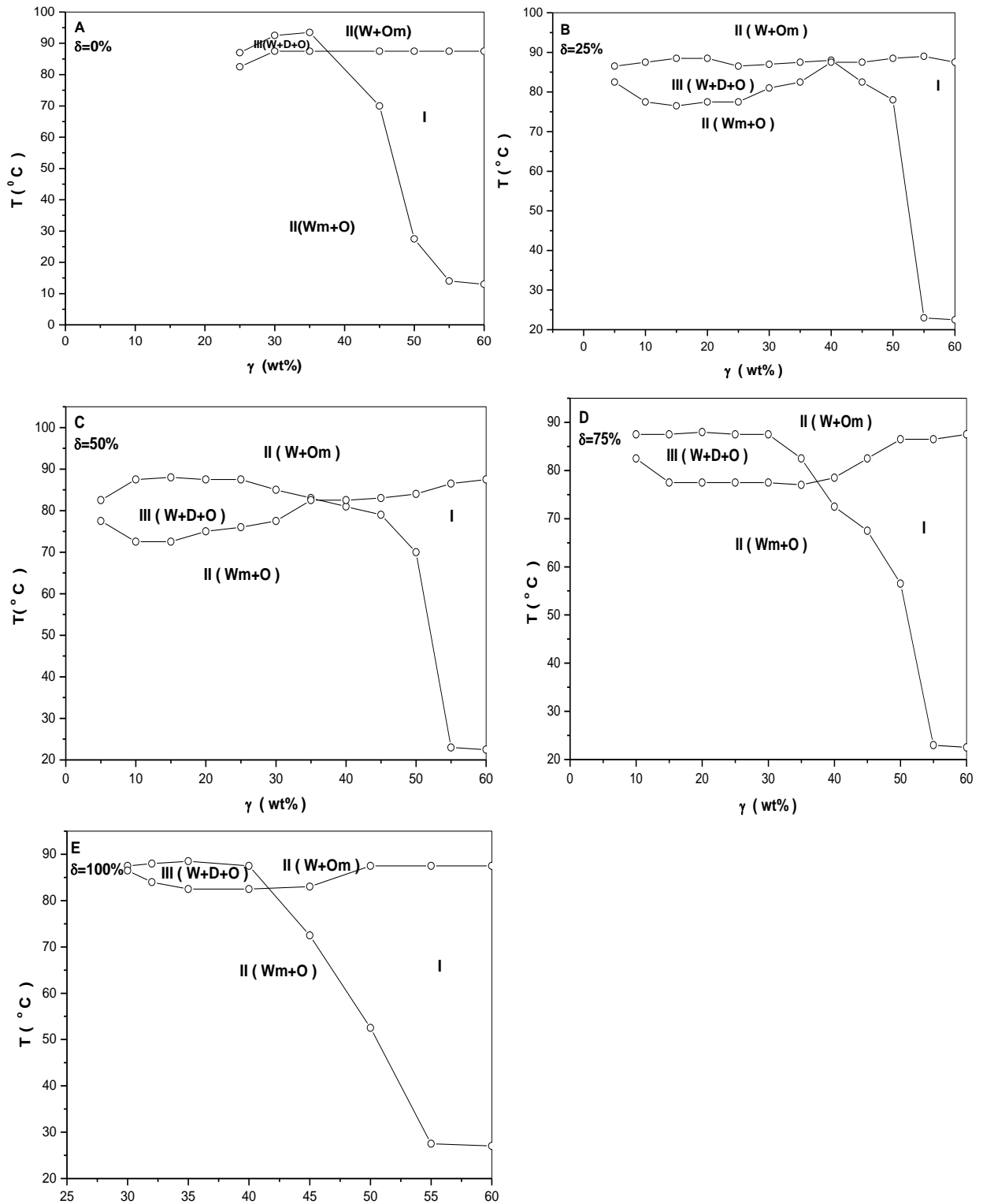


Fig. 4.43: Phase behavior of the System: Water/ L₁₆₉₅/ EMDG/ MCT as a function of δ , γ (wt%) and temperature at constant Oil/(Oil + Water) weight ratio, $\alpha = 50$ (wt%).

2-As a Function of δ, α and Temperature at Constant γ .

Fig. 4.44 shows the phase boundaries of the system: Water/ L₁₆₉₅/ EMDG/ MCT for fixed surfactant concentration (i.e. $\delta = 25$ wt% for $\gamma = 31$ wt%), while varying the temperature and weight ratios of oil and water.

At low oil contents (low α values i.e. $\alpha < 20$ wt%) a one phase region is observed, this region extends for the range of temperatures from 10 to 90°C. This region contains at $\alpha < 5$ wt% a lamellar liquid crystal phase which was identified as a very viscous transparent region. This one phase region is a water continuous microemulsions. The one phase region extends at high temperatures in a narrow range of temperature (i.e. 75°C - 85°C), for values α from 20 to 55 wt%. For these values of α and temperature below this range a two phase region is observed (W_m+O) which contains a water continuous emulsion (W_m) with excess oil (O). On the other hand, at temperature above this range another two phase region (W+O_m) is observed which contains an oil continuous emulsion (O_m) in excess with water (W), when the oil content increases (i.e. $\alpha < 55$ wt%) a new one phase region appears at a wider temperature range (i.e. 55°C \leq T \leq 85°C) which contains beside the oil continuous microemulsions a lamellar liquid crystal phase at temperatures near 55°C and also at very high oil content (i.e. $\alpha > 95$ wt%).

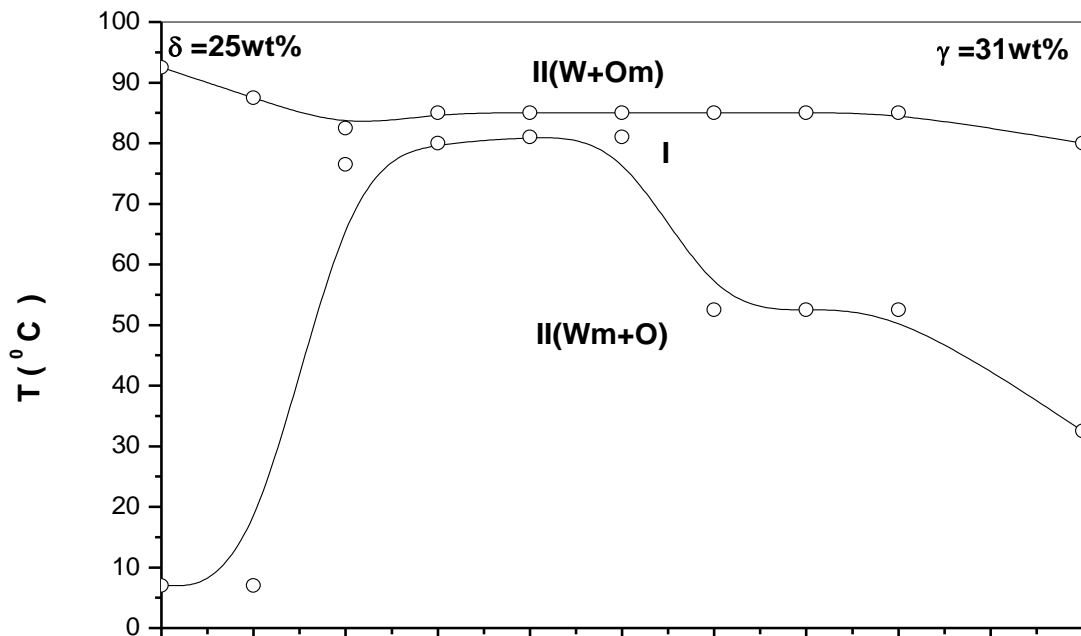


Fig. 4.44: Vertical section through the phase prism for the system: Water/ L₁₆₉₅/ EMDG/ MCT at constant surfactant concentration (γ) equals 31 wt% and constant EMDG weight content in the mixture of surfactant (δ) and equals 25 wt% as a function of temperature and $Oil/(Oil + Water)$ weight ratio, α (wt%).

3-As a Function of δ, γ and Constant Temperature at $\alpha = 50\text{wt}\%$.

Fig. 4.45 (A and B) shows the phase behavior of the system: Water/ L₁₆₉₅/ EMDG/ MCT at $\alpha = 50$ wt% as a function of δ and γ (wt%) at constant temperatures ($T = 80$ and 85°C). At 80°C a fish phase diagram is observed. L₁₆₉₅ is mainly dissolved in water at low δ and low γ but at $\gamma > 45$ wt% the one phase microemulsion appears. With increasing δ the three-phase body starts at low value of δ (i.e. $\delta = 12.5$ wt%) and low values of γ (i.e. $\gamma = 17.5$ wt %). The minimum amount of surfactant necessary to form a one phase microemulsion is decreased $\gamma = 38$ wt% at $\delta = 65$ wt%. At 85°C a fish phase diagram is observed.

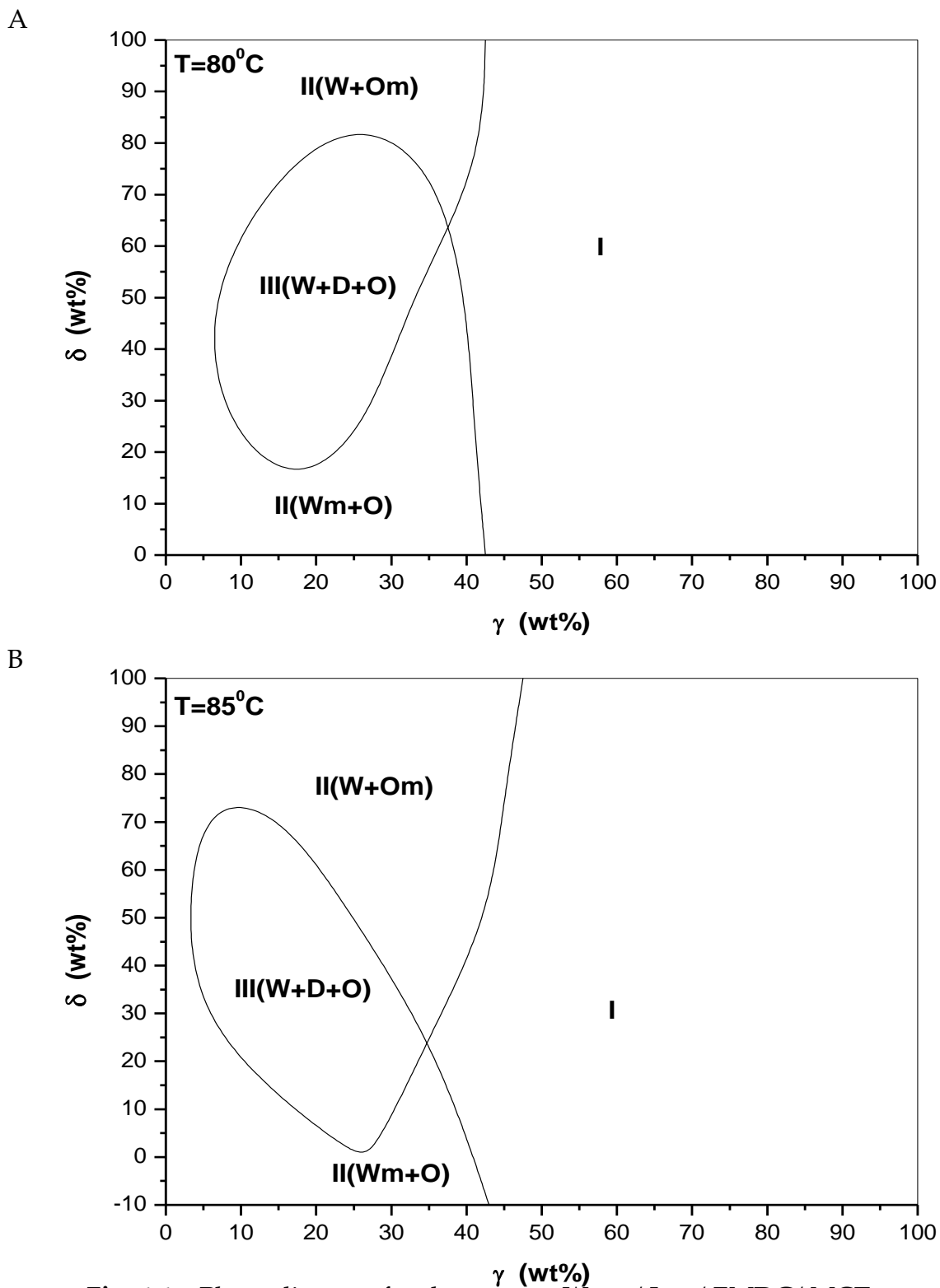


Fig. 4.45: Phase diagram for the system: Water/ L₁₆₉₅/ EMDG/ MCT at constant temperature ($T = 80^{\circ}\text{C}$ (A) and 85°C (B)) as a function of δ and γ (wt%). The Oil/(Oil + Water) weight ratio, $\alpha = 50$ (wt%).

L_{1695} remains dissolved in the water and the same II (Wm+O) \rightarrow III (W+D+O) \rightarrow II (W+Om) phase sequence is seen as δ increases. However the minimum amount of surfactant necessary to form a one phase microemulsion is shifted to low δ indicating that less EMDG is present in the microemulsion. With increasing the concentration of EMDG the three-phase body III (W+D+O) appears at low concentration of surfactant (γ). But the amount of surfactant needed to form one phase microemulsion is decreased to reach its minimum amount at $\delta = 23.5$ wt%, $\gamma = 35$ wt%.

Phase Behavior of the System O: Water/ S₁₅₇₀/ EMDG/ MCT

1-As a Function of δ , γ and Temperature at $\alpha = 50$ wt%.

Fig. 4.46 shows the temperature-composition phase diagram of the system: Water/ S₁₅₇₀/ EMDG/ MCT mixture for δ (wt%) = 0%(A), 25%(B), 50%(C), 75%(D) and 100%(E) at $\alpha = 50$ wt%. With the addition of EMDG the homogeneous microemulsion region (fish tail) becomes wider and the efficiency of the surfactant mixture increases (i.e. $\bar{\gamma} = 51$ wt% for $\delta = 0$ wt% to $\bar{\gamma} = 22.5$ wt% for $\delta = 25$ wt%). The temperature interval of the three phase body increases with increasing δ , and the whole three phase region moves upward in temperature scale, the mean temperature moves around 80 and 82.5 in the temperature scale (i.e. $\bar{T} = 82.5^\circ\text{C}$ at $\delta = 0$ wt%, $\bar{T} = 80^\circ\text{C}$ at $\delta = 50$ wt%), but the one phase region becomes wider with increasing EMDG/ S₁₅₇₀ ration from $\delta = 0$ wt% to 50 wt% and this region shifted downward in the temperature scale when increasing the EMDG/ S₁₅₇₀ ratio,

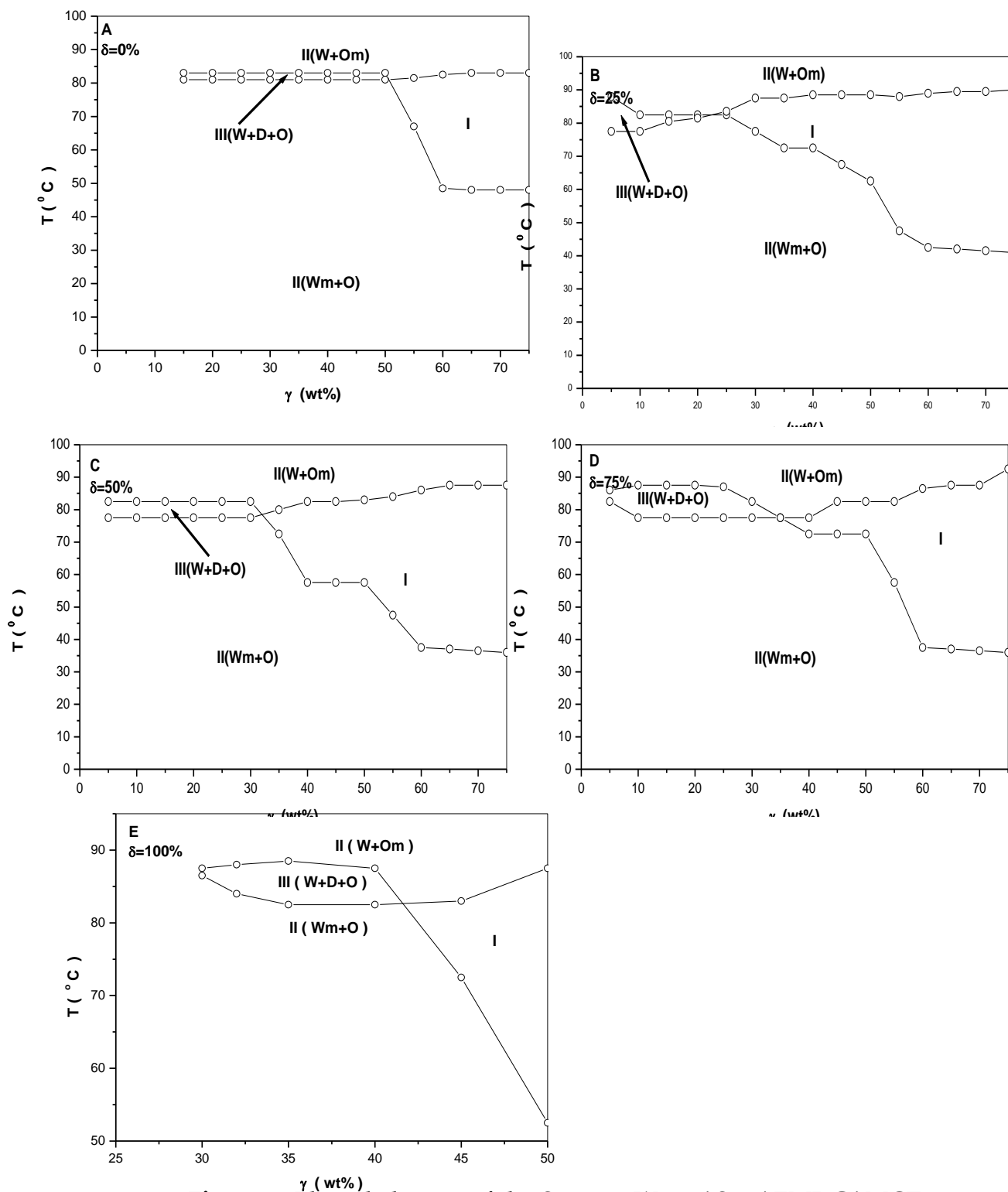


Fig. 4.46: Phase behavior of the System: Water/ S_{1570} / EMDG/ MCT as a function of δ , γ (wt%) and temperature at constant $Oil/(Oil + Water)$ weight ratio, $\alpha = 50$ (wt%).

the three phase body region becomes wider at high concentration of EMDG (i.e. $\delta = 75$ wt% and $\delta = 100$ wt%). At very high concentration $\delta = 100$ wt% the one phase region is the biggest for all and it appears at low concentration of surfactant and move down ward in the temperature scale but the three phase body becomes the wider for all.

It is important to note that for high content of surfactant (i.e. 60 wt%) the one phase region appears at lower temperatures (i.e. 40°C). Increasing the surfactant content decreases the temperature at which the one phase appears. For high temperatures (i.e. $T > 85^\circ\text{C}$), the transition temperature from one phase to two phase is dependent on the surfactant content. It increases when γ increases.

2-As a Function of δ, α and Temperature at Constant γ .

Fig. 4.47 shows the phase behavior of the system: Water/ S_{1570} / EMDG/ MCT at fixed surfactant concentrations (i.e. $\delta = 25$ wt% for $\gamma = 23.1$ wt%), while varying the temperature and weight ratios of oil and water (i.e. α (wt%)). In this Figure (i.e. **Fig. 4.47**) we can see that the one-phase microemulsion region is formed at high temperatures and low oil/ water ratio ($\alpha \leq 10$ wt%). Increasing oil-to-water ratio more than $\alpha = 10$ wt% the one-phase microemulsion does not appear at any $Oil/(Oil + Water)$ ratio or any temperature.

3-As a Function of δ, γ and Constant Temperature at $\alpha = 50$ wt%.

Fig. 4.48 shows the phase diagram of the system: Water/ S_{1570} / EMDG/ MCT at $\alpha = 50$ wt% as a function of δ and γ (wt%) at $T = 80^\circ\text{C}$. The surfactant (S_{1570}) mainly dissolved in water to form II (W_m+O), a fish type phase diagram is observed where a two phase II (W_m+O) where the surfactant (S_{1570}) is mainly dissolved in water is observed at low δ (i.e. $\delta < 20$ wt %) and γ (i.e. $\gamma < 30$ wt %) values.

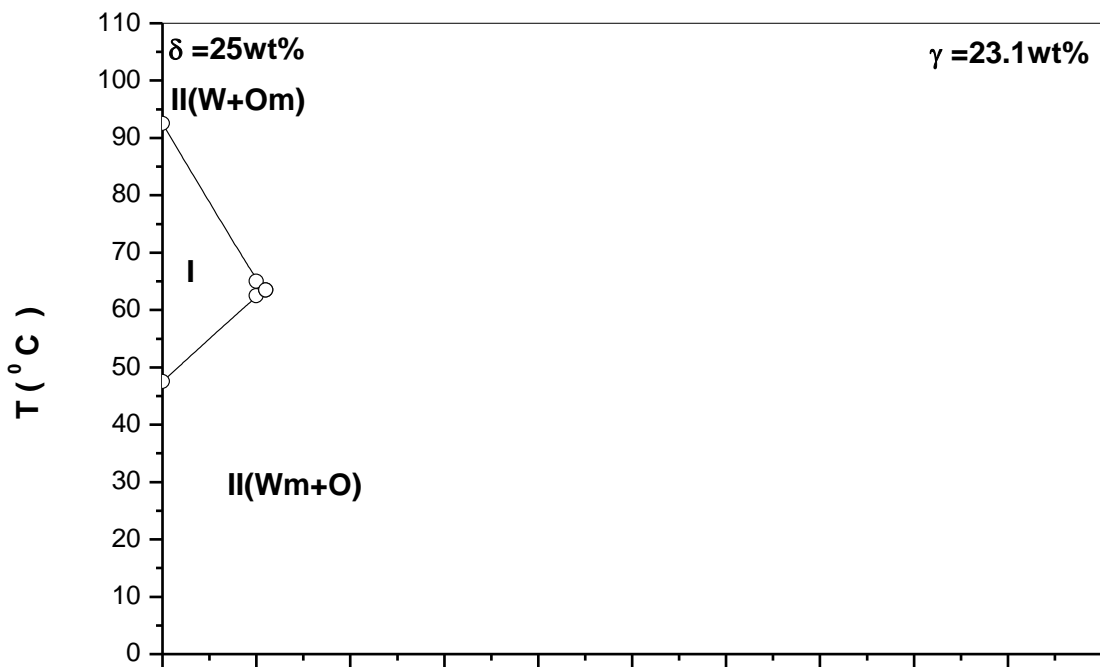


Fig. 4.47: Vertical section through the phase prism for the system: Water/ S_{1570} / EMDG/ MCT at constant surfactant concentration (γ) equals 23.1 wt% and constant EMDG weight content in the mixture of surfactant (δ) and equals 25 wt% as a function of temperature and $Oil/(Oil + Water)$ weight ratio, α (wt%).

Increasing δ values for the same range of γ values a transition from two phase to three phase body III (W+D+O) is observed. The three phase body extends from $\delta = 20$ wt% to $\delta = 80$ wt%.

Increasing the concentration of the surfactant EMDG (i.e. increasing δ) the three-phase body III (W+D+O) disappeared and the two-phase region II (W+Om) is formed at low concentration of surfactant S_{1570} . On the other hand, there is no change on the formation of the one-phase microemulsion, exists also at high concentration of surfactant. For surfactant concentration above $\gamma = 50$ wt% a one-phase body is formed which extend over all of the range of δ .

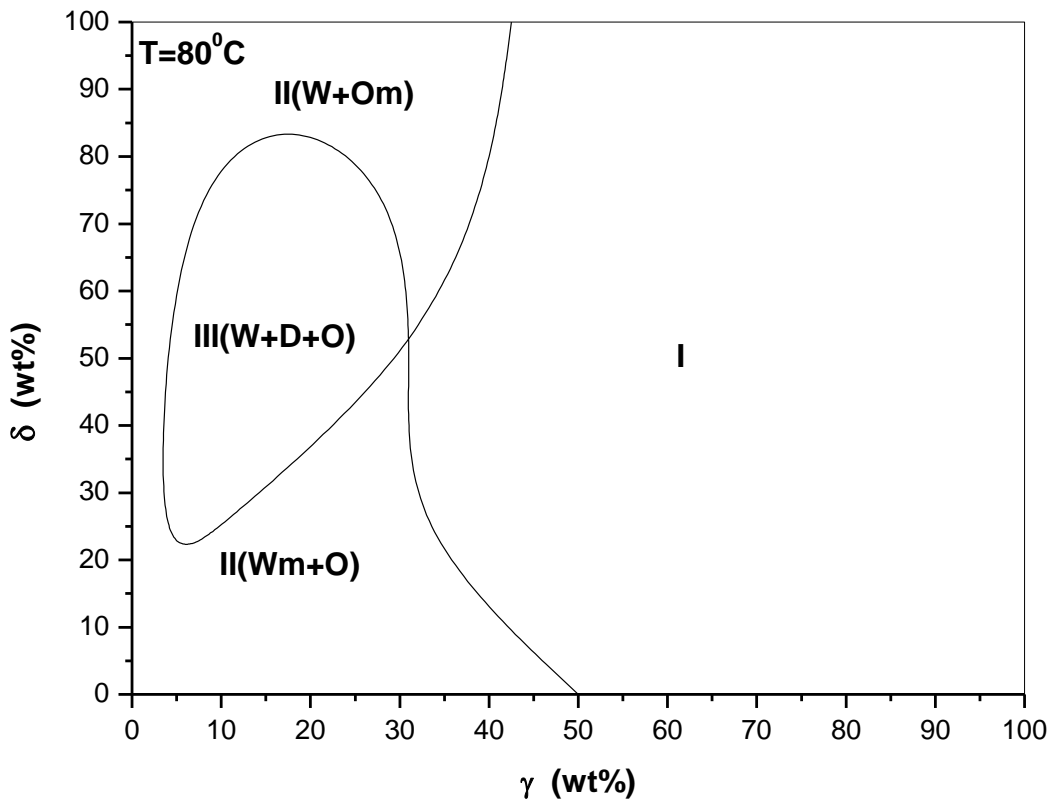


Fig. 4.48: Phase diagram for the system: Water/ S_{1570} / EMDG/ MCT at constant temperature ($T = 80^{\circ}\text{C}$) as a function of δ and γ (wt%). The $Oil/(Oil + Water)$ weight ratio, $\alpha = 50$ (wt%).

IV.1.4 Discussion of the Phase Behavior

a- Variation of amphiphile content (γ , (wt%)), ratios (δ , (wt%)) and temperature (T) at constant weight ratio of oil in the mixture of oil and water (i.e. $\alpha = 50$ wt%).

Firstly, we explored the effect of PG weight content on the phase behavior of the system: Water/ Surfactant/ PG/ Oil as a function of temperature and surfactant concentration, and demonstrating the role of PG and oil type in forming microemulsions. Secondly we studied the effect of increasing the hydrophobicity of the surfactant by substituting the L₁₆₉₅ by sucrose stearate (S₁₅₇₀) and by mixing the sucrose esters with EMDG on the temperature range on the three-phase body and single-phase microemulsion region. In the following we will discuss the effect of these factors on the phase behavior.

System 1: Water/ L₁₆₉₅/ PG/ Oil

When R(+)-limonene is used as oil phase, the presence of PG in the system will not induce the formation of 3 ϕ region over all of the range of surfactant and PG concentrations neither over all of the range of temperatures studied. This absence of a three-phase body indicates being beyond the tricritical point of the mixture. The concentration of L₁₆₉₅ needed for the formation of one phase region in the ternary system: Water/ L₁₆₉₅/ R(+)-limonene is lower than the concentration of mixed L₁₆₉₅ + PG needed. Increasing the ratio of PG in the mixture will increase the concentration of

mixed L₁₆₉₅ + PG needed for the formation of one phase region, and also affects the temperature at which this one phase begins to appear. In the case where IPM is used as the oil phase, the presence of PG will induce the formation of 3 ϕ . Increasing the ratio of PG will decrease the efficiency of the surfactant and will increase the phase inversion temperature, $(\bar{T})_{(PIT)}$. In the case where MCT is used as the oil phase, increasing the ratio of PG in the system will increase the efficiency of the surfactant, and when the PG content in the mixed surfactant and PG reaches 50 wt% (i.e. $\delta = 50$ wt%), no 3 ϕ region is observed over all the range of T and γ in the system. On the other hand, increasing the ratio of PG will increase the phase inversion temperature. The ternary system: Water/ PG/ Oil show a separation into two liquid phases. **Tables 4.1 and 4.2** and **Fig. 4.49** summarizes these results.

Table 4.1: Summary of the results of the system: Water/ L₁₆₉₅/ PG/ Oil at constant $Oil/(Oil + Water)$ weight ratio, $\alpha = 50$ wt%, and variable δ (wt%), γ (wt%) and T (°C).

δ (wt%)	R(+)-limonene			IPM			MCT		
	γ_{min} or $\bar{\gamma}$ (wt%)	T or \bar{T} (°C)	Phases	γ_{min} or $\bar{\gamma}$ (wt%)	T or \bar{T} (°C)	Phases	γ_{min} or $\bar{\gamma}$ (wt%)	T or \bar{T} (°C)	Phases
0	32.5	80	No 3 ϕ formation	25	72.5	No 3 ϕ formation	37.5	87.5	3 ϕ formation
25	50	55		50	82	3 ϕ Formation	60	91	
40	62.5	55		62	85		50	82.5	
50	No formation of 1 ϕ Two solid and liquid phases			65	92.5	No formation of 1 ϕ	45	87.5	No 3 ϕ
75				Two solid and liquid phases					
90							Two solid and liquid phases		
100	Two liquid phases			Two liquid phases			Two liquid phases		

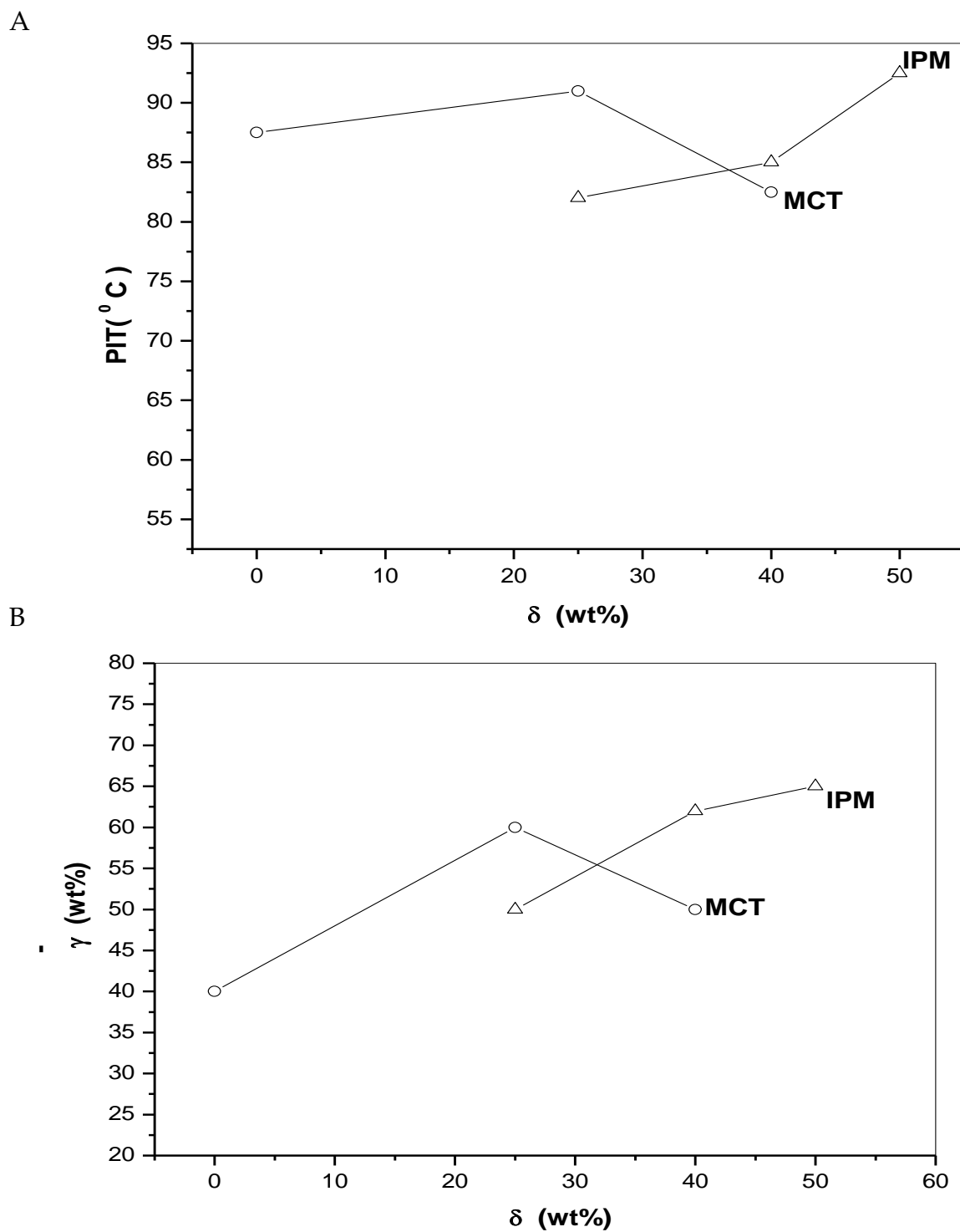


Fig. 4.49: Phase inversion temperature $\bar{T}_{(PIT)}$ (°C) [A] and the mean concentration ($\bar{\gamma}$) in wt% [B], for the system: Water/ L₁₆₉₅/ PG/ Oil at constant $Oil/(Oil + Water)$ weight ratio, $\alpha = 50$ wt%, and variable δ (wt%).

Table 4.2: Summary of the analysis of the system: Water/ L₁₆₉₅/ PG/ Oil at constant $Oil/(Oil + Water)$ weight ratio, $\alpha = 50$ wt%, and variable δ (wt%), γ (wt%) and T (°C).

Oil	Quaternary	Ternary
R(+)-limonene	No 3 ϕ formation Only 1 ϕ region Increase PG \rightarrow increase γ_{min}	$\gamma_{minR(+)-limonene} > \gamma_{minIPM}$ $T_{R(+)-limonene} > T_{IPM}$
IPM	Formation of 3 ϕ Increase PG \rightarrow increase $\bar{\gamma}$ and increase \bar{T}	
MCT	Formation of 3 ϕ Increase PG \rightarrow increase $\bar{\gamma}$ and increase \bar{T}	

System 2: Water/ S₁₅₇₀/ PG/ Oil

In the case where R(+)-limonene and IPM are used as the oil phase, the presence of PG will not induce the formation of 3 ϕ region in the phase diagram. This absence of a three-phase body indicates being beyond the tricritical point of the mixture. Increasing the ratio of PG in the system will decrease the amount of surfactant needed for the formation of one-phase region and will also decrease the temperature at which the one-phase region is formed. In the case of ternary system: Water/ S₁₅₇₀/ R(+)-limonene and Water/ S₁₅₇₀/ IPM, the concentration of surfactant needed for the formation of one-phase in the case of R (+)-limonene is lower than that needed for the

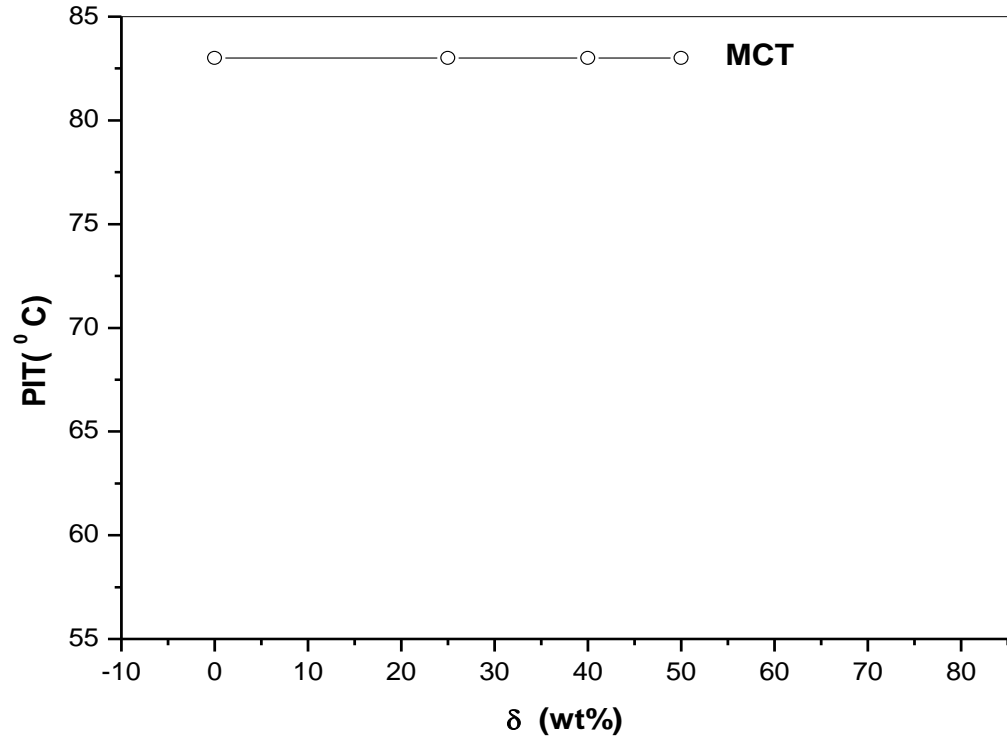
system containing IPM. The temperature at which the one phase is formed at the concentration where the one phase appears is lower in the case of the system containing R(+)-limonene than that containing IPM.

When MCT is used as the oil phase, 3 ϕ region is observed in the absence and presence of PG. Increasing the ratio of PG will not affect the efficiency of the surfactant and nor the phase inversion temperature. **Tables 4.3 and 4.4 and Fig. 4.50** summarize these results.

Table 4.3: Summary of the results of the system: Water/ S_{1570} / PG/ Oil at constant $Oil/(Oil + Water)$ weight ratio, $\alpha = 50$ wt%, and variable δ (wt%), γ (wt%) and T ($^{\circ}C$).

δ (wt%)	R(+)-limonene			IPM			MCT		
	γ_{min} or $\bar{\gamma}$ (wt%)	T or \bar{T} ($^{\circ}C$)	Phases	γ_{min} or $\bar{\gamma}$ (wt%)	T or \bar{T} ($^{\circ}C$)	Phases	γ_{min} or $\bar{\gamma}$ (wt%)	T or \bar{T} ($^{\circ}C$)	Phases
0	25	65.5	No 3 ϕ formation	42.5	75	No 3 ϕ formation	52	83	3 ϕ formation
25	24	61		32.5	71		52	83	
40	24	56.5		25	68		52	83	
50	20	56		17.5	67.5		52	83	
75	20	58		60	50				
100	Two liquid phases			Two liquid phases			Two liquid phases		

A



B

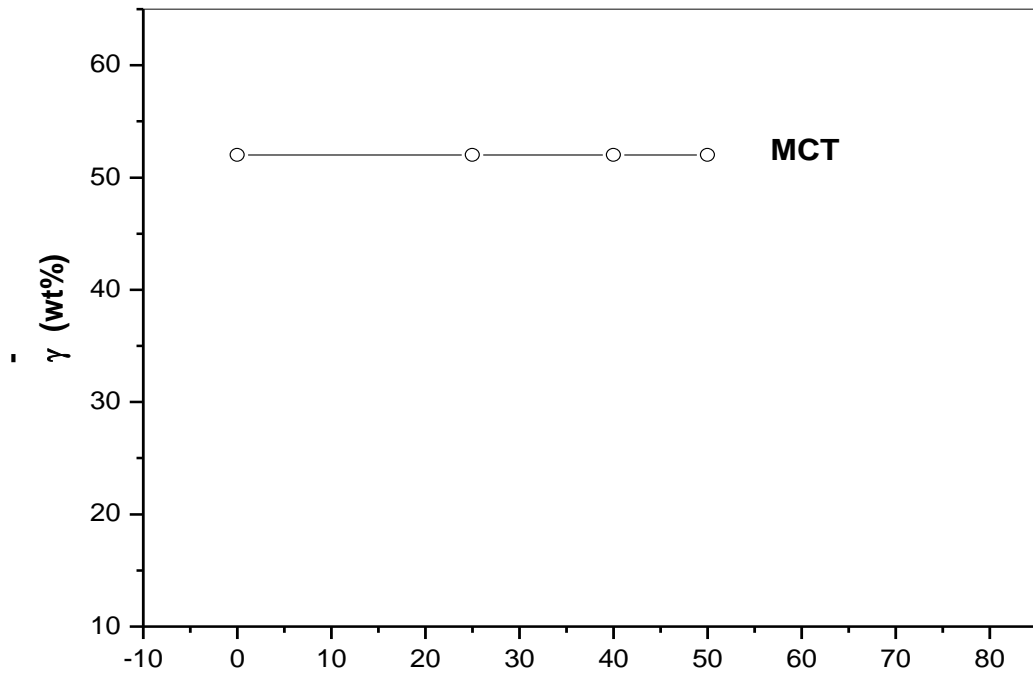


Fig. 4.50: Phase inversion temperature δ (wt%) (PIT) (°C) [A] and the mean concentration ($\bar{\gamma}$) in wt% [B], for the system: Water/ S_{1570} / PG/ Oil at constant $Oil/(Oil + Water)$ weight ratio, $\alpha = 50$ wt%, and variable δ (wt%).

Table 4.4: Summary of the analysis of the system: Water/ S₁₅₇₀/ PG/ Oil at constant $Oil/(Oil + Water)$ weight ratio, $\alpha = 50$ wt%, and variable δ (wt%), γ (wt%) and T (°C).

Oil	Quaternary	Ternary Water/S ₁₅₇₀ /Oil
R(+)- limonene	No 3 ϕ formation Increase PG \rightarrow decrease γ_{\min} and decrease T	1 ϕ formation $\gamma_{\min \text{ R(+)-limonene}} < \gamma_{\min \text{ IPM}}$
IPM	No 3 ϕ formation Increase PG \rightarrow decrease γ_{\min} and decrease T	$T_{\text{R(+)-limonene}} < T_{\text{IPM}}$
MCT	Formation of 3 ϕ Increase PG $\rightarrow \bar{\gamma}$ and \bar{T} remain constant.	
	For δ values ≥ 75 wt % $T_{\text{R(+)-limonene}} > T_{\text{IPM}}$ $\gamma_{\min \text{ R(+)-limonene}} < \gamma_{\min \text{ IPM}}$	

System 3: Water/ EMDG/ PG/ Oil

When R(+)-limonene is used as the oil phase, the 3 ϕ region is observed for high contents of PG (i.e. $75 \leq \delta < 100$ wt%). At δ values below this value no 3 ϕ region is observed. This absence of a 3-phase body indicates being beyond the tricritical point of the mixture. Increasing the ratio of PG i.e. $\delta = 25$ wt% to $\delta = 50$ wt%, the surfactant and PG concentration needed for the formation of one phase region is decreased and the temperatures at

which the one phase region is formed at the corresponding concentration of surfactant and PG increases.

In the case where IPM and MCT are used as the oil phase, no 3 ϕ region is observed in the presence of PG. The concentration of the surfactant and PG needed for the formation of the one phase region is decreased and the temperature at which the one phase region is formed increased.

The ternary systems of Water/ EMDG/ Oil , shows the presence of three phase region in the case of the two oils IPM and MCT. The efficiency ($\bar{\gamma}$) of the EMDG is higher in the case of IPM than that of MCT and the phase inversion temperature (\bar{T}) is higher in the case of IPM than of MCT. **Tables 4.5 and 4.6 and Fig. 4.51** summarize these results.

Table 4.5: Summary of the results of the system: Water/ EMDG/ PG/ Oil at constant $Oil/(Oil + Water)$ weight ratio, $\alpha = 50$ wt%, and variable δ (wt%), γ (wt%) and T ($^{\circ}$ C).

PG	R(+)-limonene			IPM			MCT		
δ (wt%)	γ_{min} or $\bar{\gamma}$ (wt%)	T or \bar{T} ($^{\circ}$ C)	Phases	γ_{min} or $\bar{\gamma}$ (wt%)	T or \bar{T} ($^{\circ}$ C)	Phases	γ_{min} or $\bar{\gamma}$ (wt%)	T or \bar{T} ($^{\circ}$ C)	Phases
0	52	52	No 3 ϕ formation	26.5	105	3 ϕ formation	42	85	3 ϕ formation
25	68	47.5							
50	35	55		55	55	No 3 ϕ	65	70	No 3 ϕ
75	45	92.5	3 ϕ formation	35	55		60	60	
100	Two liquid phases			Two liquid phases			Two liquid phases		

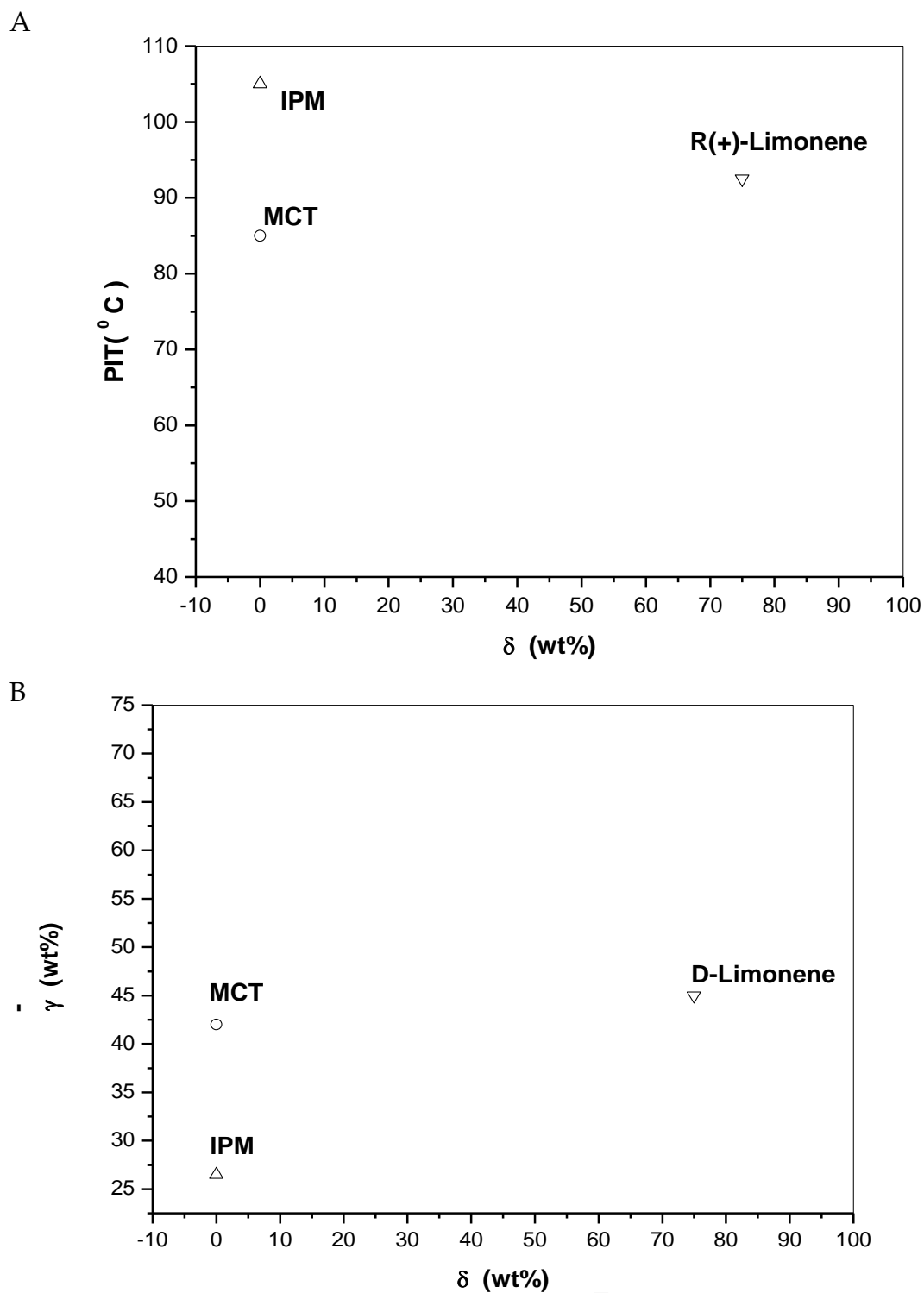


Fig. 4.51: Phase inversion temperature $\bar{T}_{(PIT)}$ (°C) [A] and the mean concentration ($\bar{\gamma}$) in wt% [B], for the system: Water/ EMDG/ PG/ Oil at constant $Oil/(Oil + Water)$ weight ratio, $\alpha = 50$ wt%, and variable δ (wt%).

Table 4.6: Summary of the analysis of the system: Water/ EMDG/ PG/ Oil at constant $Oil/(Oil + Water)$ weight ratio, $\alpha = 50$ wt%, and variable δ (wt%), γ (wt%) and T ($^{\circ}C$).

Oil	Quaternary	Ternary Water/EMDG/Oil
R(+)-limonene	No formation of 3 ϕ only 1 ϕ formed Increase PG \rightarrow decrease γ_{min} and increase T Formation of 3 ϕ for quaternary at $\delta=75wt\%$	No 3 ϕ formation
IPM	No 3 ϕ only 1 ϕ Increase PG \rightarrow decrease γ_{min} and T practically remains constant	3 ϕ formation
MCT	Increase PG \rightarrow decrease γ_{min} and decrease T	

System 4: Water/ L₁₆₉₅/ EMDG/ Oil

In the case where R(+)-limonene is used as the oil phase, the 3 ϕ region is observed for δ values varying from 25 to 50 wt%. The efficiency ($\bar{\gamma}$) of the mixed surfactant systems is increased (i.e. $\bar{\gamma}$ decreases) when the EMDG content increases from $\delta = 25$ wt% to $\delta = 50$ wt%, and the phase inversion temperature is slightly increased. In the absence of EMDG (i.e. $\delta = 0$ wt%) no three phase region is observed and also in the absence of L₁₆₉₅ (i.e. $\delta = 100$ wt%) no 3 ϕ region is observed. The L₁₆₉₅ content needed for the

formation of the one phase region for $\delta = 0$ wt% is lower than that of EMDG in the system where $\delta = 100$ wt%. The temperature at which the one phase region is formed in the ternary system containing L₁₆₉₅ is higher than that in the ternary system containing EMDG.

Using IPM as the oil phase, the ternary system: Water/ L₁₆₉₅/ IPM no three phase region is observed. The presence of EMDG will induce the formation of three phase region. Increasing the ratio of EMDG in the mixed surfactant content will increase the efficiency (i.e. decrease $\bar{\gamma}$ values) of the mixed surfactants and will decrease the phase inversion temperature (\bar{T}). The phase inversion temperature is higher in the ternary system: Water/ EMDG/ IPM than these of the quaternary system where L₁₆₉₅ is present.

In the case where MCT is used as the oil phase, the three phase region is present for the ternary and quaternary systems. In the ternary systems Water/ L₁₆₉₅/ MCT (i.e. $\delta = 0$ wt%) and Water/ EMDG/ MCT (i.e. $\delta = 100$ wt%) the efficiency of the surfactant ($\bar{\gamma}$) in the system containing L₁₆₉₅ is higher than that containing EMDG. The phase inversion temperature (\bar{T}) in the system containing L₁₆₉₅ is higher than that containing EMDG.

For the quaternary systems, increasing the ratio of EMDG in the mixed surfactants content will increase the efficiency (i.e. decrease the values of $\bar{\gamma}$) of the mixed surfactants and will decrease the phase inversion temperature. EMDG is more hydrophobic surfactant than L₁₆₉₅ thus one expects to obtain higher values for the PIT in the case where L₁₆₉₅ is present than in the case where EDMG is present. **Tables 4.7 and 4.8 and Fig. 4.52** summarize the results of these systems.

Table 4.7: Summary of the results of the system: Water/ L₁₆₉₅/ EMDG/ Oil at constant $Oil/(Oil + Water)$ weight ratio, $\alpha = 50$ wt%, and variable δ (wt%), γ (wt%) and T (°C).

EMDG	R(+)-limonene			IPM			MCT		
δ (wt%)	γ_{min} or $\bar{\gamma}$ (wt%)	T or \bar{T} (°C)	Phases	γ_{min} or $\bar{\gamma}$ (wt%)	T or \bar{T} (°C)	Phases	γ_{min} or $\bar{\gamma}$ (wt%)	T or \bar{T} (°C)	Phases
0	32.5	80	No 3 ϕ formation	25	70	No 3 ϕ formation	37.5	87.5	3 ϕ formation
25	21	85	3 ϕ formation	28	87.5	3 ϕ formation	41	85	
50	16.5	90		28	72.5		36	82.5	
75	41	80	No 3 ϕ Only 1 ϕ formation	23.5	72	37	78		
100	52	60		27	95	42	83		

Table 4.8: Summary of the analysis of the system: Water/ L₁₆₉₅/ EMDG/ Oil at constant $Oil/(Oil + Water)$ weight ratio, $\alpha = 50$ wt%, and variable δ (wt%), γ (wt%) and T (°C).

Oil	Quaternary	Ternary Water / Surfactant / Oil
R(+)-limonene	<p>3ϕ formation for δ values $25 \leq \delta < 75$wt%</p> <p>Increase EMDG \rightarrow increase \bar{T} decrease $\bar{\gamma}$</p>	<p>$\gamma_{\min L1695} < \gamma_{\min EMDG}$</p> <p>$T_{L1695} > T_{EMDG}$</p>
IPM	<p>3ϕ formation</p> <p>Increase EMDG \rightarrow decrease \bar{T} decrease $\bar{\gamma}$</p> <p>$\bar{\gamma}_{\text{quaternary}} > \bar{\gamma}_{\text{ternary EMDG}}$</p> <p>$\bar{T}_{\text{quaternary}} < \bar{T}_{\text{ternary EMDG}}$</p> <p>$\bar{\gamma}_{\text{quaternary}} > \bar{\gamma}_{\text{ternary L1695}}$</p> <p>$\bar{T}_{\text{quaternary}} > T_{\text{ternary L1695}}$</p>	
MCT	<p>3ϕ formation</p> <p>Increase EMDG \rightarrow decrease \bar{T} decrease $\bar{\gamma}$</p> <p>$\bar{\gamma}_{\text{quaternary}} < \bar{\gamma}_{\text{ternary EMDG}}$</p>	<p>$\bar{\gamma}_{L1695} < \bar{\gamma}_{EMDG}$</p> <p>$\bar{T}_{L1695} > \bar{T}_{EMDG}$</p>

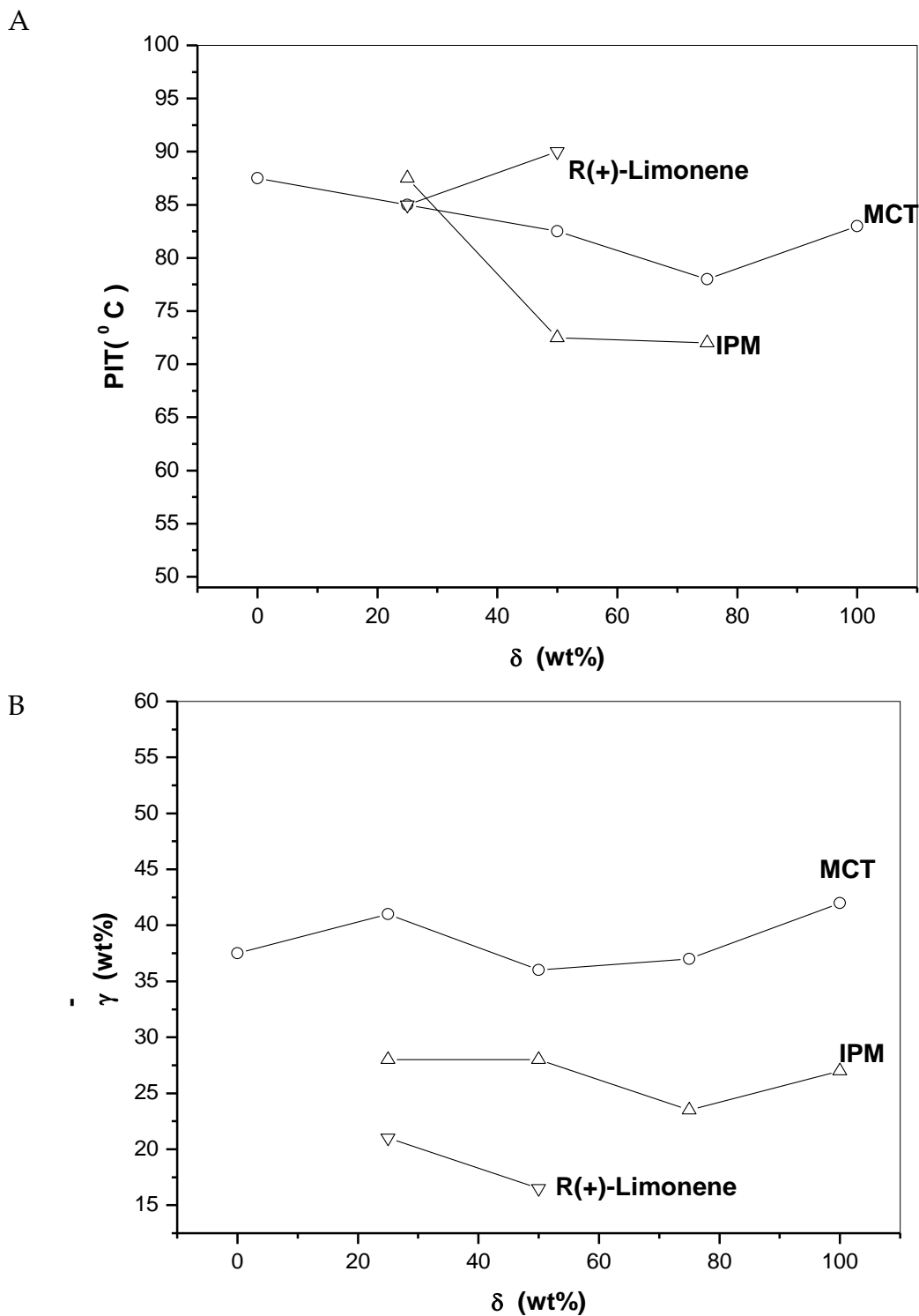


Fig. 4.52: Phase inversion temperature $\bar{T}_{(PIT)}$ (°C) [A] and the mean concentration ($\bar{\gamma}$) in wt% [B], for the system: Water/ L₁₆₉₅/ EMDG/ Oil at constant $Oil/(Oil + Water)$ weight ratio, $\alpha = 50$ wt%, and variable δ (wt%).

System 5: Water/ S₁₅₇₀/ EMDG/ Oil

When R(+)-limonene is used as the oil phase no three phase region is observed for the ternary and quaternary system. This absence of a three-phase body indicates being beyond the tricritical point of the mixture. In the ternary system: Water/ S₁₅₇₀/ R(+)-limonene (i.e. $\delta = 0$ wt%) the concentration of S₁₅₇₀ needed for the formation of the one phase region is lower than the concentration of EMDG needed in the system: Water/ EMDG/ R(+)-limonene (i.e. $\delta = 100$ wt%) while the temperature needed for the EMDG containing system is lower than that needed for the S₁₅₇₀ containing system.

In the quaternary system, increasing the ratio of EMDG in the mixed surfactants content will increase the concentration of mixed surfactants needed for the formation of the one phase region and will increase slightly the temperature at which the one phase is formed at these concentrations.

In the case where IPM is used as the oil phase, the three phase region is formed for high contents of EMDG in the mixed surfactants contents (i.e. $\delta \geq 75$ wt%) and for the ternary system: Water/ EMDG/ IPM (i.e. $\delta = 100$ wt%). For the ternary system: Water/ S₁₅₇₀/ IPM (i.e. $\delta = 0$ wt%) no three phase is observed neither in the quaternary systems where $\delta = 25$ wt% and 50 wt%. Increasing the content of EMDG from $\delta = 25$ to 50 wt% will decrease the concentration of mixed surfactant systems needed for the formation of one phase region and also decreases the temperature at which this one phase region is formed.

Using MCT as the oil phase, three phase region is present for the ternary and quaternary systems. In the ternary system: Water/ S₁₅₇₀/ MCT the efficiency of the S₁₅₇₀ is lower than that needed from the EMDG in the

system: Water/ EMDG/ MCT. The phase inversion temperature (\bar{T}) is also slightly lower for S₁₅₇₀ containing system than for EMDG containing one. Increasing the ratio of EMDG in the mixed surfactant contents will decrease the efficiency (i.e. increase the values of $\bar{\gamma}$) of the mixed surfactants and will decrease the phase inversion temperature (\bar{T}). **Table 4.9 and 4.10 and Fig. 4.53** summarizes the results of these systems.

Table 4.9: Summary of the results of the system: Water/ S₁₅₇₀/ EMDG/ Oil at constant $Oil/(Oil + Water)$ weight ratio, $\alpha = 50$ wt%, and variable δ (wt%), γ (wt%) and T (°C).

δ (wt%)	R(+)-limonene			IPM			MCT		
	γ_{min} or $\bar{\gamma}$ (wt%)	T or \bar{T} (°C)	Phases	γ_{min} or $\bar{\gamma}$ (wt%)	T or \bar{T} (°C)	Phases	γ_{min} or $\bar{\gamma}$ (wt%)	T or \bar{T} (°C)	Phases
0	25	65	No 3 ϕ formation	42	75	No 3 ϕ formation	51	82.5	3 ϕ formation
25	19	65		15	67.5		22.5	82.5	
50	30	70		5	62.5		32.5	80	
75	34	70		13	80	35	82		
100	52	60		27	92	42	87		

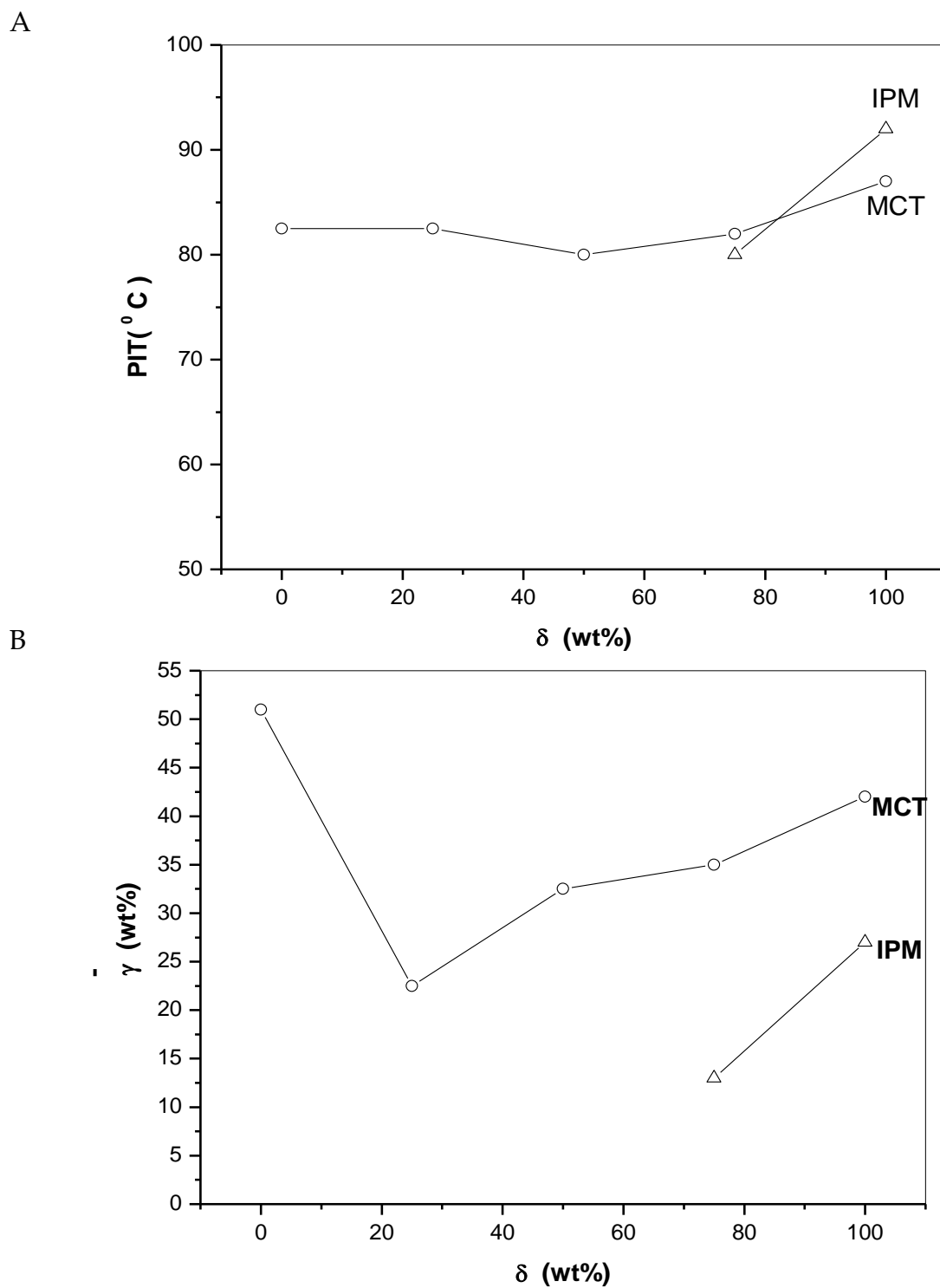


Fig. 4.53: Phase inversion temperature $\bar{T}_{(PIT)}$ (°C) [A] and the mean concentration ($\bar{\gamma}$) in wt% [B], for the system: Water/ S_{1570} / EMDG/ Oil at constant $Oil/(Oil + Water)$ weight ratio, $\alpha = 50$ wt%, and variable δ (wt%).

Table 4.10: Summary of the analysis of the system: Water/ S_{1570} / EMDG/ Oil at constant $Oil/(Oil + Water)$ weight ratio, $\alpha = 50$ wt%, and variable δ (wt%), γ (wt%) and T (°C).

Oil	Quaternary	Ternary
R(+)-limonene	No 3 ϕ formation Increase EMDG \rightarrow increase γ_{\min} increase T	$\gamma_{\min S_{1570}} < \gamma_{\min EMDG}$ $T_{S_{1570}} > T_{EMDG}$
IPM	3 ϕ for $\delta \geq 75\%$ For 1 ϕ increase EMDG, decrease γ_{\min} and decrease T For 3 ϕ increase EMDG, increase $\bar{\gamma}$ and increase \bar{T}	
MCT	Increase EMDG \rightarrow increase $\bar{\gamma}$ and decrease \bar{T}	$\bar{\gamma}_{S_{1570}} > \bar{\gamma}_{EMDG}$ $\bar{T}_{S_{1570}} < \bar{T}_{EMDG}$

As a general conclusion, 1,2-Propandiol(PG) which is a substitute of methanol, ethanol and propanol dissolve mainly in the water-rich phase. Adding PG that is completely miscible with water increases the mutual solubility between water and amphiphile. This makes T_{β} rise but T_{α} drops, adding PG to the system of: Water/ amphiphile/ Oil decreases the hydrophobicity of the amphiphile. Increasing the concentration of PG in the mixture with a given oil makes \bar{T} rise with nonionic amphiphile. This behavior was observed in the systems where the three phase body appears such as with the system: Water/ L_{1695} / PG/ Oil where the oils was IPM and MCT and the system: Water/ S_{1570} / PG/ MCT. Varying the hydrophobicity of

the amphiphile by changing the chain length of the hydrophobic part if the head part stays the same as in the case of the nonionic surfactants L₁₆₉₅ and S₁₅₇₀ (chain lengths 12 and 18, respectively), makes \bar{T} drop. EMDG is also a nonionic surfactant with an HLB = 13.5 smaller than that of L₁₆₉₅ (HLB = 16) and S₁₅₇₀ (HLB = 15) which means that EMDG is the most hydrophobic surfactant between the three surfactants studied. As we can see in the systems: Water/ Surfactant/ PG/ MCT, \bar{T}_{L1695} is bigger than that of \bar{T}_{S1570} for the three phase bodies formed as expected. EMDG does not show a formation of three phase body. The system: Water/ surfactant/ PG/ IPM also shows the same behavior that $\bar{T}_{L1695} > \bar{T}_{S1570}$. Considering the effect of changing the chain length of oil or its nature if the amphiphile remains the same, increasing the effective carbon number of the oil will rise T_α , this decreases the tendency of nonionic amphiphile to leave the water-rich phase for the oil-rich phase as T raises, accordingly, \bar{T} rises with nonionic amphiphiles with rising the effective chain length of oils. In the case of the oils used in this research R(+)-limonene, IPM and MCT. R(+)-limonene is a cyclic terpene with an effective chain length of 7 carbons with a molar volume of 162 cm³/mol, IPM is a polar straight chain oil with an effective carbon number of 17 and a molar volume of 270 cm³/mol, MCT is triglyceride branched oil forming a fork like shape with an effective carbon number of about 20 and a molar volume of 530 cm³/mol. It is suggested that the \bar{T} in MCT containing system to be the higher and this case was observed in the systems: Water/ L₁₆₉₅/ PG/ Oil for the oils IPM and MCT and also in the system: Water/ S₁₅₇₀/ PG/ Oil for the cases where the three phase region was formed (see **Table 4.11**) .

EMDG increase the hydrophobicity of the mixed surfactants but the behavior of the system will not change in tendency as we can see in (Table 4.12).

Table 4.11: Summary of the analysis of the results of the System: Water/ Surfactant/ PG/ Oil at constant $Oil/(Oil + Water)$ weight ratio, $\alpha = 50$ wt%, and variable δ (wt%), γ (wt%) and T (°C).

Water/Surfactant/PG/MCT	Water/Surfactant/PG/IPM
$\bar{T}_{L1695} > \bar{T}_{S1570}$	$\bar{T}_{L1695} > \bar{T}_{S1570}$
$\bar{\gamma}_{L1695} > \bar{\gamma}_{S1570}$	$\bar{\gamma}_{L1695} > \bar{\gamma}_{S1570}$

Table 4.12: Summary of the analysis of the results of the System: Water/ Surfactant/ EMDG/ Oil at constant $Oil/(Oil + Water)$ weight ratio, $\alpha = 50$ wt%, and variable δ (wt%), γ (wt%) and T (°C).

Oil	Ternary
R(+)-limonene	$\gamma_{\min L1695} > \gamma_{\min S1570}$ $T_{L1695} > T_{S1570}$
IPM	$\gamma_{\min L1695} < \gamma_{\min S1570}$ $T_{L1695} < T_{S1570}$
MCT	$\bar{\gamma}_{L1695} < \bar{\gamma}_{S1570}$ $\bar{T}_{L1695} > \bar{T}_{S1570}$

b- Variation of weight ratio of oil in the mixture of oil and water (i.e α (wt%)) and temperature (T) at constant mixed amphiphile content (γ , (wt%)), and ratios (δ , (wt%)).

The systems studied are presented in the following table:

Table 4.13: System used in the study of variation of $Oil/(Oil + Water)$, α (wt %) as function of (T (°C)) for constant γ (wt%) and δ (wt%).

No.	System	γ (wt%)	δ (wt%)	Fig.
1.	Water/L₁₆₉₅/PG/Oil			
a.	Water/L ₁₆₉₅ /PG/IPM	26	0	4.18.A
b.	Water/L ₁₆₉₅ /PG/IPM	35.5	25	4.18.B
2.	Water/S₁₅₇₀/PG/Oil			
a.	Water/S ₁₅₇₀ /PG/R(+)-limonene	20	0	4.13.A
b.	Water/S ₁₅₇₀ /PG/R(+)-limonene	20	25	4.13.B
c.	Water/S ₁₅₇₀ /PG/IPM	31	0	4.21.A
d.	Water/S ₁₅₇₀ /PG/IPM	26	25	4.21.B
e.	Water/S ₁₅₇₀ /PG/MCT	35.5	25	4.28
3.	Water/L₁₆₉₅/EMDG/Oil			
a.	Water/L ₁₆₉₅ /EMDG/R(+)-limonene	26	25	4.33.A
b.	Water/L ₁₆₉₅ /EMDG/R(+)-limonene	31	50	4.33.B
c.	Water/L ₁₆₉₅ /EMDG/IPM	26	25	4.38.A
d.	Water/L ₁₆₉₅ /EMDG/IPM	31	50	4.38.B
e.	Water/L ₁₆₉₅ /EMDG/MCT	31	25	4.44
4.	Water/S₁₅₇₀/EMDG/Oil			
a.	Water/S ₁₅₇₀ /EMDG/IPM	16.6	25	4.41
b.	Water/S ₁₅₇₀ /EMDG/MCT	23.1	25	4.47

System1: Water/ L₁₆₉₅/ PG/ Oil

The system was studied only with IPM as the oil phase. For the ternary system: Water/ L₁₆₉₅/ IPM (i.e. $\delta = 0$ wt %) the surfactant content used was 20 wt%. A one phase region was observed for the range of temperatures varying from 0 to 80°C and the range of α values varying from 0 (wt %) at 0°C to 15 (wt %) at 50 to 80°C. a two phase regions were formed for all of the range of T and α (wt %) values bigger than those mentioned above. At low temperatures a (W_m + O) two phase region is formed and at high T a (W + O_m) two phase region is formed.

For the quaternary system: Water/ L₁₆₉₅/ PG/ IPM (i.e. $\delta = 25$ wt %), when increasing the surfactant content to $\gamma = 35.5$ wt%, the formation of one phase region is observed for the range of temperature varying from 0 to 90°C and the range of α values varying from 0 (wt%) at 90°C to 20 (wt%) at 80 to 90°C. For all the values of α (wt%) bigger than these concentrations the two phase region (W_m + O) and (W + O_m) is formed. From these results we can say that the addition of PG and increasing of the mixed surfactant content in the mixture will increase and shifts the one phase region upward along the temperature scale also shifts this region to $\alpha = 20$ wt%.

System 2: Water/ S₁₅₇₀/ PG/ Oil

2. A: Water / S₁₅₇₀/ PG/ R (+)-limonene
2. B: Water/ S₁₅₇₀/ PG/ IPM
2. C: Water/ S₁₅₇₀/ PG/ MCT

In these systems we observed that a one phase region is observed at $\delta = 0$ wt% with the two oils R (+)-limonene and IPM while no one phase region is observed with MCT.

This one phase region is extended over all of the range of α values in the case of R (+)-limonene while it extends from $\alpha = 60$ wt% to 100 wt% in the case of IPM. It is also wider in the R (+)-limonene for high α values than in the case of IPM. R (+)-limonene is less hydrophobic oil than IPM

Adding PG to the ternary system: Water/ S₁₅₇₀/ Oil (i.e. $\delta = 25$ wt %). A one phase region is observed over all of the range of α values in the case of R (+)-limonene and IPM but for α values bigger than 55 wt% in the case of MCT. For low α values $\alpha < 15$ wt% the range of temperature over which the one phase appears is the same for R (+)-limonene and IPM (i.e. $47 < T < 77^\circ\text{C}$). In the case of high α values > 85 wt% the range of temperature over which the one phase appears is slightly wider in the case of R (+)-limonene than IPM and MCT. **Table 4.14** summarizes these results. As we mentioned previously adding PG will increase the mutual solubility of surfactant and water and will induce the formation of the one phase region as we observed it with the three oils. The extension of the one phase region is also related to the hydrophobicity of the oil which increases when one passes from R (+)-limonene to IPM then to MCT.

Table 4.14: Summary of the results of the system: water/ S₁₅₇₀/ PG/ Oil, for variable $Oil/(Oil + Water)$ weight ratio, α (wt %) and temperature (°C).

Oil (γ (wt %))	R(+)-limonene	IPM	MCT
$\delta = 0$ wt%	$\gamma = 20$ wt%	$\gamma = 31$ wt%	$\gamma = 31$ wt%
$\alpha < 15$ wt%	$47 < T < 77$	No 1 ϕ formation	No 1 ϕ formation
$15 < \alpha < 65$ wt%	$60 < T < 77$	No 1 ϕ formation	No 1 ϕ formation
$\alpha = 100$ wt%	$0 < T < 95$	$60 < T < 100$	No 1 ϕ formation
Oil (γ (wt %))	R(+)-limonene	IPM	MCT
$\delta = 25$ wt%	$\delta = 20$ wt%	$\delta = 26$ wt%	$\delta = 35.5$ wt%
$\alpha < 15$ wt%	$47 < T < 77$	$47 < T < 77$	No 1 ϕ formation
$0 < \alpha < 50$ wt%	$60 < T < 77$	$60 < T < 80$	No 1 ϕ formation
$\alpha = 100$ wt%	$20 < T < 100$	$30 < T < 100$	$30 < T < 100$

System3: Water/ L₁₆₉₅/ EMDG/ Oil

In the case of δ values = 25 wt% and for the three oils, the one phase region extends over all of the range of α values over the range of temperature R (+)-limonene gave the wider one phase region.

Again the chemical structure of R (+)-limonene improves itself on the system. In the case of δ values = 50 wt%, R (+)-limonene also gave a wider one phase region over the scale of temperatures compared to IPM, (MCT, not studied). **Table 4.15** summarizes these results.

Table 4.15: Summary of the results of the system: Water/ L₁₆₉₅/ EMDG/ Oil, for variable $Oil/(Oil + Water)$ weight ratio, α (wt %) and temperature (°C).

Oil (γ (wt %))	R(+)-limonene	IPM	MCT
$\delta = 25$ wt%	$\gamma = 26$ wt%	$\gamma = 26$ wt%	$\gamma = 31$ wt%
$0 < \alpha < 10$	$17 < T < 95$	$5 < T < 80$	$5 < T < 95$
$\alpha = 50$ wt%	$80 < T < 95$	$77.5 < T < 80$	$80 < T < 85$
$\alpha = 100$ wt%	$20 < T < 110$	$5 < T < 80$	$35 < T < 85$
Oil (γ (wt %))	R(+)-limonene	IPM	-----
$\delta = 50$ wt%	$\gamma = 31$ wt%	$\gamma = 31$ wt%	-----
$0 < \alpha < 10$ wt%	$18 < T < 95$	$18 < T < 110$	-----
$\alpha = 50$ wt%	$40 < T < 95$	$90 < T < 110$	-----
$\alpha = 100$ wt%	$20 < T < 110$	$35 < T < 110$	-----

System 4: Water/ S₁₅₇₀/ EMDG/ oil

Table 4.16: Summary of the results of the system: water/ S₁₅₇₀/ EMDG/ Oil, for variable $Oil/(Oil + Water)$ weight ratio, α (wt %) and temperature (°C).

Oil (γ (wt %))	IPM	MCT
$\delta = 25$ wt%	$\gamma = 16.6$ wt%	$\gamma = 23.1$ wt%
$0 < \alpha < 10$ wt%	$47 < T < 67$	$47 < T < 95$
$\alpha = 50$ wt%	$60 < T < 70$	No 1 ϕ
$\alpha = 100$ wt%	$40 < T < 100$	No 1 ϕ

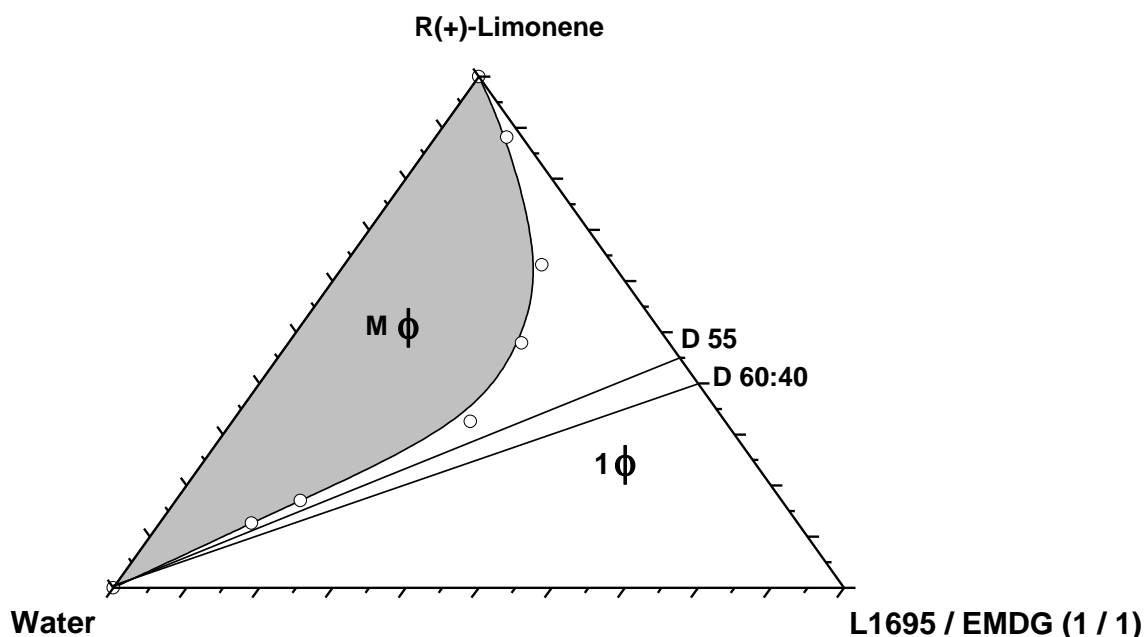
As we can see in **Table 4.16**, the one phase region extends over all of the range of α values, when IPM is used as the oil phase while in the case of MCT this one phase is vary small and had a triangle shape with a height equals 10 wt%. The behavior of MCT corresponds to it chemical structure and also is affected by the fact the mixed surfactant system $S_{1570} + \text{EMDG}$ is more hydrophobic than that of $L_{1695} + \text{EMDG}$ and thus is less able to solubilize oil in water. R (+)-limonene is not studied here but according to these results it is expected to behave like IPM or even to give a wider one phase channel on the temperature scale.

IV.1.5 Pseudoternary Phase Diagram

The pseudoternary phase diagrams of the different systems studied are shown in the (Fig. 4.54 to 4.57). The translucent and low-viscosity area is presented in the phase diagrams as a microemulsion one phase area (1ϕ), the conversion from water continuous microemulsion region to oil continuous region passes through a bicontinuous isotropic region. The remainder of the phase diagram represents the turbid region, represented as multiphase ($M\phi$) and conventional emulsions based on visual identification.

Fig. 4.54 shows the pseudoternary phase behavior of the systems: Water/ L_{1695} / EMDG/ R (+)-Limonene (A) and Water/ L_{1695} / EMDG/ EtOH/ R (+)-Limonene (B). The weight ratio of L_{1695} / EMDG = 1 in the two systems and the weight ratio of EtOH/ R (+)-Limonene = 1 in the system (B). From these two figures we observe that a one phase region is extended over all of range of water dilution which means that the maximum water solubilization W_m equals 100%. In system (A) this extension is found for initial mixed surfactant content equals 55wt% (i.e. dilution line 55). While in system (B), this extension is found for initial mixed surfactant concentration equals 30wt% (i.e. dilution line 30). The total microemulsion area on the pseudoternary phase diagram (A_T) is 61.6% and 74.2% for the two systems, respectively. Table 4.17 summarizes the results of these two systems.

A



B

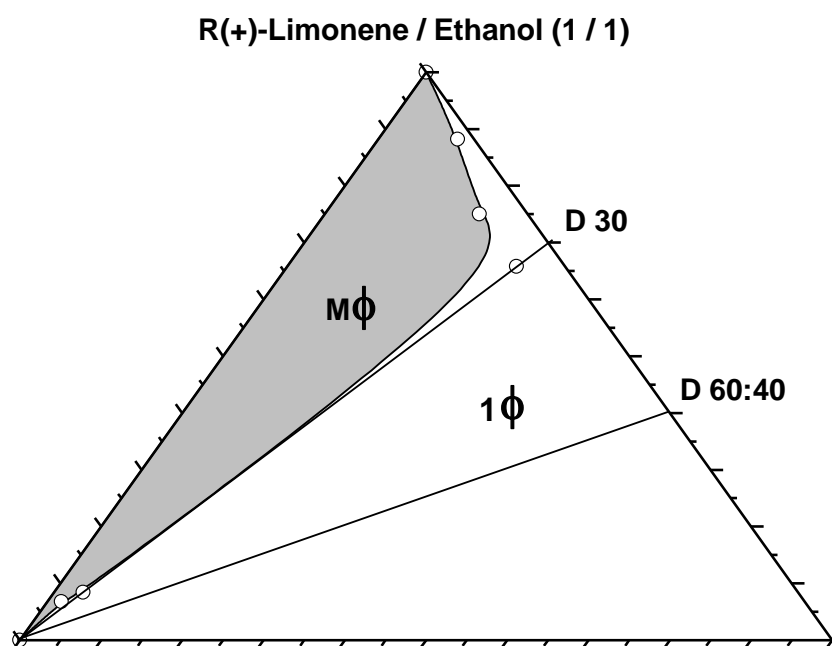


Fig. 4.54: Phase diagrams of the systems: Water/ L₁₆₉₅/ EMDG / R (+)-Limonene (A) and Water / L₁₆₉₅ / EMDG / EtOH / R (+)-Limonene (B) at 25°C. The weight ratio of L₁₆₉₅/ EMDG = 1 in the two systems (A), and (B), and that of R (+)-Limonene/ Ethanol = 1 in the system (B). The one phase region is designated by 1φ, and the multiple phase region is designated by Mφ.

Table 4.17: Summary of the results of the pseudoternary phase behavior of the system: Water/ L₁₆₉₅/ EMDG/ EtOH/ R (+)-Limonene at 25°C.

System	L ₁₆₉₅ /EMDG (<i>weight ratio</i>)	EtOH/R(+)-Limonene (<i>weight ratio</i>)	Dilution line for maximum water solubilization (W _m)	W _m (wt%)	A _T (%)
A	1	0	55	100	61.6
B	1	1	30	100	74.2

Fig. 4.55 shows the pseudoternary phase behavior of the systems: water/ L₁₆₉₅/ EMDG/ R (+)-Limonene (A) and Water/ L₁₆₉₅/ EMDG/ R (+)-Limonene (B). The weight ratio of L₁₆₉₅/ EMDG = 1/3 in the two systems and that of EtOH / R (+)-Limonene = 1 in system (B). In **Fig. 4.55 (A)** we observe that the maximum water solubilization (W_m) which equals 60 wt% is observed at initial surfactant content equals 70 wt% (i.e. dilution line 70). The minimum content of surfactant S_m needed for the maximum amount of solubilized water is 31 wt%. A separation to multiple phase region is observed above this concentration of water then again a new one phase region highly viscous is observed at 65 wt% water content and extends to 80 wt% water which is liquid crystal phase. Above this concentration of water a multiple phase region is again observed. The total one phase region (A_T) observed in the pseudo ternary phase region is 47.2%.

In **Fig. 4.55 (B)** the one phase region is extended over all of the range of water contents at the dilution line 40 (i.e. initial mixed surfactant content equals 40 wt%) as the minimum mixed surfactants initial content capable of forming continuous phase region. The total one phase region (A_T) observed

in the pseudoternary phase region is 66.1%. **Table 4.18** summarizes the results of these two systems.

A

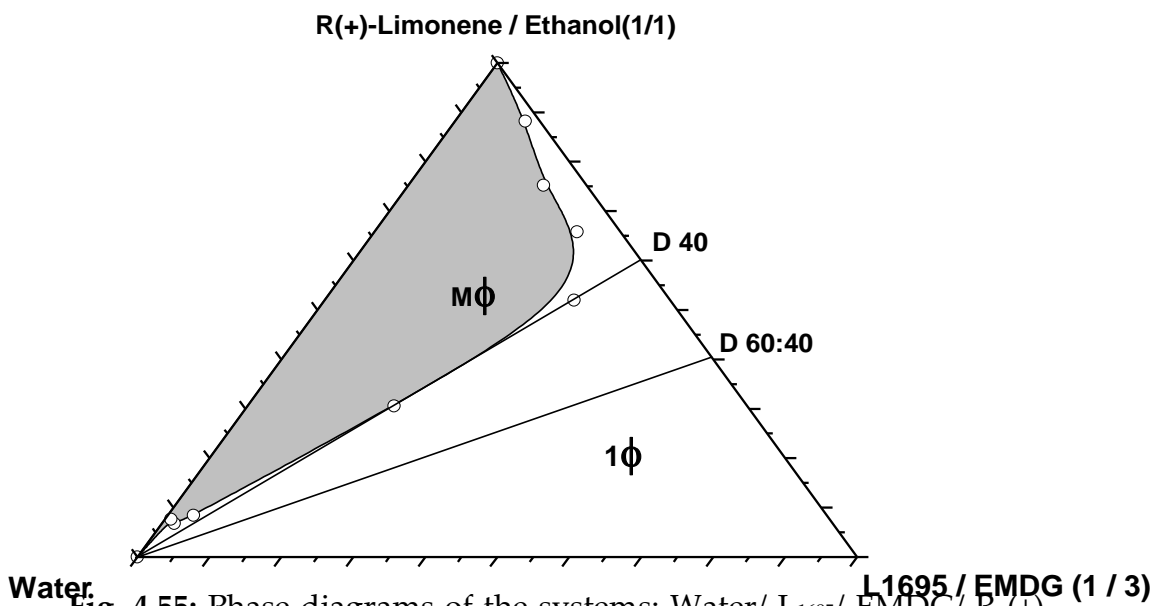
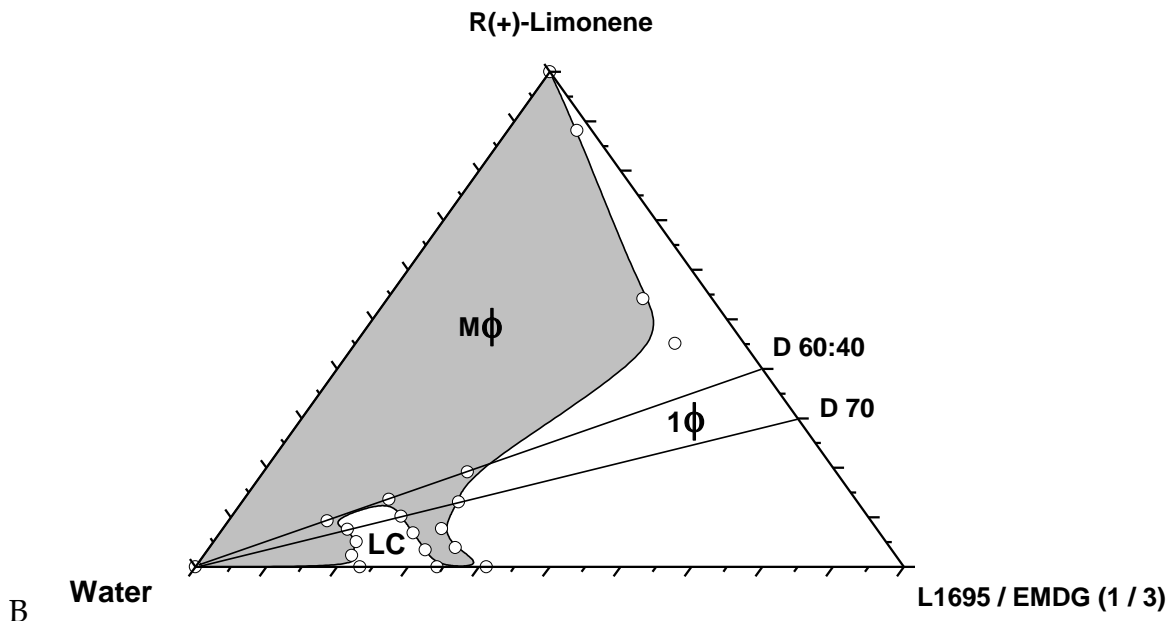


Fig. 4.55: Phase diagrams of the systems: Water/ L₁₆₉₅/ EMDG/ R (+)-Limonene (A) and Water/ L₁₆₉₅/ EMDG/ EtOH/ R (+)-Limonene (B) at 25°C. The weight ratio of L₁₆₉₅/ EMDG = 1/3 in the two systems (A), and (B), and that of R (+)-Limonene/ Ethanol = 1 in the system B. The one phase region is designated by 1φ, and the multiple phase region is designated by Mφ.

Table 4.18: Summary of the results of the pseudoternary phase behavior of the system: Water/ L₁₆₉₅/ EMDG/ EtOH/ R (+)-Limonene at 25°C.

System	L ₁₆₉₅ /EMDG $\left(\begin{matrix} \textit{weight} \\ \textit{ratio} \end{matrix}\right)$	EtOH/R(+)-limonene $\left(\begin{matrix} \textit{weight} \\ \textit{ratio} \end{matrix}\right)$	Dilution line for maximum water solubilization (W _m)	W _m (wt%)	A _T (%)	S _m (wt%)
A	1/3	0	70	60	47.2	31
B	1/3	1	40	100	66.1	∞

Fig. 4.56 shows the pseudo ternary phase behavior of the systems: Water/ L₁₆₉₅/ EMDG/ IPM (A) and Water/ L₁₆₉₅/ EMDG/ EtOH/ IPM (B). The weight ratio of L₁₆₉₅/ EMDG = 1 in the two systems and that of EtOH/ IPM = 1 in system (B).

In **Fig. 4.56 A** we observe that the one phase region extends over all of the range of water contents for high initial mixed surfactant concentration which equals 95wt% (i.e. dilution line 95). This one phase region extends from oil continuous region to liquid crystal region and finally water continuous region. For initial mixed surfactant contents below 95 wt% (i.e. dilution line 95) the one phase region extends to a maximum water solubilization (W_m) which equals 35 wt% at the dilution line 65 (i.e. initial mixed surfactant concentration = 65 wt%). The total one phase region (A_T) observed in the pseudo ternary phase diagram equals 49.2%. The minimum amount of surfactant required to obtain the maximum amount of solubilized water (S_m) is 42 wt% .

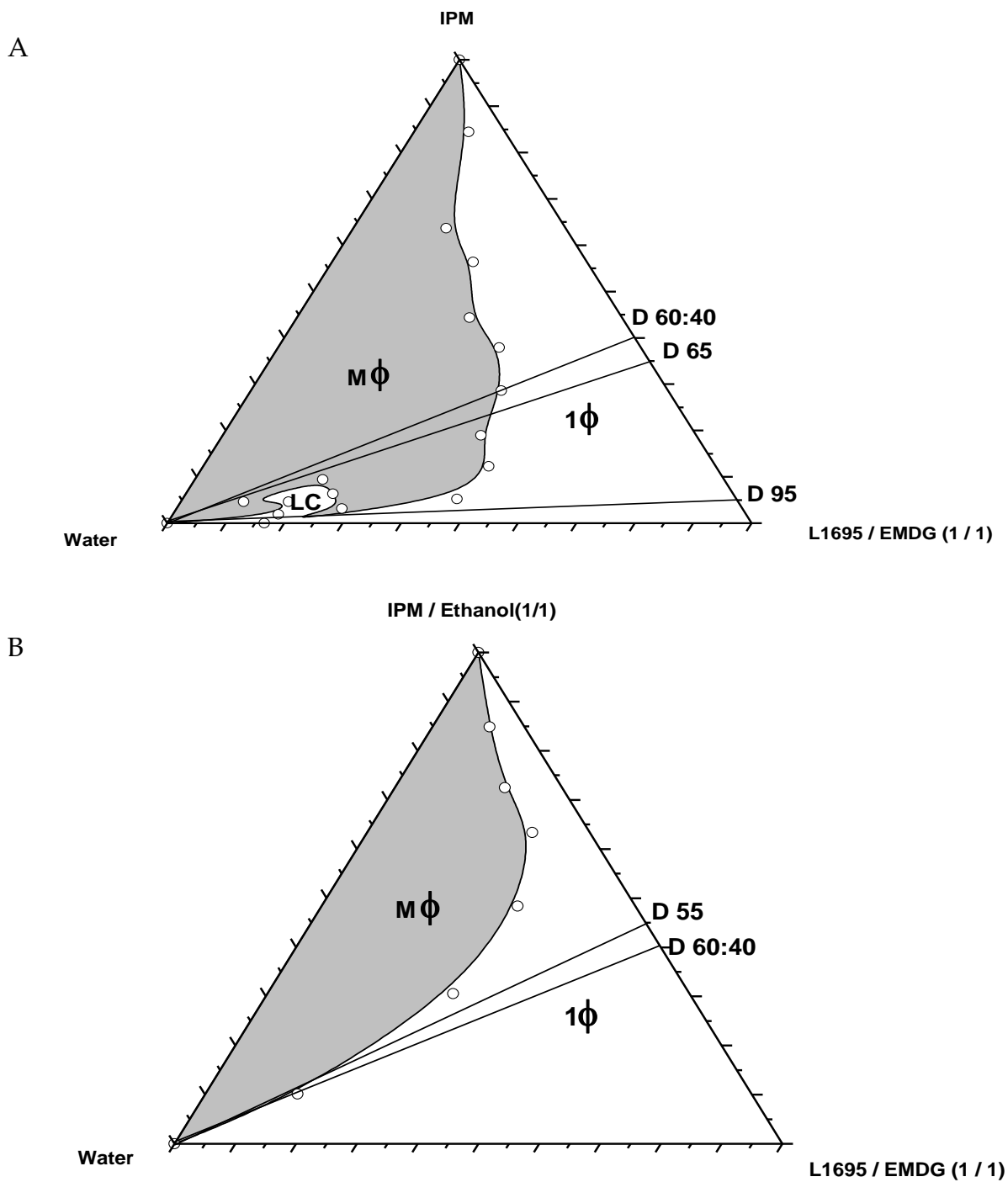


Fig. 4.56: Phase diagrams of the systems: Water/ L₁₆₉₅/ EMDG/ IPM (A) and Water / L₁₆₉₅/ EMDG / EtOH / IPM (B) at 25°C. The weight ratio of L₁₆₉₅/ EMDG = 1 in the two systems (A), and (B), and that of IPM/ Ethanol = 1 in the system (B). The one phase region is designated by 1 ϕ , and the multiple phase region is designated by M ϕ .

In Fig. 4.56 (B), the one phase region extends over all of the range of water content at the dilution line 55 (i.e. initial mixed surfactant content =55wt %). The total one phase region (A_T) observed in the pseudo ternary phase diagram equals 61.2%. Table 4.19 summarizes the results of these two figures.

Table 4.19: Summary of the results of the pseudoternary phase behavior of the system: Water/ L₁₆₉₅/ EMDG/ EtOH/ IPM at 25°C.

System	L ₁₆₉₅ /EMDG (<i>weight ratio</i>)	EtOH/IPM (<i>weight ratio</i>)	Dilution line for maximum water solubilization (W_m)	W_m (wt%)	A_T (%)	S_m (wt%)
A	1	0	95 65	100 35	49.2	42
B	1	1	55	100	61.2	∞

Fig. 4.57 shows the pseudo ternary phase behavior of the systems: Water/ L₁₆₉₅/ EMDG/ IPM (A) and Water/ L₁₆₉₅/ EMDG/ EtOH/ IPM (B). The weight ratio of L₁₆₉₅/ EMDG = 1/3 in the two systems and that of EtOH/ IPM = 1 in system (B).

In Fig. 4.57 (A), we can see that the one phase region does not form from the first beginning of adding water to the mixtures of surfactants and oil. After the addition of about 10wt% of water on the dilution line 40 the one phase region forms and extends to about 35wt% water. This behavior is observed for all the dilution lines in the phase diagram and gave a twisted bottle shape for the one phase region.

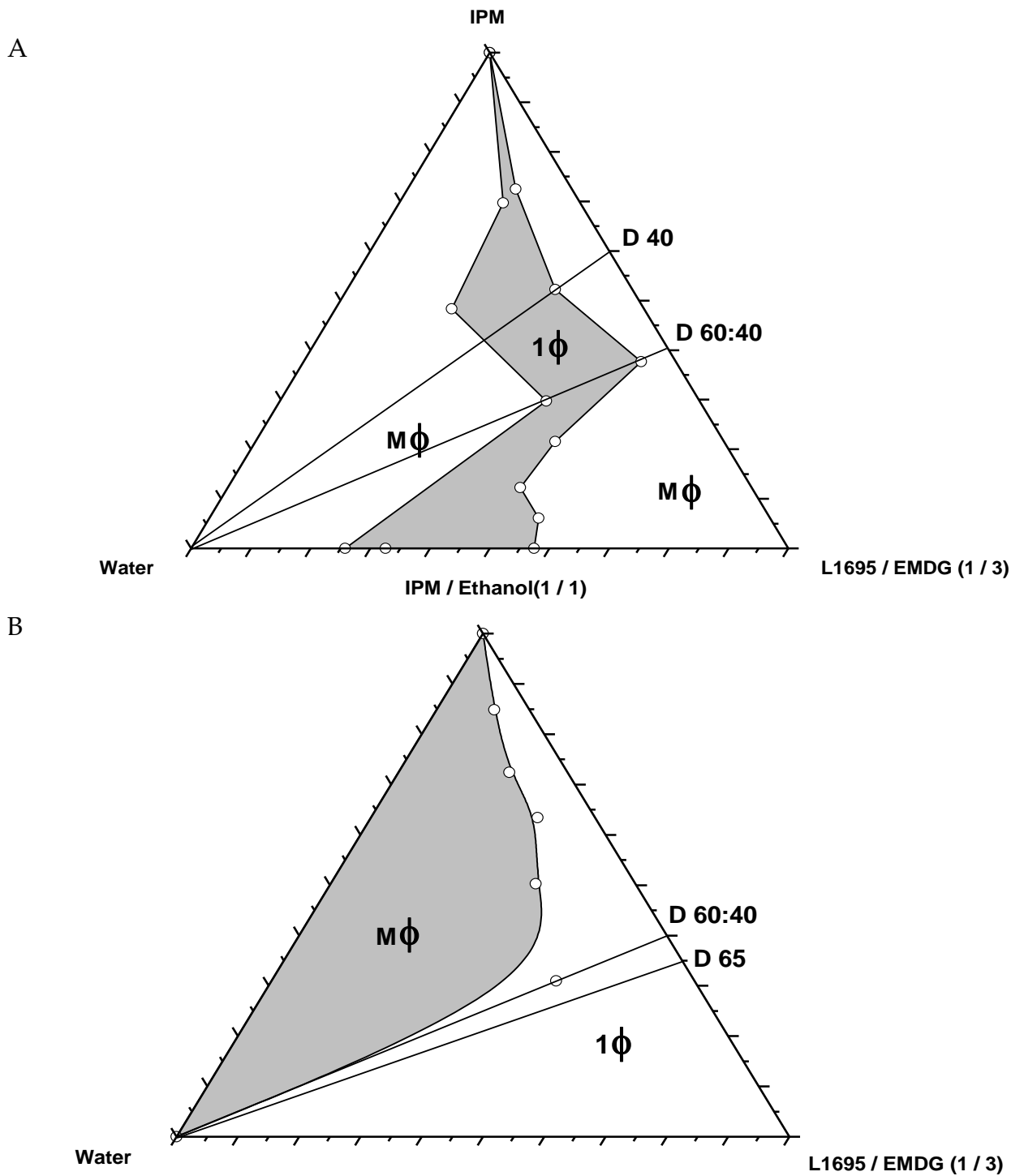


Fig. 4.57: Phase diagrams of the systems: Water/ L₁₆₉₅/ EMDG/ IPM (A) and Water/ L₁₆₉₅/ EMDG/ EtOH/ IPM (B) at 25°C. The weight ratio of L₁₆₉₅/ EMDG = 1/3 in the two systems (A), and (B), and IPM/ Ethanol = 1 in the system (B). The one phase region is designated by 1φ, and the multiple phase region is designated by Mφ.

The total area of the one phase region (A_T) is 23.5% of the pseudoternary phase diagram. The minimum amount of surfactant needed to obtain the maximum amount of solubilized water, $S_m = 28.2$ wt%.

In **Fig. 4.57 B**, the one phase region extends over all the water content on the dilution line 65 (i.e. initial mixed surfactant weight content = 65wt %). The total area of the one phase region (A_T) equals 56.6%. **Table 4.20** summarizes the results of these systems.

Table 4.20: summary of the results of the pseudoternary phase behavior of the system: Water/ L_{1695} / EMDG/ EtOH/ IPM at 25°C.

System	L_{1695} /EMDG (<i>weight ratio</i>)	EtOH/IPM (<i>weight ratio</i>)	Dilution line for maximum water solubilization (W_m)	W_m (wt%)	A_T (%)	S_m (wt%)
A	1/3	0	40	10-35	23.5	28.2
B	1/3	1	65	100	56.6	∞

In these two systems we studied the effect of changing the ratio of EMDG in the mixed surfactants $L_{1695} + \text{EMDG}$, and the effect of adding ethanol to the oleic phase. As we can see in the two systems containing R(+)-limonene and IPM, decreasing the ratio of L_{1695} in the mixed surfactants $L_{1695} + \text{EMDG}$ from 1 to 1/3 decreases the extension of the phase region (W_m) and decreases the total microemulsion area.

EMDG is more hydrophobic surfactant than L_{1695} with HLB = 13.5 compared to HLB = 16 for L_{1695} , increasing its ratio in the mixture of surfactants will decrease the affinity of water to the mixed surfactants and will affect the extension of the one phase region.

As we can observe, the initial surfactant concentration (dilution line) where we obtained a maximum water solubilization is lower in the case of high content of L₁₆₉₅ (i.e. L₁₆₉₅/ EMDG = 1). This behavior is also observed when ethanol is added to the oil phase, this behavior is explained by the fact that alcohol increases the flexibility of the interfacial layer which enables more water to be solubilized in the system.

Changing the type of the oil from R (+)-limonene to IPM also affects the total one phase region and the extent of water solubilization. R (+)-limonene is less hydrophobic oil than IPM, therefore the total area of the one phase region observed with R (+)-limonene is greater than that observed with the IPM.

IV.2 Microemulsion Structure

To better understand the microemulsion systems formed in the previous systems, we investigated the microstructure of some of these systems using electrical conductivity and self-diffusion NMR.

IV.2.1 Electrical Conductivity

Salts are practically insoluble in the oil phase, therefore their addition to the mixture will not affect the solubility of mixed nonionic surfactants in the oil. On the other hand, solubilization of salt in the aqueous phase will change its chemical potential and will shift the mixture towards the three phase formation by changing the conditions of solubility of the mixed nonionic amphiphiles.

It was also found that adding salt to the mixture decreases the area of the one phase region in the phase diagram ⁽¹⁰⁹⁻¹¹²⁾.

Adding aqueous solution of a trace of salt (NaCl, 0.05M) to the mixture of mixed nonionic amphiphiles and oil will make the microemulsion mixture and practically the aqueous phase in it electrically conducting.

When measuring the electrical conductivity (κ) of the microemulsion one can find a change in the κ within rather a narrow interval upon varying either the temperature and the composition of the system.

Electrical Conductivity of the System: Water/ L₁₆₉₅/ EMDG/ IPM

The electric conductivity (κ) along the homogeneous channel of the system: Water/ L₁₆₉₅/ EMDG/ IPM. **Table 4.21, Figures(4.58 and 4.59)** show the points where we measured κ and the values obtained as a function of α wt% and T (°C). As we can observe from **Fig. 4.59(A)** the electrical conductivity increases linearly with the temperature for all the α values measured. For α values ≥ 30 wt% the electrical conductivity was measured for temperature above 80°C since the one phase region is present at these high temperatures.

In **Fig. 4.59 (B)** we can see that κ decreases from the water-rich region (i.e. low α values) to the oil-rich region (i.e. high α values). In the region close to $\alpha = 90$ wt% the electrical conductivity is very sensitive to even slight variation of temperature.

Table 4.21: Electrical conductivity of the system: Water/ L₁₆₉₅/ EMDG/ IPM ($\gamma = 31$ wt%, $\delta = 50$ wt%) as a function of α (wt%) and temperature ($^{\circ}\text{C}$).

Composition (wt%) Water/L ₁₆₉₅ /EMDG/IPM	α (wt%)	T ($^{\circ}\text{C}$)	Electrical Conductivity (κ) (S cm^{-1})
69.0/ 15.5/ 15.5/ 0	0	60	4.61×10^{-3}
62.1/ 15.5/ 15.5/ 6.9	10	70	4.26×10^{-3}
55.17/ 15.5/ 15.5/ 13.8	20	80	4.02×10^{-3}
48.27/ 15.5/ 15.5/ 20.7	30	90	3.74×10^{-3}
34.5/ 15.5/ 15.5/ 34.5	50	92	2.78×10^{-3}
20.7/ 15.5/ 15.5/ 48.27	70	93	1.64×10^{-3}
13.8/ 15.5/ 15.5/ 55.17	80	94	7.43×10^{-4}
6.9/ 15.5/ 15.5/ 62.1	90	95.3	1.265×10^{-4}
0/ 15.5/ 15.5/ 96	100	96	3×10^{-7}

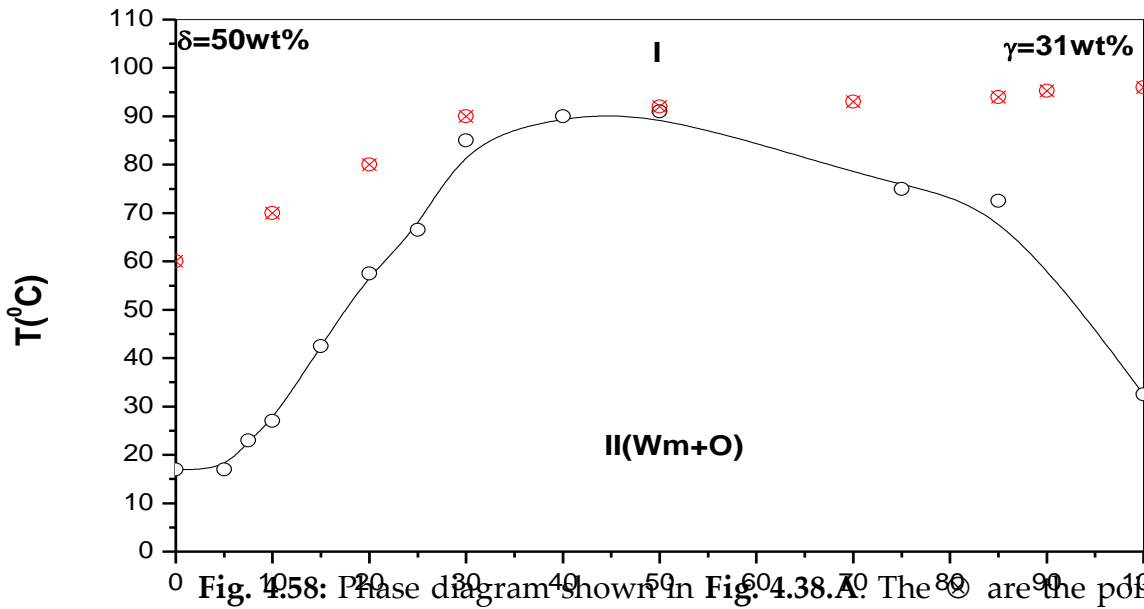


Fig. 4.58: Phase diagram shown in Fig. 4.38.A. The \odot are the points where we measured the electrical conductivity in the system: Water/ L₁₆₉₅/ EMDG/ IPM, at $\gamma = 31$ wt% and $\delta = 50$ wt% for variable α (wt%) and T ($^{\circ}\text{C}$).

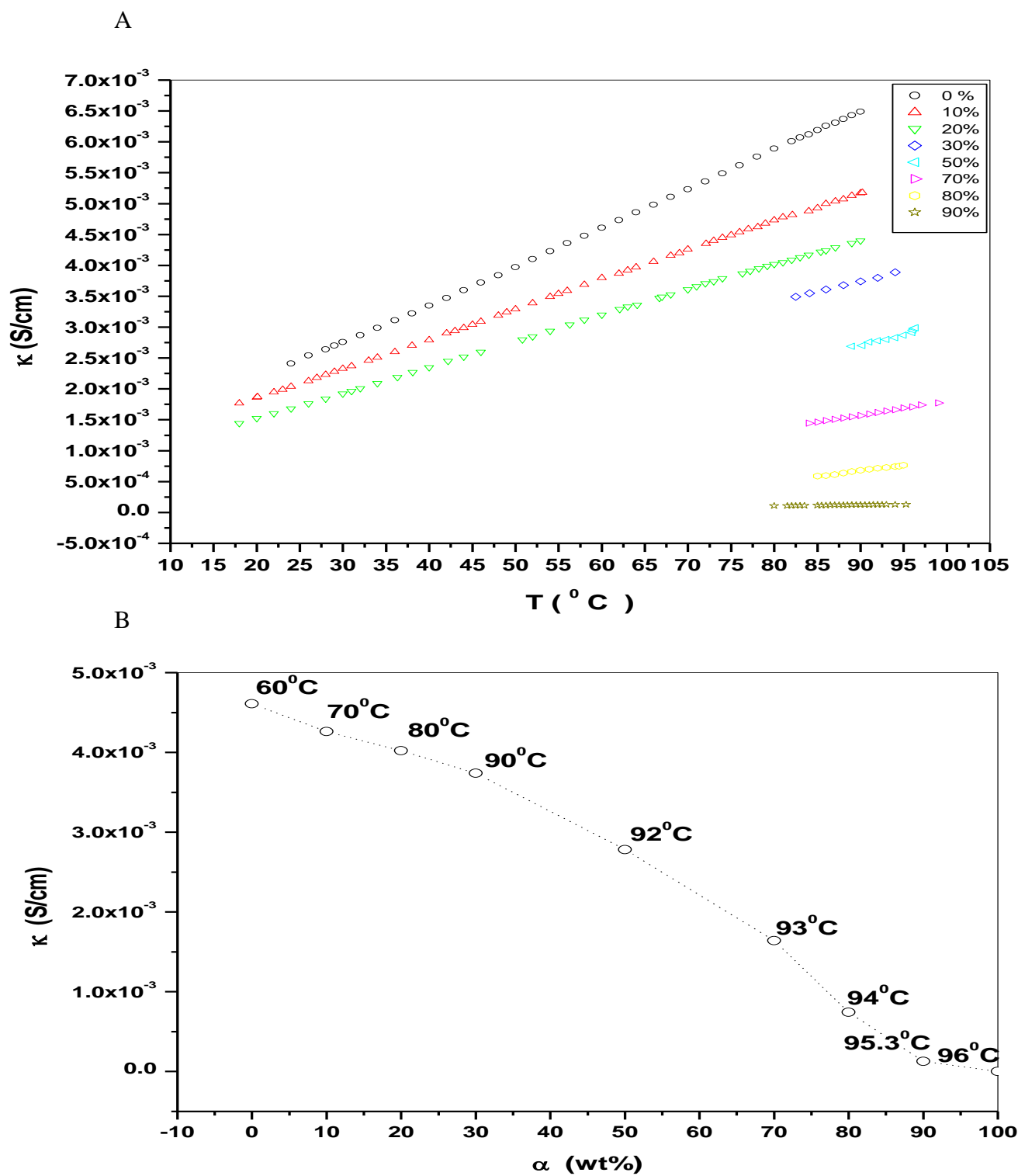


Fig. 4.59: Plot of κ as a function of T ($^{\circ}\text{C}$) (A) and as a function of $Oil/(Oil + Water)$ weight ratio, α (wt %) (B) For the system: Water/ L_{1695} / EMDG/ IPM ($\gamma = 31$ wt%, $\delta = 50$ wt%) at points presented in Fig. 4.58.

Electrical Conductivity of the System: Water/ L₁₆₉₅/ EMDG/ R(+)-Limonene

Table 4.22, Figures (4.60 and 4.61) show the points where κ was measured and the values obtained as a function of α (wt%) and T(°C) for the system: Water/ L₁₆₉₅/ EMDG/ R(+)-limonene. Fig. 4.61 (A) shows the electrical conductivity behavior as a function of T for different α values. For α values = 0 wt%, no oil present in the system, the electrical conductivity increases linearly with temperature.

For $10 \leq \alpha \leq 30$ wt% values the electrical conductivity have a sigmoidal behavior as one increases temperature (i.e. it increases linearly with T, then decreases and again increases).

For $\alpha \geq 50$ wt% the electrical conductivity again increases linearly as one increases temperature.

As we can see in the (Fig. 4.61 (B)) where κ is plotted versus α with raising temperature, κ decreases from the water-rich to the oil-rich side and at the region close to $\alpha = 90$ wt% the electrical conductivity is very sensitive to slight variation of temperature like the case of the system: Water/ L₁₆₉₅/ EMDG/ IPM. We also observe in Fig. 4.61 (B) a sudden change of κ within a rather narrow interval upon varying either the composition at fixed temperature (T), or temperature at fixed main composition.

By using different types of oil the electric conductivity κ differs. From the Figures (4.60 and 4.61) we can find that despite the increase in electrical conductivity in both oils R(+)-Limonene and IPM the values of κ with R(+)-Limonene are smaller than in the case of IPM. This can be explained by the chemical structure of both oils and their capability to penetrate between the chains of surfactants to the interface, IPM which has a linear structure as an oil-phase will give the water the mobility and this will increase the

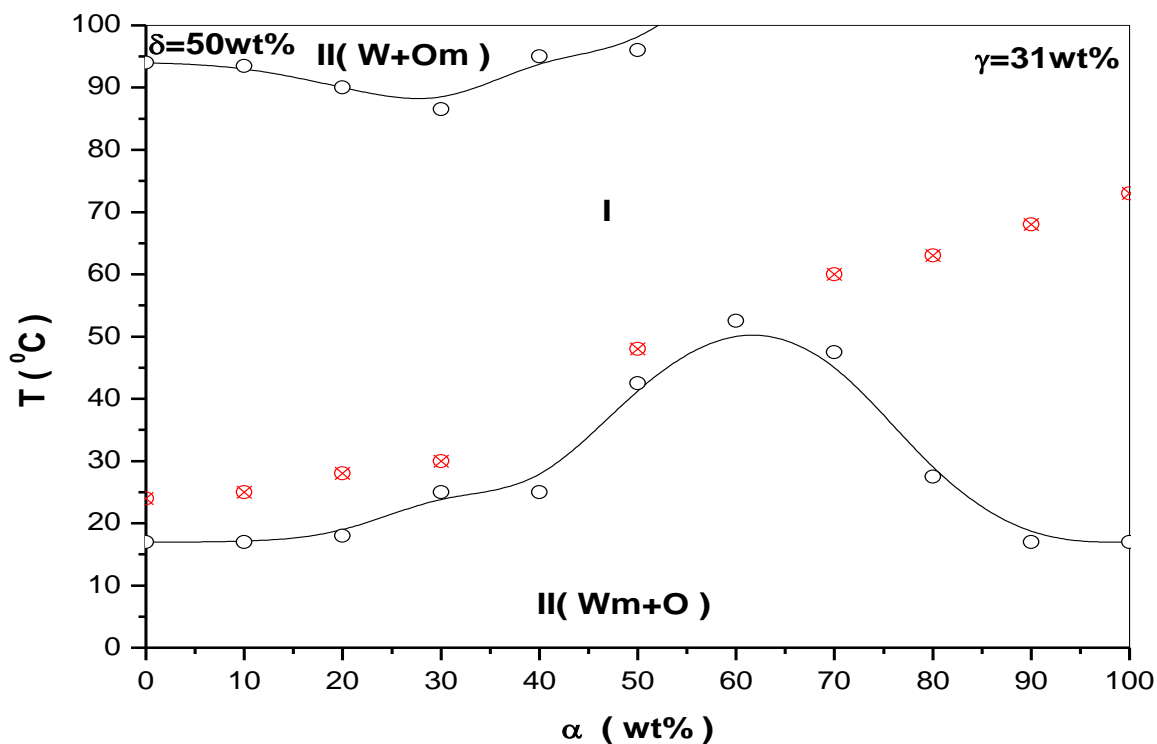


Fig. 4.60: Phase diagram shown in Fig. 4.33.B. The \otimes are the points where we measured the electrical conductivity in the system: Water/ L₁₆₉₅/ EMDG/ R (+)-limonene. At $\gamma = 31$ wt% and $\delta = 50$ wt% for variable α (wt%) and T (°C).

conductivity, because there is enough space for water to move around the droplets (micelles), while R(+)-Limonene which have a cyclic structure, will decrease the space for water to move between the droplets (micelles) and this will decrease the conductivity of the system for α values between 10 and 30 wt%. Raising the temperature the collision probability between the droplets increases and the opening and reforming of droplets will increase the mobility of water and the electrical conductivity will again rise with temperature. In addition the possibility of percolation becomes larger and the formation of water channels will increase the electrical conductivity of the system.

Table 4.22: Electrical conductivity of the system: Water/ L₁₆₉₅/ EMDG / R(+)-limonene ($\gamma = 31$ wt%, $\delta = 50$ wt%) as a function of α (wt%) and temperature ($^{\circ}\text{C}$).

Composition (wt%) Water/L ₁₆₉₅ /EMDG/R(+)-limonene	α (wt%)	T ($^{\circ}\text{C}$)	Electrical conductivity(κ) (S cm^{-1})
69.0/ 15.5/ 15.5/ 0	0	24	2.41×10^{-3}
62.1/ 15.5/ 15.5/ 6.9	10	25	1.79×10^{-3}
55.17/ 15.5/ 15.5/ 13.8	20	28	1.61×10^{-3}
48.27/ 15.5/ 15.5/ 20.7	30	30	1.52×10^{-3}
34.5/ 15.5/ 15.5/ 34.5	50	48	1.21×10^{-3}
20.7/ 15.5/ 15.5/ 48.27	70	60	6.03×10^{-4}
13.8/ 15.5/ 15.5/ 55.17	80	63	2.18×10^{-4}
6.9/ 15.5/ 15.5/ 62.1	90	68	4.7×10^{-6}
0/ 15.5/ 15.5/ 96	100	73	1×10^{-7}

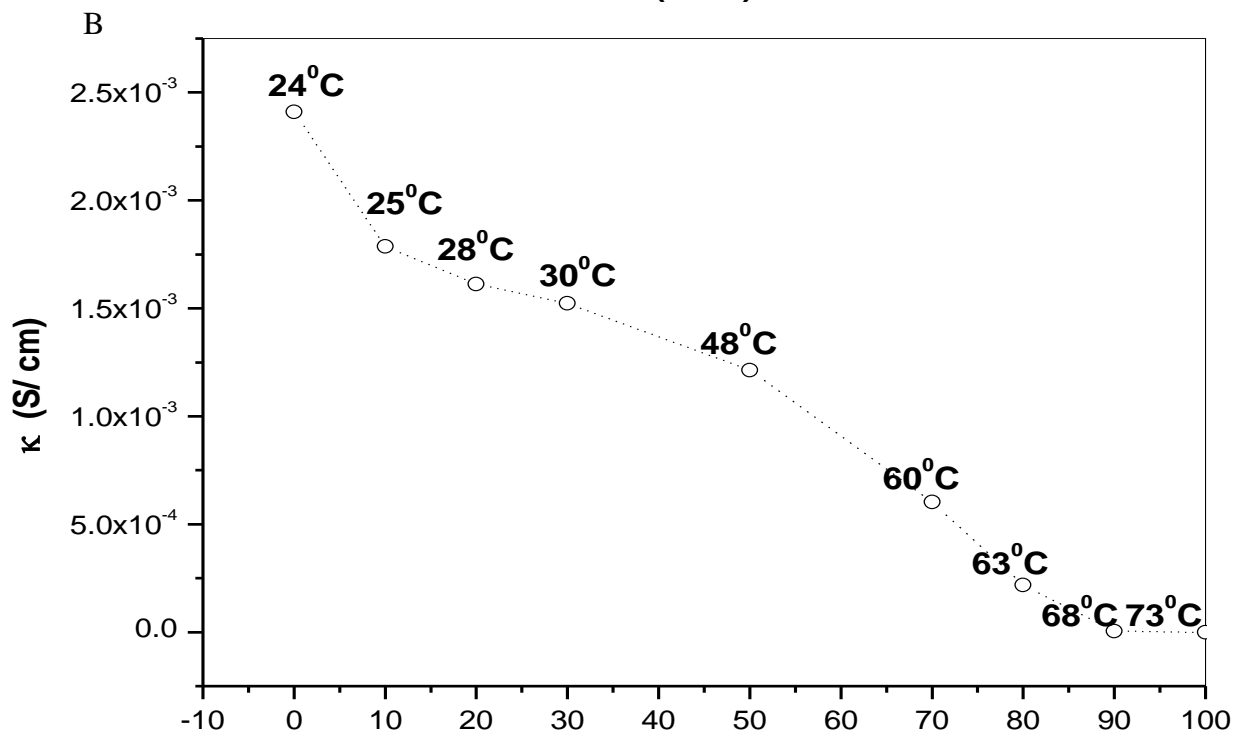
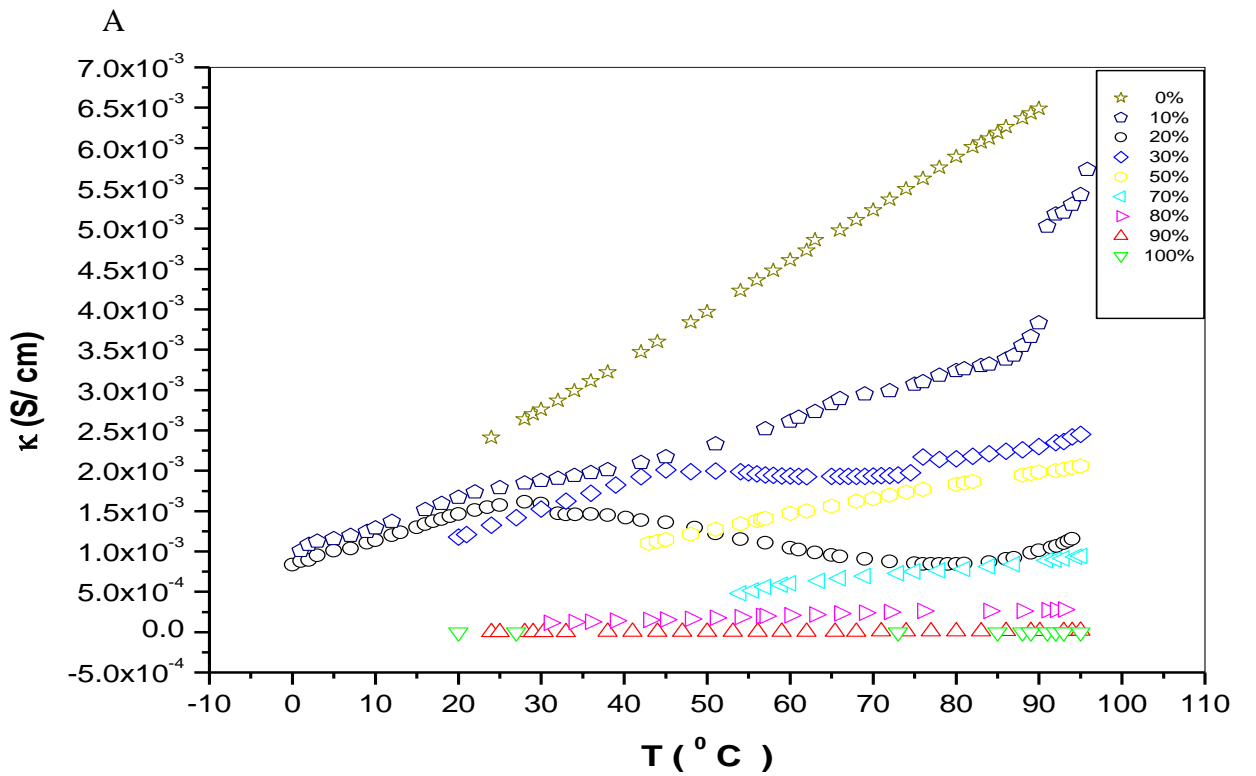


Fig. 4.61: Plot of κ as a function of T ($^{\circ}\text{C}$) (A) and as a function of $Oil/(Oil + Water)$ weight ratio, α (wt%) (B) for the system: Water/ L_{1695} / EMDG/ R(+)-limonene ($\gamma = 31$ wt% and $\delta = 50$ wt%) at the points indicated in (Fig. 4.60).

IV.2.2 Pulsed Gradient Spin-Echo (PGSE)-NMR

Confinement and obstruction of molecules have a major effect on the molecular self-diffusion coefficients and thus can provide some direct insight into solution structure of organized systems.

Studies of microemulsions using self diffusion techniques have demonstrated a considerable structural variability including O/ W and W/ O droplet type structures (see Fig. 4.62) as well as bicontinuous structure depending on composition, salinity, co-solvent, co-surfactant, temperature, etc. ⁽¹¹³⁻¹²⁰⁾ . Low and equal diffusion coefficient of the surfactant and the dispersed medium characterize the two extremes O/ W and W/ O. The solvent molecules in these extremes have a diffusion coefficient close to what is found in the neat liquid, reduced only by obstruction from the dispersed particles. High diffusion coefficients for all the constituents characterize the bicontinuous structures.

The isotropic region in which both oil and water show rapid diffusion is often referred to as bicontinuous microemulsion ⁽¹²¹⁾ , and there has been considerable debate about the microstructure of bicontinuous microemulsions. The lamellar structures, interconnected rods, and cubic liquid crystalline phases have been proposed, but now the most general representation of a bicontinuous microemulsion is one of zero or close to zero mean curvature structures with infinite curved channels of oil and water. As shown in see Fig. (4.62 and 1.2), where the water on the hydrophilic side of the surfactant monolayer is continuously connected in the three dimensions and the same is true of the oil on the hydrophobic side. As the system parameters are changed, such as temperature for

microemulsions based on nonionic surfactants, the spontaneous mean curvature will change and the system will gradually move away from bicontinuity.

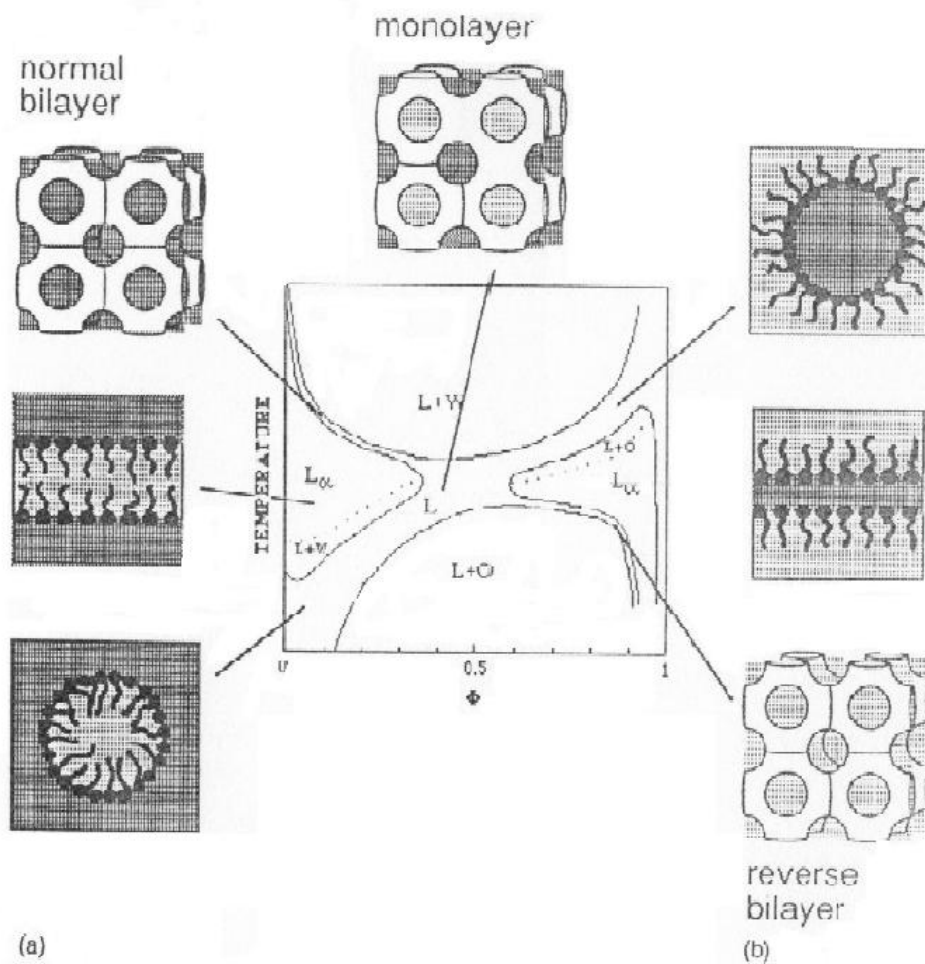


Fig. 4.62: Effects of temperature and oil volume fraction (Φ or α) on the surfactant monolayer spontaneous curvature and on the surfactant oil water phase behavior for a system containing a fixed surfactant concentration. At low or zero content of oil (a) at low water content (b). At similar water and oil contents, a bicontinuous structure with a surfactant monolayer separating the water and oil domains can be stable ⁽⁶⁾.

The phase behavior of the system: Water/ L₁₆₉₅/ EMDG/ IPM has been examined and described in detail in the phase behavior section of this thesis. Such a two-dimensional phase diagram at constant atmospheric pressure, a constant surfactant concentration (i.e. γ) of 26 wt% (A) and 31 wt% (B) and a constant weight ratio of L₁₆₉₅ and EMDG (i.e. δ) of 25 wt% (A) and 50 wt% (B) is shown in **Fig. 4.63**. **Table 4.23** summarizes the results obtained from self diffusion measurements. The system exhibits an isotropic channel extending from the lower left to the upper right corner of the temperature versus $Oil/(Oil + Water)$ diagram shown in (**Fig. 4.63**). The observed diffusion coefficients, D , and D_0 which denotes the diffusion coefficient of the neat component at the same temperature. Where used to determine the relative diffusion coefficients D/ D_0 .

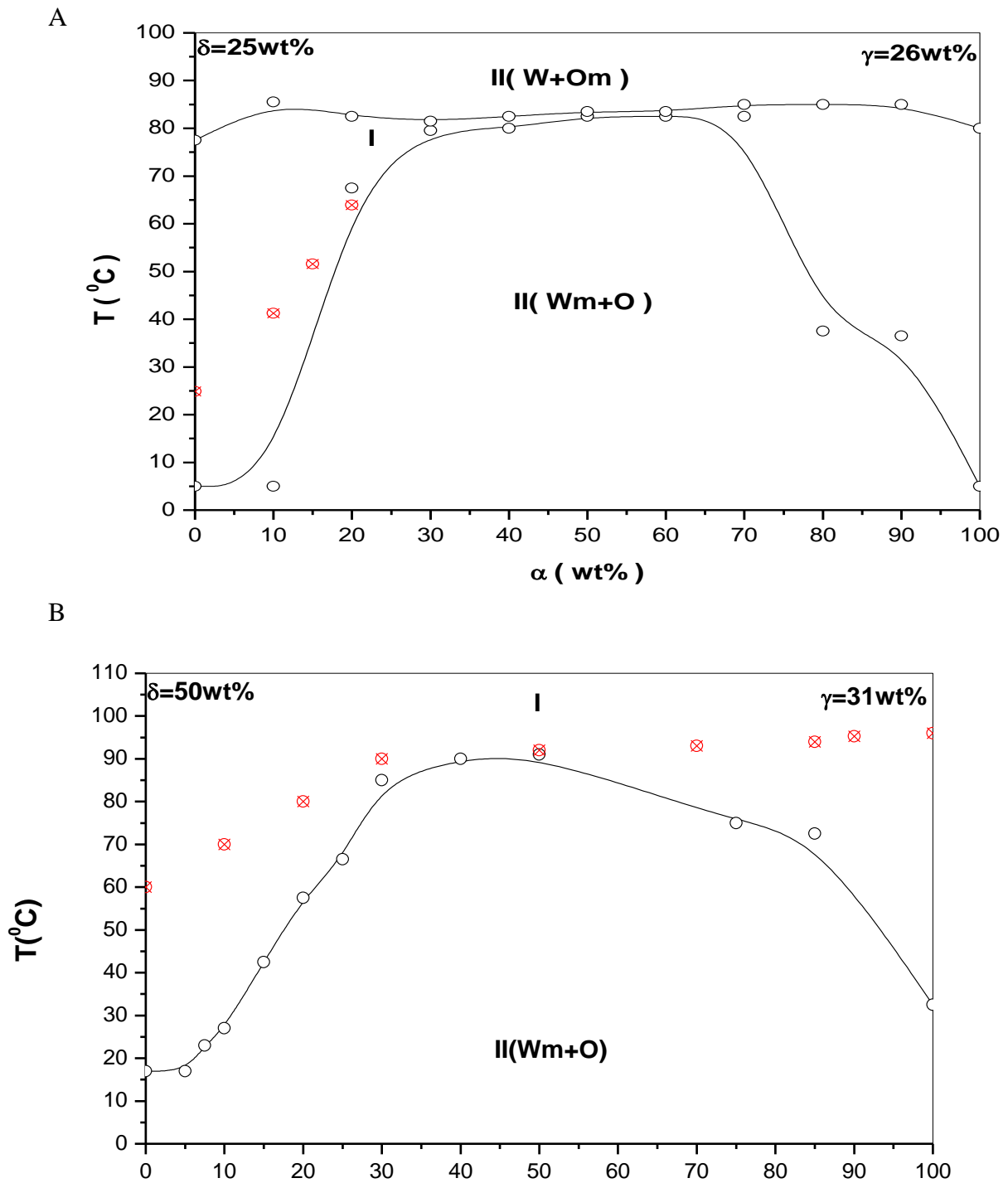


Fig. 4.63: Schematic phase diagram of the system: Water/ L₁₆₉₅/ EMDG/ IPM, (see Fig. 4.38 A and B), where the mixed surfactants content (i.e. γ) are 26 wt% in (A) and 31 wt% in (B). The EMDG ratio (i.e. δ) is 25 wt% in (A) and 50 wt% in (B). The cross filled circles \otimes are experimental points investigated by self diffusion-NMR measurements.

Table 4.23: Self-diffusion coefficients in the system Water/ L₁₆₉₅/ EMDG/ IPM as function of α (wt%) and T (K) for constant $\gamma = 31$ wt% and $\delta = 50$ wt%.

Composition (wt%) Water/L ₁₆₉₅ /EMDG/IPM	α (wt%)	T (K)	Observed Diffusion coefficient $D \times 10^{-10}$ (m ² /s)			Relative diffusion coefficient D/D_0	
			EMDG	water	IPM	Water	IPM
69/ 15.5/ 15.5/ 0	0	297.89	0.697	11.87	-----	0.874	-----
65.55/ 15.5/ 15.5/ 3.45	5	297.89	0.697	11.27	2.057×10^{-3}	0.83	1×10^{-3}
63.83/ 15.5/ 15.5/ 5.17	7.5	307.06	0.554	13.79	3.988×10^{-3}	0.624	1.54×10^{-3}
62.1/ 15.5/ 15.5/ 6.9	10	314.27	0.487	14.91	6.05×10^{-3}	0.441	1.94×10^{-3}
58.65/ 15.5/ 15.5/ 10.35	15	324.58	0.399	19.18	8.366×10^{-3}	0.366	2.06×10^{-3}
55.17/ 15.5/ 15.5/ 13.83	20	336.92	0.315	22.95	4.86×10^{-2}	0.326	8.72×10^{-3}
51.76/ 15.5/ 15.5/ 17.28	25	353.39	-----	29.48	1.061	0.312	0.125
48.28/ 15.5/ 15.5/ 20.72	30	365.94	-----	34.57	2.34	0.306	0.2
34.5/ 15.5/ 15.5/ 34.5	50	353.39	-----	15.22	2.46	0.161	0.29
17.28/ 15.5/ 15.5/ 51.72	75	353.39	-----	9.92	2.845	0.105	0.335
10.35/ 15.5/ 15.5/ 58.65	85	365.94	-----	11.87	4.215	0.105	0.36
0/ 15.5/ 15.5/ 69	100	336.92	-----	-----	3.465	-----	0.622

Fig. 4.64 shows the relative self-diffusion coefficients of oil and water in the system: Water/ L₁₆₉₅/ EMDG/ IPM in the points presented in the (**Fig. 4.63**). We can see the strong temperature and composition dependence of the diffusion coefficients of both water and oil. The full lines are drawn through approximate mean values of D/D_0 , with respect to temperature, at each composition point. D/D_0 for water decreases from a value of about 0.87 to approximately 0.1, while D/D_0 for oil increases from 1×10^{-3} to 0.6 when the weight fraction of oil is increased. The surfactant diffusion can also be monitored, and the values obtained can help in structure elucidations.

The very large variations in D_{water} and D_{oil} on varying the weight fraction of oil is striking. Evidently, there is a smooth transition from O/W structure at low oil to water ratio to W/O at high ratio, while at approximately equal amounts of oil to water, there is rapid diffusion (D/D_0 of around 0.3) of both components, indicating a structural arrangement where neither component is confined into closed domains.

Fig. 4.65, Tables 4.23 and 4.24 show the relative self-diffusion coefficients of $D^{\text{water}} / D_0^{\text{water}}$ as a function of temperature and the oil content in the microemulsion samples of the system: Water/ L₁₆₉₅/ EMDG/ IPM at different mixed surfactants contents (i.e. $\gamma = 26$ and 31 wt%) and at different ratios of surfactants (i.e. $\delta = 25$ and 50 wt%). **Fig. 4.63** shows these points in the phase diagram. In **Fig. 4.65** we observe that the $D^{\text{water}} / D_0^{\text{water}}$ values are decreases as α increase and are higher in the case where the surfactants content is $\gamma = 26$ wt% than in the case where $\gamma = 31$ wt%. in these two cases EMDG ratio was changed from $\delta = 50$ wt% to $\delta = 25$ wt%. L₁₆₉₅ is more hydrophilic than EMDG, one expects that increasing the content of L₁₆₉₅ as in the case of $\delta = 25$ wt% will increase the attachment of water to the mixed

surfactants in the microemulsion and the D^W / D_0^W in the case of $\delta = 25$ wt% will be lower than these with $\delta = 50$ wt%.

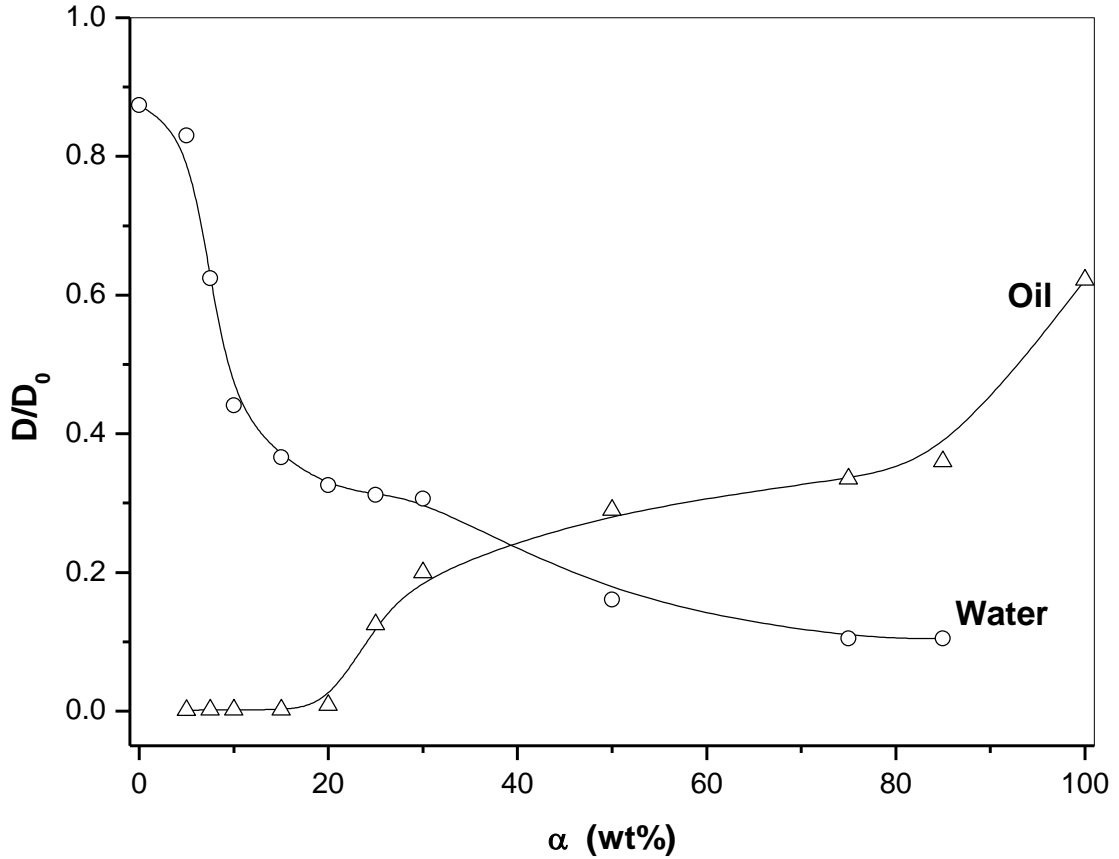


Fig. 4.64: Relative diffusion coefficients, D/D_0 , for the system: Water/ L_{1695} / EMDG/ IPM as a function of the weight fraction of $Oil/(Oil + Water)$, (α) for $\gamma = 31$ wt% and $\delta = 50$ wt%, where (\circ)-are the relative diffusion coefficient of the water and (Δ)-is for the oil.

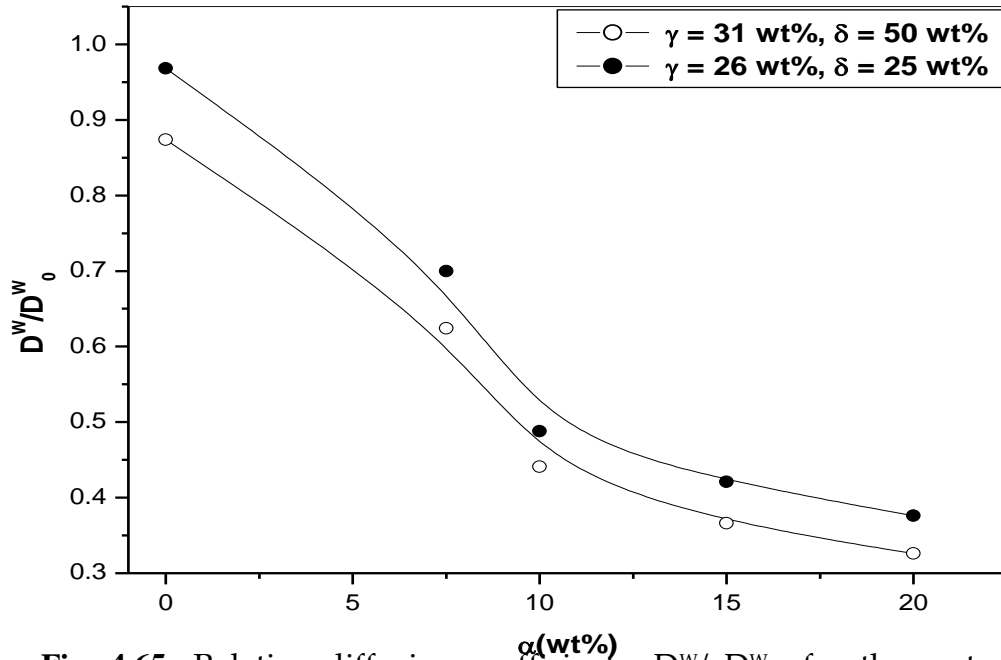


Fig. 4.65: Relative diffusion coefficients, D^W/D_0^W , for the system: Water/ L₁₆₉₅/ EMDG/ IPM as a function of the weight fraction of *Oil/(Oil+Water)*, (α) for different surfactant and co-surfactant concentrations, (\circ) $\gamma = 31$ wt%, $\delta = 50$ wt%, and (\bullet) $\gamma = 26$ wt%, $\delta = 25$ wt%.

This is not the case in our system. This behavior indicates that the concentration of surfactant (γ) in the system is the dominant factor that determines the values of D^W/D_0^W .

Fig. 4.66, **Tables 4.23 and 4.24** show the relative self diffusion coefficient of D^0/D_0^0 as a function of temperature and the oil content in the microemulsion sample in the system: Water/ L₁₆₉₅/ EMDG/ IPM at different mixed surfactant contents (i.e. $\gamma = 26$ and 31 wt%) and different ratios of surfactant (i.e. $\delta = 25$ and 50 wt%). **Fig. 4.63** ($\gamma = 31$ wt%, $\delta = 50$ wt%) and **Fig. 4.63** ($\gamma = 26$ wt%, $\delta = 25$ wt%). In this Figure we observe that D^0/D_0^0 values increases as α increase.

When $\gamma = 31$ wt% and $\delta = 50$ wt% the oil is more confined in the core of the microemulsion than that in the case of $\gamma = 26$ wt% and $\delta = 25$ wt%. This is manifested in the higher values of D^0/D_0^0 in the case of $\gamma = 31$ wt% than that of $\gamma = 26$ wt%.

From these two **Fig. (4.65 and 4.66)** one can conclude that the mixed surfactants content in the microemulsion system may have the dominant role in determining the microstructure of the microemulsions.

The hydrophilicity of the mixed surfactants affects also the diffusivity of both oil and water but can not have the major role in determining the microstructure compared with the mixed surfactant content.

Table 4.24: Self-diffusion coefficients in the system Water/ L₁₆₉₅/ EMDG/ IPM as function of α (wt%) and T (K) for constant $\gamma = 26$ wt% and $\delta = 25$ wt%.

Composition (wt%) Water/L ₁₆₉₅ /EMDG/IPM	α (wt%)	T (K)	Observed Diffusion coefficient $D \times 10^{-10}$ (m ² /s)			Relative diffusion coefficient D/D_0	
			EMDG	Water	IPM	Water	IPM
69/ 15.5/ 15.5/ 0	0	297.89	1.11	13.15	-----	0.968	1.3×10^{-3}
63.83/ 15.5/ 15.5/ 5.17	7.5	307.06	0.880	15.47	5.9×10^{-3}	0.7	2.28×10^{-3}
62.1/ 15.5/ 15.5/ 6.9	10	314.27	0.7774	16.49	13.69×10^{-3}	0.488	4.39×10^{-3}
58.65/ 15.5/ 15.5/ 10.35	15	324.58	0.634	22.06	16.29×10^{-2}	0.421	4.01×10^{-2}
55.17/ 15.5/ 15.5/ 13.83	20	336.92	0.5	26.47	49.24×10^{-2}	0.376	8.84×10^{-2}

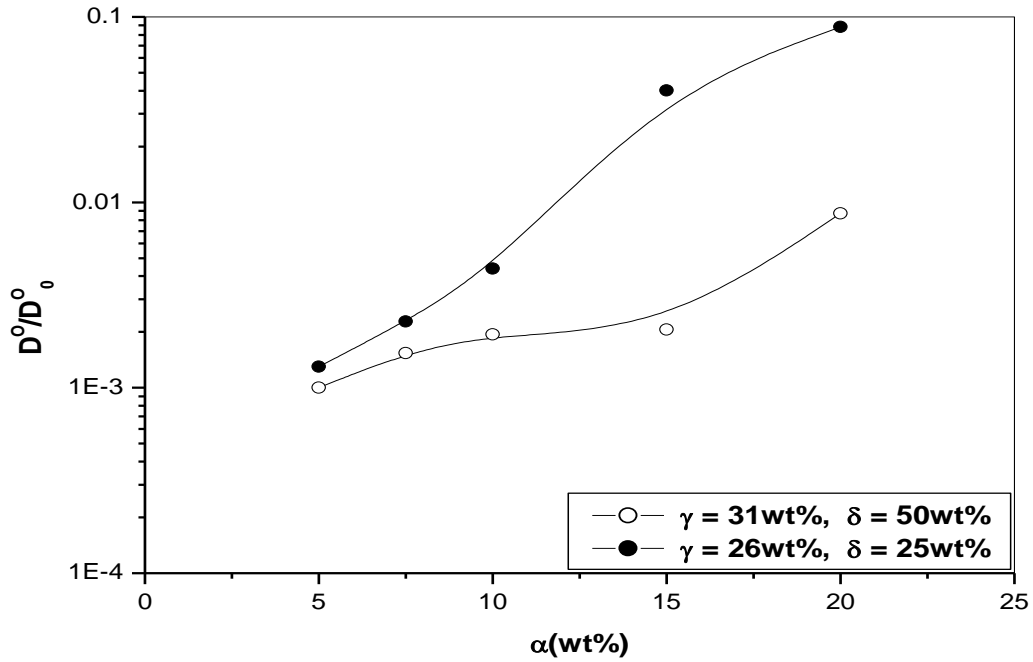


Fig. 4.66: Relative diffusion coefficients, D°/D°_0 , for the system: Water/ L₁₆₉₅/ EMDG/ IPM as a function of the weight fraction of Oil/(Oil + Water), (α) for different surfactant and co-surfactant concentrations, (\circ) $\gamma = 31$ wt%, $\delta = 50$ wt%, and (\bullet) $\gamma = 26$ wt%, $\delta = 25$ wt%.

For self diffusion spheres in a continuous phase a modified Stokes-Einstein equation may be used to calculate the hydrodynamic radius R_H of the micelles in the water-rich region (i.e. α values below 15 wt%)

$$R_H = \frac{kT}{6\pi\eta D_{obs}} \quad (7)$$

where k (J/K) is the Boltzman constant, T (K) is the absolute temperature, η (Pa.s) is the viscosity of the medium (i.e. water), and D_{obs} (m²/s) is the EMDG self diffusion coefficient.

The D_{obs} of the EMDG were used since the EMDG is the one that have higher volume between the two mixed surfactants used L₁₆₉₅ and

EMDG. For the system with $\gamma = 31$ wt% and $\delta = 50$ wt% the values of hydrodynamic radius for the water rich region (i.e. $\alpha < 20$ wt%) are presented in **Table 4.25 and Fig. 4.67**, and those of the system with $\gamma = 26$ wt% and $\delta = 25$ wt% are presented in **Table 4.26** and shown in **Fig. 4.68**.

Table 4.25: Hydrodynamic radius of the system: Water/ L₁₆₉₅/ EMDG/ IPM as function of α (wt%) for ($\gamma = 31$ wt%, $\delta = 50$ wt%).

Composition (wt%) Water/ L ₁₆₉₅ / EMDG /IPM	α (wt%) = $\frac{IPM}{Water + IPM} \times 100\%$	R_H (nm)
65.55/ 15.5/ 15.5/ 3.45	5	3.6
63.83/ 15.5/ 15.5/ 5.17	7.5	5.6
62.1/ 15.5/ 15.5/ 6.9	10	7.3
58.65/ 15.5/ 15.5/ 10.35	15	10.8
55.17/ 15.5/ 15.5/ 13.83	20	17.4

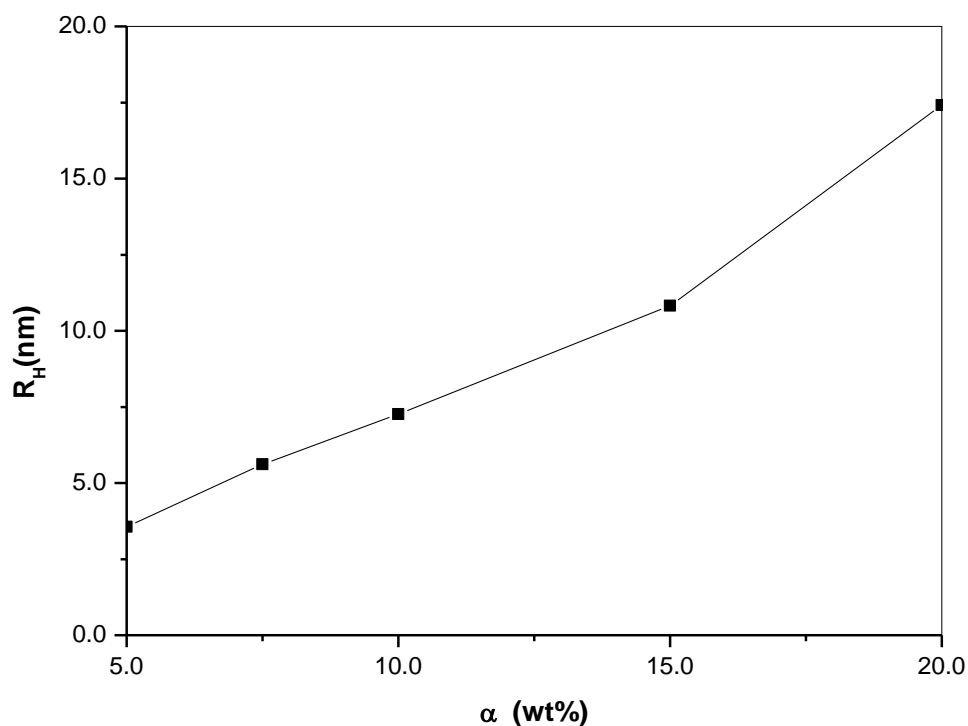


Fig. 4.67: Hydrodynamic radius for the system: Water/ L₁₆₉₅/ EMDG/ IPM as function of *Oil/(Oil + Water)* weight ratio, α (wt%) for ($\gamma = 31$ wt%, $\delta = 50$ wt%).

Table 4.26: Hydrodynamic radius of the system: Water/ L₁₆₉₅/ EMDG/ IPM as function of α (wt%) for ($\gamma = 26$ wt%, $\delta = 25$ wt%).

Composition (wt%) Water/ L ₁₆₉₅ / EMDG /IPM	α (wt%) = $\frac{IPM}{Water + IPM} \times 100\%$	R_H (nm)
65.55/ 15.5/ 15.5/ 3.45	5	2.2
63.83/ 15.5/ 15.5/ 5.17	7.5	3.5
62.1/ 15.5/ 15.5/ 6.9	10	4.6
58.65/ 15.5/ 15.5/ 10.35	15	6.8
55.17/ 15.5/ 15.5/ 13.83	20	11.00

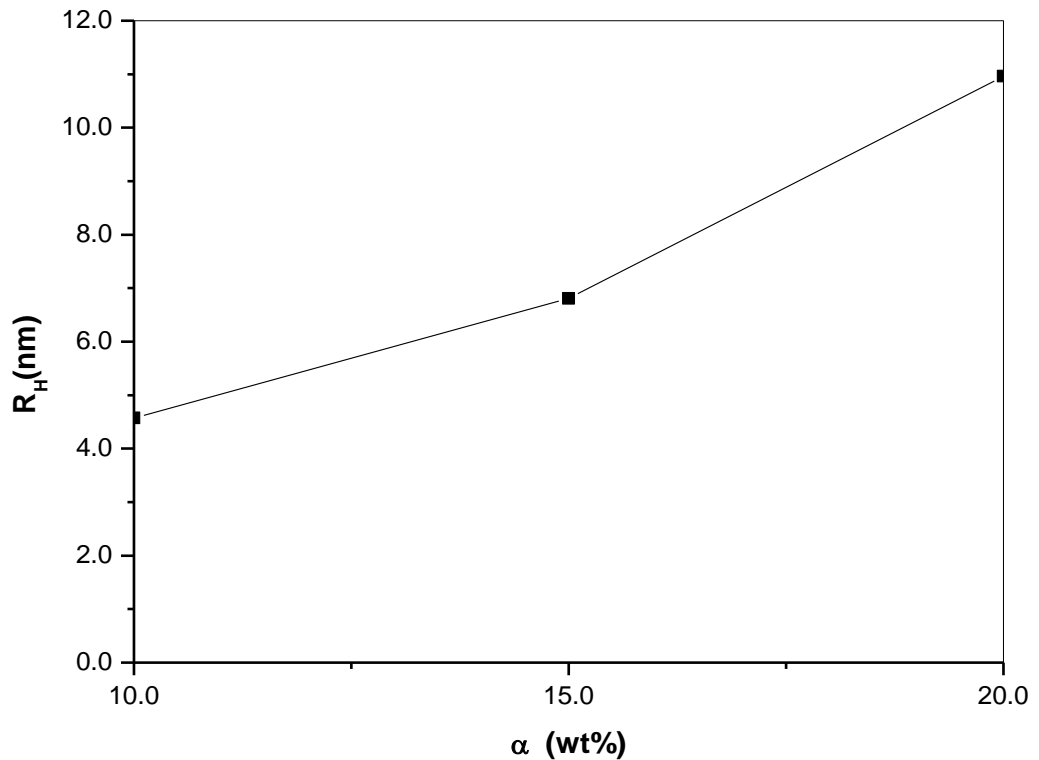


Fig. 4.68: Hydrodynamic radius for the system: Water/ L₁₆₉₅ / EMDG/ IPM as function of *Oil/(Oil + Water)* weight ratio, α (wt%) for ($\gamma = 26$ wt%, $\delta = 25$ wt%).

From **Table 4.25**, one can observe that for water contents ≥ 85 wt% (i.e. $\alpha \leq 15$ wt%) where oil-in-water (O/ W) droplets exist the hydrodynamic radius is below 11 nm. On the other hand, **Table 4.26** shows that the hydrodynamic radius for $\alpha \leq 15$ wt% is below 7 nm. These observation demonstrate that the EMDG is the dominant surfactant in determining the dimensions of the droplets.

Fig. (4.67 and 4.68), shows the increase of R_H as the oil content increases. One expects that increasing oil content will increase D of the surfactant but because of the formation of the droplet and the swelling

mechanism the volume of droplets become larger and the surfactants diffusion become slower, therefore the D_{obs} of EMDG decreases as the R_H increases.

Assuming spherical aggregates with no oil penetration into the mixed surfactants film, the area per polar head group (a) can be estimated from the R_H and the ratio of the volume fraction of oil to the volume fraction of EMDG (ϕ_0 / ϕ_s) is determined by the relation ⁽¹²²⁾

$$a = \frac{3v_s}{R_H} \left(1 + \frac{\phi_0}{\phi_s}\right) \quad (8)$$

where v_s is the EMDG molecular volume which equals 1200 \AA^3 .

For water content equals 90 wt% (i.e. $\alpha = 10$ wt%) the obtained value of a is 75 \AA^2 for the system with $\gamma = 31$ wt% and $\delta = 50$ wt% and 88 \AA^2 for the system with $\gamma = 26$ wt% and $\delta = 25$ wt%. This indicates that increasing the quantity of EMDG in the system makes it more packed.

It should be noticed that in the analysis above the effect of L₁₆₉₅ on swollen O/ W micelle size is not taken in consideration. Since it is assumed to be dispersed at the interface between the EMDG molecules.

IV.3 Solubilization in Microemulsion

IV.3.1 Introduction

Solubilization of pharmaceutical active ingredients and transdermal drug delivery of active substance to the target organ at relevant level is one of the successful methods used in pharmaceutical formulations ⁽¹²³⁾ . Microemulsions were suggested during the last decades as an oral vehicle for cutaneous release of drugs for both hydrophilic and hydrophobic drugs. Compounds which are able to form nontoxic microemulsions and solubilize high quantity of the drug are the most suitable for application in pharmaceutical formulations.

Solubilization and deposition of the drug in the microemulsion depend on the microstructure of these microemulsions ⁽¹²⁴⁾ . Microemulsions show high potential of incorporation of large fraction of lipophilic and hydrophilic phases and therefore have favorable solvent properties ^(125,126) .

The water-miscible surfactant molecules contain both a hydrophobic and hydrophilic portion can solubilize many poorly water-soluble drugs. When the surfactant monomer concentration reaches the critical micelle concentration the surfactants can self-assemble to form micelles. So the surfactant can solubilize drug molecules by either a direct co-solvent effect or by uptake into micelles ⁽¹²⁷⁾ . The addition of the co-solvent (ethanol) to the oil phase turned the oil phase into better solvent and allowed significant solubilization of the surfactant into the oil with the formation of inverse micelles. The co-solvent is necessary to increase the hydrophilicity of the surfactants. However due to its amphiphilic character it will redistribute

also as a co-surfactant and not just as a co-solvent (i.e. it has the ability to participate in the self-assembly with the surfactant)⁽¹²⁸⁾.

Oil-in-water (O/ W) microemulsion have been prepared using certain nonionic surfactants⁽¹²⁹⁾, adding short chain alcohols (such as ethanol) to some of our systems will induce the formation of both W/ O and O/ W microemulsions⁽¹²⁹⁾. The phase behavior of our systems was characterized by a single continuous microemulsion region starting from pseudo-binary solution (micellar system containing surfactant and oil phase) and proceeding to the microemulsion water corner, which means that there is no phase separation will occur and the structural changes occurring in the isotropic phase develop continuously.

In our research work, we studied the solubilization of sodium diclofenac which is used as analgesic, anti-inflammatory, anti-rhumatic or anti-pyretic, in our microemulsion systems.

The systems used in this study are summarized in the following:

- (1) Water/ L₁₆₉₅ + EMDG (1/1)/ R(+)-limonene, **(Fig 4.53)**
- (2) Water/ L₁₆₉₅/ EMDG (1/1)/ R(+)-limonene + EtoH (1/1), **(Fig. 4.54)**
- (3) Water/ L₁₆₉₅/ EMDG (1/1)/ IPM, **(Fig. 4.55)**
- (4) Water / L₁₆₉₅/ EMDG (1/1)/ IPM + EtoH (1/1), **(Fig. 4.56)**.

on the dilution line D 60:40.

The objective of this study is to explore the ability of our microemulsions systems, to solubilze diclofenac sodium, and to study the effect of co-solvent (i.e. ethanol) and other components on the solubilization capacity of the diclofenac sodium.

IV.3.2 Results and discussion

In the **Table 4.27** we present the solubility of sodium diclofenac in each component of the microemulsion systems at 25°C.

Table 4.27: Diclofenac sodium solubility at 25°C in the different microemulsion components.

Medium	Diclofenac sodium solubility (ppm)
R(+)-limonene	SC < 120
IPM	SC < 120
Ethanol	6340 < SC < 6530
Water	2206 < SC < 2279
R(+)-limonene / Ethanol	5350 < SC < 5480
IPM / Ethanol	4520 < SC < 4660

Dilution a micellar solutions consisting of R(+)-limonene (A), R(+)-limonene + EtOH (B), IPM (C), IPM + EtOH (D) as the oil phase and sucrose ester (L₁₆₉₅), and etoxylated mono diglyceride (EMDG) as the surfactant with an a queues phase (water), caused gradual microstructure transitions ⁽¹²⁴⁾. The solubilization capacity (SC) of diclofenac sodium along the dilution lines, where the weight ratio for R(+)-limonene/ L₁₆₉₅/ EMDG (A) is 2:1.5:1.5, R(+)-limonene/ EtoH/ EMDG/ L₁₆₉₅ (B) is 1:1:1.5:1.5, IPM/ L₁₆₉₅/ EMDG (C) is 2:1.5:1.5 and IPM/ EtoH/ L₁₆₉₅/ EMDG (D) is 1:1:1.5:1.5, (**see Tables (4.28 - 4.31) and Fig. (4.69-4.72)**)

Table 4.28: Solubilization capacity (SC) of diclofenac sodium in the system: Water/ L₁₆₉₅ + EMDG (1/1)/ R(+)-limonene, along the dilution line D 60:40, at constant temperature (T = 25°C).

Composition (wt%) Water/L ₁₆₉₅ /EMDG/R(+)-limonene	α (wt%) $\frac{R(+)-Limonene}{Water + R(+)-Limonene}$	Maximum solubilization capacity (SC)
0/ 30/ 30/ 40	100	>115450
10/ 27/ 27/ 36	78	<110350
20/ 24/ 24/ 32	61.5	>133480
40/ 18/ 18/ 24	37.5	<125960
80/ 6/ 6/ 8	9.1	<81645

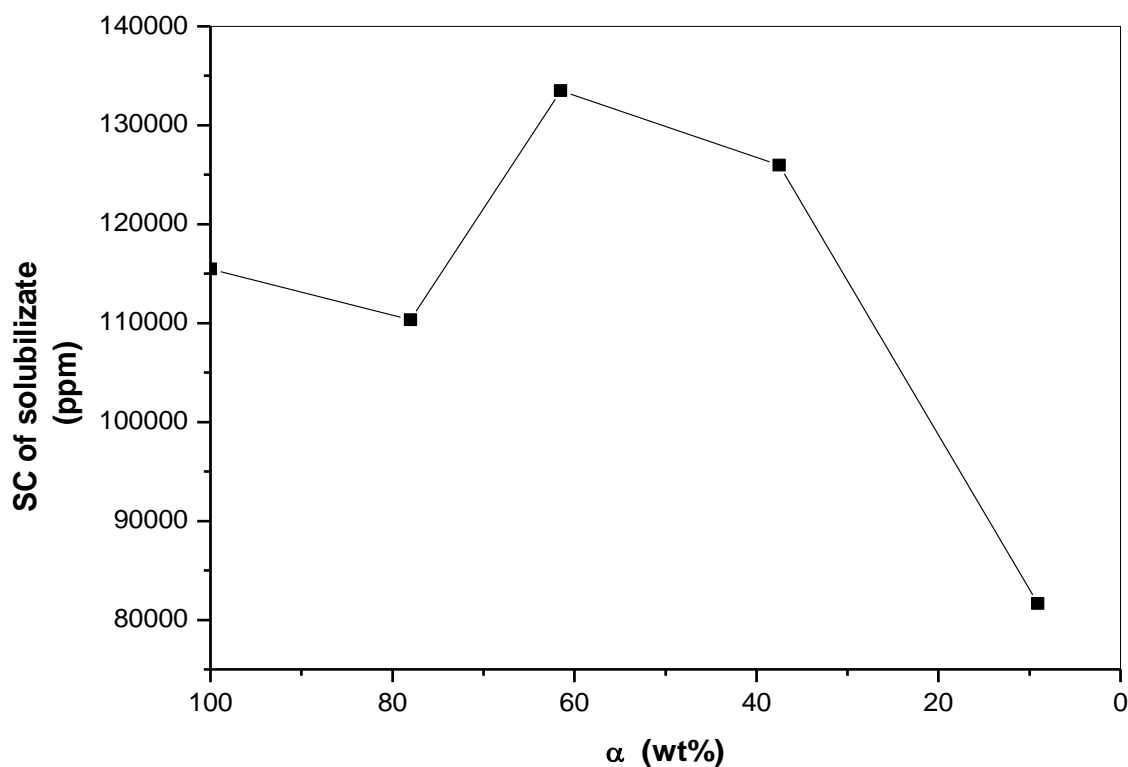


Fig. 4.69 : Solubilization capacity (SC) curve of Diclofenac sodium along the dilution line D 60:40 at 25°C, in the system: Water/ L₁₆₉₅ + EMDG (1/1)/ R(+)-limonene.

Table 4.29: Solubilization capacity (SC) of diclofenac sodium in the system: Water/ L₁₆₉₅ + EMDG (1/1)/ R(+)-limonene + EtOH (1/1), along the dilution line D 60:40, at constant temperature (T = 25°C).

Composition (wt%)	α (wt%)	Maximum solubilization capacity (SC)
Water/L ₁₆₉₅ /EMDG/R(+)-limonene/ EtOH	$\frac{R(+)-Limonene}{Water + R(+)-Limonene}$	
0/ 30/ 30/ 20/ 20	100	>163830
20/ 24/ 24/ 16/ 16	44	>152760
40/ 18/ 18/ 12/ 12	23	>164910

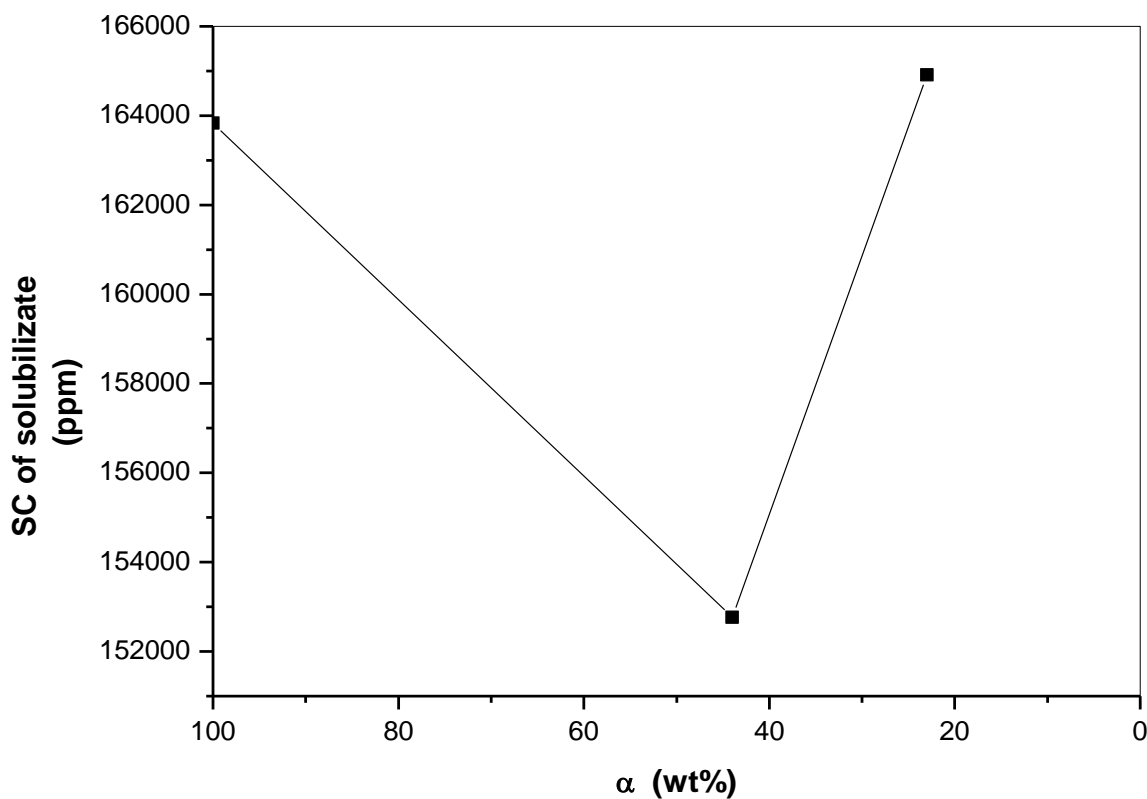


Fig. 4.70 : Solubilization capacity (SC) curve of Diclofenac sodium along the dilution line D 60:40 at 25°C, in the system: Water/ L₁₆₉₅ + EMDG (1/1)/ R(+)-limonene + EtOH (1/1).

Table 4.30: Solubilization capacity (SC) of diclofenac sodium in the system: Water/ L₁₆₉₅ + EMDG(1/1)/ IPM, along the dilution line D 60:40, at constant temperature (T = 25°C).

Composition (wt%) Water/L ₁₆₉₅ /EMDG/IPM	α (wt%) = $\frac{IPM}{Water + IPM} \times 100\%$	Maximum solubilization capacity(SC)
0/ 30/ 30/ 40	100	<142122
10/ 27/ 27/ 36	78.3	<142765
20/ 24/ 24/ 32	61.5	<156650
25/ 22.5/ 22.5/ 30	54.5	<94450

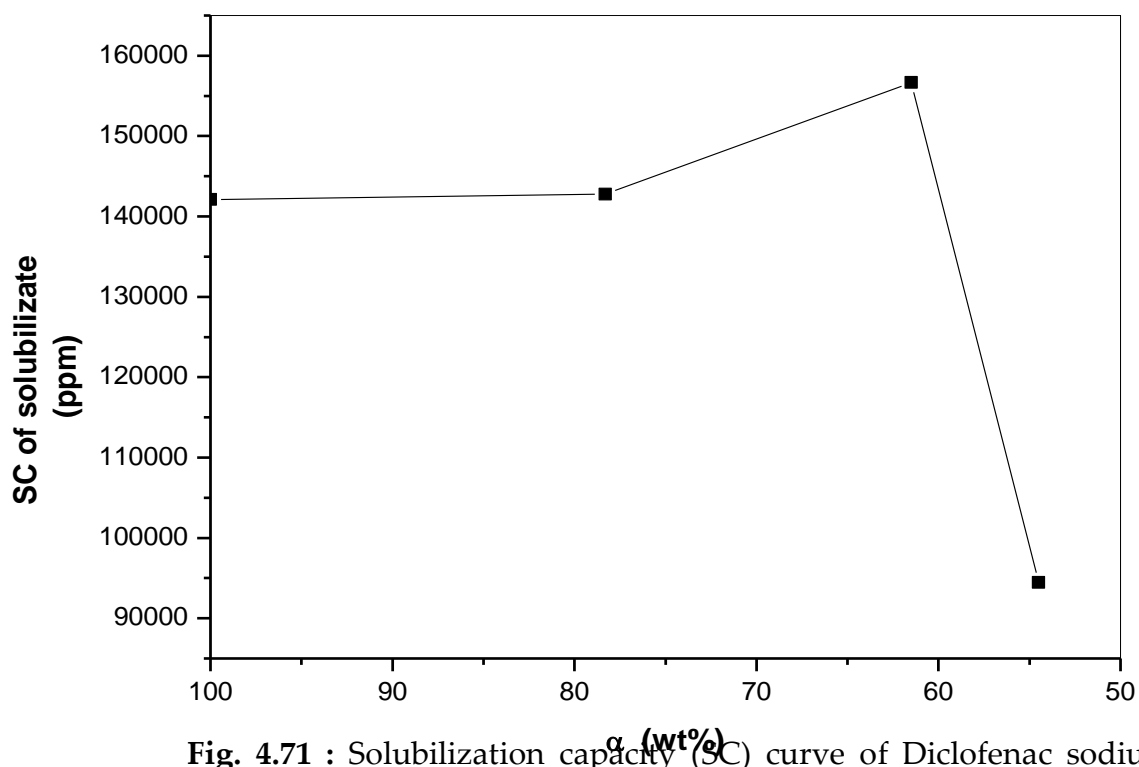


Fig. 4.71 : Solubilization capacity (SC) curve of Diclofenac sodium along the dilution line D 60:40 at 25°C, in the system: Water/ L₁₆₉₅ + EMDG(1/1)/ IPM.

Table 4.31: Solubilization capacity (SC) of diclofenac sodium in the system: Water/ L₁₆₉₅ + EMDG (1/1)/ IPM + EtOH (1/1), along the dilution line D 60:40, at constant temperature (T = 25°C).

Composition (wt%) Water/L ₁₆₉₅ /EMDG/IPM/EtOH	α (wt%) = $\frac{IPM}{Water + IPM} \times 100\%$	Maximum solubilization capacity (SC)
0/ 30/ 30/ 20/ 20	100	>164910
20/ 24/ 24/ 16/ 16	44	>167550
40/ 18/ 18/ 12/ 12	23	>177440
60/ 12/ 12/ 8/ 8	11.8	<146515

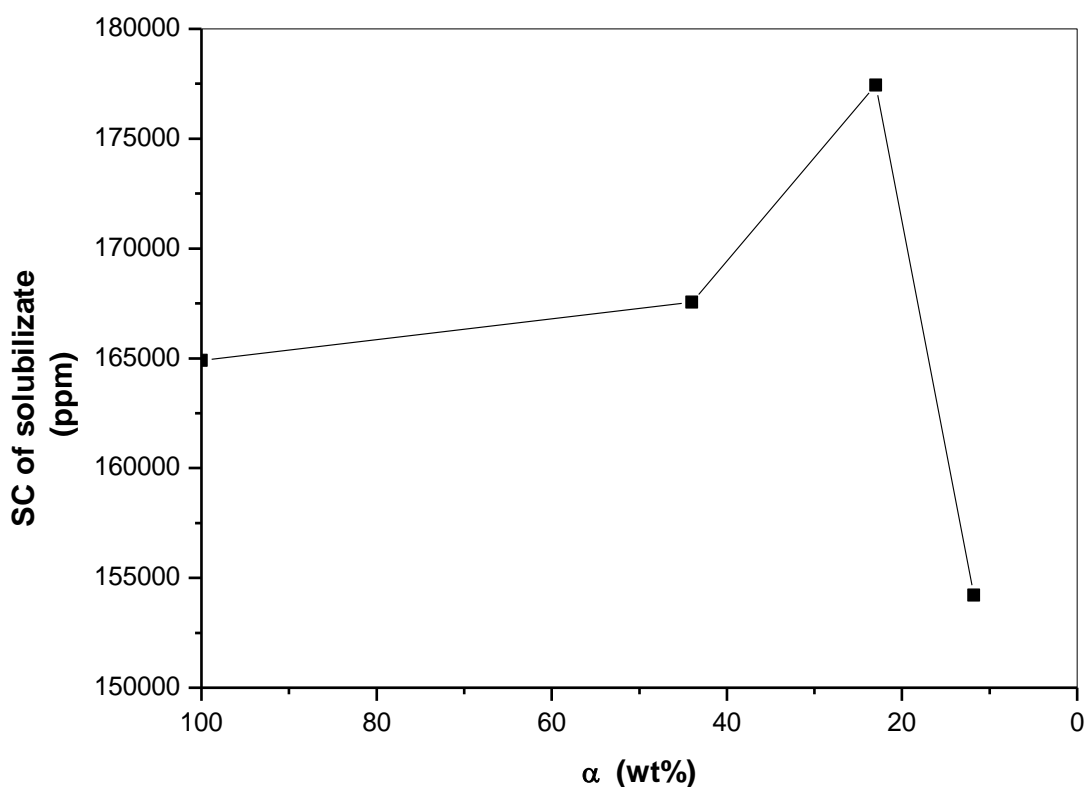


Fig. 4.72 : Solubilization capacity (SC) curve of Diclofenac sodium along the dilution line D 60:40 at 25°C, in the system: Water/ L₁₆₉₅ + EMDG (1/1)/ IPM + EtOH (1/1).

We can see in these tables and figures, that the solubilization capacity of sodium diclofenac in the microemulsion system is largely higher than that in each component alone (see Table 4.27).

The solubilization capacity curves in (Fig. 4.69), can be divided into three regions which indicate the microstructure transition along the dilution line. The first region indicates the formation of W/ O microstructure. The second region indicates the transition from W/ O microstructure to a bicontinuous microemulsion to an O/ W microstructure occurs.

In the first region ($78 < \alpha < 100$), the solubilization capacity decreases. The decrease in the solubilization capacity can be attributed to the decrease in the interfacial area as the micelle swell.

In the second region ($37.5 < \alpha < 78$), the solubilization capacity increases and reaches a maximum at $\alpha = 61.5$ wt% where in accordance with self-diffusion NMR results, the system has a bicontinuous microstructure which have the higher interfacial area and the higher flexibility .

In the third region ($\alpha < 37.5$) the solubilization capacity is decreased. These results indicates that the interface O/ W is not favorable for the solubilization of sodium diclofenac.

In the system: Water/ L₁₆₉₅/ EMDG/ R(+)-limonene + EtOH(1/1), the values of the solubilization capacity are higher than those obtained in the absence of ethanol.

A similar behavior was observed in the solubilization capacity curve, which is divided also to three regions . The maximum solubilization capacity is obtained at α value equals 23 wt%. If we suppose that ethanol is in the oil phase the α value for maximum solubilization capacity is at $\alpha = 37.5$ wt%. From this curve one concludes, that the bicontinuous region on

the dilution line is wider than in the case of the system: Water/ L₁₆₉₅/ EMDG/ R(+)-limonene.

In the case of the system: Water/ L₁₆₉₅/ EMDG/ IPM, two main regions are observed in the solubilization capacity curve. The first region where the microstructure is W/ O, the solubilization capacity increases until it reaches a maximum at α value = 61.5 wt% which indicates the presence of bicontinuous structure. The second region where the microstructure is O/ W and the solubilization capacity decreases, which also indicates that the O/ W microstructure is not favorable for the solubilization of sodium diclofenac.

In the system: Water/ L₁₆₉₅/ EMDG/ IPM + EtOH (1/1), the values of the solubilization capacity are higher than those obtained in the absence of ethanol. A two regions are also observed in the solubilization capacity curve. For the W/ O microstructure the solubilization capacity increases until it reaches a maximum at the bicontinuous region then it decreases in the O/ W microemulsion region.

It is observed also in this case that ethanol extends the bicontinuous region cause of the increase of interfacial flexibility and interfacial area.

It is also important to note that the values of the solubilization capacity obtained in the case where IPM is present as the oil phase , are higher than those obtained in the case where R(+)-limonene is present. This is referred to the fact that the interfacial area in the microemulsion containing IPM is higher than that containing R(+)-limonene.

CHAPTER FIVE

GENERAL CONCLUSIONS

V. General Conclusions:

This research work investigated the following subjects in the domain of mixed surfactants systems:

1. Study of the phase behavior and exploring the factors affecting it.
2. Elucidation of the microstructure of the mixed surfactants systems.
3. Revelation of the possibility of solubilization of pharmaceutical active ingredients in the microemulsions formed using these mixed surfactants.

In the following we redraw the general conclusions varied from these subjects:

1. Study of the phase behavior:

- a. **Variation of γ, δ (wt %) and T at constant $\alpha = 50$ wt% in the system: Water/ Surfactant / PG/ Oil.**

In the case where the three phase region was formed increasing PG content (i.e. δ Values) increases the $\bar{\gamma}$ and \bar{T} . The \bar{T}_{MCT} bigger than \bar{T}_{IPM} and the $\bar{\gamma}_{MCT}$ is also bigger than $\bar{\gamma}_{IPM}$. For the three surfactants used which mean that the effective carbon of the oil which is the highest with MCT between the three oils, is the dominant factor determining the phase behavior. R(+)-limonene which is the less hydrophobic one does not form three phase in the majority of the cases studied indicating that the systems

studied are beyond the tricritical point of the system and no three phase can be formed.

The type of the surfactant also affects the behavior where $\bar{T}_{L1695} > \bar{T}_{S1570} > \bar{T}_{EMDG}$, $\bar{\gamma}_{L1695} > \bar{\gamma}_{S1570} > \bar{\gamma}_{EMDG}$ corresponding to the fact that L1695 is most hydrophilic one. With HLB = 16, while HLB of S1570 = 15 and that of EMDG = 13.5.

In the case when the one phase was formed beside the two phase and no three phase was observed (i.e. the case of R (+)-limonene) the minimum amount of surfactant and co-surfactant needed for the formation of 1 phase region $\gamma_{\min S1570} < \gamma_{\min L1695} < \gamma_{\min EMDG}$ which means that S1570 is a solubilization improver.

a.2 In the system: Water/ Sucrose Ester/ EMDG/ Oil

The three-phase region is observe for the three oils and in this case $\bar{\gamma}_{R(+)\text{-limonene}} < \bar{\gamma}_{IPM} < \bar{\gamma}_{MCT}$ and $\bar{T}_{IPM} < \bar{T}_{R(+)\text{-limonene}} < \bar{T}_{MCT}$, this indicates that the type of surfactant mixture affect the phase behavior beside the type of oil and a microstructural effects such as the type of droplets formed and the presence of channels interfere beside the chemical structure.

In the case where MCT was used as the oil phase $\bar{\gamma}_{L1695} < \bar{\gamma}_{S1570}$ and $\bar{T}_{L1695} > \bar{T}_{S1570}$ which is also in accordance with the fact that L1695 is more hydrophilic than S1570.

In the case of the formation of one phase beside two phase also S1570 was observed as a solubilization improver.

b. Variation of α (wt %) and T at constant γ and δ (wt %).

A one phase region channel was extended from low values of α to high values in the systems: Water/ S₁₅₇₀ / PG/ Oil and in the system: Water/ L₁₆₉₅/ EMDG/ Oil. The width of the one phase region on the temperature scale depends on the nature of oil and its effective carbon number.

c. Pseudo-ternary phase behavior at constant T.

In these two systems we studied the effect of changing the ratio of EMDG in the mixed surfactants L₁₆₉₅ + EMDG, and the effect of adding ethanol to the oleic phase. As we can see in the two systems containing R(+)-limonene and IPM, decreasing the ratio of L₁₆₉₅ in the mixed surfactants L₁₆₉₅ + EMDG from 1 to 1/3 decreases the extension of the phase region (W_m) and decreases the total microemulsion area.

EMDG is more hydrophobic surfactant than L₁₆₉₅ with HLB = 13.5 compared to HLB = 16 for L₁₆₉₅, increasing its ratio in the mixture of surfactants will decrease the affinity of water to the mixed surfactants and will affect the extension of the one phase region.

As we can observe, the initial surfactant concentration (dilution line) where we obtained a maximum water solubilization is lower in the case of high content of L₁₆₉₅ (i.e. L₁₆₉₅/ EMDG = 1/3). This behavior is also observed when ethanol is added to the oil phase, this behavior is explained by the fact that alcohol increases the flexibility of the interfacial layer which enables more water to be solubilized in the system.

Changing the type of the oil from R (+)-limonene to IPM also affects the total one phase region and the extent of water solubilization. R (+)-

limonene is less hydrophobic oil than IPM, therefore the total area of the one phase region observed with R (+)-limonene is greater than that observed with the IPM.

2. Elucidation of the microstructure of the mixed surfactant systems.

a. By electrical conductivity.

By using different types of oil the electric conductivity (κ) differs. From the Figures (**Fig. 4.59 and Fig. 4.60**) we find that despite the increase in electrical conductivity in both oils R(+)-Limonene and IPM the values of κ with R(+)-Limonene are smaller than in the case of IPM. This can be explained by the chemical structure of both oils and their capability to penetrate between the chains of surfactants to the interface, IPM which have a linear structure as oil-phase will give the water the mobility and this will increase the conductivity, because there is enough space for water to move around the droplets (micelles), while R(+)-Limonene which have a cyclic structure, will decrease the space for water to move between the droplets (micelles) and this will decrease the conductivity of the system for α values between 10 and 30 wt%. Raising the temperature the collision probability between the droplets increases and the opening and reforming of droplets will increase the mobility of water and the electrical conductivity will again rise with temperature. In addition the possibility of percolation becomes larger and the formation of water channels will increase the electrical conductivity of the system.

b. By self-diffusion NMR.

The very large variations in D_{water} and D_{oil} on varying the weight fraction of oil are striking. Evidently, there is a smooth transition from O/ W structure at low oil to water ratio to W/ O at high ratio, while at approximately equal amounts of oil to water, there is rapid diffusion (D/D_0 of around 0.3) of both components, indicating a structural arrangement where neither component is confined into closed domains.

This is not the case in our system. This behavior indicates that the concentration of surfactant (γ) in the system is the dominant factor that determines the values of D^W/D_0^W .

From these two **Fig. (4.64 and 4.65)** one can conclude that the mixed surfactants content in the microemulsion system may have the dominant role in determining the microstructure of the microemulsions.

The hydrophilicity of the mixed surfactants affects also the diffusivity of both oil and water but can not have the major role in determining the microstructure compared with the mixed surfactant content.

From **Table 4.25**, one can observe that for water contents ≥ 85 wt% (i.e. $\alpha \leq 15$ wt %) where oil-in-water (O/ W) droplets exist the hydrodynamic radius is below 11 nm. On the other hand, **Table 4.26** shows that the hydrodynamic radius for $\alpha \leq 15$ wt% is below 7 nm. These observation demonstrate that the EMDG is the dominant surfactant in determining the dimensions of the droplets.

Fig. (4.66 and 4.67), shows the increase of R_H as the oil content increases. One expects that increasing oil content will increase D of the surfactant but because of the formation of the droplet and the swelling mechanism the volume of droplets become larger and the surfactants

diffusion become slower, therefore the D_{obs} of EMDG decreases as the R_H increases.

Assuming spherical aggregates with no penetration of oil into the mixed surfactant film, the estimation of the area per polar head group indicates that increasing the quantity of EMDG in the system makes it more packed.

3. Revelation of the possibilities of solubilization of pharmaceutical ingredients

As we have seen in the self-diffusion NMR results, at $\alpha = 61.5$ wt% the system has the bicontinuous microstructure which is the one capable to solubilize the maximum amount of solubilizate. A cause of its high flexibility and its high interfacial area.

Adding ethanol will increase the flexibility of the interface and its area , and will permit to obtain a maximum solubilization capacity at α values lower than those observed in the case where ethanol was absent. For all the system studied, those containing ethanol, permit higher solubilization capacity.

It is also important to note that the values of the solubilization capacity obtained in the case where IPM is present as the oil phase , are higher than those obtained in the case where R (+)-limonene is present. This is referred to the fact that the interfacial area in the microemulsion containing IPM is higher than that containing R (+)-limonene

CHAPTER SIX

REFERENCES

VI. References

1. J.P. Hoar, J.H. Schluman. *Nature*. **152**, 102 (1943).
2. V.R. Kokatnur, U.S. Pat., 2,111,000 (1935).
3. D. Bowden, J. Holmstine, U.S. Pat., 2,045,455 (1936).
4. J. Sjoblom, R. Lindberg, S.E. Friberg, *Adv. Colloid Interface Sci.*, **65**, 125 (1996).
5. T. Hellweg, *Curr. Opin. Colloid Interface Sci.*, **7**, 50 (2002).
6. S. Qutubuddin, in: D.O. Shah (Ed.). *Micelles, Microemulsions, and Monolayers*, Marcel Dekker, New York, 1998, P.305.
7. B.P. Binks, J. Meunier, O. Abillon, D. Langevin, *Langmuir*, **5**, 415 (1989).
8. R. Strey, *Colloid Polym. Sci.*, **272**, 1005 (1994).
9. K. Shinoda, B. Lindman, *Langmuir*, **3**, 135 (1987).
10. S.E. Friberg, *J. Dispersion, Sci. Technol.*, **6**, 317 (1985).
11. A.M. Bellocq, J. Biais, P. Bothorel, B. Clin, G. Fourche, P. Lalanne, B. Lemaire, B.Lemanceau, D. Roux, *Adv. Colloid Interface Sci.*, **20**, 167 (1984).
12. C. Solans, R. Pons, H. Kunieda, in: C. Solans, H. Kunieda (Eds.), *Industrial Applications of Microemulsions*, Marcel Dekker, New York, 1997, P.1.
13. S.R. Dungan, in: C. Solans, H. Kunieda (Eds.), *Industrial Applications of Microemulsions*, Marcel Dekker, New York, 1997, P.148.
14. H. Jamels, *Agricultural Research Service*, 1998.
15. D. F. Evans, H. Wennerstrom, *The colloidal domain, where physics, chemistry, biology and technology meet*, 2nd ed. Wiley-VCH, New York, 2001, pp. 539-570.
16. P. Ekwall, *Acta Acad, Aboensis (Math. Phys.)*, **4**, 1 (Dissertation) (1927).

17. P. Ekwall , I. Danielsson, L. Mandell, *Kolloid-Z.*, **169**, 113 (1960).
18. P. Ekwall, Microemulsions and liquid crystals, In: *Advances in liquid Crystals*, **Vol. 1**, (G.H. Brown Ed.), Academic Press, London, 1975, pp.1-142.
19. G. Gillberg, H. Lehtinen, S. Friberg, *J. Colloid Interface Sci.*, **33**, 40 (1970).
20. P. Ekwall, I. Danielsson, P. Stenius, in: M. Kerker (Ed.), *Surface Chemistry and Colloid*, MTP, Rev. Sci., Phys. Chem. Ser., 1, **Vol.7**, Butter Worths, London, 1972. P.97.
21. K. Shinoda, T. Ogawa, *J. Colloid Interface Sci.*, **24**, 56 (1967).
22. K. Shinoda, H. Saito, *J. Colloid Interface Sci.*, **26**, 70 (1968).
23. K. Shinoda, H. Takeda, *J. Colloid Interface Sci.*, **32**, 642 (1970).
24. Johan Sjoblem, Ritva lindberg and stig E. Friberg, *Advances in Colloid and interface science*, **95**, 125-287 (1996).
25. C. Tanford, *The Hydrophobic Effect: Formation of Micelles and Biological Membranes*. Wiley , New York, 1989.
26. M.J. Rosen, *Surfactants and Interfacial Phenomena*, 2nd Ed., Wiley-Interscience, New York, 1989.
27. K. Meguro, M. Ueno, K. Esumi, in: M. Schick(Ed.), *Nonionic Surfactant , Phsical Chemistry*, Dekker, New York, 1987, P.109.
28. B. Lindman, H. Wennerstrom, *Topics Curr. Chem.*, **87**, 1 (1980).
29. H. Kunieda, A. Nakano, M. Akimaru, The Effect of Mixing of Surfactant on Solubilization in a Microemulsion system, *J. Colloid and inter. Sci.*, **170**, 78-84 (1995).
30. M. Kahlweit, R. Strey, *Angew. Chem. Int. Ed. Engl.*, **24**, 654-668 (1985).
31. M. Kahlweit, R. Strey, P. Firman, D. Haase, J. Jen, R. Schomacker, *Langmuir*, **4**, 499 (1988).
32. M. Kahlweit, R. Strey, G. Busse, *J. Phys. Chem.*, **89**, 163 (1985).

33. M. Kahlweit, R. Strey, R. Schomacker, D. Hasse, *Langmuir*, **5**, 307 (1989).
34. R.B. Griffiths, B. Widom, *Phys. Rev.*, **A 8**, 2173 (1973).
35. M. Kahlweit, R. Strey, G. Busse, *Phys. Rev.*, **E 47**, 4197 (1993).
36. O.P. Ward, F. Jianwen, L. Zuyi, *Enzyme Microb. Technol.*, **20**, 52 (1996).
37. J.O. Rich, B.A. Bedell, J.S. Dordick, *Biotechnol. Bioeng.*, **45**, 426 (1995).
38. G.B. Oguntimein, H. Erdmann, R.D. Schmid, *Biotechnol. Lett.*, **15**, 175 (1993).
39. N. Garti, V. Clement, M. Leser, A. Aserin, M. Fanun, *J. Molecular Liquids*, **80**, 253-296 (1999).
40. A.N.P. Wood, R. Fernandez-LaFuente, D.A. Cowan, *Biotechnol.*, **51**, 57 (1996).
41. M. Nishinohara, H. Kohyama, H. Yamamura, Japan. Pat., JP. 50,101,309 (1975).
42. T. Nagahama, K. Hasegawa, T. Nakajima, Y. Ito, Taisho Pharm.Co., Ttd., PCT Int. Appl., Wo 9744124 AL (1997).
43. H. Kunieda, K. Shioguchi, T. Tagawa, Mitsubishi Chem. Ind., Japanese Patent, 10 043 573 A2 (1998).
44. T. Watanabe, S. Yoshikawa, *Shokuin Kogyo*, **14**, 65 (1971).
45. C. Gallegos, J. Munoz, A. Guerrero, M. Berjano, ACS symp. Ser. 578 (Structure and Flow in Surfactant Solutions), 217 (1994).
46. D.C. Clark, P.J. Wilde, D.R. Wilson, R. Wustneck, *Food Hydrocolloids*, **6**, 173 (1992).
47. D. Abran, F. Boucher, T. Hamanaka, K. Hiraki, Y. Kito, K. Koyama, R.M. Leblanc, H. Machida, G. Munger, M. Seidou, M. Tessier, *J. Colloid Interface Sci.*, **128**, 230 (1989).

48. S.C. Sethi, S.D. Adyanthaya, S.D. Deshpande, R.G. Kelkar, N. Natarajan, S.S. Katti, *J. Surf. Sci. Technol.*, **2**, 103 (1986).
49. Kawaguchi, Takeshi, Nagoya Kogyo Daigaku Gakuho, **35**, 269 (1983).
50. S. Konoo, H. Ogawa, H. Mizuno, N. Iso, *J. Jpn. Soc, J. Food Sci. Technol.*, **43**, 880 (1996).
51. C.C. Akoh, C.V. Nwosu, *J. Am. Oil Chem. Soc.*, **69**, 14 (1992).
52. B. Jarvis, A.W. Holmes, *J. Chem. Technol. Biotechnol.*, **32**, 224 (1982).
53. T. Olesen, PCT-International. Patent Application, WO 91/ 04669 (1991).
54. I. Niiya, T. Maruyama, M. Imamura, M. Okada, T. Matsumato, *J. Food Sci. Technol.*, **20**, 199 (1973).
55. Rikagaku Kenkyusho, Japanese-Examined-Patent, 5616158 (1981).
56. K. Farooq, Z.U. Haque, *J. Dairy Sci.*, **75**, 2672 (1992).
57. T. Maruyama, Y. Kinoshita, I. Niiya, M. Imamura, *J. Food Sci. Technol.*, **20**, 399 (1973).
58. J.W. Cappel, R.N. Cronemiller, U.S. Patent, 4668 522 (1987).
59. W. Seibel, A. Menger, H.G. Ludewig, F. Bretschneider, *Getreide, Mehl Brot*, **30**, 325 (1976).
60. W.J. Brabbs, C.A. Hong. Procter and Gamble Co., U.S. Patent, 4, 503, 080.
61. C. Gallegos, C. Calahorro, J. Munoz, M. Berjano, A. Guerrero, *Comun. Jorn. Com. Esp. Deterg.*, **22**, 283 (1991).
62. M.A. Thevenin, J.L. Grossiord, M.C. Poelman, *Int. J. Pharm.*, **137**, 177 (1996).
63. S. Keipert, G. Schulz, *Pharmazie*, **49**, 195 (1994).
64. Y. Hayashi, S. Yoshioka, Y. Aso, A.L.W. Po, T. Terao, *Pharm. Res.*, **11**, 337 (1994).
65. J.T.H. Ong, E. Manoukian, *Pharm. Res.*, **5**, 704 (1988).

66. N. Garti, V. Clement, M. Fanun, M.E. Leser, *J. Agri. Food Chem.*, **48**, 3945 (2000).
67. M. Fanun, E. Wachtel, B. Antalek, A. Aserin, N. Garti, *Colloids and Surf. A: Physicochem. Eng. Aspects*, **180**, 173-186 (2000).
68. M.A. Thevenin, J.L. Grossiord, M.C. Poelman, *Int. J. Pharma.*, **137**, 177 (1996).
69. M.A. Pes, K. Aramaki, N. Nakamura, H. Kunieda, *J. Colloid Interface Sci.*, **178**, 666 (1996).
70. M.A. Bolzinger-Thevenin, J.L. Grossiord, M.C. Poelman, *Langmuir*, **15**, 2307 (1999).
71. L. Lehman, S. Keipert, M. Gloor, *Eur. J. Pharm. Biopharm*, **52**, 129 (2001).
72. R. Nagarajan, C.C. Wang, *J. Colloid Interface Sci.*, **178**, 471 (1996).
73. T. Iwanaga, M. Suzuki, H. Kunieda, *Langmuir*, **14**, 5775 (1998).
74. A. Martino, E. W. Kaler, *Langmuir*, **11**, 779 (1995).
75. R. Nagarajan, C.C. Wang, *Langmuir*, **16**, 5242 (2000).
76. S. Ray, S.P. Moulik, *Langmuir*, **10**, 2511 (1994).
77. H. Tanojo, J. A. Bouwstra, H. E. Junginger, H. E. Boddé, *J. Therm. Anal. Cal.*, **57**, 313 (1999).
78. P. M. Mehl, *Thermochim. Acta.*, **255**, 297 (1995).
79. P. M. Mehl, *Thermochim. Acta.*, **272**, 201 (1996).
80. M. Kreilgaard, *Advanced Drug Delivery Reviews*, **54 Suppl.1**, S77 (2002).
81. Y. Tokuoka, H. Uchiyama, M. Abe, S. D. Christian, *Langmuir*, **11**, 725 (1995).
82. N. Kanei, Y. Tamura, H. Kunieda, *J. Colloid Interface Sci.*, **218**, 2113 (1999).
83. N. Garti, A. Yaghmur, M.E. Leser, V. Clement, H.J. Watzke, *J. Agric. Food Chem.*, **49**, 2552 (2001).

84. A. Yaghmur, A. Aserin, N. Garti, *Colloids Surf. A: Physicochem. Eng. Aspects*, **194**, 175 (2001).
85. Mitsubishi-Kasei Foods Corp., "Ryoto Sugar Ester Technical Information", 1982.
86. Stepan Europe, "Neobee M5 Technical Information" Voreppe, France, 1990.
87. British Pharmacopoeia, **Version 4.0**, United Kingdom for HMSO, London, 2000.
88. M. Kahlweit, R. Strey, G. Busse, *Phys. Rev.*, E **47**, 4197 (1993).
89. M. Fanun, R. Aserin, N. Garti, Sucrose ester microemulsions as microreactores for model Maillard reaction, *Colloids Surf. A.*, **194**, 175-187 (2001).
90. M. Fanun, E. Wachtel, B. Antalek, A. Aserin, N. Garti, A study of the microstructure of four-component sucrose ester microemulsions by SAXS and NMR, *Colloids Surf. A.*, **180**, 173-186 (2001).
91. O. Glatter, D. Orthhaber, A. Strander, G. Scherf, M. Fanun, N. Garti, V. Clement, M.E. Leser, Sugar ester nonionic microemulsions: structural characterization, *J. Colloid Interface Sci.*, **241**, 215-225 (2001).
92. N. Garti, A. Aserin, I. Tiunova, M. Fanun, A DSC study of water behavior in water-in-oil microemulsions stabilized by sucrose esters and butanol, *Colloids surf. A.*, **170**, 1-18 (2000).
93. N. Garti, V. Clement, M. Fanun, M.E. Leser, Some characteristics of sugar ester nonionic microemulsions in view of possible food applications, *J. Agri. Food Chem.*, **48**, 3945-3956 (2000).
94. S. Ezrahi, A. Aserin, M. Fanun, N. Garti, Sub-zero temperature behavior of water in microemulsions, In: Thermal behavior of

- dispersed systems Surfactant Science Series, **Vol. 93** (N. Garti, Ed.) Marcel Dekker Inc., New York, 2000, pp. 59-120.
95. N. Garti, A. Aserin, M. Fanun, Nonionic sucrose ester microemulsions for food applications. Part 1: Water solubilization, *Colloids surfaces A.*, **164**, 27-38 (2000).
 96. N. Garti, V. Clement, M.E. Leser, A. Aserin, M. Fanun, Sucrose ester microemulsions, *J. Mol. Liquids*, **80**, 253-296 (1999).
 97. Larry D. Rayan, Eric W. Kaler, *Colloids and Surfaces, A: Physicochem. Eng. Aspects*, **176**, 69-83 (2001).
 98. Larry D. Rayan, Kai-V. Schubert, Eric W. Kaler, *Langmuir*, **13**, 1510-1518 (1997).
 99. Larry D. Rayan, Eric W. Kaler, *Langmuir*, **13**, 5222-5228 (1997).
 100. M. Kahlweit, R. Strey, G. Busse, *J. Phys. Chem.*, **94**, 3881 (1990).
 101. N.Garti, A. Aserin, S. Ezrahi, I. Tiunova, G. Bercovic, Water behavior in nonionic surfactant systems. Part 1:Sub-zero behavior of water in nonionic microemulsions studied by DSC., *J. Colloid Interface Sci.*, **178**, 60-68 (1996).
 102. N. Garti, A. Aserin, I. Tiunova, S. Ezrahi. Sub-zero temperature behavior of water in nonionic microemulsions, *J. Thermal Anal.*, **51**, 63-78 (1998).
 103. N. Garti, A. Aserin, I. Tiunova, M. Fanun, A DSC study of water behavior in water-in-oil microemulsions stabilized by sucrose esters and butanol, *Colloids Surf. A: Physicochem. Eng. Aspects*, **170**, 1-18 (2000b).
 104. D. Waysbort, S. Ezrahi, A. Aserin, R. Givati, N. Garti. ¹H NMR study of a U-type nonionic microemulsions. *J. Colloid Interface Sci.*, **188**, 282-295 (1997).

105. K. Shinoda, S. Friberg, Correlation between solution behavior of surfactants and solubilization microemulsions or emulsions type in surfactant/ water/ oil systems. In *Emulsions and solubilization*, Wiley, New York, 1986 , pp 11-50.
106. N. Garti, A. Aserin, M. Fanun, Nonionic sucrose ester microemulsions for food applications. Part 1: Water solubilization, *Colloids Surf. A: Physicochem. Eng. Aspects*, **164**, 27-38 (2000a).
107. G. Li, X. Kong, R. Guo, X. Wang. Interrelation of carbon numbers in microemulsions, *J. Surface Sci. Technol.*, **5**, 29-45 (1989).
108. D. Wu, A. Chen, C.S. Johnson, An improved Diffusion-ordered spectroscopy experiment incorporating bipolar-gradient pulses, *J. Magn. Reson.*, **115**, 260-264 (1995).
109. R. Zana, Microemulsions, *Hetrogeneous Chem. Rev.*, **1**, 145-157 (1994).
110. M. Kahlweit, G. Busse, J. Winkler, Electric conductivity in microemulsions, *J. Phys. Chem.*, **99**, 5605-5614 (1993).
111. M. Kahlweit, How to prepare microemulsion at prescribed temperature, oil and brine, *J. Phys. Chem.*, **99**, 1281-1284 (1995).
112. K. Aramaki, H. Kunieda, M. Ishitobi, T. Tagawa, Effect of added salt on three phase behavior in a sucrose monolaurate systems, *Langmuir*, **13**, 2266-2270 (1997).
113. B. Lindman, N. Kamenka, T.M. Kathopoulis, B. Brun, P.G. Nilsson, Translational diffusion and solution structures in microemulsions, *J. Phys. Chem.*, **84**, 2485-2490 (1980).
114. E.O. Stejskal, Reminiscences about the development of Pulsed Field Gradient Spin Echo NMR (PFGSE), In: *Encyclopedia of Nuclear Magnetic Resonance*, (E.O. Stejskal, Ed.), Wiley, New York, USA, 1995, pp. 657-658.

115. O. Gatter, D. Orthhaber, A. Strander, G. Scherf, M. Fanun, N. Garti, V. Clement, M.E. Leser, Sugar ester nonionic microemulsions: structural characterization, *J. Colloid Interface Sci.*, **241**, 215-225 (2001).
116. K. Shinoda, M. Araki, A. Sadaghiani, A. Khan, B. Lindman, Lecithin-based microemulsions-phase-behavior and microstructure, *J. Phys. Chem.*, **95**, 989-993 (1991).
117. F.D. Blum, S. Pickup, B.W. Ninham, S.J. Chen, D.F. Evans, Structure and dynamics in three-component microemulsions, *J. Phys. Chem.*, **89**, 711-713 (1985).
118. U. Olsson, K. Shinoda, B. Lindman, Change of the structure of microemulsions with the HLB of nonionic surfactants as revealed by NMR self-diffusion studies, *J. Phys. Chem.*, **90**, 4083-4088 (1986).
119. P.G. Nilsson, B. Lindman, Water self-diffusion in nonionic surfactants solutions: hydration and obstruction effects, *J. Phys. Chem.*, **87**, 4756-4761 (1983).
120. B. Lindman, K. Shinoda, M. Jonstromer, A. Shinodara, Change of organized solutions (microemulsions) structure with small changes in surfactant composition as revealed by NMR self-diffusion studies, *J. Phys. Chem.*, **92**, 4702-4706 (1988).
121. L.E. Scriven, *Nature*, **263**, 123 (1976).
122. A. Arridsson, O. Soderman, *Langmuir*, **7**, 3567-3572 (2001).
123. M. Kreilgaard, Influence of microemulsion on cutaneous drug delivery, *Adv. Drug Delivery Reviews*, **54 Suppl. 1**, S77-S98 (2002).
124. A. Spornath, A. Yagmur, A. Aserin, R.E. Hoffman, N. Garti, Food grade microemulsions based on nonionic emulsifiers: media to enhance lycopene solubilization, *J. Agric. Food Chem.*, **50**, 6917-6922 (2002).

125. S.R. Dungan, Microemulsions in foods: properties and applications. In Industrial Applications of Microemulsions; C. Solans, H. Kunieda Eds., **Vol. 66**, Marcel Dekker Inc., New York, 1997, pp. 148-170.
126. K. Holmberg, Quarter Century progress and new horizons in microemulsions. In Micelles. Microemulsions. and Monolayers; O. Shah Ed., Marcel Dekker Inc.: New York, 1998, pp.161-192.
127. G. Strickly, *Pharmaceutical Research*, **21, No.2**, 201-228 (2004).
128. O. Glatter, D. Orthaber, A. Strandner, G. Scherf, M. Fanun, N. Garti, *Colloid Interface Sci.*, **241**, 215-225 (2001).
129. N. Garti, A. Yagmur, M.E. Leser, V. Clement, H.J. Watzke, Improved oil solubilization in oil/ water food grade microemulsions in the presence of polyols and ethanol, *J. Aric. Food Chem.*, **49**, 2552-2562 (2001).